2(mix)

LR 25491
OCTOBER 1972

CR 114519

AVAILABLE TO THE PUBLIC

FINAL REPORT

EXPERIMENTAL HINGELESS ROTOR CHARACTERISTICS AT FULL SCALE FIRST FLAP MODE FREQUENCIES

INCLUDING ROTOR FREQUENCY RESPONSE TO SHAFT OSCILLATIONS

by W.A. Kuczynski

PHASE 3: CONTRACT NAS2 - 5419

Submitted to:

U.S. Army Air Mobility Research
and Development Laboratory
Ames Directorate,
Moffet Field, California

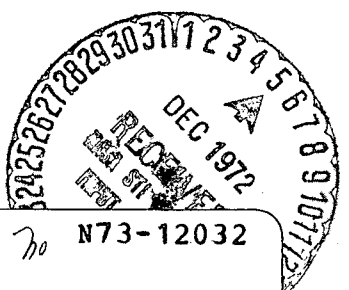

LOCKHEED-CALIFORNIA COMPANY • BURBANK
A DIVISION OF LOCKHEED AIRCRAFT CORPORATION

250

LR 25491
OCTOBER 1972

FINAL REPORT

EXPERIMENTAL HINGELESS ROTOR CHARACTERISTICS AT FULL SCALE FIRST FLAP MODE FREQUENCIES

INCLUDING ROTOR FREQUENCY RESPONSE TO SHAFT OSCILLATIONS

by W.A. Kuczynski

PHASE 3: CONTRACT NAS2 - 5419

Submitted to:

U.S. Army Air Mobility Research
and Development Laboratory
Ames Directorate,
Moffet Field, California

LOCKHEED-CALIFORNIA COMPANY • BURBANK
A DIVISION OF LOCKHEED AIRCRAFT CORPORATION

FOREWORD

The results of the third phase of the Lockheed/U. S. Army Air Mobility Research and Development Laboratory (AMRDL) (Ames Directorate) "High Advance Ratio Research Program" (Contract NAS2-5419) are presented in this document. The research effort spanned the period from October 1971 to August 1972.

The success of this endeavor is directly attributable to the diligent efforts of the various AMRDL and Lockheed people who supported the program. Particular credit is due Mr. David Sharpe, the AMRDL Project Engineer.

PRECEDING PAGE BLANK NOT FILMED

SUMMARY

Phase 3 of the Lockheed/AMRDL (Ames Directorate) "High Advance Ratio Research Program" has been successfully completed. The primary objectives of the program were to experimentally determine the rotor frequency response to shaft pitching and rolling oscillations and to acquire steady response and frequency response data at high advance ratios for hingeless rotors with typical, full-scale, first flap mode natural frequencies. The acquisition of these experimental results would greatly enhance the hingeless rotor data bank established during the first two phases of the program.

Two minor modifications of the test model were required to fulfill these goals. First, the turnbuckles which had been used to manually position the model in pitch and roll, were replaced with electrically controlled hydraulic actuators. This provided the remotely operable shaft oscillation capability required for the frequency response tests. In order to obtain a lower flapping frequency, a set of 'supersoft' hub flexures were fabricated. The flapwise stiffness of these new restraints was 1/4 of the value for the softest flexure previously tested. (The rotor equipped with the 'supersoft' flexures is identified as configuration 5.)

Secondary objectives of the program included the further evaluation of both the Phase 2 hub moment feedback control system and the Phase 1 simplified rigid blade flapping theory with respect to shaft oscillations.

The experimental program was composed of three types of tests.

- open loop steady state tests where the rotor was excited with steady θ_o, θ_s, θ_c and α inputs
- open loop frequency response tests with sinusoidal swashplate (θ_o, θ_s and θ_c) and shaft (α, ϕ) excitations
- closed loop frequency response tests with sinusoidal shaft excitations.

The steady state tests were conducted with only configuration 5. Three rotor speeds (550, 850 and 1,000 rpm) were tested which corresponded to non-dimensional flap frequencies (P) of 1.28, 1.15 and 1.125. The maximum advance ratios attained for each frequency were $\mu = 0.93$ at P = 1.28 and $\mu = 0.82$ at P = 1.15. P = 1.125 was only tested at $\mu = 0$. The experimental data which are presented include steady rotor hub and shaft moments and lift and the harmonic content of the blade flapping moments at three radial positions.

Open loop frequency response tests with swashplate excitations were also conducted with only rotor configuration 5. Linear hub moment transfer functions were acquired at advance ratios from $\mu = 0$ to 0.93 for P = 1.28 and $\mu = 0$ to 0.61 with P = 1.15.

Since frequency response testing with shaft oscillations was initiated during the Phase 3 program, tests were conducted with rotor configuration 1 (identified as such during the Phase 1 program) and configuration 5. Linear transfer functions with respect to shaft pitch and roll were determined for flap frequencies from P = 1.15 to 1.56 and at advance ratios ranging from $\mu = 0$ to 0.93.

Two tests were performed with configuration 1 in a closed loop mode. The specific objective was to determine the effectiveness of the Phase 2 hub moment feedback control system in relieving the rotor response to the shaft excitations. Advance ratios of $\mu = 0$ and $\mu = 0.28$ at a rotor speed of 800 rpm were considered.

The discussion of the third phase of the "High Advance Ratio Research Program," presented in this report, draws heavily upon the Phase 1 and Phase 2 documentation. This is particularly true in the descriptions of the test article, the data acquisition and analysis systems, and the theoretical analysis. The bulk of the text is devoted to the presentation and examination of representative experimental results. All the analyzed test data are documented in appendices in tabular and/or graphical formats.

TABLE OF CONTENTS

LIST OF FIGURES

LIST OF FIGURES (Continued)

LIST OF FIGURES (Continued)

LIST OF FIGURES (Continued)

LIST OF FIGURES (Continued)

LIST OF FIGURES (Continued)

LIST OF FIGURES (Continued)

LIST OF FIGURES (Continued)

LIST OF FIGURES (Continued)

LIST OF TABLES

SECTION 1

INTRODUCTION

The Lockheed/AMRDL (Ames Directorate) "High Advance Ratio Research Program" is a systematic investigation of the characteristics of hingeless rotors over an advance ratio range and at conditions which are applicable to pure helicopter, compound helicopter and slowed rotor flight vehicles. The goals of the program are being achieved by means of small scale rotor model testing in the AMRDL (Ames) 7 x 10 foot wind tunnel and associated simplified theoretical analyses.

Three phases of the research have been completed. The first, for which Reference 1 constitutes the program final report, was finished in February 1971. That effort included the investigation of hingeless rotor flapping stability and response to steady swashplate control and angle of attack excitations at low rotor lift levels. Tests were conducted at advance ratios from 0 to 2.15 for a large envelope of rotors defined by Lock number (γ) and nondimensional flapping frequency (P).

The Phase 2 effort (Reference 2) expanded the investigations to hingeless rotor frequency response with respect to swashplate (θ_o, θ_s, θ_c) excitations. The rotor model was also equipped with a hub moment feedback control system and the steady and frequency response characteristics of the resulting closed loop system were studied. The Phase 2 rotor configurations and test conditions were among those considered during Phase 1 to assure consistency with previous data.

The Phase 3 program, for which this document represents the contract final report, sought to expand the reservoir of experimental hingeless rotor data which had already been established. The expansion was accomplished in two ways. First, the test model was modified to free the rotor shaft in pitch and roll. This change made it possible to determine the experimental rotor frequency response to shaft pitch and roll oscillations. These data were acquired

for the Phase 2 rotor configurations and frequency response test conditions, again for data consistency.

The second means of enlarging the data bank was to test the 7-1/2 foot diameter rotor with a reduced hub stiffness. This was accomplished by softening the blade flexures in the flapwise direction. This modification facilitated a significant expansion of the previously tested advance ratio/flap frequency (μ/P) envelope. Full-scale flapping frequencies were achieved. All of the types of tests formerly conducted, plus frequency response with respect to rotor shaft oscillations, were performed with the softened rotor hub configuration.

Two secondary objectives of the Phase 3 program were to continue both the evaluation of the Phase 2 feedback control system and the assessment of the validity of the simplified rigid blade mathematical model.

Current plans call for another research program involving the High Advance Ratio Rotor Model. This investigation will have as its objectives the determination of the effects of blade stall and inflow on hingeless rotor dynamic characteristics. To this end, the rotor model will be tested at high lift levels. The experimental portion of the program is presently scheduled for February 1973. The AMRDL (Ames) 7 x 10 foot wind tunnel will again be the test site.

SECTION 2
SYMBOLS

a	lift curve slope
a_1	longitudinal rotor tilt, pitch up positive, deg
b	number of rotor blades
b_1	lateral rotor tilt, roll right positive, deg
c	blade chord, ft
c_m	pitching moment coefficient $c_m = \frac{kM_H}{\pi R^3 \rho(\Omega R)^2}$
c_l	rolling moment coefficient $c_l = \frac{kL_H}{\pi R^3 \rho(\Omega R)^2}$
k	ratio of the one-per-rev blade flap bending moment at r = 0 in. to the one-per-rev blade flap bending moment at r = 3.3 in.
l	vertical distance from model pitch and roll pivots to rotor plane, in.
$m_\alpha(\psi)$	nondimensional aerodynamic excitation of blade flapping by rotor angle of attack
$m_{\dot{\alpha}}(\psi)$	nondimensional aerodynamic excitation of blade flapping by rotor pitch rate
$m_{\theta_o}(\psi)$	nondimensional aerodynamic excitation of blade flapping by collective pitch
$m_{\dot{\phi}}(\psi)$	nondimensional aerodynamic excitation of blade flapping by rotor roll rate
r	blade radial station measured from the center of rotation, in.
v	rotor induced velocity, ft/sec
x	nondimensional blade radial station x = r/R
A	feedback control system gain parameter

$C(\psi)$ nondimensional aerodynamic damping of blade flapping

C_T rotor thrust coefficient

$$C_T = \text{THRUST}/\pi R^2 \rho(\Omega R)^2$$

HM total rotor hub moment, in.-lb

$$HM = \sqrt{M_H^2 + L_H^2}$$

$K(\psi)$ nondimensional aerodynamic spring rate of blade flapping

K_θ rotor stiffness, in.-lb/deg

L feedback control system lag parameter

L_H rotor hub roll moment resolved from rotating blade flapping moments measured at r = 3.3 in., roll right positive, in.-lb, L_H is equivalent to L_R (3.3 in.) in References 1 and 2

L_s rotor shaft roll moment, roll right positive, in.-lb

M_β rotating blade flapping moment, in.-lb

$$M_\beta(\psi) = M_{\beta_o} - \sum_{i=1}^{n} \left[M_{\beta_{ic}} \cos(i\psi) + M_{\beta_{is}} \sin(i\psi) \right]$$

M_{β_o} constant component of rotating blade flapping moment, in.-lb

$M_{\beta_{ic}}$ cos $(i\psi)$ harmonics of rotating blade flapping moment, in.-lb

$M_{\beta_{is}}$ sin $(i\psi)$ harmonics of rotating blade flapping, in.-lb

M_H rotor hub pitch moment resolved from rotating blade flapping moments measured at r = 3.3 in., in.-lb, pitch up positive, M_H is equivalent to M_R (3.3 in.) in References 1 and 2

M_s rotor shaft pitch moment, pitch up positive, in.-lb

P nondimensional blade flapping frequency

R rotor blade radius, ft

SM	total rotor shaft moment, in.-lb

$$SM = \sqrt{M_s^2 + L_s^2}$$

α	rotor shaft pitch angle, pitch up positive, deg
β_i	blade flapping angles i = 1, 2, 3, 4, deg
γ	Lock number
θ_c	lateral cyclic pitch, deg
θ_s	longitudinal cyclic pitch, deg
θ_o	collective pitch, deg
μ	advance ratio
σ	rotor solidity, $\sigma = bc/\pi R$
ϕ	rotor shaft roll angle, roll right positive, deg
ω	excitation frequency, rad/sec
Γ	feedback system cyclic control phase angle, deg
Δ	feedback control system phase angle, deg
ψ	rotor azimuth angle, deg
Ω	rotor rotational frequency, rad/sec

SECTION 3

MODEL DESCRIPTION

The versatility of the 7-1/2 foot diameter Lockheed/AMRDL High Advance Ratio Rotor Model has been developed during the course of the High Advance Ratio Research Program. The Phase 1 test article, which is described in detail in Reference 1, was a fixed shaft, direct swashplate controlled hingeless rotor with variable Lock number and natural flapping frequency. This basic configuration was enhanced during the second phase of the research program by the addition of an automatic hub moment feedback control system with variable gain, time constant and phasing capabilities. The bandwidths of the remotely controlled collective and cyclic pitch hydraulic actuators were also extended to permit meaningful frequency response testing. A description of the Phase 2 model can be found in Reference 2.

During the Phase 3 effort the capabilities of the rotor model were further expanded in two ways. First, the rotor hub flapping stiffness was reduced by fabricating a very soft set of flapping flexures (hereafter referred to as the 'supersoft' flexures). These flexures are characterized by a flapwise EI of 11.5×10^3 lb-in.^{2} and a chordwise EI of 1.97×10^6 lb-in.^{2} over the radial expanse r = 1.74 in. $\rightarrow$ 4.55 in. Two specimens were fatigue tested, each to more than one million cycles, without failure, in order to establish a safe rotor moment endurance limit.

The analytically determined natural frequencies of the rotor blade with the 'supersoft' flexure and no tip weight are presented as a function of rotor speed in Figure 1. Shake test results of this blade configuration are also plotted on the figure. Very good agreement is noted.

For purposes of identification, the rotor equipped with the 'supersoft' flexures and no tip weight ($\gamma \simeq 5.0$) is designated configuration 5. The other rotor tested during the Phase 3 program was configuration 1 which has heretofore

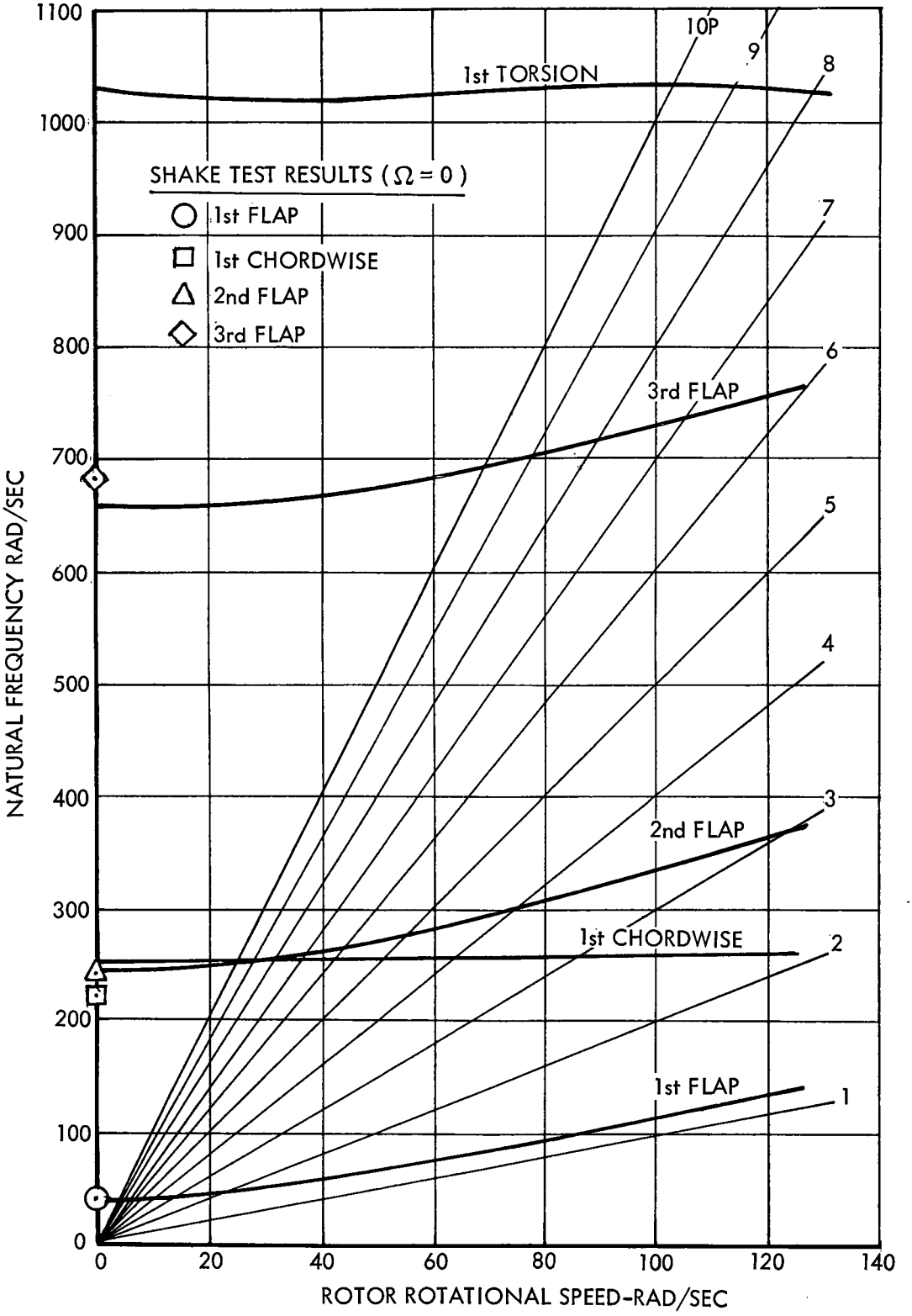

Figure 1. Coupled Blade Natural Frequencies, Configuration 5

(Reference 1) been defined as the rotor equipped with the 'soft' flexure and no tip weight. 'Soft' is characterized by stiffness values of

$$EI_{flap} = 46.5\ (10^3)\ \text{lb-in.}^2$$

$$EI_{chord} = 2.24\ (10^6)\ \text{lb-in.}^2$$

from $r = 1.74$ in. $\rightarrow 4.55$ in.

The second modification to the model consisted of installing remotely operated hydraulic actuators which controlled the rotor shaft pitch and roll positions. The break frequencies of the actuators were never reached during the test which included maximum shaft oscillation frequencies of 10 Hz in pitch and 14 Hz in roll. Thus it is known that the servo bandwidths exceed these values at the least.

The mechanization of shaft angular motion required that the model be pitched and rolled about pivots which were located 11.25 in. below the plane of the rotor. Thus an angular variation of the shaft generated linear translation of the rotor hub as well as the angular motion.

The physical characteristics of the model are summarized in Table I.

TABLE I

LOCKHEED/AMRDL HIGH ADVANCE RATIO ROTOR MODEL CHARACTERISTICS

Number of Blades:	4
Radius:	45 in.
Chord:	4.5 in.
Solidity:	0.127
Airfoil Section:	NACA 0012
Blade Twist:	0 deg
Blade Precone:	0 deg
Lock Number ($a = 2\pi$):	5.0, 3.0 (with tip weight)
First Flap Mode Natural Frequency:	Variable; tested range $1.125\Omega \rightarrow 2.32\Omega$
Blade Radially Distributed Mass and Stiffness Properties:	See Section 3 of Reference 1
Rotor Control System:	Direct swashplate or Electronic hub moment feedback
Features of Hub Moment Feedback Control System:	1st order lag filters Variable gain Variable time constant Variable control and feedback phasing
Drive System:	Two 37 HP variable frequency induction motors
Additional Model Features:	Resolved hub moments θ_o, θ_s, θ_c, α and ϕ frequency response capability Distance from model pitch and roll pivots to rotor plane = 11.25 in.

SECTION 4

DATA ACQUISITION SYSTEM

INSTRUMENTATION

The Phase 3 rotor model instrumentation consisted of all those sensors which had been installed for previous tests plus:

- a rotor shaft bending strain gage bridge aligned with blades 1 and 3 (ψ = 0° and 180°) and located 2 inches below the plane of the rotor and
- a linear position potentiometer which measured the model roll actuator ram position and thus the rotor shaft roll angle.

DATA RECORDING EQUIPMENT

The equipment utilized to record data for off-line analysis consisted of the following:

- AMRDL DATEX System
- Honeywell Medium Band Analog Tape Recorder
- Honeywell Viscorder (direct-write oscillograph)

A description of each of these devices can be found in Section 4 of Reference 1.

In order to maximize the visibility of the data while the test was in progress, a transfer function analyzer was used to determine rotor hub moment frequency response with respect to a selected excitation (i.e., θ_o, θ_s, θ_c, α, ϕ). X-Y-Y plotters were driven with the analyzer gain and phase signals. Thus hub pitching and rolling moment transfer functions were immediately available in a graphical form. These on-line data greatly enhanced the selection of excitation frequencies, especially at near resonance conditions.

Table II summarizes the Phase 3 data acquisition system.

TABLE II

SUMMARY OF THE PHASE 3 HIGH ADVANCE RATIO ROTOR MODEL DATA ACQUISITION SYSTEM

DATUM	INSTRUMENTATION	DATA ACQUISITION EQUIPMENT
Flap Bending Moment at Sta 22.3	Flap Bending Strain Gage at Sta 22.3	V, T+
Flap Bending Moment at Sta 13.15	Flap Bending Strain Gage at Sta 13.15	V, T+
Flap Bending Moment at Sta 3.3	Flap Bending Strain Gage at Sta 3.3	V, T
Flap Bending Moment at Sta 2.4	Flap Bending Strain Gage at Sta 2.4	*
Rotating Shaft Bending Moment	Strain Gage at $\psi = 0°$ 2 in. below rotor plane	V, T
Resolved Rotor Hub Pitching and Rolling Moments at Sta 3.3	4-Flap Bending Strain Gages at Sta 3.3	V, T, D
Chord Bending Moment at Sta 13.15	Chord Bending Strain Gage at Sta 13.15	*
Chord Bending Moment at Sta 2.4	Chord Bending Strain Gage at Sta 2.4	V, T
Blade Torsion Moment at Sta 9.28	Torsion Gage at Sta 9.28	V, T+
Pitch Link Tension/Compression Load	Pitch Link Tension/Compression Strain Gage	V, T+
Instantaneous Pitch Angle of Blade No. 1	Blade Feathering Position Potentiometer (Pot.)	V, T
Body Moments and Forces	Body Mounted Strain Gage Balance	D (LIFT ON T+)
Applied Longitudinal Cyclic Pitch (θ_s)	Longitudinal Cyclic Pitch Actuator Position Pot.	V, T, D
Applied Lateral Cyclic Pitch (θ_c)	Lateral Cyclic Pitch Actuator Position Pot.	V, T, D
Applied Collective Pitch (θ_o)	Collective Pitch Actuator Position Pot.	V, T, D
Rotor Shaft Pitch Angle (α)	Model Pitch Actuator Linear Position Pot.	V, T, D
Rotor Shaft Roll Angle (ϕ)	Model Roll Actuator Linear Position Pot.	V, T, D
Longitudinal Control Input (θ_{long})	Longitudinal Control Input Pot.	V, D
Lateral Control Input (θ_{lat})	Lateral Control Input Pot.	V, D
Pitch Feedback Control Signal (δ_s)	Direct - Voltage Measurement	V, D
Roll Feedback Control Signal (δ_c)	Direct - Voltage Measurement	V, D
Fore - Aft Model Acceleration	Accelerometer	V
Oscillator Output	Direct - Voltage Measurement	V, T
Rotor Rotational Speed	One-Per-Rev Magnetic Pickup	V, T, D
Body Moments and Forces	Wind Tunnel Balance	D
Tunnel Dynamic Pressure	Wind Tunnel Pitot Static Probe	D
Tunnel Temperature	Wind Tunnel Temperature Probe	D

V = Visicorder (Oscillograph), T = Analog Tape, D = Datex

* Datum not recorded because slip rings unavailable.

\+ Recorded on tape only during steady state tests.

SECTION 5

TEST PROGRAM

The test program was conducted at the facilities of the Ames Directorate of the U. S. Army Air Mobility Research and Development Laboratory (AMRDL) at Moffett Field, California. One week of whirl testing (February 23 - 29, 1972) was performed in the AMRDL Model Preparation Area following a thorough functional check of the model and data acquisition system. The wind tunnel tests spanned four consecutive weeks beginning on March 20, 1972 and were conducted in the AMRDL 7 x 10 foot wind tunnel. For a description of the tunnel, including the installation of the 7-1/2 foot diameter High Advance Ratio Rotor Model, the reader is referred to Pages 33 - 36 of Reference 1.

Three types of tests were required to fulfill the objectives of the research program. They were:

- open loop steady state response tests wherein steady collective pitch (θ_o) cyclic pitch (θ_s and θ_c) and rotor shaft angle of attack (α) excitations were applied to the rotor;
- open loop frequency response tests where sinusoidally varying θ_o, θ_s, θ_c, α and rotor shaft roll (ϕ) excitations were applied to the rotor;
- and closed loop frequency response tests with sinusoidally varying α and ϕ excitations.

The open loop steady state response tests and the frequency response tests with θ_o, θ_s and θ_c excitations were performed on configuration 5 ('supersoft' flexure without tip weight) only. The aim was to obtain experimental rotor response data at combinations of nondimensional flapping frequency (P) and advance ratio (μ) not previously tested. Frequency response tests with α and ϕ excitations were conducted with both configurations 1 and 5 since this type of testing was initiated during this phase of the research program. Closed loop frequency response tests with α and ϕ excitations were meant to compliment similar closed loop Phase 2 data with swashplate excitations (θ_o, θ_s, and θ_c) and thus only configuration 1 was considered.

Since exactly the same types of tests were performed during the whirl and wind tunnel activities, it is possible to summarize the total test program in one table (Table III). The summary contains the rotor configurations and conditions tested for each of the three types of tests as well as the data acquired.

DISCUSSION OF TEST RESULTS

As has been the case with previous phases of this research program, the test activity was quite successful and resulted in a large amount of experimental data. With the exception of rotor frequency response with respect to α and ϕ, the results are essentially the same as those obtained during the Phase 1 and Phase 2 programs. Improvements in test techniques and data analysis methods indicated by the previous experience and the addition of a shaft bending moment measurement have changed the type of data and the presentation slightly.

In the following discussion, the results from the three types of tests will be presented separately. In the interest of brevity, the details regarding the test procedures and data analysis methods which are common to the Phase 1 and Phase 2 programs will be referenced wherever possible. Emphasis will be placed on those tests and results which were initiated during the current phase of the program.

Open Loop Steady State Tests

These tests consisted of exciting the rotor with steady θ_o, θ_s, θ_c and α excitations at various rotor rotational speeds and forward velocities. Each of the four excitations was applied independently at several magnitudes in order to obtain data from which linear rotor shaft, hub flapping and blade flapping moment derivatives and lift derivatives could be determined. All of the rotor moment response data for the steady state tests were determined by a harmonic analysis (over 40 rotor cycles) of digitized analog signals. The collective pitch, cyclic pitch and angle of attack angles were measured by linear potentiometers, the outputs of which were recorded with a steady data sampling system.

TABLE III

HIGH ADVANCE RATIO RESEARCH PROGRAM PHASE 3 TEST CONDITIONS

Type of Test	Config	γ	RPM	μ	P	Excitations	Excitation Frequencies	Data Acquired
Open Loop Steady State Response	5	5	1000	0	1.125	θ_o, θ_s	0	Steady rotor shaft and hub moments and lift. Radially distributed blade flap bending moments
			850	0 0.27 0.36 0.51 0.60 0.72 0.75 0.81	1.15	$\theta_o, \theta_s, \theta_c, \alpha$		
			550	0 0.41 0.56 0.79 0.92	1.28	$\theta_o, \theta_s, \theta_c, \alpha$		
Open Loop Frequency Response	5	5	850	0 0.27 0.36 0.51 0.60	1.15	$\theta_o, \theta_s^s, \theta_c$	0 → 32 Hz	Rotor transfer functions
				0 0.27 0.36 0.51 0.60	1.15	α, ϕ	0 → 14 Hz	
			550	0 0.41 0.79 0.92	1.28	$\theta_o, \theta_s^s, \theta_c$	0 → 32 Hz	
				0	1.28	α, ϕ	0 → 10 Hz	
	1	5	800	0 0.28 0.38 0.54 0.64	1.33	α, ϕ	0 → 14 Hz	
			550	0 0.41 0.56 0.78 0.93	1.56	α, ϕ	0 → 14 Hz	
Closed Loop Frequency Response*	1	5	800	0 0.28	1.33	α^ϕ	0 → 10 Hz	Closed loop transfer functions

* Closed Loop Control System Configuration (A = 0.5, L = 0, Δ = 0 deg)

The steady state whirl test ($\mu = 0$) results indicate that the induced inflow has both a linear and a non-linear effect on the rotor response. The variation of rotor thrust with collective pitch at $\mu = 0$ clearly demonstrates the non-linear influence. For example, experimental rotor thrust versus collective pitch for configuration 5 at three rotor speeds is presented in Figure 2. At low thrust levels the reduction in the effective blade angle of attack due to the inflow is very non-linear, generating a corresponding non-linear thrust-θ_o relationship. At higher thrust levels the inflow tends to be approximately linear. This inflow characteristic is easily understood from simple momentum theory from which it can be shown that for $\mu = 0$

$$\frac{v}{\Omega R} = \sqrt{\frac{C_T}{2}} \qquad (1)$$

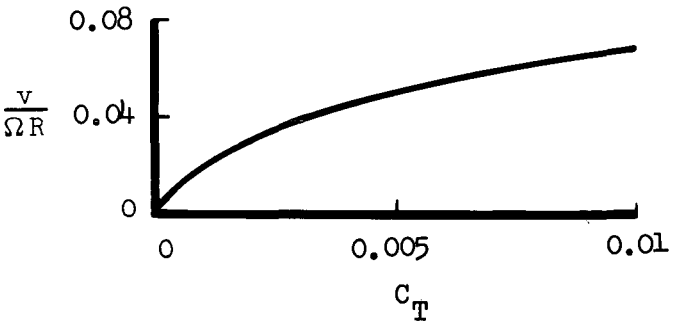

A similar non-linear characteristic at low thrust levels can also be seen in Figure 3 where the rotor hub pitching (M_H) and rolling (L_H) moments due to longitudinal cyclic pitch (θ_s) are plotted for three thrust levels at $\mu = 0$ and a rotor speed of 550 rpm. These data also demonstrate the effect that the inflow has upon the linear rotor moment response; namely a reduction in the magnitude of the derivative.

In the current presentation the resolved rotor hub moments are designated M_H and L_H. In previous related documentation (References 1 and 2) M_H was symbolized as M_R (3.3 in.) and L_H as L_R (3.3 in.).

The swashplate of the model was designed to permit independent excitation of longitudinal and lateral cyclic pitch. In order to demonstrate that this was in fact the case, the rotor was excited with θ_c at $\mu = 0$. Figure 4 shows the rotor response which was generated. A comparison of the moments (with

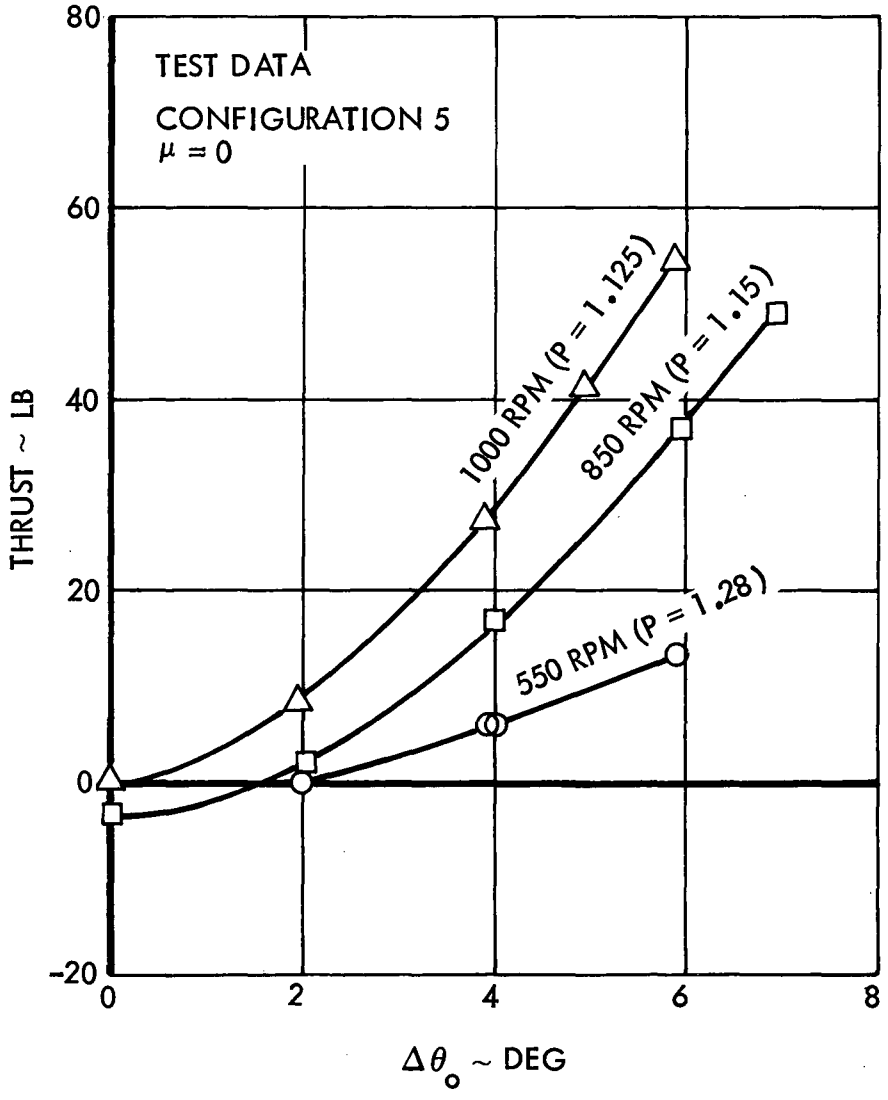

Figure 2. Rotor Thrust Versus Collective Pitch at μ = 0, Configuration 5

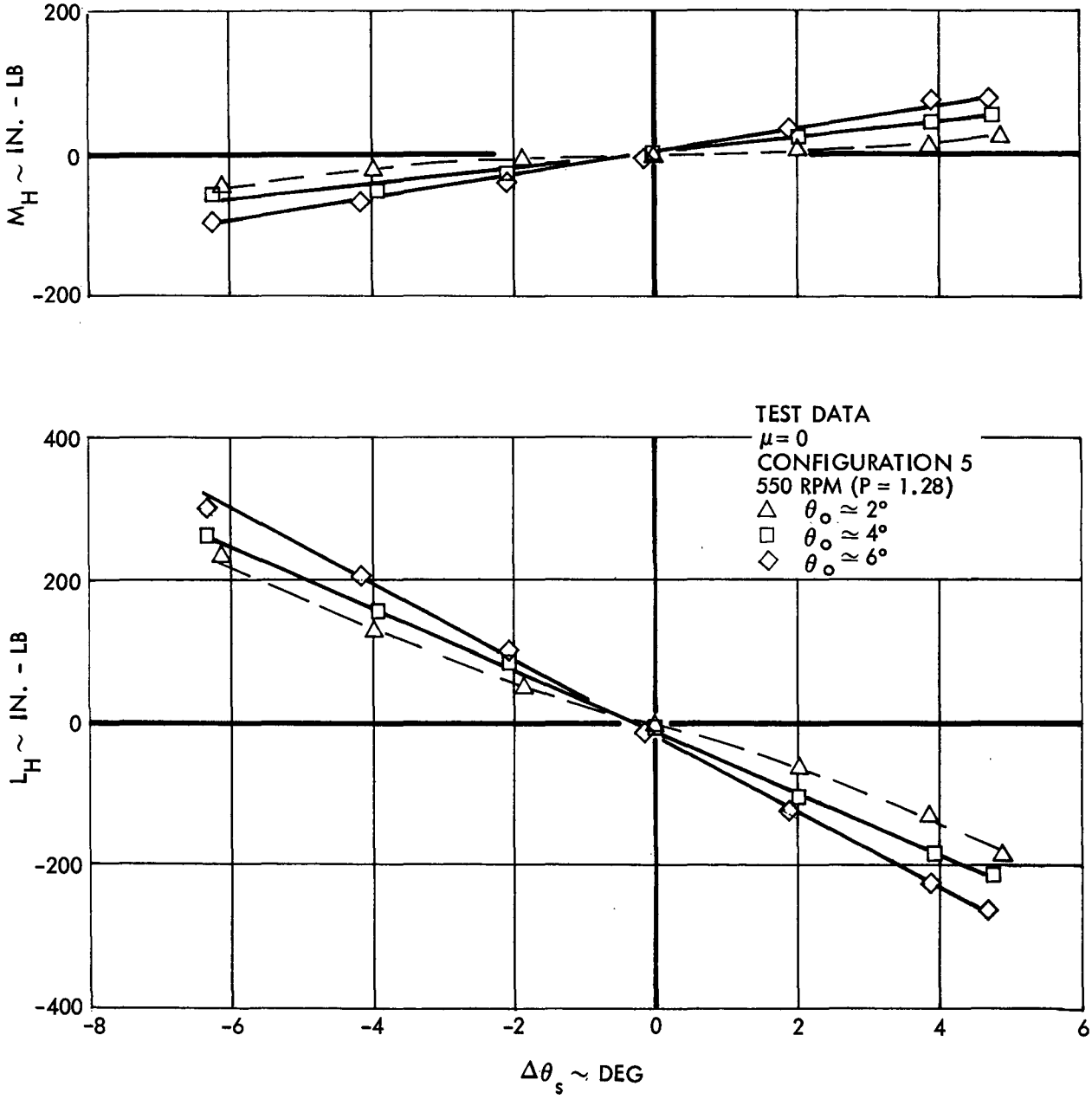

Figure 3. Rotor Hub Moment Response to Longitudinal Cyclic Pitch, $\mu = 0$, Configuration 5, 550 RPM (P = 1.28)

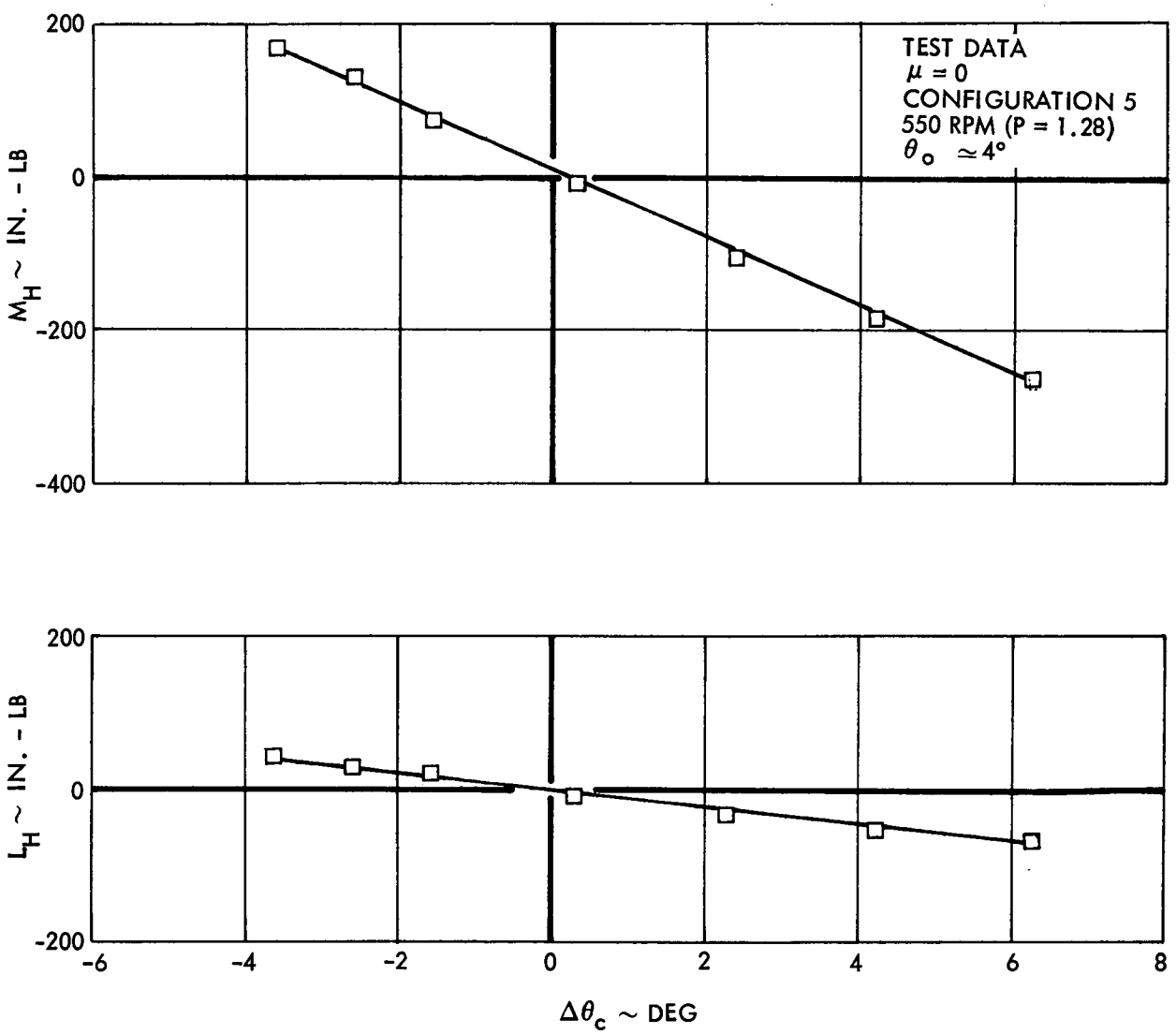

Figure 4. Rotor Hub Moment Response to Lateral Cyclic Pitch, $\mu = 0$, Configuration 5, 550 RPM (P = 1.28)

$\theta_o = 4°$) in Figures 3 and 4 confirms the symmetry of the open loop cyclic controls.

The rotor response to θ_s at 850 rpm (first flap mode frequency P = 1.15) is shown in Figure 5 and the response at 1,000 rpm (P = 1.125) in Figure 6. The characteristics of the curves are generally the same as those previously discussed.

Figure 7 presents a summary of the linear hub moment response to longitudinal cyclic pitch for $\mu = 0$. The results are presented in terms of the total hub moment derivative

$$\text{HUB MOMENT (HM)} = \sqrt{M_H^2 + L_H^2} \tag{2}$$

and its phase angle of response measured from $\psi = 0°$

$$\text{PHASE} = \text{ARCTAN}\left(-L_H/-M_H\right) \tag{3}$$

plotted versus rotor rotational speed. Noteworthy characteristics include anticipated increases in the magnitude and phase angle of response with decreasing flap frequency (P) and the larger magnitude of response at the higher rotor thrust level. The ratio of the steady hub moment derivative to the steady shaft moment (SM) derivative is also shown in Figure 7. The shaft moment data will be thoroughly discussed later in this section. Suffice it for now to note the reduction in the ratio of hub moment to shaft moment with increased rotor speed.

The individual hub and shaft moment derivatives used to generate the data in Figure 7, i.e.,

$$\frac{\partial M_H}{\partial \theta_s}, \frac{\partial L_H}{\partial \theta_s}, \frac{\partial M_s}{\partial \theta_s}, \frac{\partial L_s}{\partial \theta_s} \tag{4}$$

were determined using a linear least squares curve fit. All of the steady state data at $\mu = 0$ are tabulated in Appendix A. The derivatives from the least squares curve fit and the deviation of each individual data point from the statistical line are also listed.

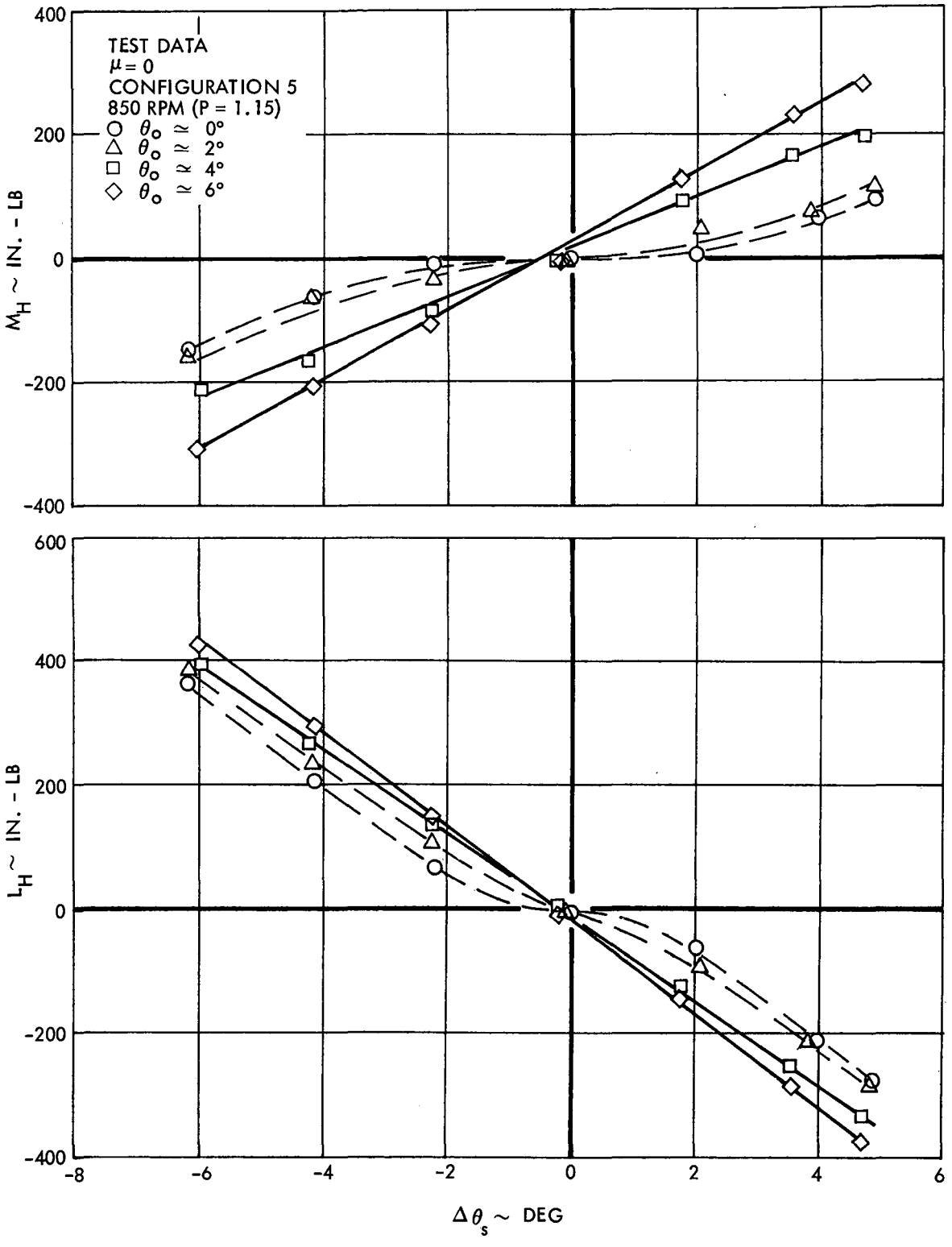

Figure 5. Rotor Hub Moment Response to θ_s, μ = 0, Configuration 5, 850 RPM (P = 1.15)

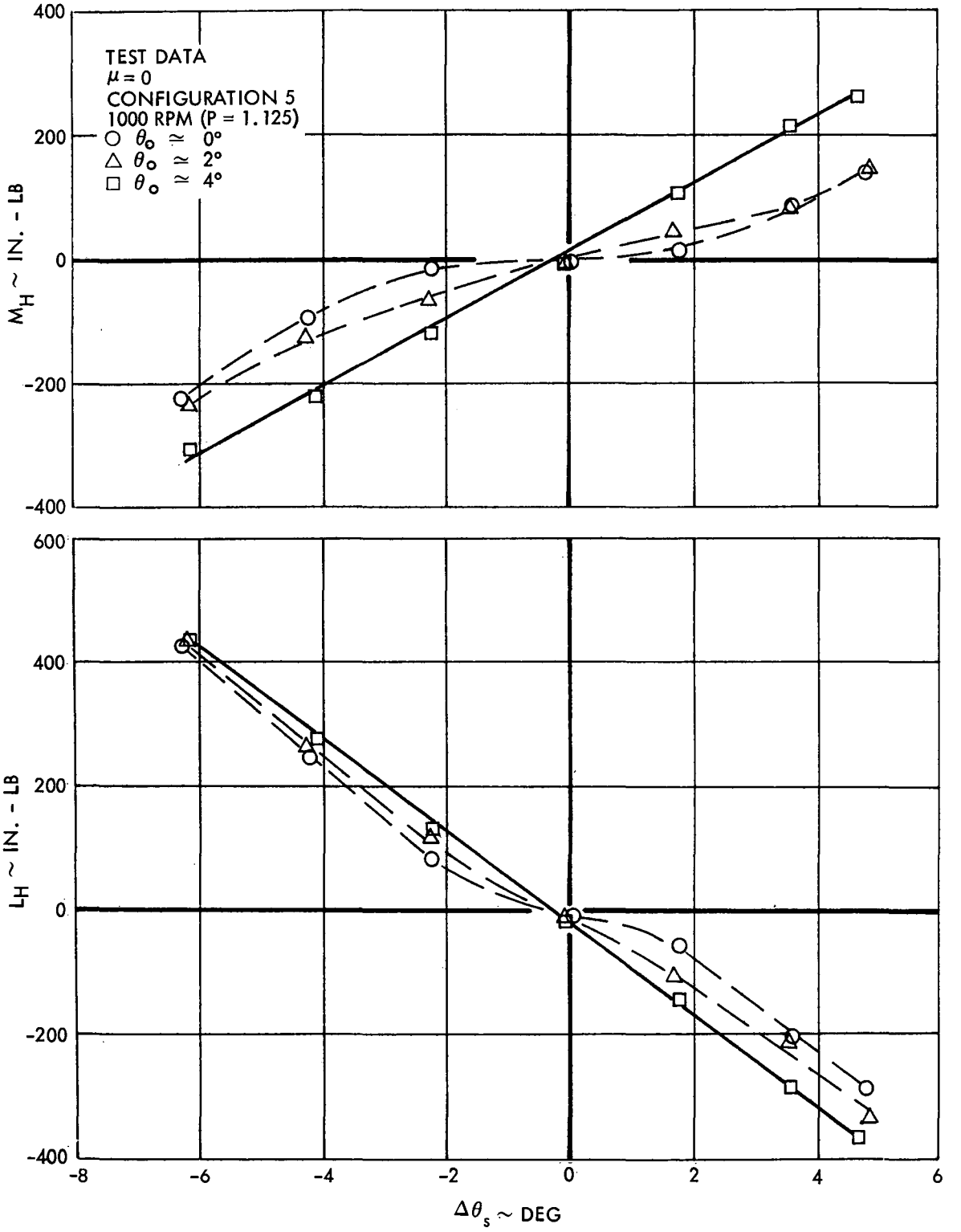

Figure 6. Rotor Hub Moment Response to θ_s, μ = 0, Configuration 5, 1000 RPM (P = 1.125)

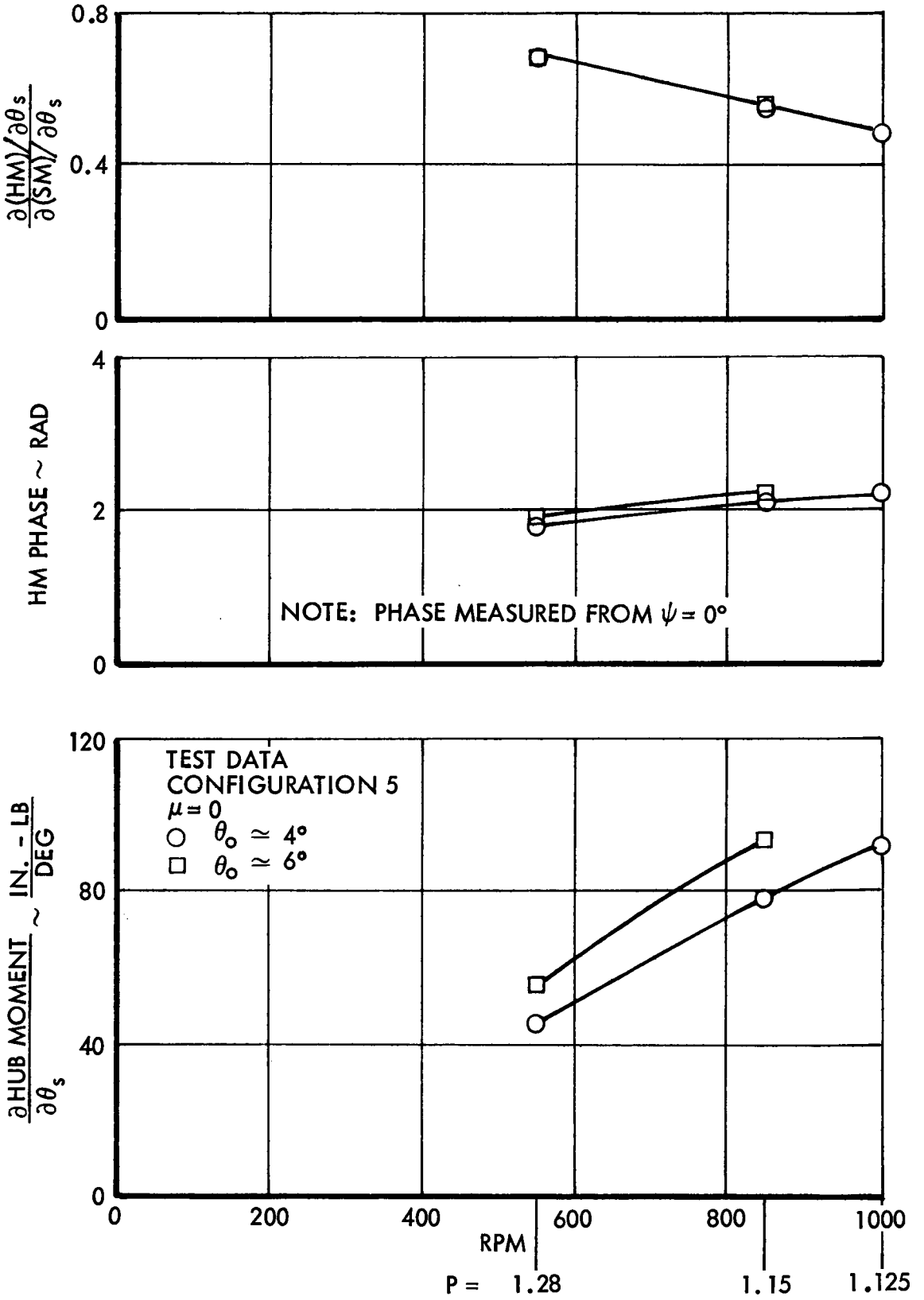

Figure 7. Linear Rotor Hub and Shaft Moment Derivatives with Respect to θ_s for $\mu = 0$

Forward flight data were acquired at rotor speeds of 550 and 850 rpm. The test procedure was the same as that used during the Phase 1 test (Reference 1). Briefly this means that the rotor was disturbed from a trim state with either a θ_o, θ_s, θ_c or an α excitation. Each excitation was applied independently at several magnitudes. The rotor was nominally unloaded and the aerodynamic environment was linear (low tip Mach number and blade angles below stall values).

An example of the quality (and linearity) of the data is shown in Figure 8. The measured rotor hub pitching and rolling moments are plotted versus collective pitch for a rotor rotational speed of 550 rpm and advance ratios ranging from 0.41 to 0.92. The data manifest very little scatter and the slopes of the curves are very definitely linear. The expected increase in the magnitude of the response with increased μ is noted.

As indicated previously, the rotor shaft moment was measured during the Phase 3 test program (it was not measured during the Phase 1 and Phase 2 tests). A rotating signal aligned with blades 1 and 3 (ψ = 0° and 180°) was recorded on tape and harmonically analyzed at 1Ω to determine the steady pitching (M_s) and rolling (L_s) components of the total shaft moment. An example of these data for the conditions shown in the previous figure are shown in Figure 9. It can be seen that the linearity of the shaft moment data and the hub moment data are approximately the same.

Despite the consistency between shaft and hub moment results indicated by Figure 8 and 9 it is important to recognize several sources of inexactness in the shaft moment data. First, the accuracy of the calculation of the harmonic components M_s and L_s depends upon the accuracy of the rotor frequency, Ω. As demonstrated in Appendix A of Reference 2, very small errors in frequency can generate significant errors in the magnitude and phase of the harmonic components. The most likely source of error in Ω is caused by slight variations in the rotor speed during the test. The analytical procedure for calculating Ω from the experimental data (i.e. counting rpm blips) can also introduce slight errors. It is noted that an imprecise value of Ω does not affect the values of M_H and L_H because they are resolved signals and therefore the steady component of the harmonic analyses. It is further noted that M_H

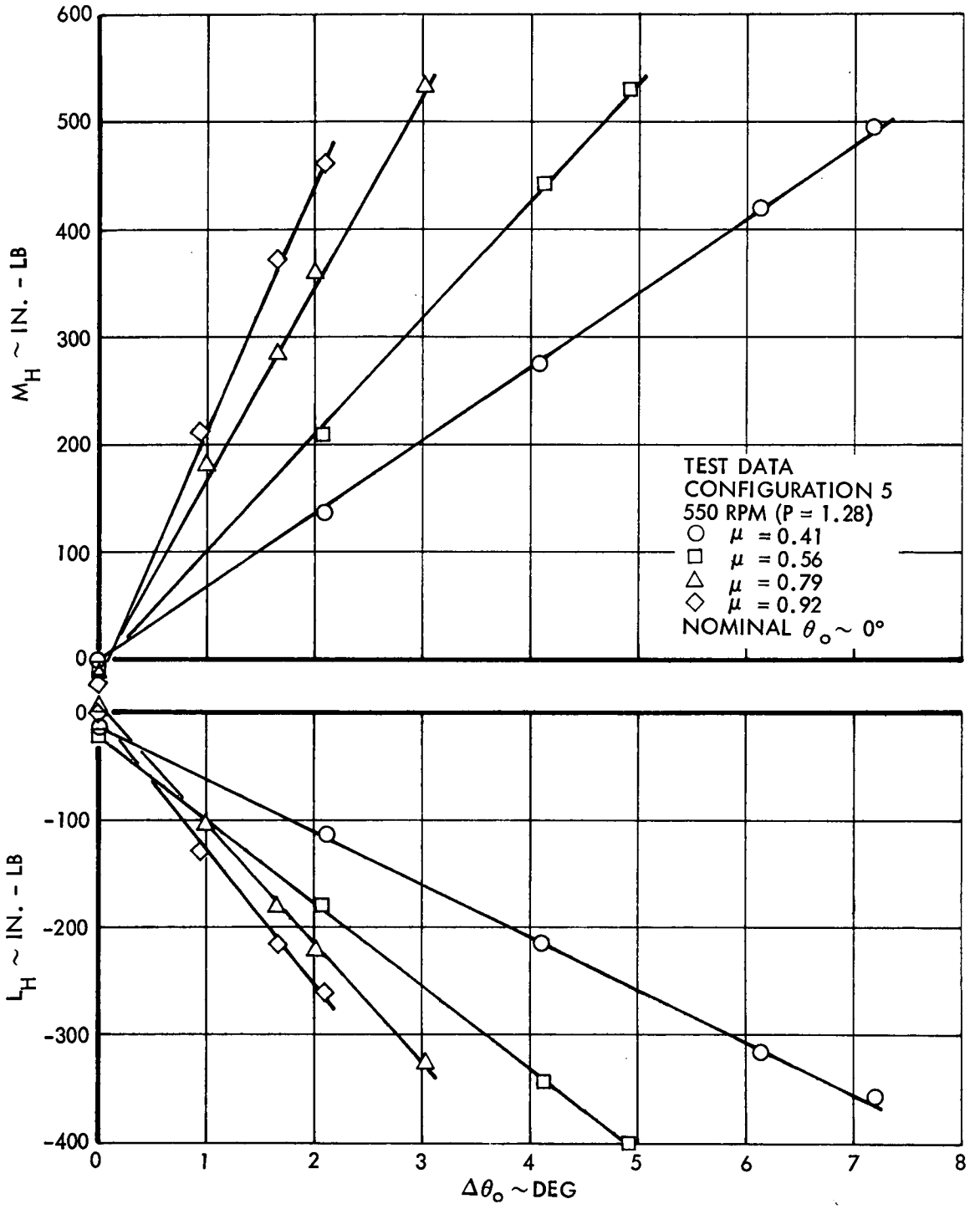

Figure 8. Rotor Hub Moment Response to Collective Pitch, Configuration 5, 550 RPM (P = 1.28)

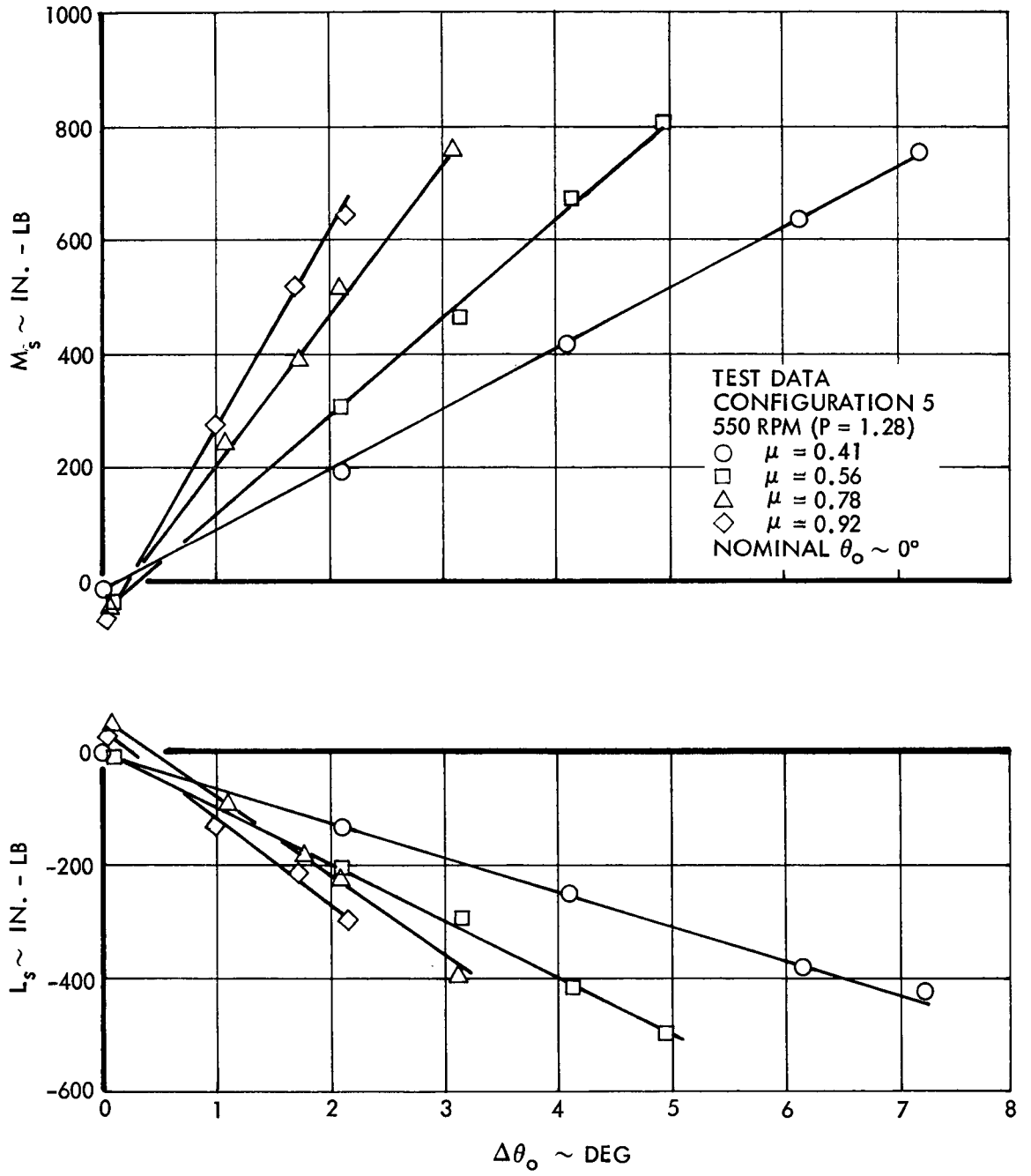

Figure 9. Rotor Shaft Moment Response to Collective Pitch, Configuration 5, 550 RPM (P = 1.28)

and L_H are calculated from the response of all four blades, whereas M_s and L_s are influenced by only blades 1 and 3.

Two other factors which influence shaft moments are the shear loads at the center of rotation due to inplane loading and the tilt of the thrust vector. These do not affect the hub flap moments. They do, however, contribute to the measured shaft moment because the shaft bending strain gage is located approximately two inches below the plane of the rotor, viz,

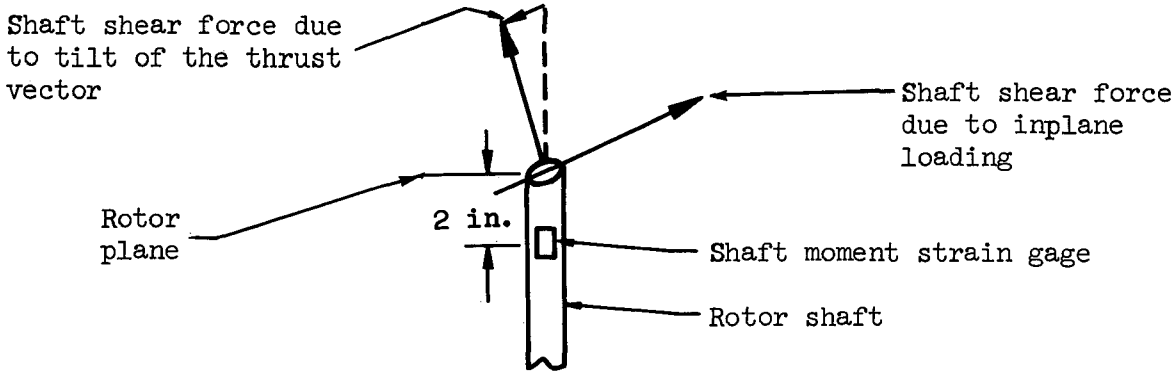

Although each of these three effects are minor,

- maximum error in Ω $\sim 0.2\%$
- maximum shaft moment due to inplane shear forces $\sim$10 in.-lb
- maximum shaft moment due to tilt of thrust vector $\sim$20 in.-lb

they do introduce scatter into the shaft moment results. This will be evident in the following presentation of data.

All of the steady state rotor moment response data are conveniently summarized in subsequent curves as total moment derivatives and their phase angles of response (measured relative to $\psi = 0°$).

$$\text{PHASE ANGLE} = \text{ARCTAN} \left(\frac{-L}{-H}\right) \qquad (5)$$

The derivatives are calculated using a linear least squares curve fit. The data used in their determination plus the calculated values of the shaft and hub moment derivatives and the deviation of each datum from the satistical curves are tabulated in Appendix A.

The rotor response to collective pitch is shown in Figure 10 for the two tested rotor speeds, 550 rpm and 850 rpm, which correspond to blade first flap mode natural frequencies of 1.28Ω and 1.15Ω. The total hub moment derivative, its phase angle of response and the ratio of the magnitudes of hub moment and shaft moment derivatives are plotted versus advance ratio. Shaft moment phase is approximately the same as hub moment phase and thus is not shown. The characteristics of the curves are similar to previous experimental results (References 1 and 2). That is, the magnitude of the response derivative increases with increased advance ratio and decreased flap frequency. Noteworthy also is the nearly constant phase angle of response over the tested advance ratio range for both rotor speeds. As discussed earlier in this section, the shaft moment data are subject to contamination by shear loads and rpm variations which accounts for the scatter in the

$$\frac{\partial HM/\partial\theta_o}{\partial SM/\partial\theta_o} \tag{6}$$

curves.

The results of the steady state tests with longitudinal and lateral cyclic pitch excitations are shown in Figures 11 and 12.

There was one steady state test condition which yielded a non-linear rotor moment response. It was with configuration 5 at 550 rpm and $\mu = 0.41$ with an α-excitation. The data are plotted in Figure 13. This non-linear behavior suggests that induced inflow is still an important consideration even at advance ratios as high as $\mu = 0.40$.

The test results with steady state angle of attack variations are presented in Figure 14. A change in sign of the hub roll moment derivative at $\mu = 0.27$ (850 rpm) is indicated by the phase angle of response varying from less than to greater than π radians. This characteristic was also observed during high

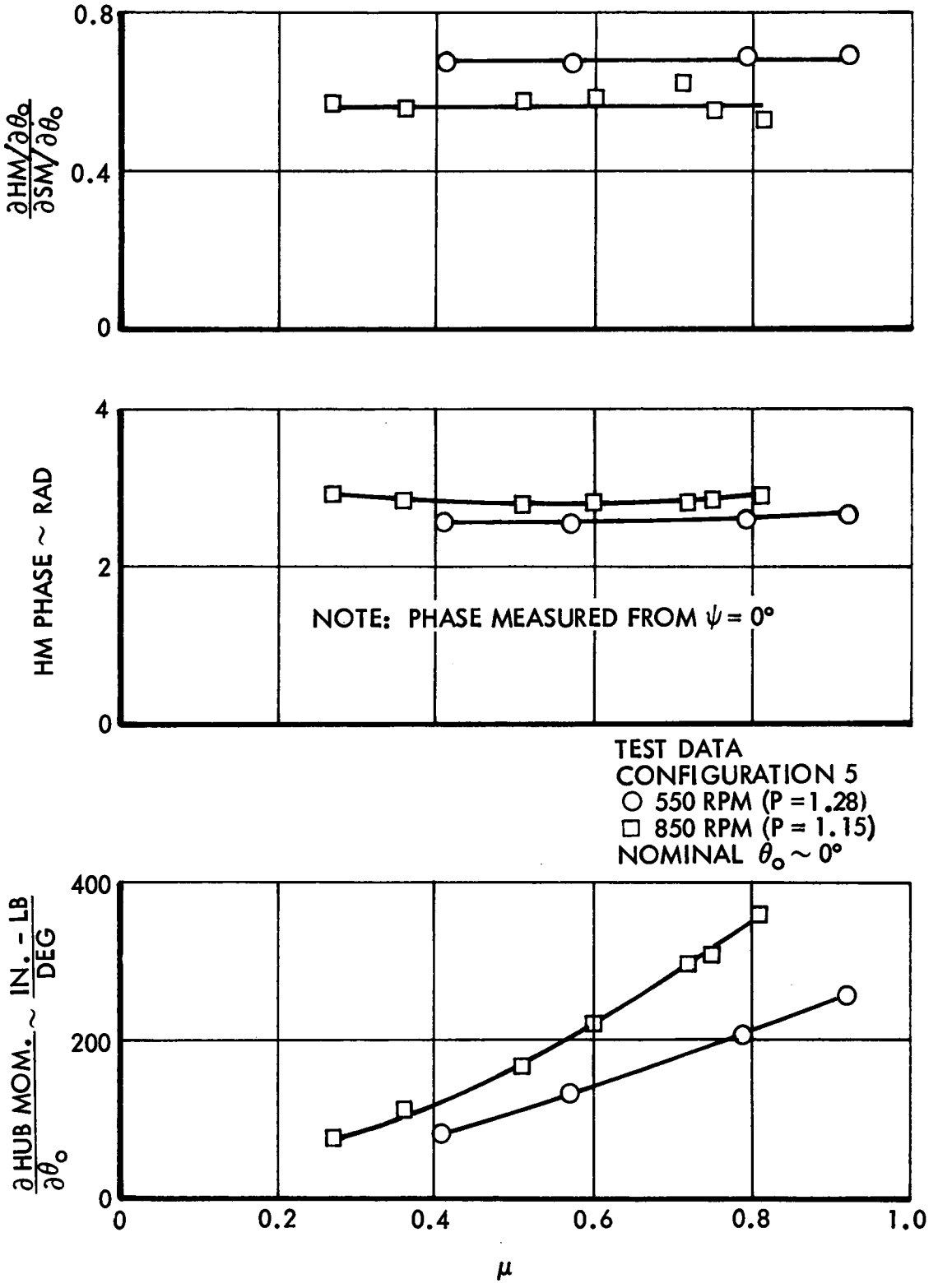

Figure 10. Rotor Hub and Shaft Moment Derivatives with Respect to θ_o, Configuration 5

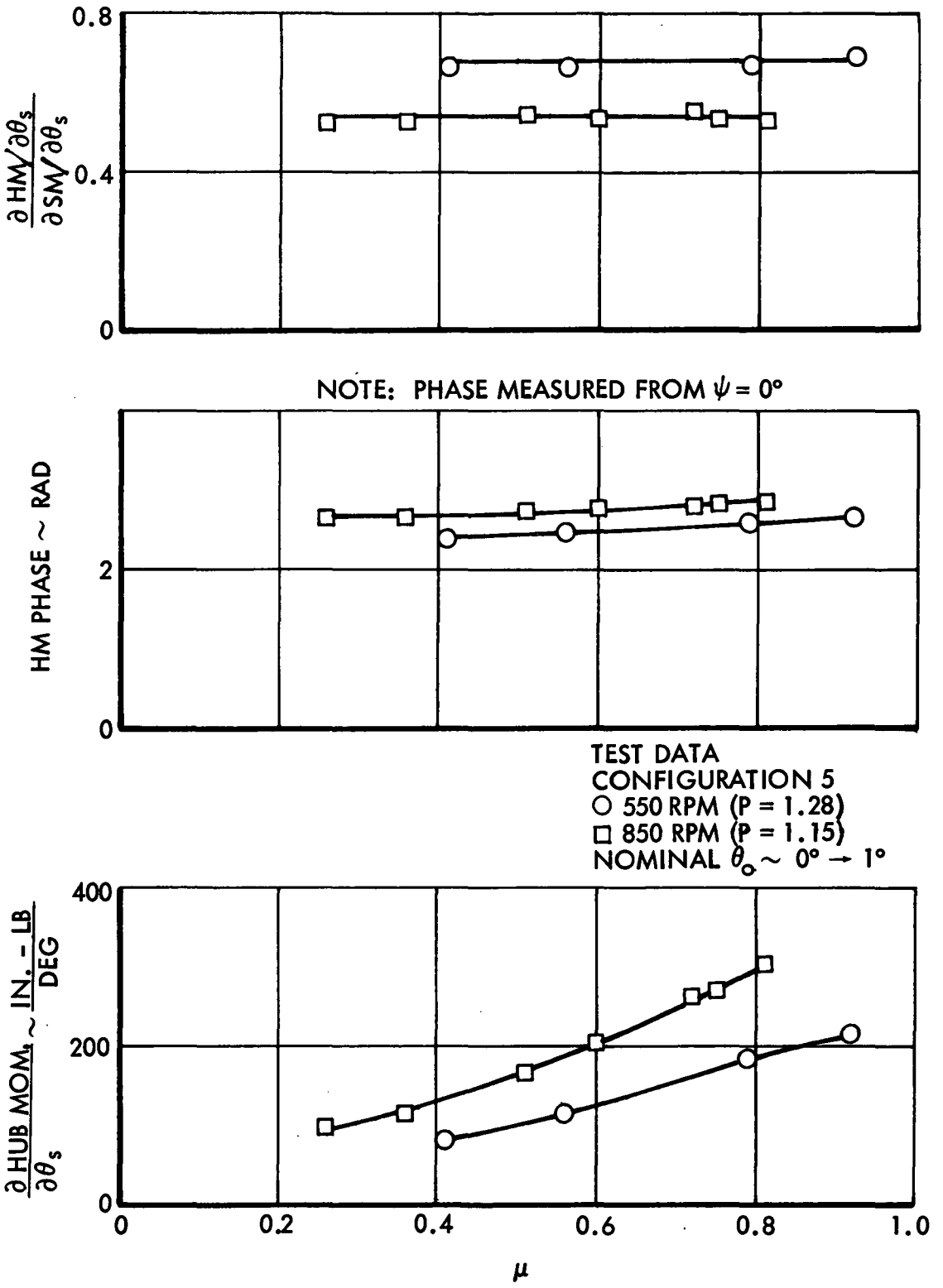

Figure 11. Rotor Hub and Shaft Moment Derivatives with Respect to θ_s, Configuration 5

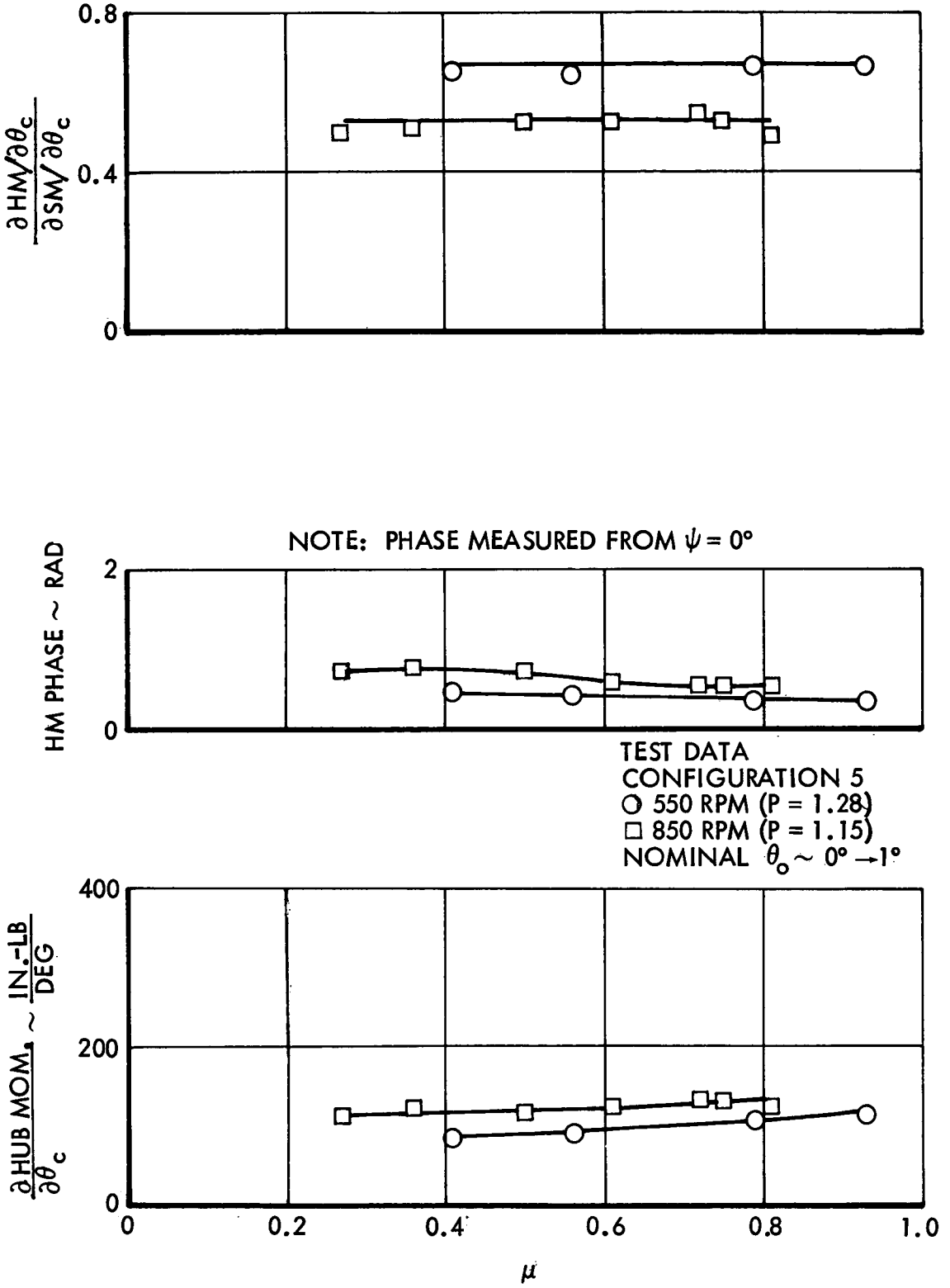

Figure 12. Rotor Hub and Shaft Moment Derivatives with Respect to θ_c, Configuration 5

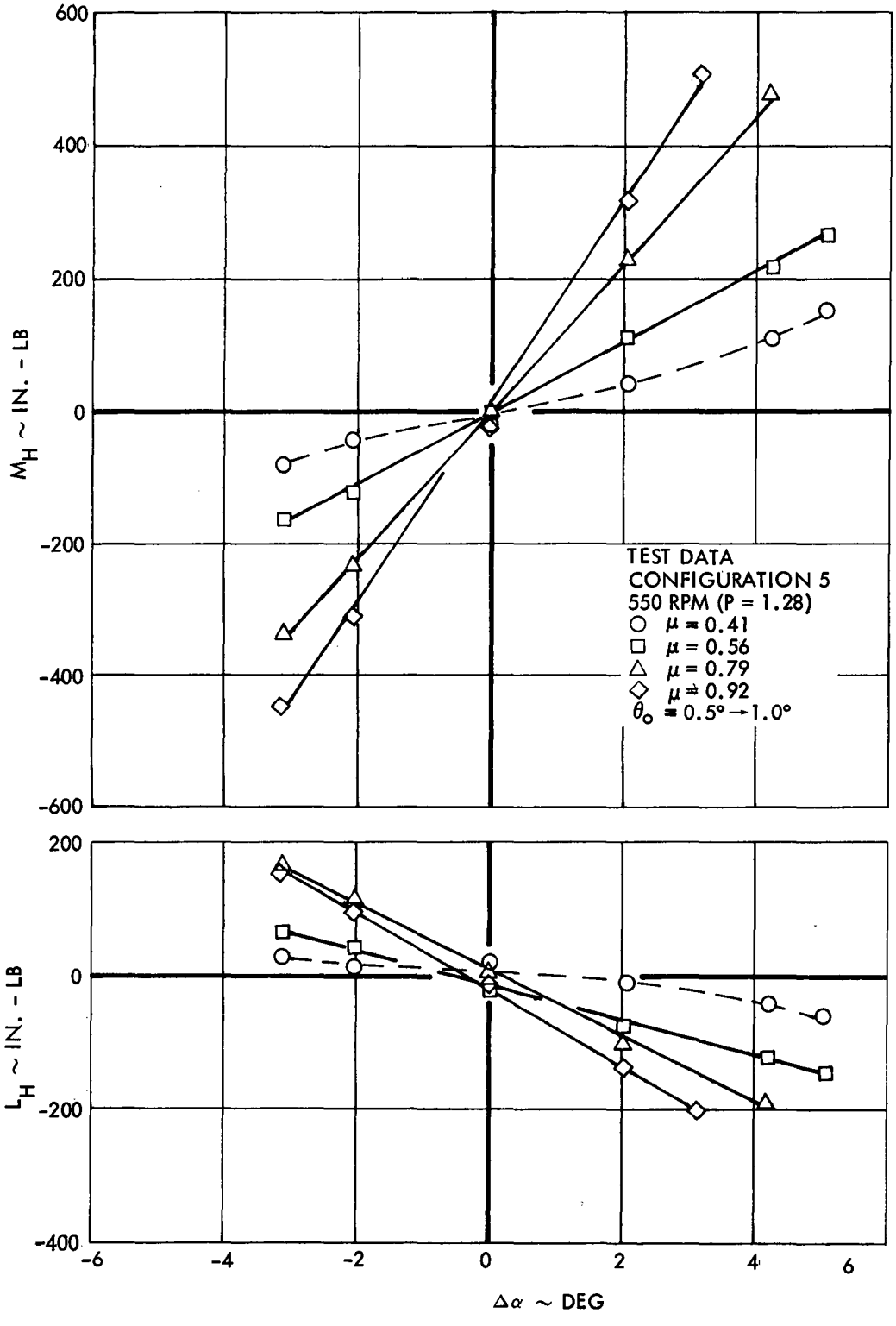

Figure 13. Rotor Hub Moment Response to α, Configuration 5, 550 RPM (P = 1.28)

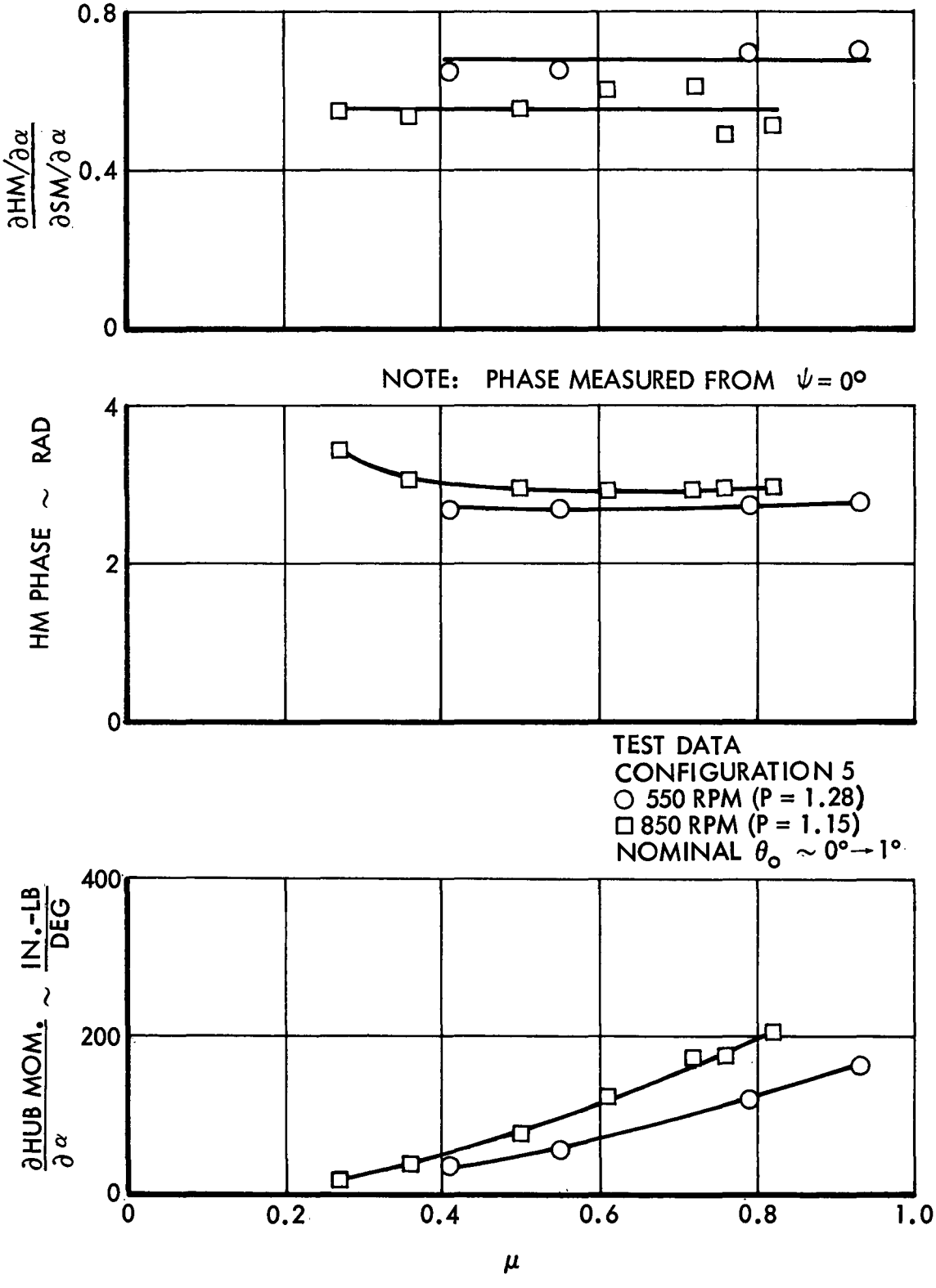

Figure 14. Rotor Hub and Shaft Moment Response Derivatives with Respect to α, Configuration 5

rpm (P = 1.17) steady state α-tests of configuration 1 (Reference 2), and is thought to be caused by induced inflow.

The rotor lift which was generated during the application of θ_o, θ_s, θ_c and α disturbances is summarized in Figure 15. The lift is expressed in terms of blade loading coefficient (C_T/σ) derivatives versus advance ratio. The slight negative lift generated by lateral cyclic pitch at high advance ratios was not previously discovered experimentally. It is probable that it would have been if a least squares linear curve fit of the test data had been used rather than a hand faired curve fit. It is noted that a simple theoretical model incorporating a two mode approximation for blade flapping and periodic aerodynamic spring, damping and excitation functions also predicts this characteristic. All of the lift data from which these derivatives were calculated are listed in Appendix A, as are the deviations of each data point from the curve fit line.

The harmonic content of a single blade flapping moment has also been extracted from the steady state test data. The digitized analog output of a flap strain gage located at 3.3 inches from the center of rotation of blade 1 has been Fourier analyzed at harmonic frequencies up to 4Ω. Typical results of this analysis are shown in Figure 16, where the derivatives with respect to θ_o are plotted versus μ for the 850 rpm tests. Similar data for all the steady state test conditions are plotted in Appendix A. The experimental data from which the derivatives were calculated are also tabulated therein.

The total blade flapping moment is expressed as

$$\begin{aligned} M_\beta\ (@r = 3.3\text{ in.}) = M_{\beta_o} &- M_{\beta_{1c}} \cos\psi - M_{\beta_{1s}} \sin\psi \\ &- M_{\beta_{2c}} \cos 2\psi - M_{\beta_{2s}} \sin 2\psi \\ &- M_{\beta_{3c}} \cos 3\psi - M_{\beta_{3s}} \sin 3\psi \\ &- M_{\beta_{4c}} \cos 4\psi - M_{\beta_{4s}} \sin 4\psi \end{aligned} \qquad (7)$$

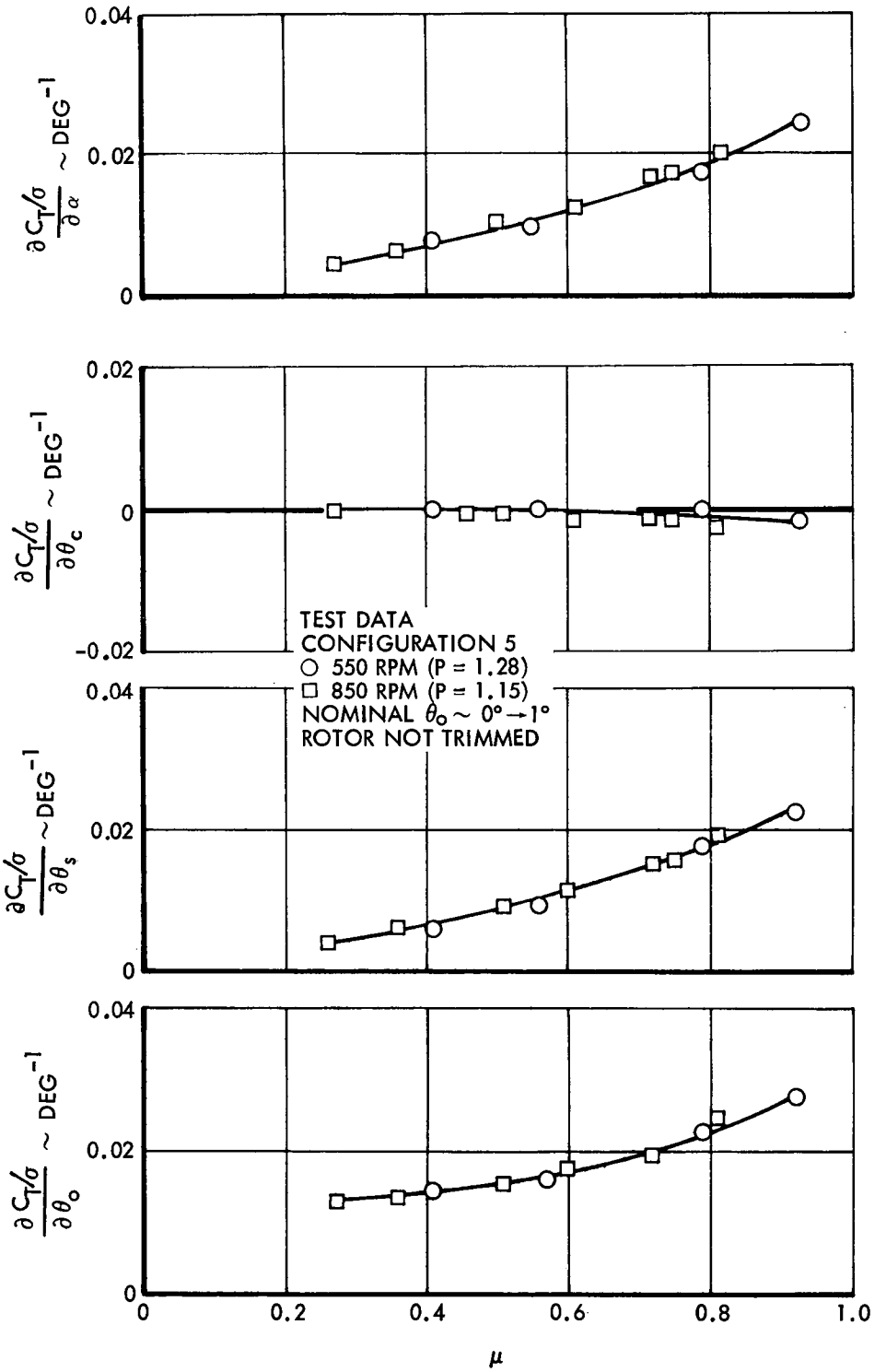

Figure 15. Rotor Lift Derivatives Versus μ

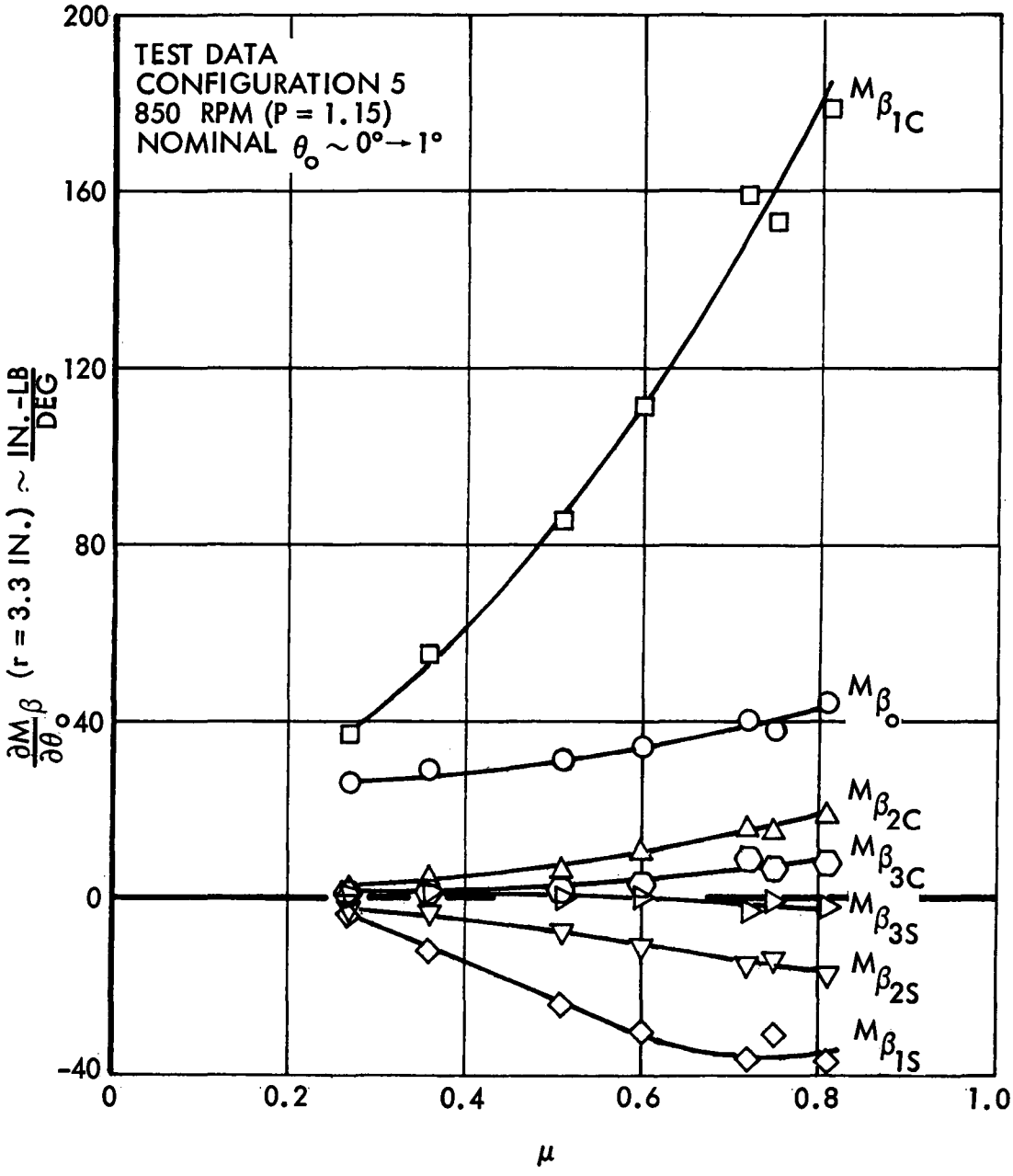

Figure 16. Harmonic Content of Blade Flapping, Configuration 5, 850 RPM (P = 1.15), Steady θ_o Excitation

The data indicate that the blade 1-per-rev response is dominant over the tested advance ratio range and that the strength of the higher harmonic flapping increases with advance ratio. This latter characteristic is expected since it coincides with a corresponding increase in the higher harmonic aerodynamic excitations (Reference 1). The 4-per-rev harmonic of the blade flapping moment derivative was not plotted since it was approximately zero for all tested conditions.

A cursory examination of Figure 16 reveals an anomaly in the data taken at $\mu = 0.72$ and 0.75. One's first inclination might be to attribute the inflection to scatter and simply fair a curve through the data (as has been done). This may be totally valid because the tests at $\mu = 0.75$ and $\mu = 0.81$ were performed at the end of the wind tunnel program and those up to and including $\mu = 0.72$ at the beginning of the test. It is conceivable (though not a certainty) that deadbands in the controls and/or the flapping stiffness (as affected by the feathering bearing slop) could have changed sufficiently to generate scatter of the magnitude indicated. The fact that the derivatives of Figure 16 are based upon data from one blade must also be considered. The hub moment derivatives previously presented (which are a function of the flapping of all 4 blades) display a much milder curvature at $\mu \sim 0.75$. It is logical to expect that the overall effect of slop and deadband would be reduced if four blade motions are averaged.

It is also possible that the characteristic is natural. Work by Dr. Robert A. Ormiston and Mr. David A. Peters of AMRDL (Ames Directorate), reported in Reference 3, indicates that an inflection in the derivative curves should occur at $\mu \sim 0.8$ due to inflow. Their results, however, suggest that the perturbation should occur over an advance ratio span of ~ 0.3 rather than the 0.05 width seen in Figure 16.

Plans are currently underway to re-enter the tunnel with the High Advance Ratio Model to conduct high lift testing. At that time data will be obtained which will resolve the peculiarity just described.

The rotor blade one-per-rev (1P) bending moment distribution has also been determined by harmonically analyzing the radially distributed flapping bending moments. Flap moments were measured at

r = 3.3 in. (x = 0.073)

r = 13.15 in. (x = 0.293)

r = 22.3 in. (x = 0.49)

on blade No. 1 and their 1P derivatives with respect to θ_o, θ_s, θ_c and α calculated. These were then nondimensionalized by one-half the shaft moment derivative (i.e., blade moment derivative at x = 0) to obtain a nondimensional distribution. The results at μ = 0 for a θ_s-excitation are plotted in Figure 17. Data for the three tested rotor speeds are presented. Both the magnitude and phase of the moments are shown as a function of nondimensional radial position (x). For a constant shaft moment the data show a decrease in the outboard flap bending moments with increased rotor rotational speed. The reason for this is that the internal loading in the structure is a function of the flapping displacement which decreases at higher rotor speeds (for a constant airload) because of increased centrifugal force. The linearity of the distributions and the nearly constant phase angle of response (with radial position) suggests that the 1P airload is concentrated over an outboard expanse of the blade.

The blade bending moment distributions for all of the forward flight test conditions and excitations have been calculated. The curves and a tabulation of the test data used to calculate the derivatives are presented in Appendix A. The forward flight distributions are very similar to those shown in Figure 17. The radial blade bending moments are not significantly affected by either advance ratio or type of excitation.

Open Loop Frequency Response Tests (Swashplate Excitations)

Open loop frequency response tests with θ_o, θ_s and θ_c excitations were conducted with configuration 5 only. The test procedures and data analysis techniques were the same as those used during the Phase 2 program (Reference 2). The problem of support stand resonance, which affected some of the Phase 2 data in the frequency range 6 to 10 Hz, was not evident (either visually or from accelerometer measurements) during these Phase 3 tests. There are probably two reasons for this. First, the magnitude of the viscous damping of

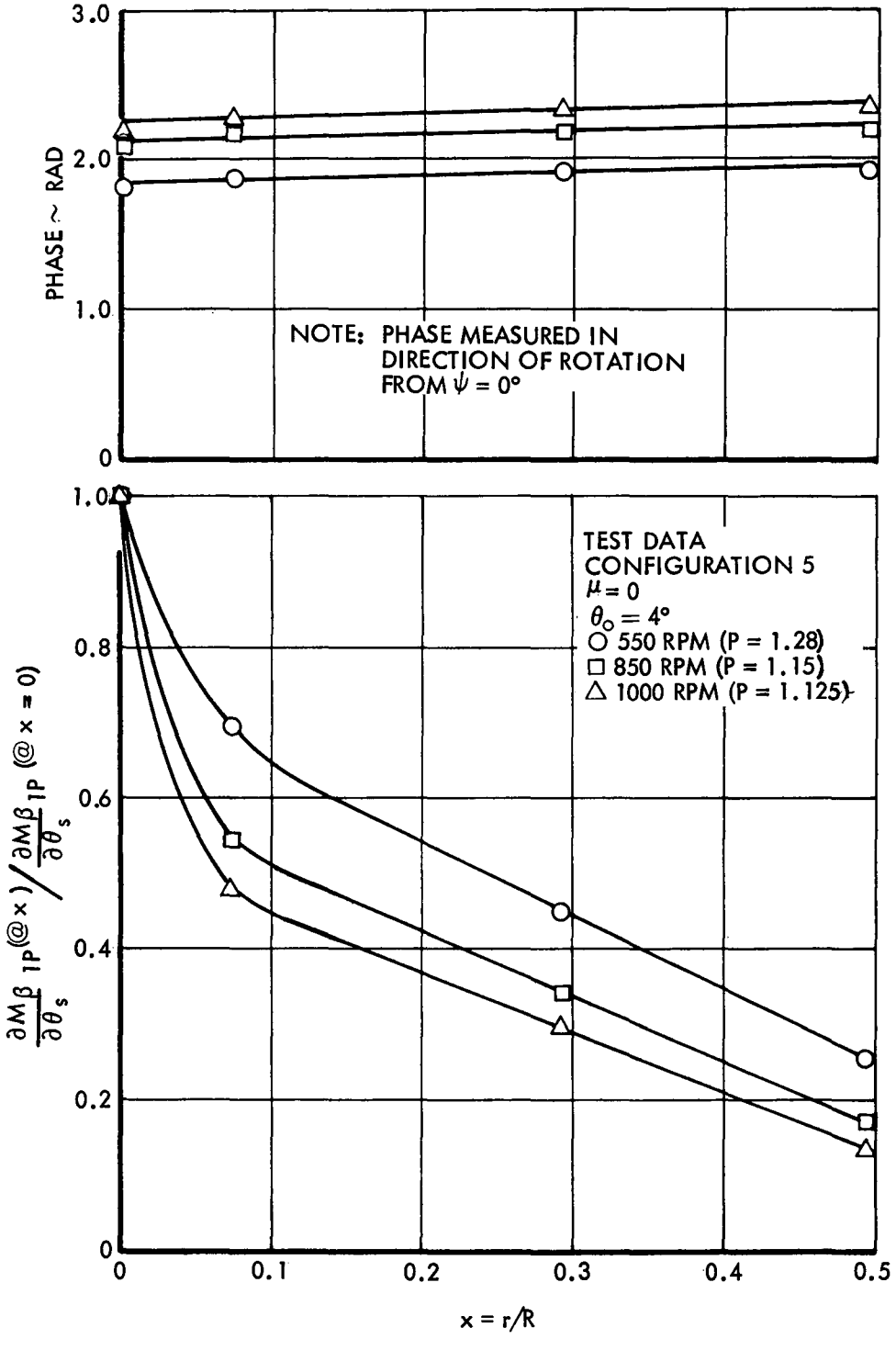

Figure 17. One-Per-Rev Blade Radial Flap Bending Moment Distribution at $\mu = 0$

the model pitch motion was increased above the previous value. Secondly, the softer rotor hub configuration may have actually added to the damping of the body mode and/or changed the relative magnitudes and phases of the motions (eigenvectors) in the mode.

There was one problem which was encountered with high frequency sinusoidal cyclic pitch excitations. The gyroscopic inertia moments which were generated in one swashplate axis by excitations in the other axis, aggravated by a servo natural frequency of approximately 40 Hz, produced coupling between longitudinal and lateral cyclic pitch. The degree of coupling was a nonlinear function of the excitation frequency (ω) and a linear function of the swashplate rotational frequency (Ω). Because of this it was reasoned that the coupling was caused by the near resonance response of the servo to the gyroscopic excitation rather than a simple overpowering of the actuator. Typical θ_c/θ_s and θ_s/θ_c couplings are shown in Figure 18.

Correcting the test data to obtain hub moment pitch and roll frequency response with respect to pure θ_s and θ_c excitations was relatively simple. It consisted of forming a complex second order linear system from moment and cyclic pitch data during the θ_s and θ_c tests which were conducted at the same excitation frequency, i.e.,

$$\begin{aligned} \theta_{s_1} \frac{\partial M_H}{\partial \theta_s} + \theta_{c_1} \frac{\partial M_H}{\partial \theta_c} &= M_{H_1} \\ \theta_{s_2} \frac{\partial M_H}{\partial \theta_s} + \theta_{c_2} \frac{\partial M_H}{\partial \theta_c} &= M_{H_2} \end{aligned} \tag{8}$$

The subscript 1 refers to data obtained when θ_s was the intended excitation and the subscript 2 when θ_c was the principal excitation. Premultiplying Eq. 8 by the inverse of the θ-matrix yields the following linear system which is solved simultaneously to obtain the moment derivatives.

$$\begin{Bmatrix} \frac{\partial M_H}{\partial \theta_s} \\ \frac{\partial M_H}{\partial \theta_c} \end{Bmatrix} \begin{bmatrix} \theta_{s_1} & \theta_{c_1} \\ \theta_{s_2} & \theta_{c_2} \end{bmatrix}^{-1} = \begin{Bmatrix} M_{H_1} \\ M_{H_2} \end{Bmatrix} \tag{9}$$

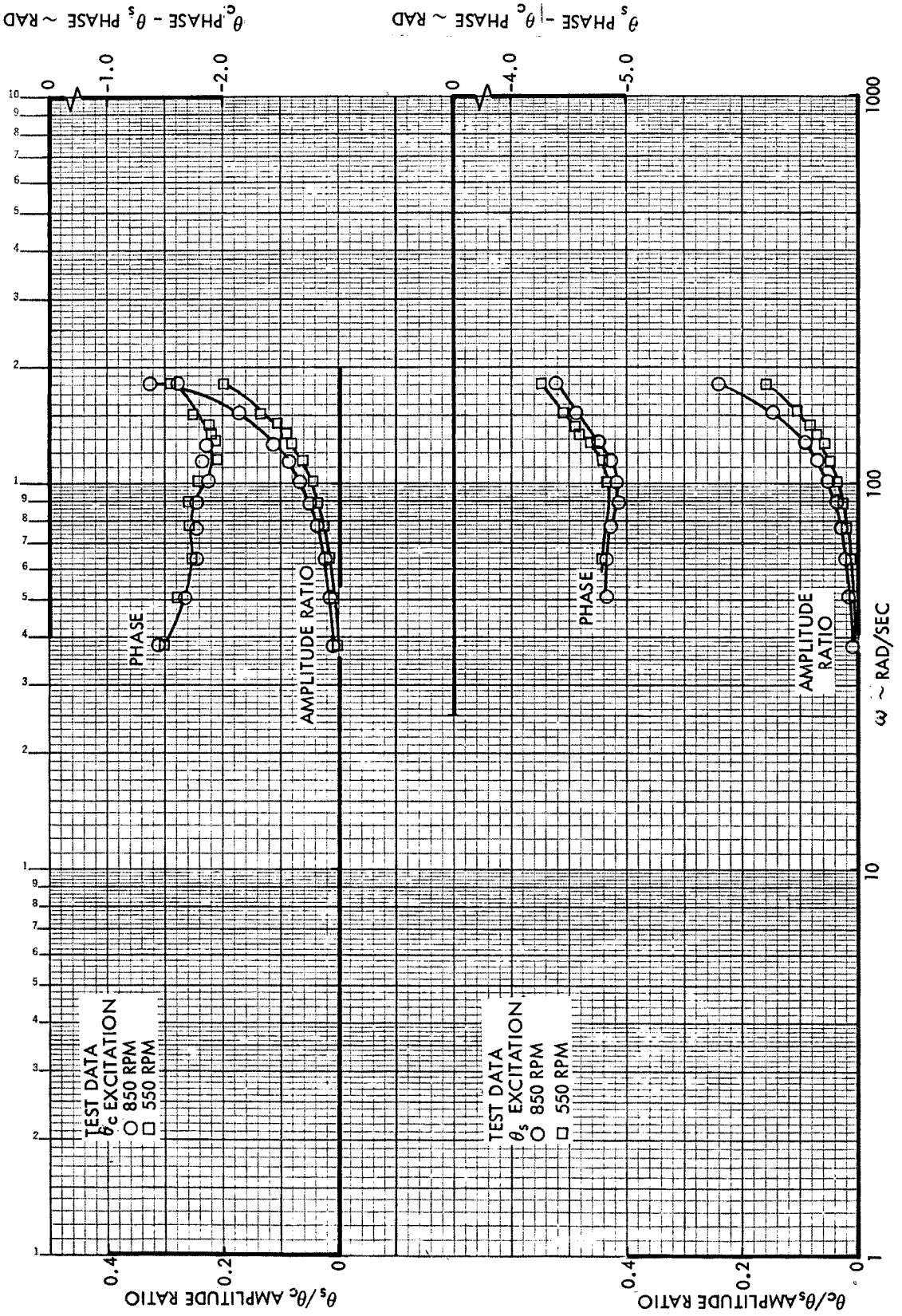

Figure 18. Cyclic Pitch Coupling at High Excitation Frequencies

Since the numbers are complex, the amplitude ratio and phase lag between the moment and the cyclic pitch are obtained directly. Most of θ_s and θ_c tests were conducted at identical frequencies. For the few tests that were not, interpolated values were used to generate one of the two linear equations. Since both θ_c and θ_s tests were not performed in hover, symmetry in the coupling was assumed.

It is noted that the frequency response data presented in Reference 2 were not corrected for the cyclic pitch coupling (the problem was not recognized at the time). The maximum excitation frequency for those tests was 22 Hz and the three tested rotor speeds were 300, 550, and 800 rpm. Based upon Figure 18, the probable coupling which existed at 22 Hz was

- 300 rpm - 4.78% coupling
- 550 rpm - 8.75% coupling
- 800 rpm - 12% coupling.

The maximum correction applied to the Phase 3 data at $\omega = 22$ Hz and 850 rpm was ~ 1 dB and $\sim 5°$ phase. It is therefore concluded that the corrections to the Phase 2, θ_s and θ_c frequency response data would have been within experimental error.

The experimental open loop rotor transfer functions with respect to swashplate excitations for configuration 5 are approximately the same as those determined for configuration 1 during the Phase 2 test. In general, the rotor response peaked when the excitation frequency was in resonance with the blade rotating first flap bending mode natural frequency. As shown in Figure 19, this occurred twice; when $\omega = (P - 1)\Omega$ and $\omega = (P + 1)\Omega$. The cited example presents the hub pitch moment frequency response to collective pitch at an advance ratio of $\mu = 0.41$ and a rotor speed of 550 rpm. The amplitude ratio M_H/θ_o is expressed in decibels (dB)

$$dB = 20 \text{ LOG}_{10} \text{ (amplitude ratio)} \qquad (10)$$

and has the dimensions in.-lb/deg. The phase lag of M_H relative to θ_o is expressed in degrees in the range $-180° \rightarrow +180°$. The measured hub roll

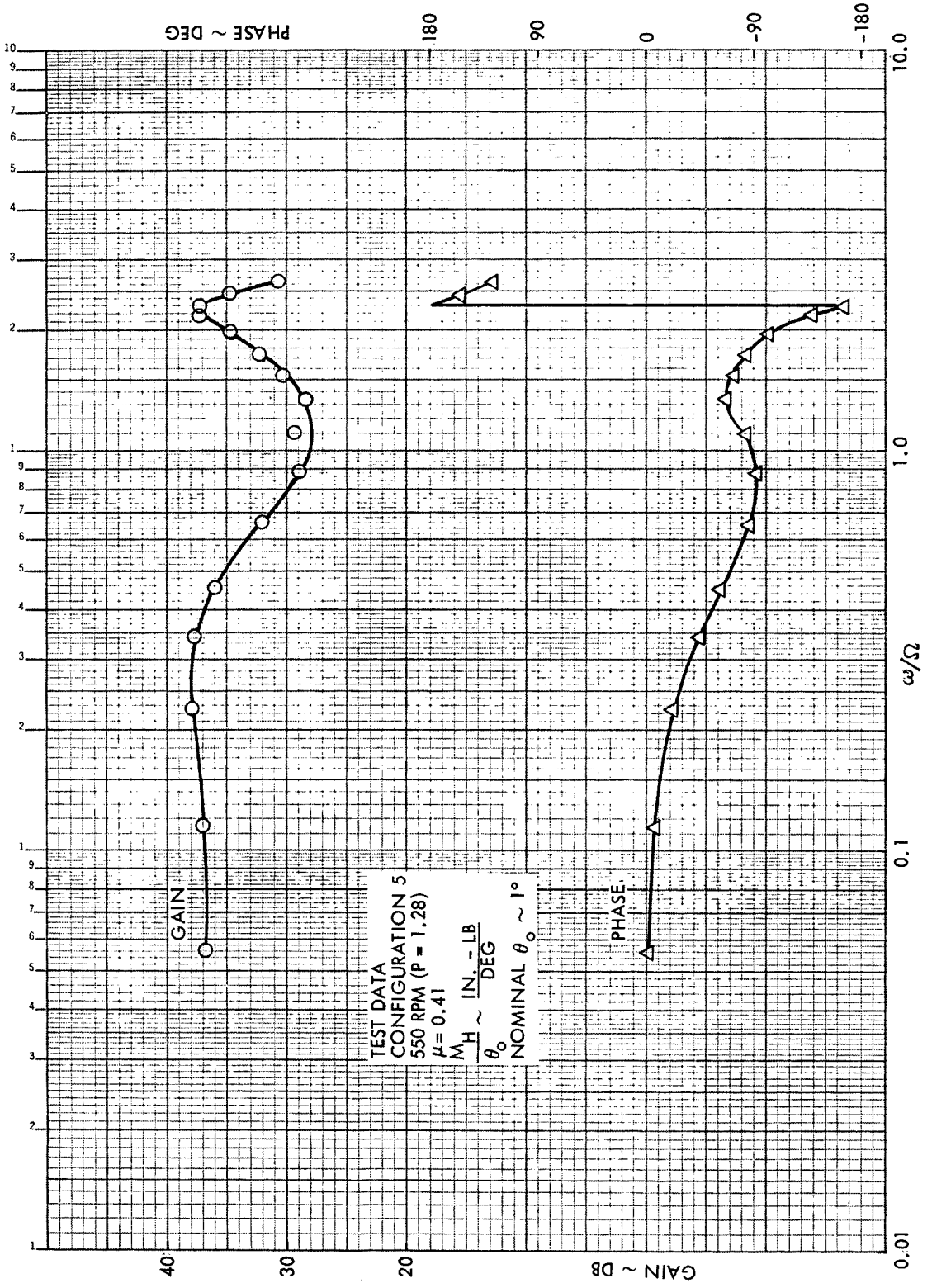

Figure 19. Rotor Hub Pitch Moment Frequency Response to θ_o, μ = 0.41, Configuration 5, 550 RPM (P = 1.28)

moment frequency response to θ_o for the same test condition is shown in Figure 20. The dissimilarity of the M_H and L_H gain curves indicates that the rotor phase angle of response, i.e.,

$$\text{PHASE ANGLE OF RESPONSE} = \text{TAN}^{-1}\left(\frac{-L_H}{-M_H}\right) \tag{11}$$

varies with the excitation frequency.

It is noted that the rotor moment transfer functions presented in this report have the dimensions in.-lb/deg. In Reference 2 the moments were nondimensionalized by an analytically determined rotor stiffness (K_θ) and presented in the form of fore-aft (a_1) and lateral (b_1) rotor angular displacements. This approach was not used for the current presentation because the assumption that a single value of K_θ is sufficient for all test conditions at a constant rotor speed is not totally valid. The procedure by which K_θ was reduced to account for the radially offset hub moment measurement is also suspect. The transfer functions in Reference 2 can be converted to the dimensions in.-lb/deg by simply adding

$$20\ \text{LOG}_{10}\ K_\theta \tag{12}$$

to the gain values which have the units deg/deg. K_θ values for the Phase 2 data are listed in Table IV of Reference 2. For those who would prefer to nondimensionalize the Phase 3 hub moment data, $20\ \text{LOG}_{10}\ K_\theta$ must be subtracted from the gains with the dimensions in.-lb./deg. K_θ values for configuration 5 which are calculated from first flap bending mode moments and deflections (see Section 7 of Reference 1) are

RPM	K_θ (@ 3.3 in.)
1000	125 in-lb/deg
850	123
550	120

An increase in the damping of blade flapping with increased advance ratio was revealed by the measured hub moment frequency response. Examples of data which demonstrate this characteristic are contained in the next four curves.

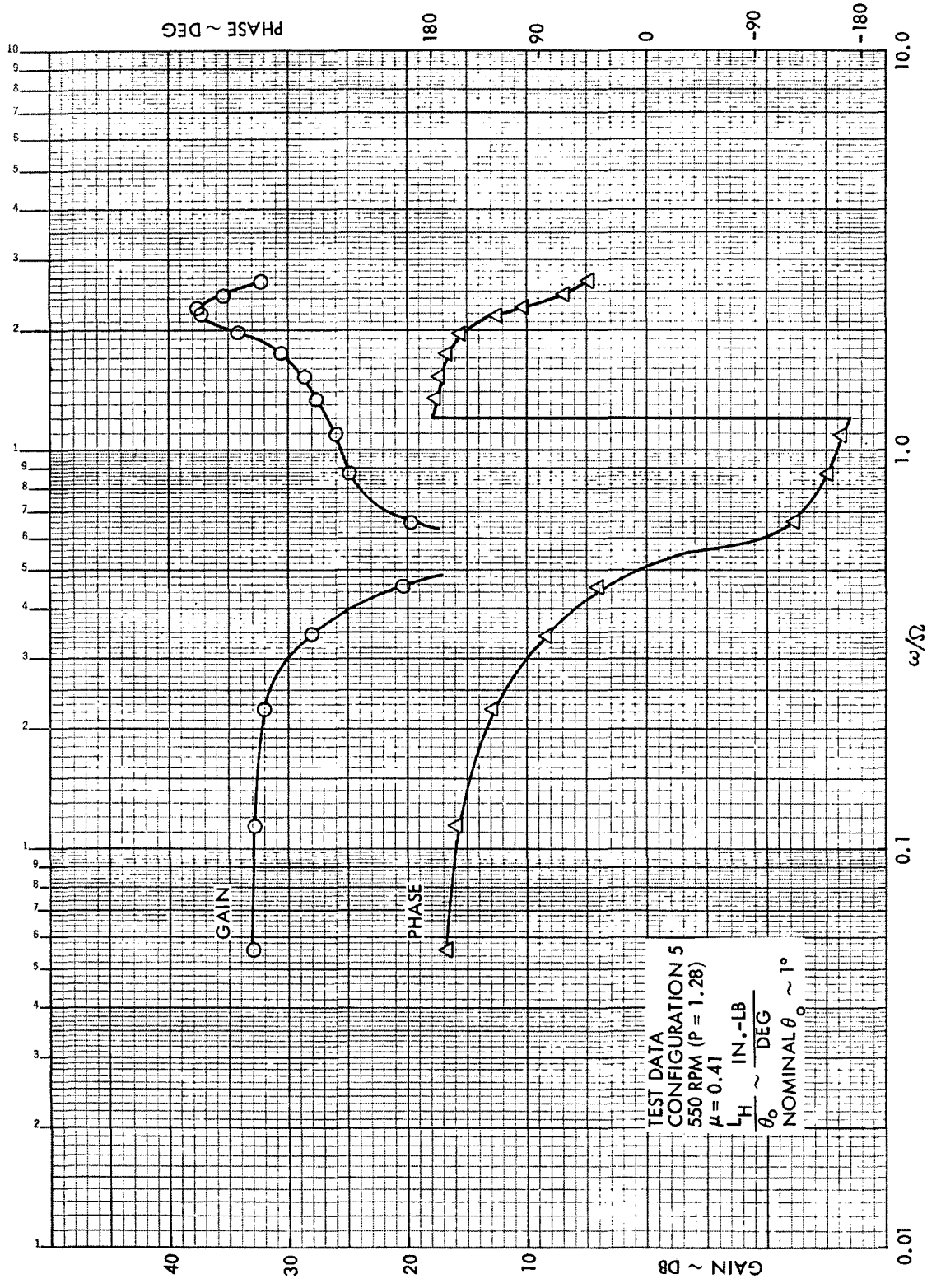

Figure 20. Rotor Hub Roll Moment Frequency Response to θ_o, μ = 0.41, Configuration 5, 550 RPM (P = 1.28)

Figures 21 and 22 present the rotor hub moment frequency response to longitudinal cyclic pitch at $\mu = 0$ and a rotor speed of 850 rpm. Similar transfer functions are plotted in Figures 23 and 24 at $\mu = 0.27$. The increase in flap damping is indicated by both the gain and the phase curves. The reduced peaking of the low frequency hub pitch moment response at $\mu = 0.27$ as compared with the response at $\mu = 0$ is indicative of greater damping. Also the rate of change in phase lag with excitation frequency of both the pitch and roll response is smaller at $\mu = 0.27$ than at $\mu = 0$. This trend is also characteristic of increased damping.

If the high frequency portions of the transfer functions at the two advance ratios are now compared, it is seen that the gain and phase curves are nearly identical or varying at the same rate. It is known that the decrease in the low frequency response is caused by induced inflow. It is suspected, therefore, that the induced velocity only has an influence on the rotor response at low frequencies. For the example shown the inflow has an effect only up to $\omega/\Omega \sim 0.2$.

Another feature of the 850 rpm frequency response data which is notable is a broad fluctuation in the hub moment gain curves centered at $\omega/\Omega \sim 0.8$. Examples of the response are shown in Figures 25 and 26 in which the hub moment transfer functions with respect to collective pitch at $\mu = 0.27$ are plotted. The characteristic in question is manifested by a peak in the pitch moment and a depression in the roll moment gain curves. It is suspected that this characteristic is caused by a mild involvement of the second flap bending mode in the response. The variations are the most prevalent when the moments are at a low level and the control input is collective pitch. If the dynamic response of the second flap mode is assumed to be relatively invariant with the tested aerodynamic environment, its influence on the total response would lessen at increased moments because of the decibel presentation.

All of the rotor hub moment frequency response data with respect to θ_o, θ_s and θ_c control inputs for configuration 5 (as delineated in Table III) are contained in Appendix B. The results are presented graphically in curves exactly like those just discussed. The experimental hub moment transfer

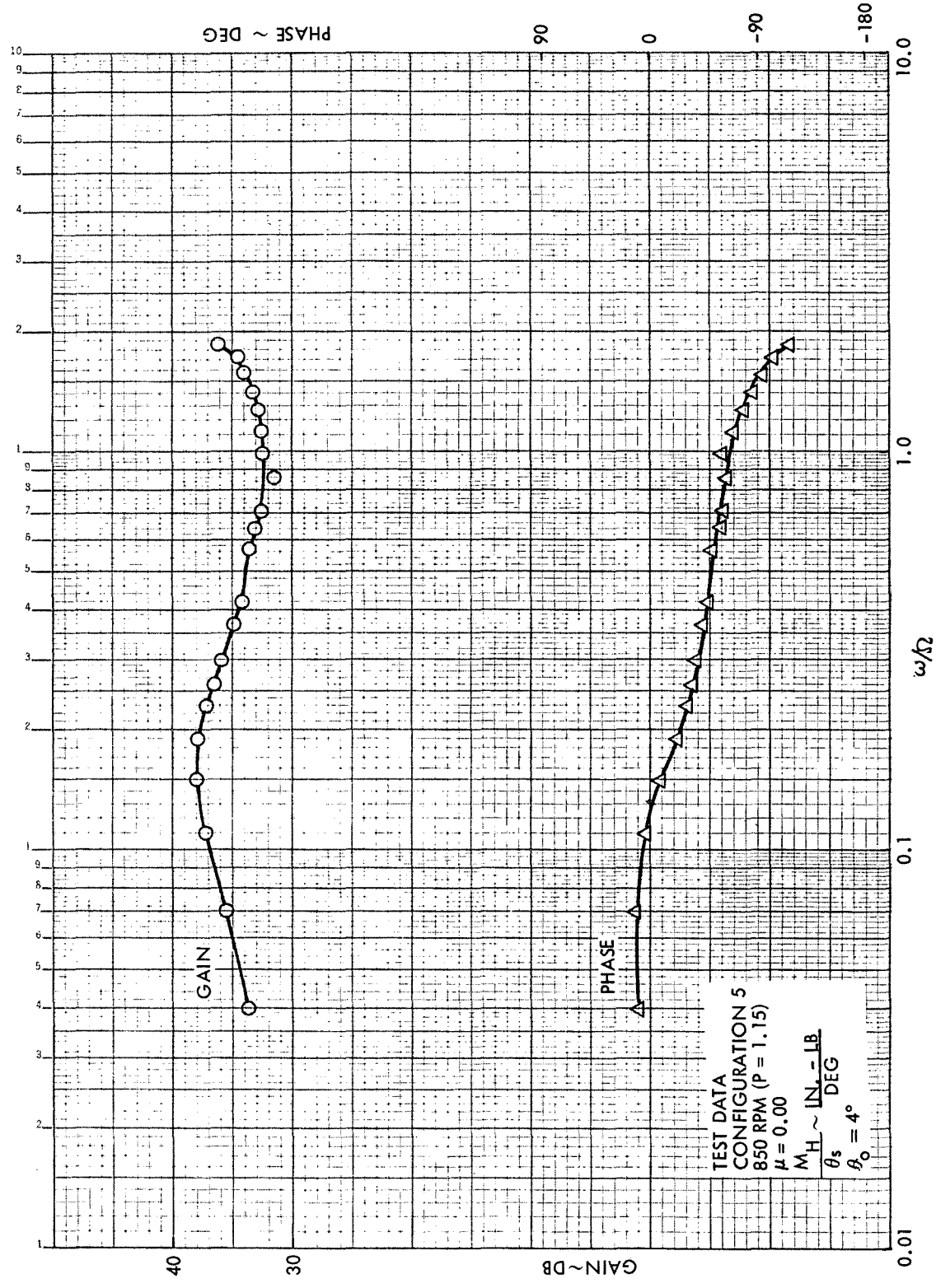

Figure 21. Rotor Hub Pitch Moment Frequency Response to θ_s, $\mu = 0$, Configuration 5, 850 RPM ($P = 1.15$)

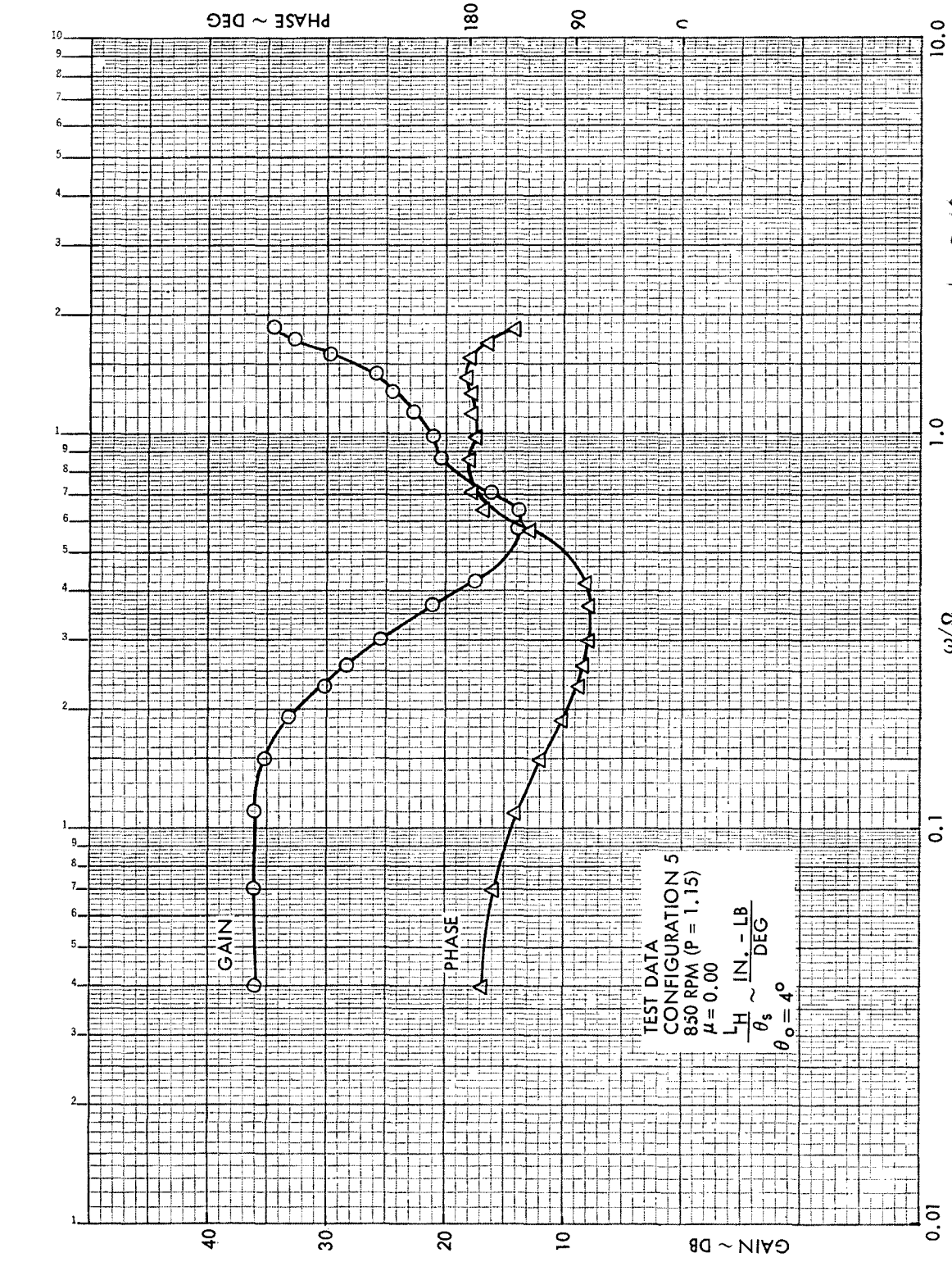

Figure 22. Rotor Hub Roll Moment Frequency Response to θ_s, μ = 0, Configuration 5, 850 RPM (P = 1.15)

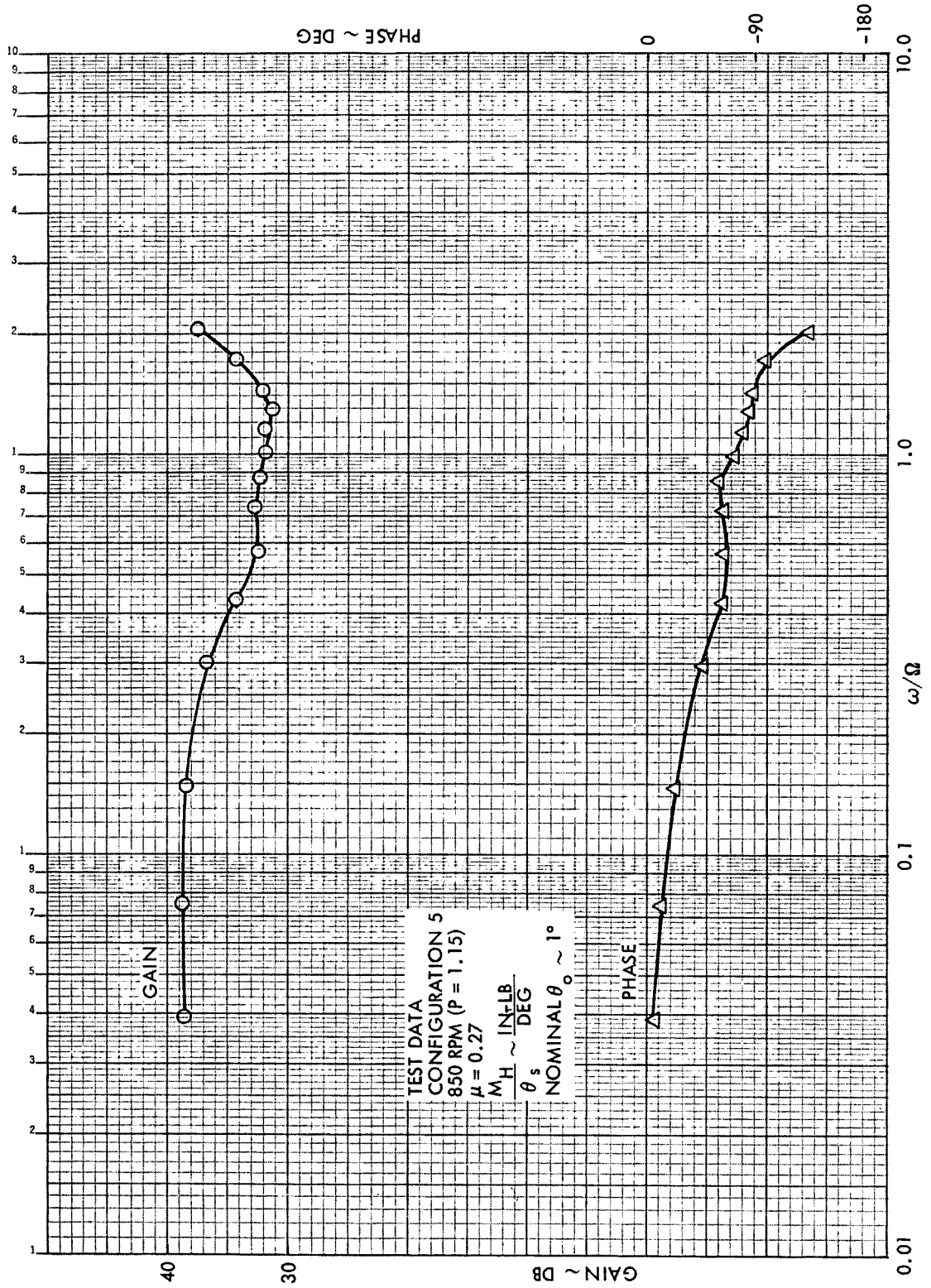

Figure 23. Rotor Hub Pitch Moment Frequency Response to θ_s, $\mu = 0.27$, Configuration 5, 850 RPM (P = 1.15)

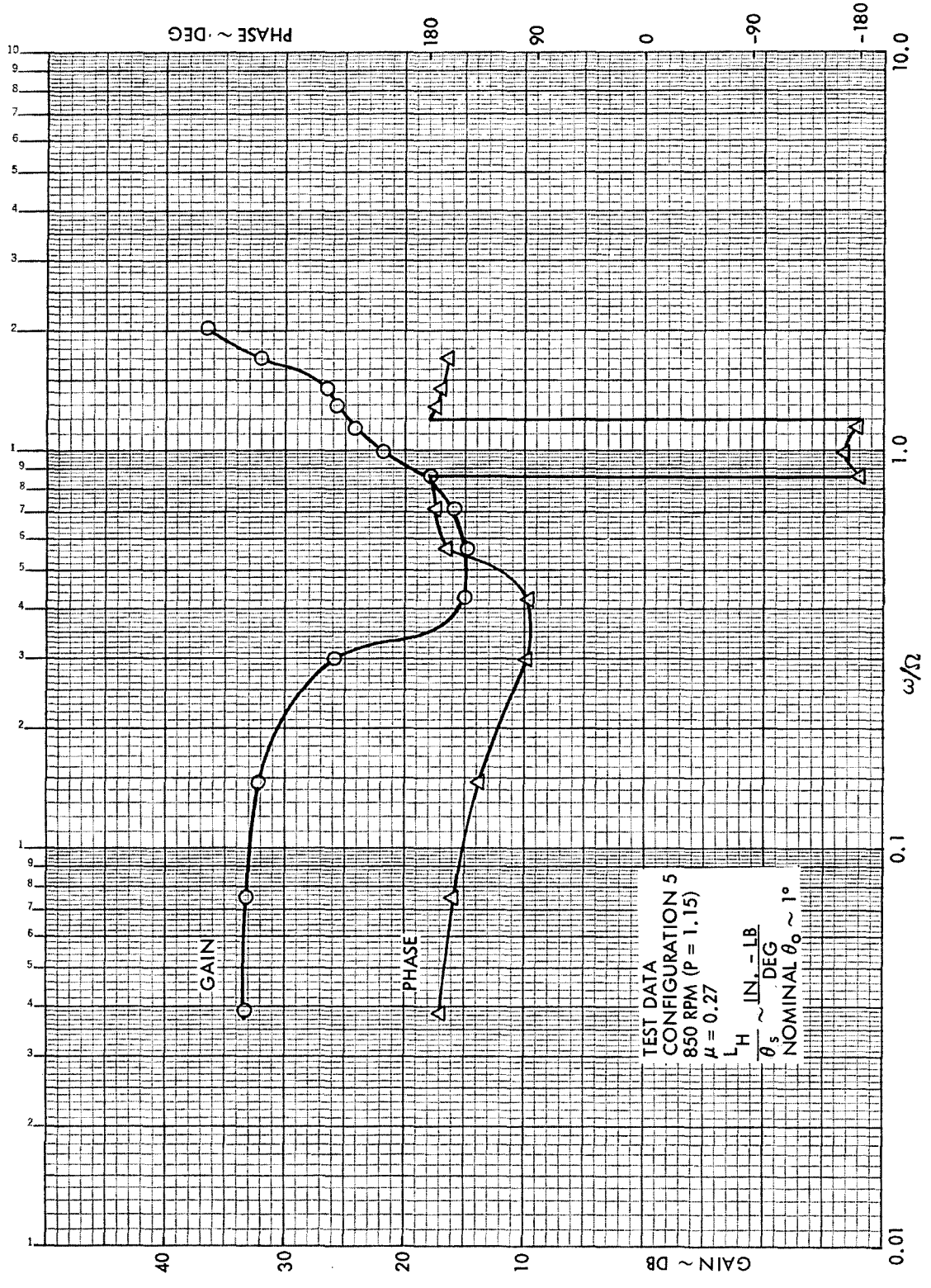

Figure 24. Rotor Hub Roll Moment Frequency Response to θ_s, μ = 0.27, Configuration 5, 850 RPM (P = 1.15)

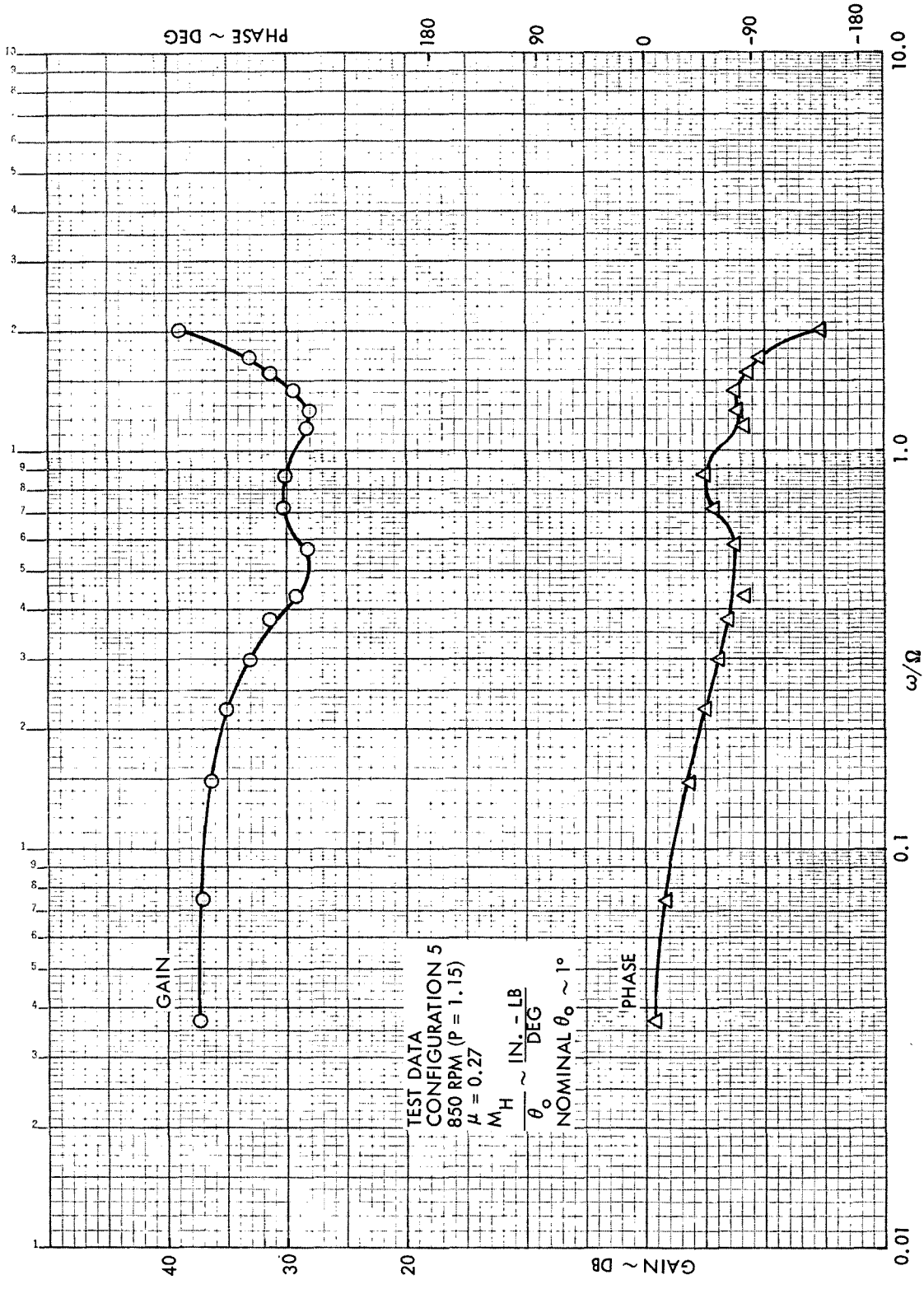

Figure 25. Rotor Hub Pitch Moment Frequency Response to θ_o, μ = 0.27, Configuration 5, 850 RPM (P = 1.15)

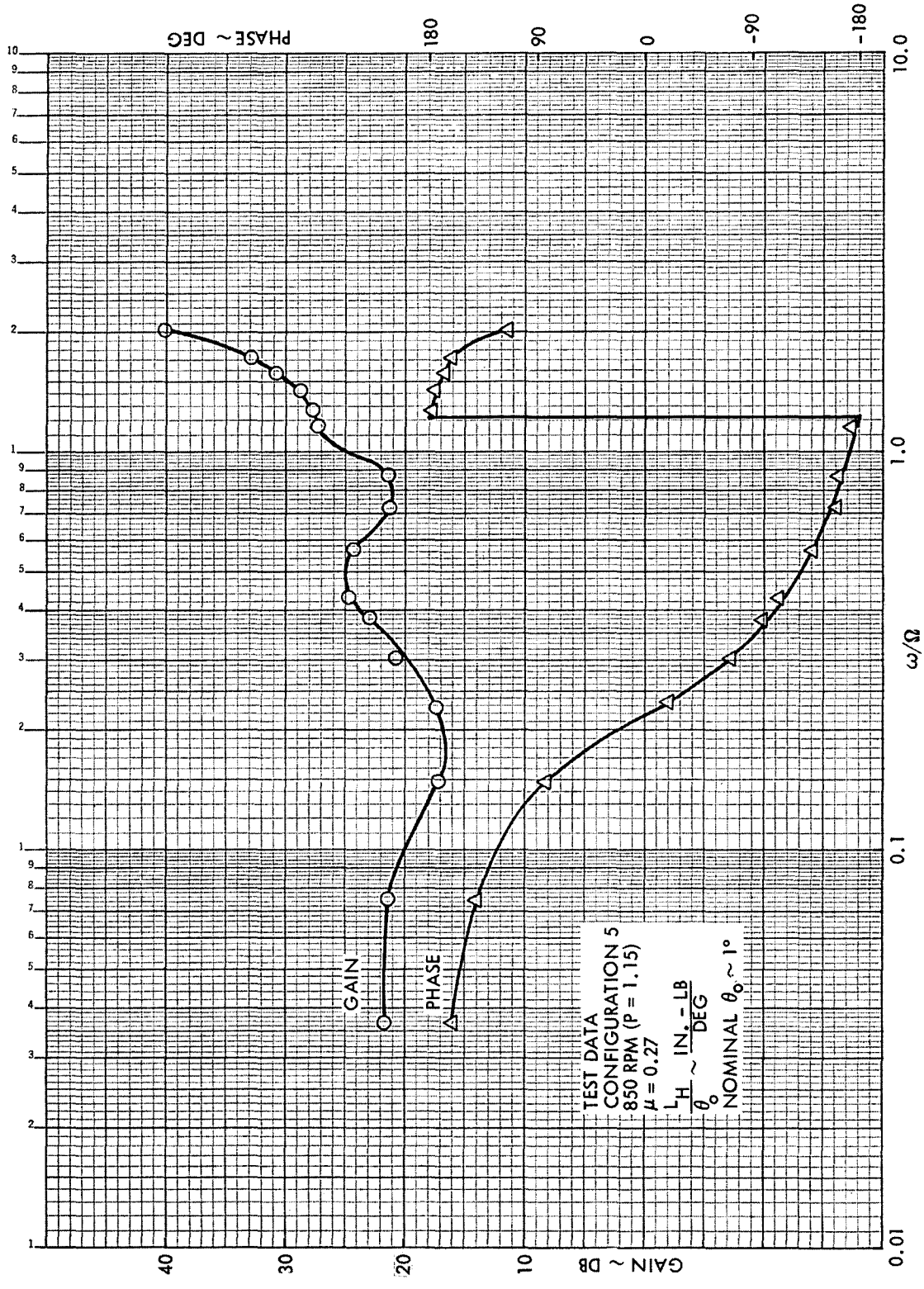

Figure 26. Rotor Hub Roll Moment Frequency Response to θ_o, μ = 0.27, Configuration 5, 850 RPM (P = 1.15)

functions have also been adjusted to the center of rotation and converted to a coefficient form. These results (including phase lag) are tabulated as a function of excitation frequency, rotor speed, and advance ratio.

Open Loop Frequency Response Tests (Rotor Shaft Excitations)

Experimental rotor frequency response with respect to shaft pitch (α) and roll (ϕ) excitations had not been acquired during previous phases of the High Advance Ratio Research Program. Therefore, both configuration 1 (soft flexure, no tip weight) and configuration 5 ('supersoft' flexure, no tip weight) were tested. The test conditions (Ω, μ) for configuration 1 are compatible with those considered during the Phase 2 program. All configuration 5 test conditions (i.e., with θ_o, θ_s, θ_c, α and ϕ excitations) are identical.

The test technique for the α and ϕ frequency response experiments was the same as for the swashplate excitations. That is, the hydraulic actuators which restrained the model in pitch and roll were driven (one at a time) with a sine wave function generator at discrete frequencies ranging from 0.5 Hz to 14 Hz. The magnitude of the input was adjusted according to the rotor response. Flexure bending moment endurance limits were respected at all times. The maximum allowable angular travel in both pitch and roll, as dictated by mechanical interference, was $\pm 5°$.

The experimental rotor frequency response data with respect to α are not of a quality comparable to the results for swashplate excitations. The primary reason for this is the large moment of inertia of the body about the pitch pivot. When the model was oscillated at high frequencies the resulting large inertia forces generated bending of the support structure. Since the pitch angular position was deduced from the actuator ram position, elastic deformations were not accounted for in the measurement.

In general the frequency response data with respect to ϕ are more reliable than those with respect to α. The model moment of inertia about the roll axis was considerably less than the inertia about the pitch axis. Also, the pitch damper was installed during the roll tests which helped to minimize unprogrammed pitch vibrations. All of the data that are suspected of being

contaminated by elastic deformations and/or support vibrations are noted as such in the presentation of the test results.

Before the experimental rotor transfer functions are discussed, it is important to recognize the content of the excitations which the rotor experiences when the shaft is oscillated. As discussed in Section 3, the pivots about which the model pitched and rolled were located below the plane of the rotor. Therefore, in addition to the angular excitations of the rotor generated by shaft variations, i.e.,

$$\begin{aligned} \alpha &= \alpha_o \sin \omega t & \phi &= \phi_o \sin \omega t \\ \dot{\alpha} &= \alpha_o \omega \cos \omega t & \dot{\phi} &= \phi_o \omega \cos \omega t \\ \ddot{\alpha} &= -\alpha_o \omega^2 \sin \omega t & \ddot{\phi} &= -\phi_o \omega^2 \sin \omega t \end{aligned} \tag{13}$$

there are also linear velocity ($\dot{\eta}$) and acceleration ($\ddot{\eta}$) excitations, e.g.,

$$\begin{aligned} \dot{\eta} &= l\dot{\alpha} \\ \ddot{\eta} &= l\ddot{\alpha} \end{aligned} \tag{14}$$

l is the distance from the pitch pivot to the rotor hub. In the curves which will be presented, the transfer functions are labeled as being with respect to α and ϕ where it is understood that the total excitation is not merely the angular displacement but the composite of the linear and angular displacements, rates and accelerations.

Several curves which illustrate the nature of the experimental rotor frequency response with respect to shaft pitch and roll are discussed below. The reader is referred to Appendix C for graphical and tabular presentations of all the test data (including those presented in the main body of this report).

The experiments conducted at $\mu = 0$ provide a good basis for evaluating the effect of support stand vibrations on the rotor data. Because the response of the rotor to the displacement, α, is zero when $\mu = 0$, the transfer functions with respect to α and ϕ oscillations should be symmetrical. Rotor hub moment frequency response data at $\mu = 0$ with α and ϕ excitations are shown in Figures 27 to 30. In the first two plots the pitch and roll response to α are presented. In the next two figures the same responses to a ϕ excitation are shown. The conditions for the two tests are identical (configuration 5, rotor speed = 850 rpm and $\theta_o = 4°$). Comparisons of M_H/α with L_H/ϕ and L_H/α

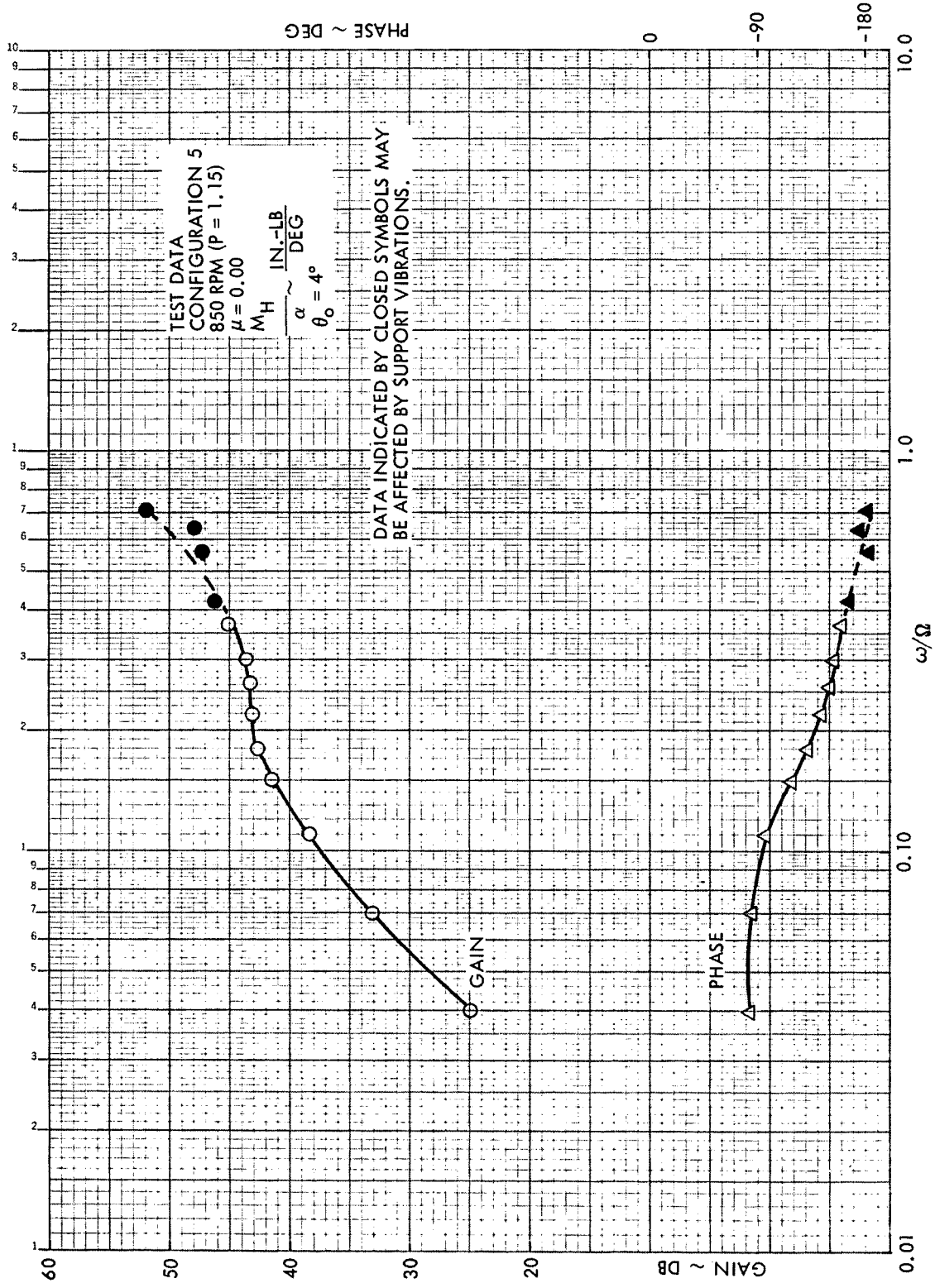

Figure 27. Rotor Hub Pitch Moment Frequency Response to Shaft Pitch, Configuration 5, μ = 0, 850 RPM (P = 1.15)

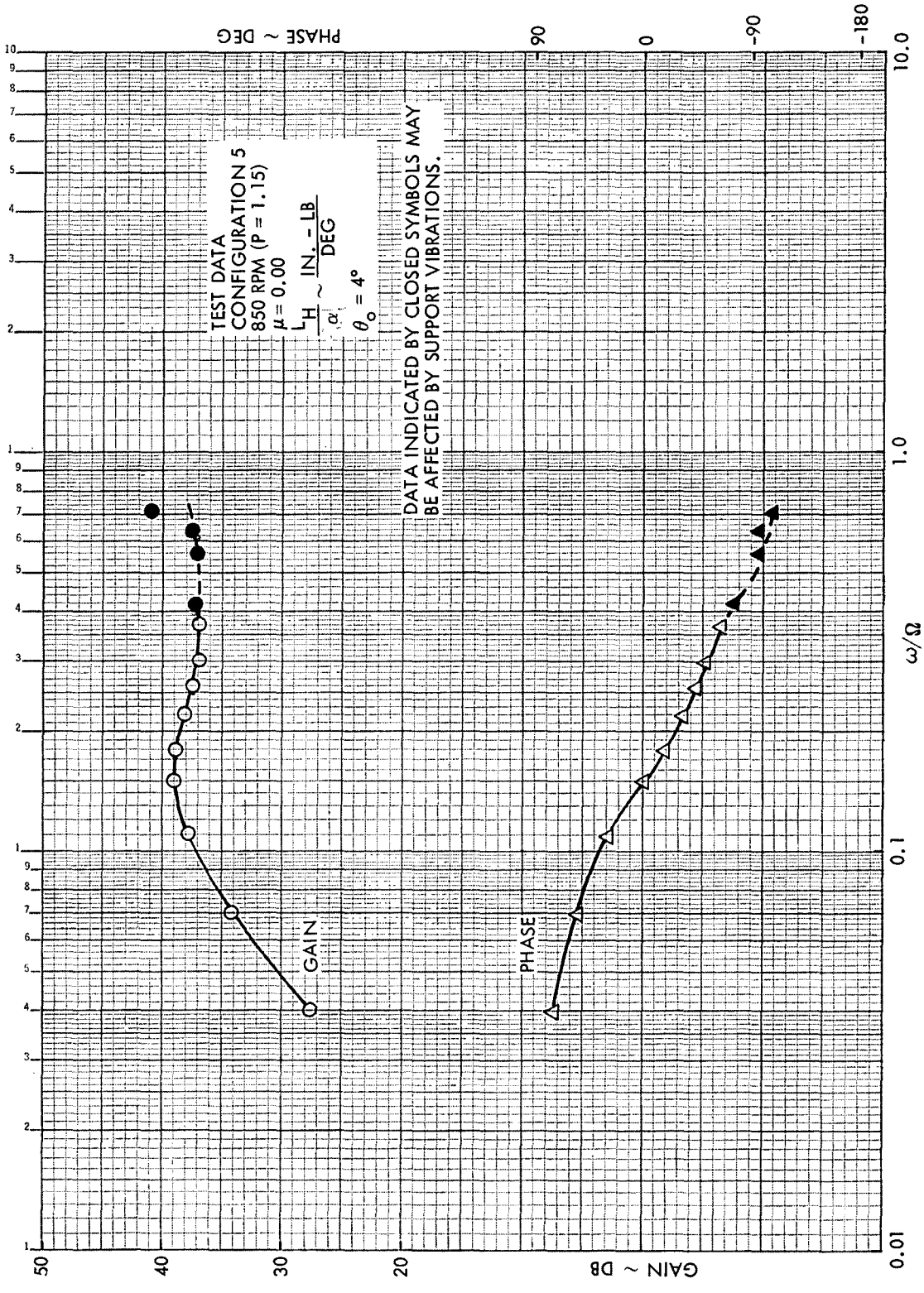

Figure 28. Rotor Hub Roll Moment Frequency Response to Shaft Pitch, Configuration 5, μ = 0, 850 RPM (P = 1.15)

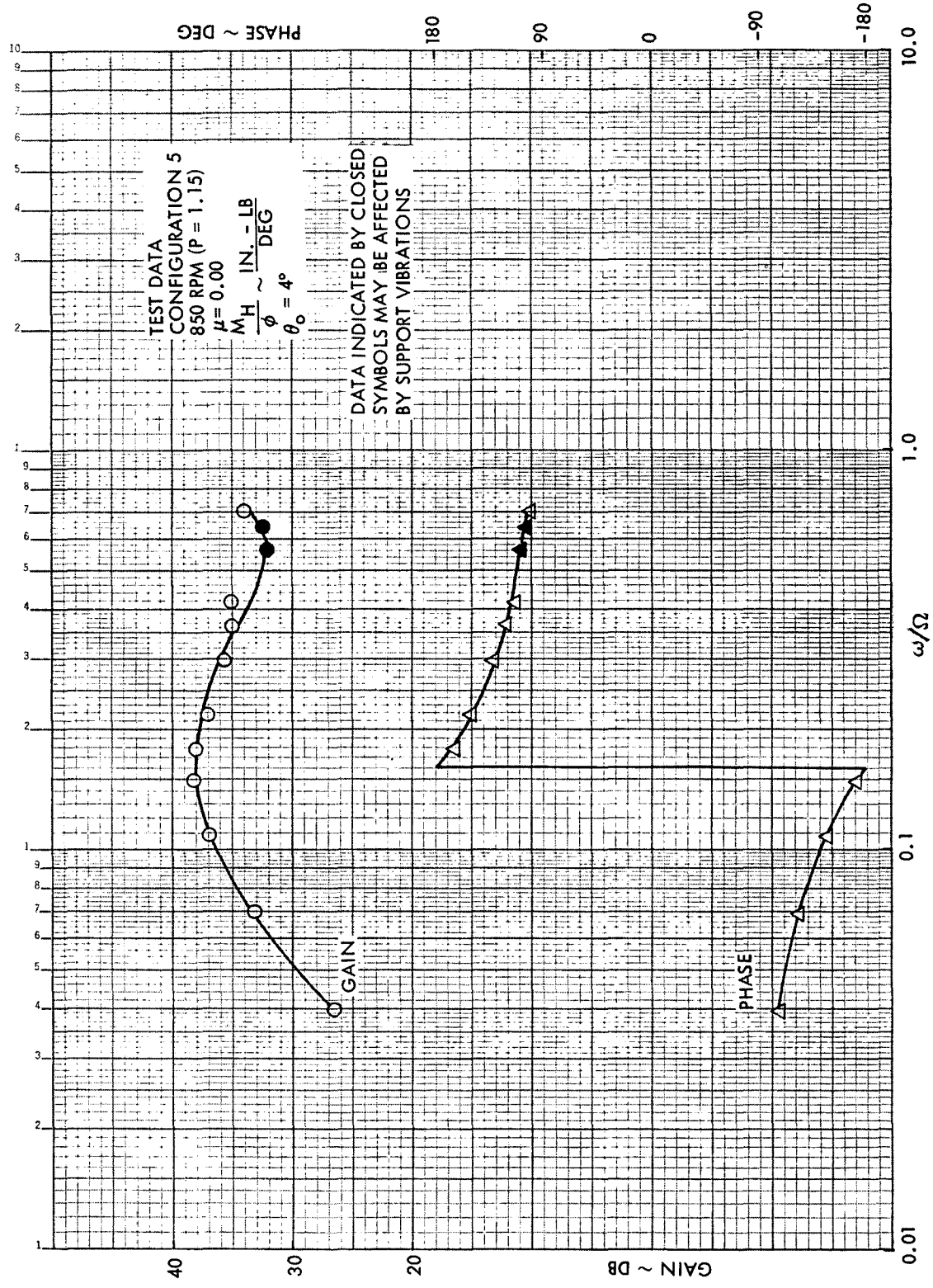

Figure 29. Rotor Hub Pitch Moment Frequency Response to Shaft Roll, Configuration 5, μ = 0, 850 RPM (P = 1.15)

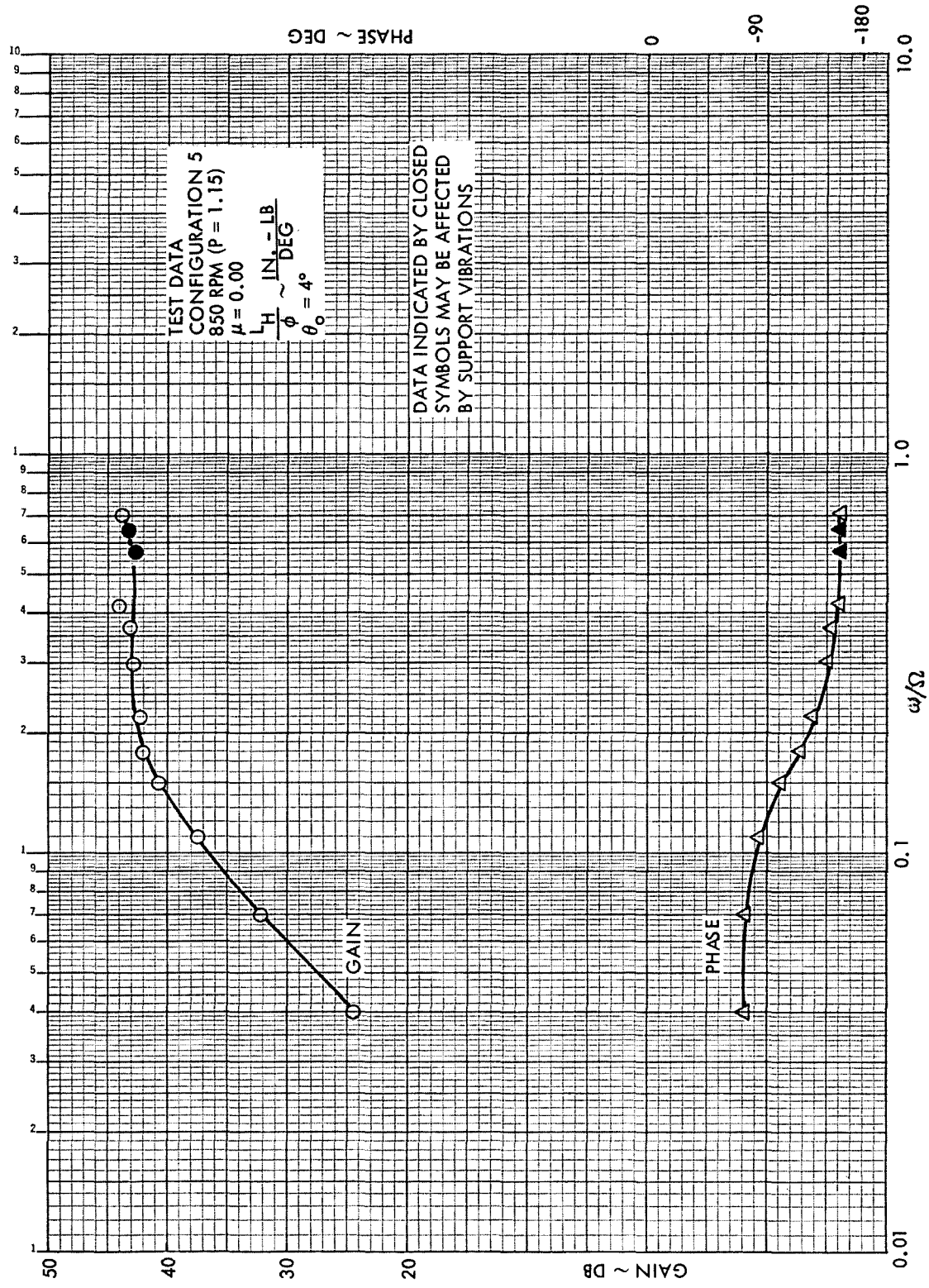

Figure 30. Rotor Hub Roll Moment Frequency Response to Shaft Roll, Configuration 5, μ = 0, 850 RPM (P = 1.15)

with M_H/ϕ reveal that the responses are approximately symmetric up to an excitation frequency of $\omega \sim 0.3\,\Omega$. The gain values generally agree to within 1 dB and phase discrepancies are almost undetectable. As the frequency ratio increases, however, the disagreement also increases until at $\omega/\Omega = 0.7$ the responses are divergent by 7 to 8 dB in gain and 30° in phase. As has been discussed previously, the roll frequency response data are considered more reliable than the pitch results.

The characteristics of the experimental data at $\mu = 0$ are quite informative. Consider, for example, the hub moment roll response to a shaft roll oscillation, L_H/ϕ (Figure 30). When the excitation frequency is small the response is low. This is due to the fact that the roll rate ($\dot{\phi}$) and roll acceleration ($\ddot{\phi}$) are small. The rotor, of course, does not respond to roll position at any advance ratio. The 90° phase lag at the low frequencies indicates the primary rotor excitation is due to $\dot{\phi}$. Since the response and excitation are in phase, the excitation is of aerodynamic origin. As the excitation frequency increases the magnitude is of both $\dot{\phi}$ and $\ddot{\phi}$ increase for a constant ϕ, thus generating the higher rotor response.

The hub pitch moment response to ϕ at $\mu = 0$ is shown in Figure 29. Again, at low excitation frequencies the phase lag is 90°. In this case the primary disturbance is the gyroscopic excitation due to $\dot{\phi}$. The peaking of the pitch response at $\omega/\Omega \sim 0.15$ is caused by the resonant response of the rotor at its natural flapping frequency.

Experimental rotor frequency response with respect to shaft roll oscillations in forward flight are shown in Figures 31 through 34. Hub pitch and roll moment data at two advance ratios ($\mu = 0.27$ and $\mu = 0.51$) are presented for configuration 5 at a rotor speed of 850 rpm. The rotor response is not affected by roll position (ϕ) and the inertia excitations due to $\dot{\phi}$ and $\ddot{\phi}$ are independent of μ at a constant excitation frequency. Therefore, the differences between the transfer functions at the two advance ratios must be due to a change in aerodynamic excitation; the primary excitation (ignoring unsteady effects) is caused by the steady roll rate, $\dot{\phi}$. From the data shown it can be seen that increased forward speed generates a slight reduction in the hub

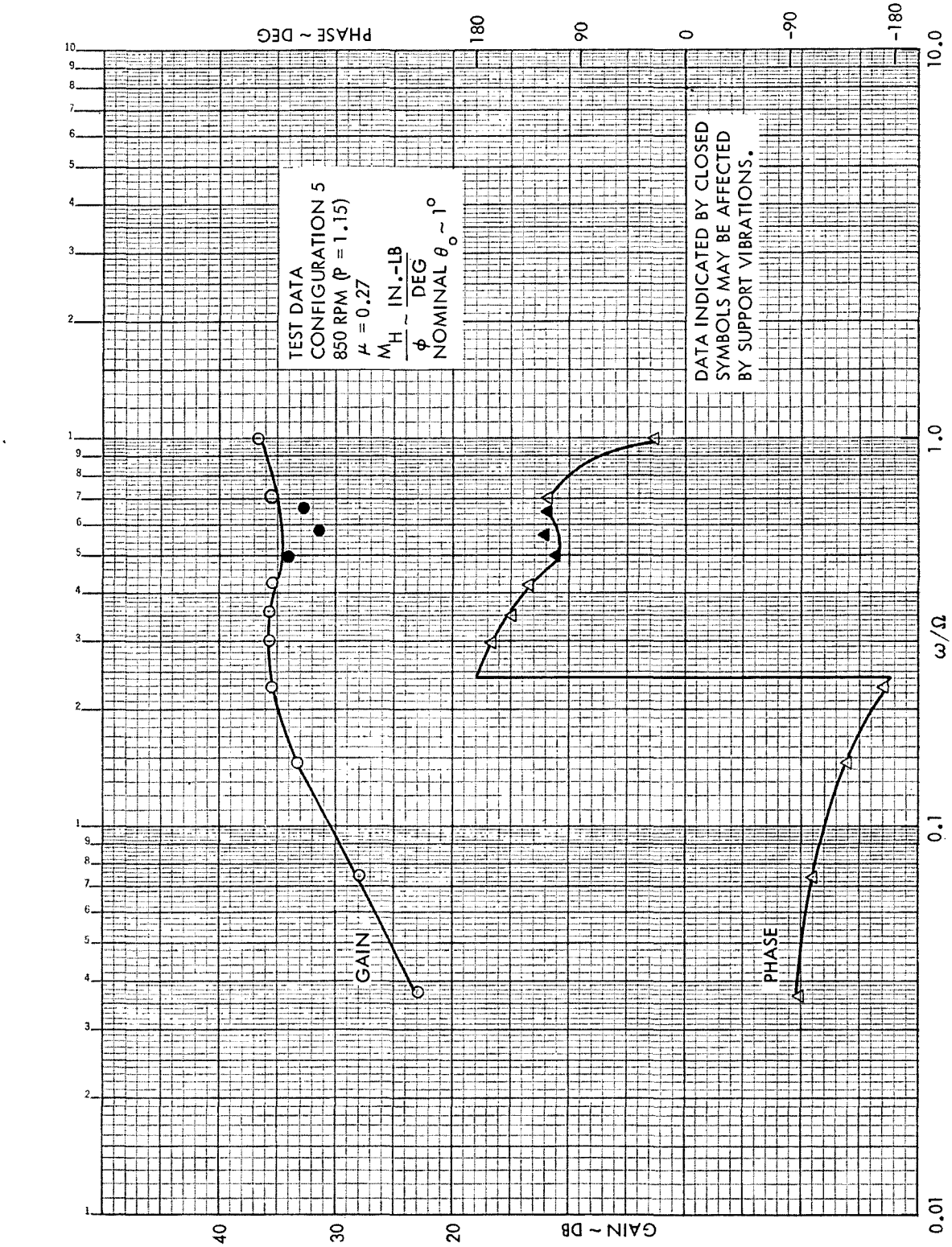

Figure 31. Rotor Hub Pitch Moment Frequency Response to Shaft Roll, Configuration 5, μ = 0.27, 850 RPM (P = 1.15)

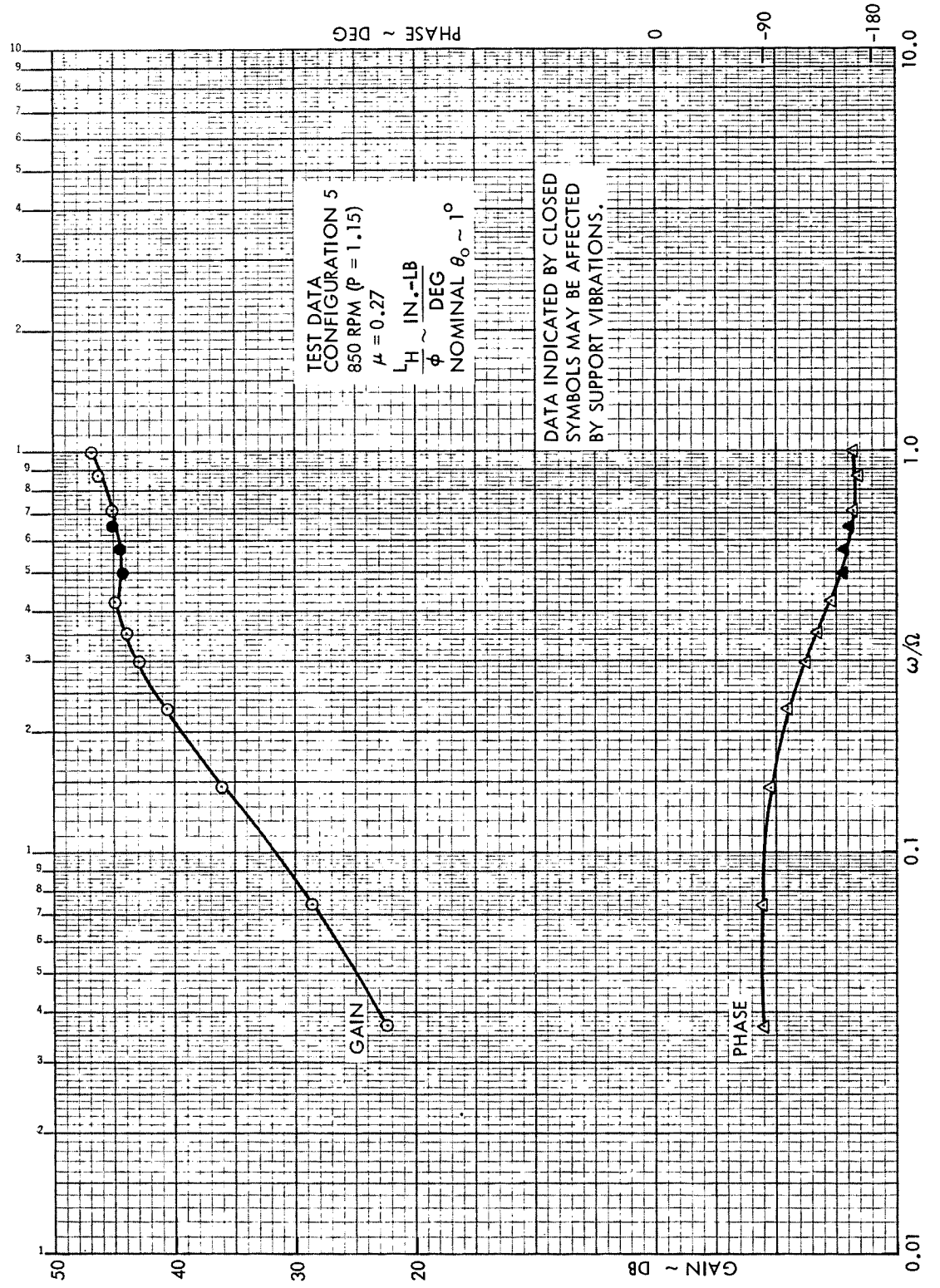

Figure 32. Rotor Hub Roll Moment Frequency Response to Shaft Roll, Configuration 5, μ = 0.27, 850 RPM (P = 1.15)

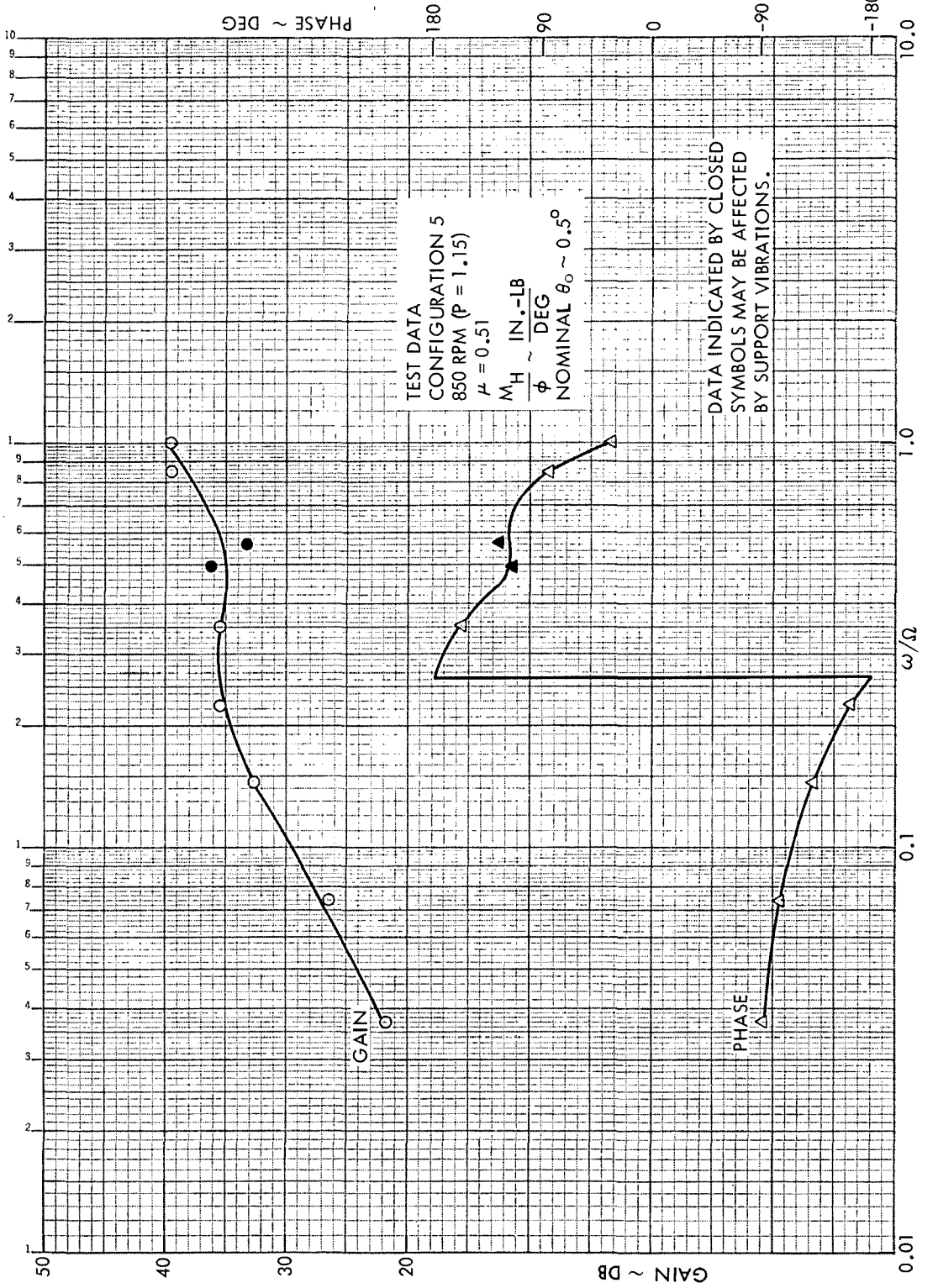

Figure 33. Rotor Hub Pitch Moment Frequency Response to Shaft Roll, Configuration 5, $\mu = 0.51$, 850 RPM (P = 1.15)

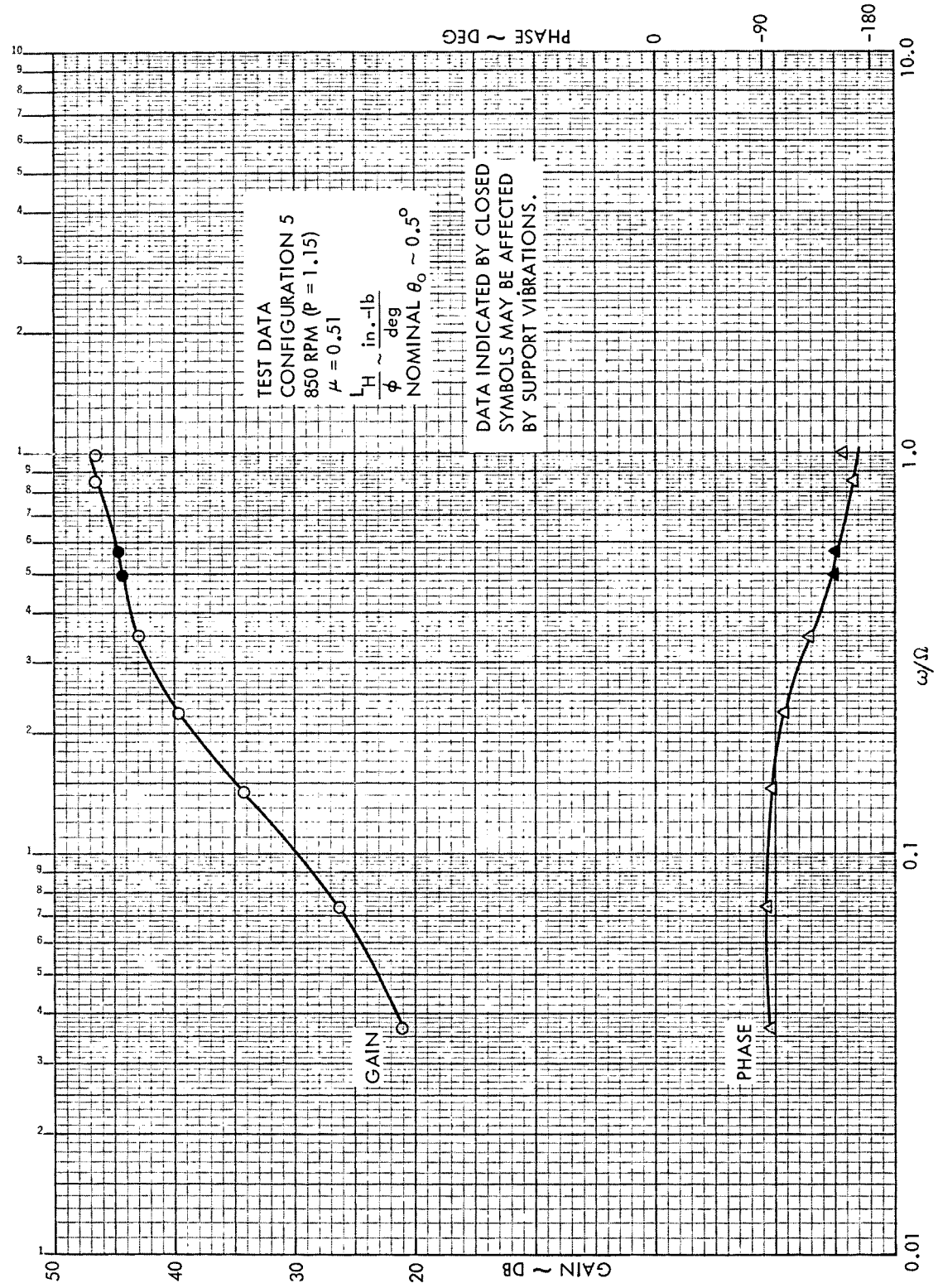

Figure 34. Rotor Hub Roll Moment Frequency Response to Shaft Roll, Configuration 5, μ = 0.51, 850 RPM (P = 1.15)

LOCKHEED CALIFORNIA COMPANY

moment response up to an excitation frequency of $\omega \sim 0.5\ \Omega$. At higher frequencies the transfer functions are the same. The phase lag of the response is also affected only slightly over the tested excitation frequency range.

Rotor frequency response to α is plotted in Figures 35 through 38 at the same test conditions (i.e., configuration 5, 850 rpm $\mu = 0.27$ and $\mu = 0.51$). By comparing similar response data at the two advance ratios, the aerodynamic effect of forward speed is seen. Based upon the roll frequency response results it is probable that most of the increased response at the higher advance ratio is due to α rather than $\dot{\alpha}$. It is noted, however, that the aerodynamic excitation of blade flapping by $\dot{\alpha}$ and $\dot{\phi}$ are not identical.

Closed Loop Frequency Response Tests (Rotor Shaft Excitations)

A major portion of the Phase 2 study was spent in determining the dynamic characteristics of hingeless rotors equipped with hub moment feedback controls. The model control system is electronic and consists of two decoupled first order lag filters which have variable gains and time constants. The resolved rotor hub pitching and rolling moments constitute the feedback signals to the control filters. The control system outputs, in turn, drive the longitudinal and lateral cyclic pitch actuators. For a complete description of the closed loop system, the reader is referred to Section 3 of Reference 2.

In order to further evaluate the first order lag feedback control system, several closed loop tests were conducted during the Phase 3 program. The object of the experiments was to determine the effectiveness of the electronic control device in alleviating the rotor response to the external disturbances generated by shaft motion. One rotor and control system configuration was considered, i.e.,

Rotor Configuration 1 ($\gamma = 5.0$)

800 rpm ($P = 1.33$)

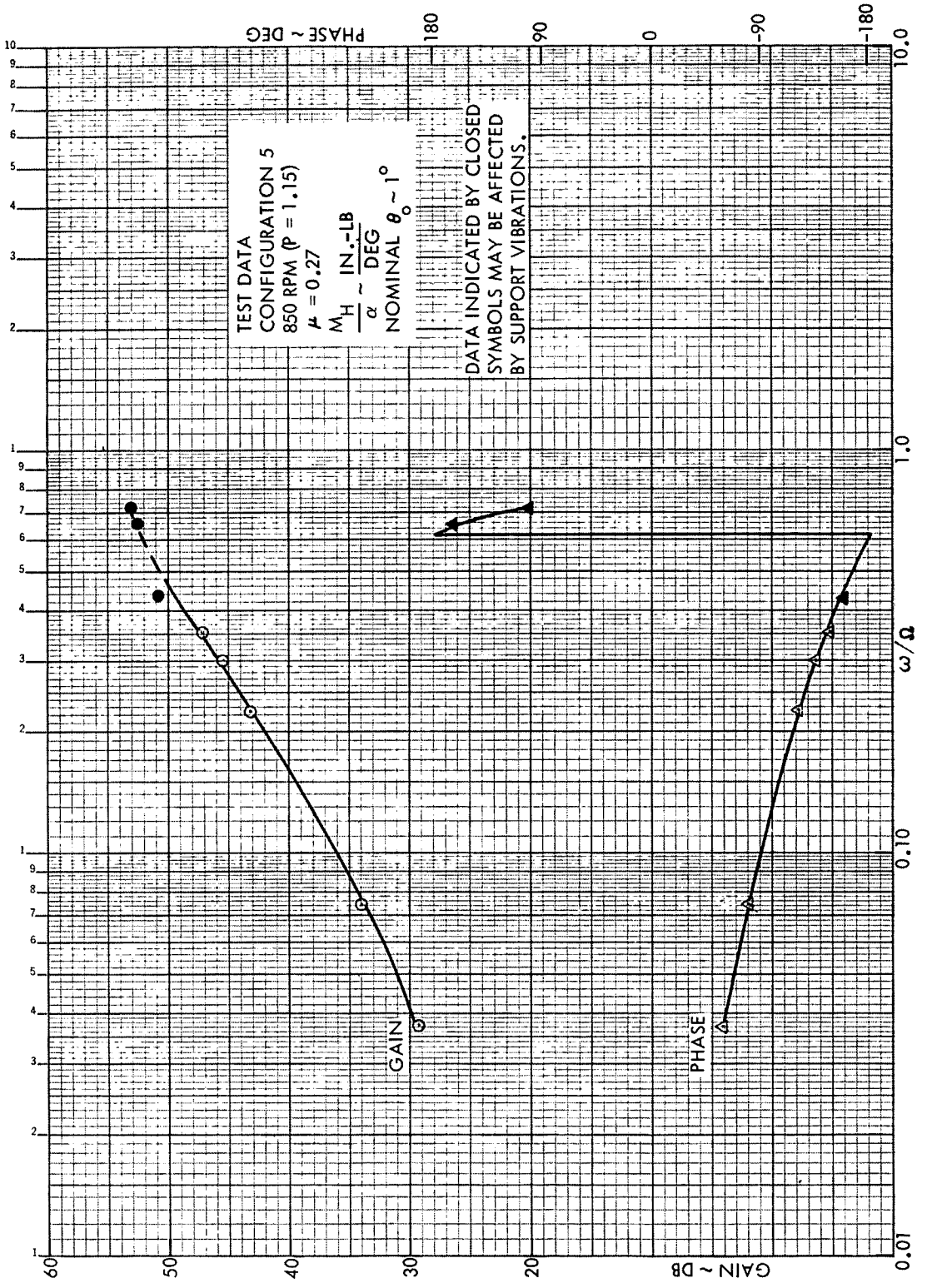

Figure 35. Rotor Hub Pitch Moment Frequency Response to Shaft Pitch, Configuration 5, μ = 0.27, 850 RPM (P = 1.15)

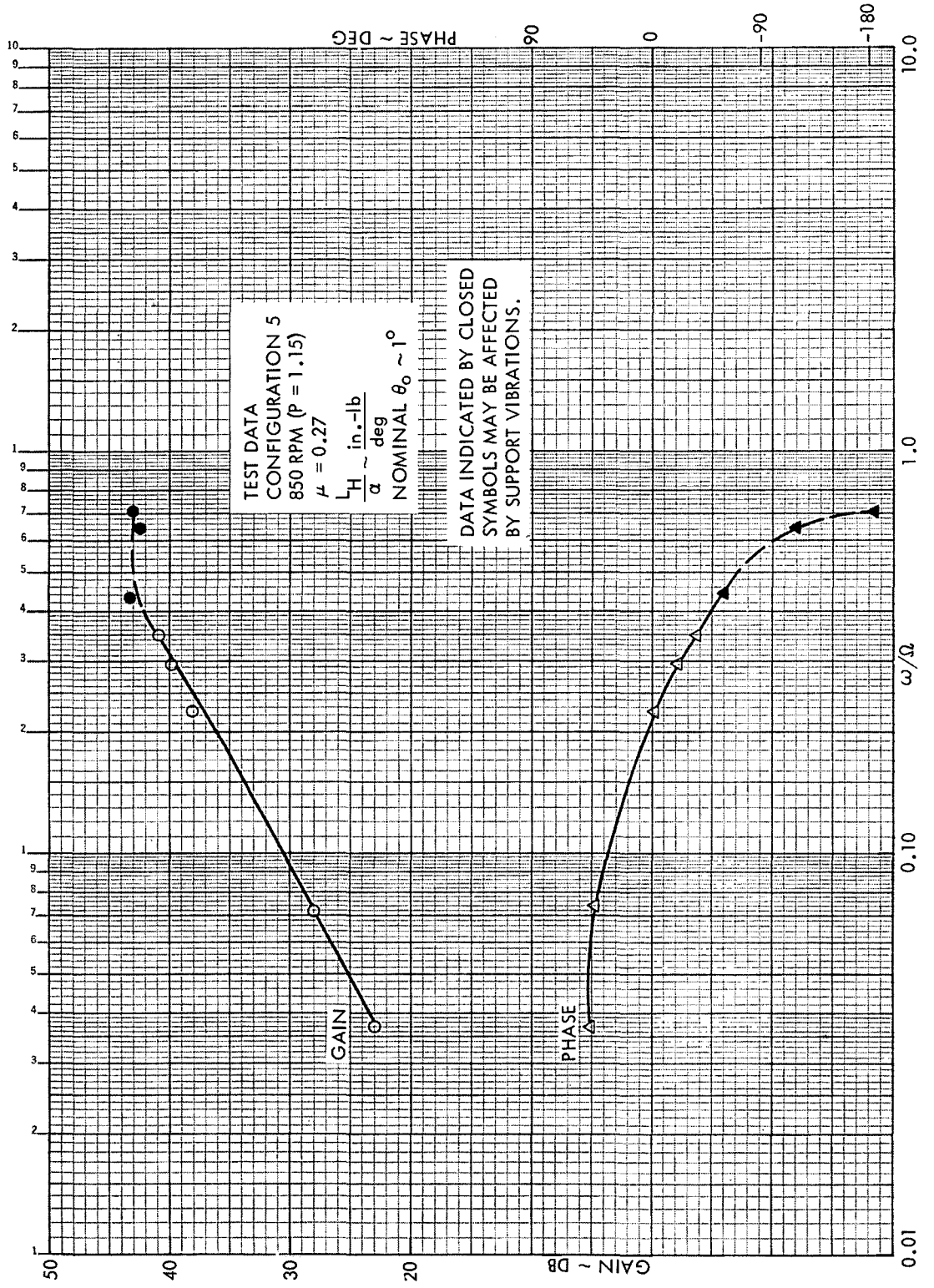

Figure 36. Rotor Hub Roll Moment Frequency Response to Shaft Pitch, Configuration 5, μ = 0.27, 850 RPM (P = 1.15)

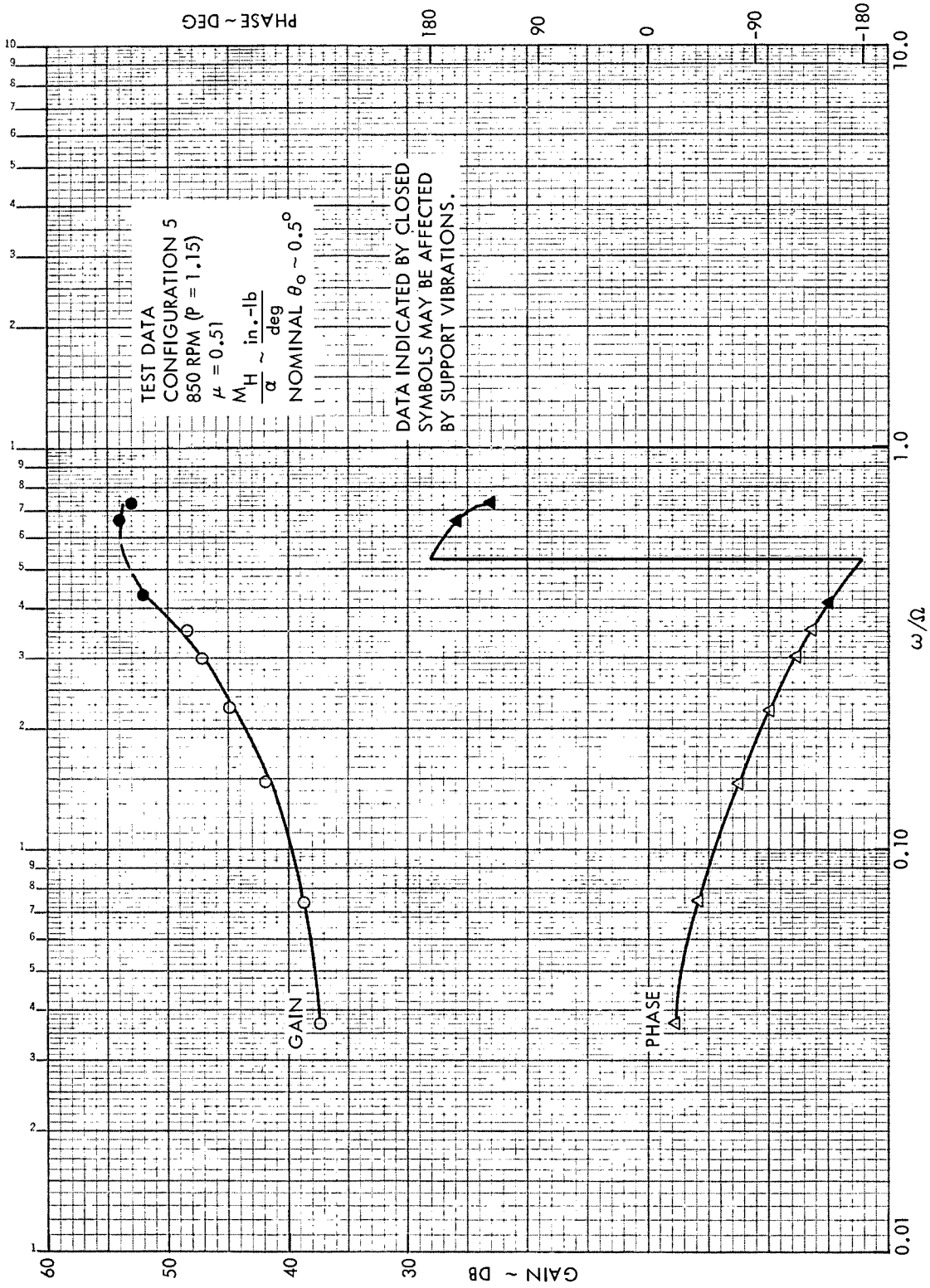

Figure 37. Rotor Hub Pitch Moment Frequency Response to Shaft Pitch, Configuration 5, μ = 0.51, 850 RPM (P = 1.15)

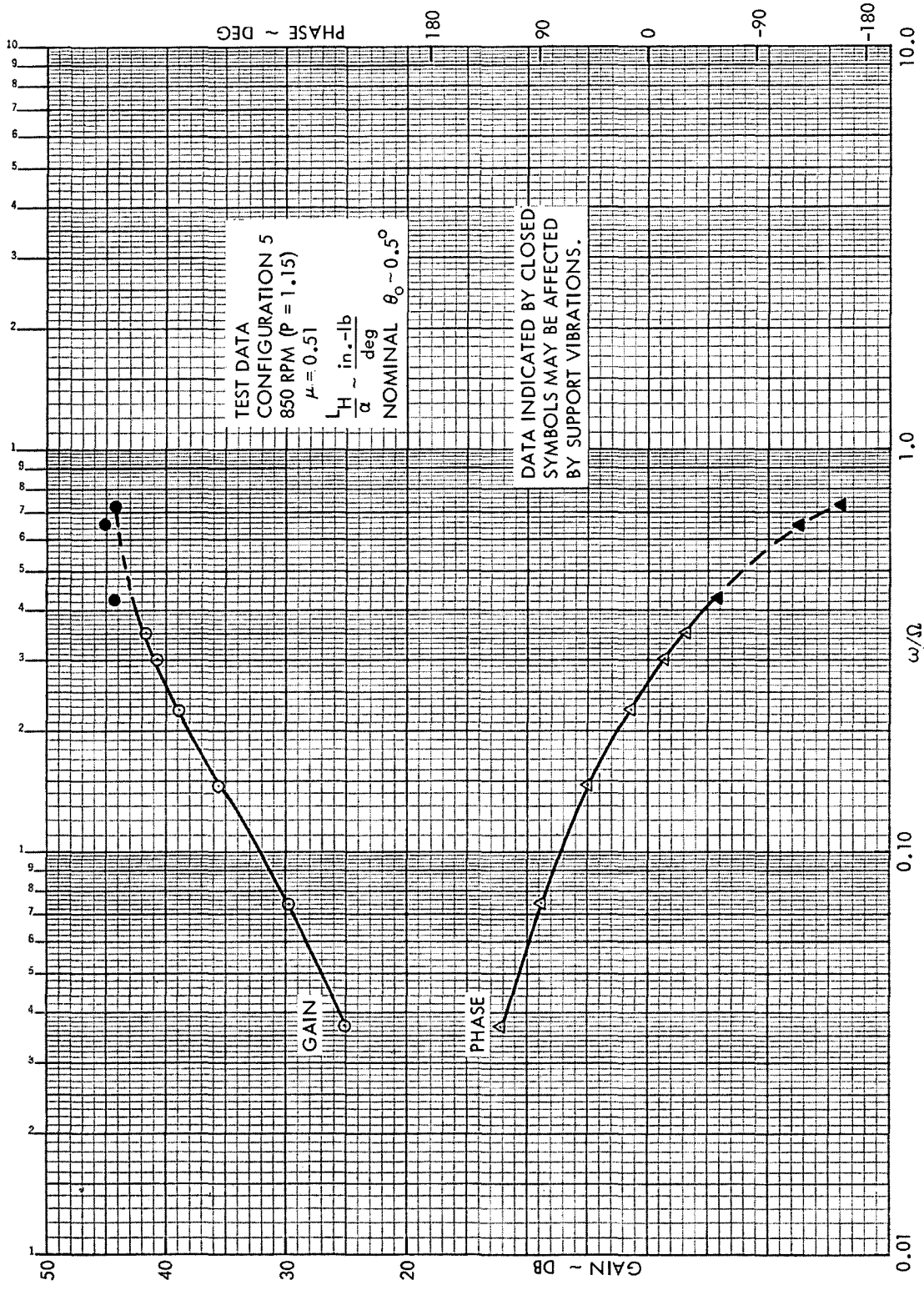

Figure 38. Rotor Hub Roll Moment Frequency Response to Shaft Pitch, Configuration 5, μ = 0.51, 850 RPM (P = 1.15)

Control System Parameters

$A = 0.5$

$L = 0$

$\Delta = 0$ deg

$\Gamma = 0$ deg

The closed loop rotor hub moment frequency response to shaft roll at $\mu = 0$ is presented in Figures 39 and 40. A comparison of these data with similar open loop results (i.e., Figures C33 and C34) indicates the feedback control system is mildly effective in alleviating the external disturbance at low excitation frequencies and ineffective or even deteriorating at higher frequencies. These characteristics are consistent with similar Phase 2 test results where a collective pitch excitation comprised the external disturbance of the closed loop system.

Closed loop frequency response test results at $\mu = 0.28$ are shown in Figures 41 and 42. For these data the excitation was shaft pitch. Generally the rotor characteristics are the same as those obtained at $\mu = 0$. The effectiveness of the control system at low frequencies is somewhat greater, however. (Comparable open loop data are plotted in Figures C25 and C26.) This is simply due to the fact that the rotor open loop response to α at $\mu = 0.28$ is greater than the response to ϕ at $\mu = 0$ and thus there is more moment response to relieve. The peaking of the closed loop response at $\omega/\Omega \sim 0.23$ is the result of a natural mode associated with the feedback control system.

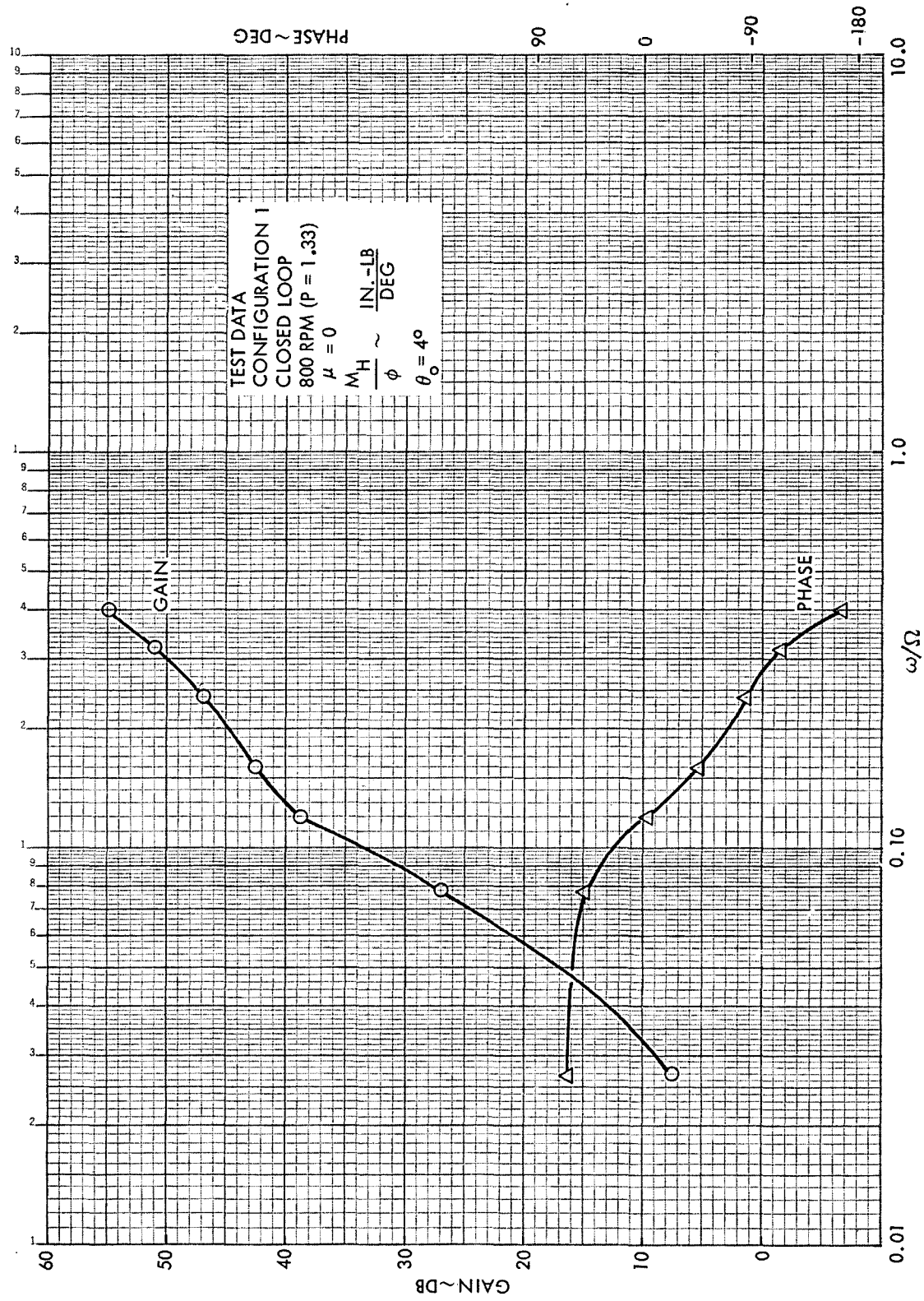

Figure 39. Closed Loop Rotor Hub Pitch Moment Frequency Response to Shaft Roll, Configuration 1, μ = 0, 800 RPM (P = 1.33), (A = 0.5, L = 0, $\Delta = \Gamma = 0°$)

LOCKHEED
CALIFORNIA COMPANY

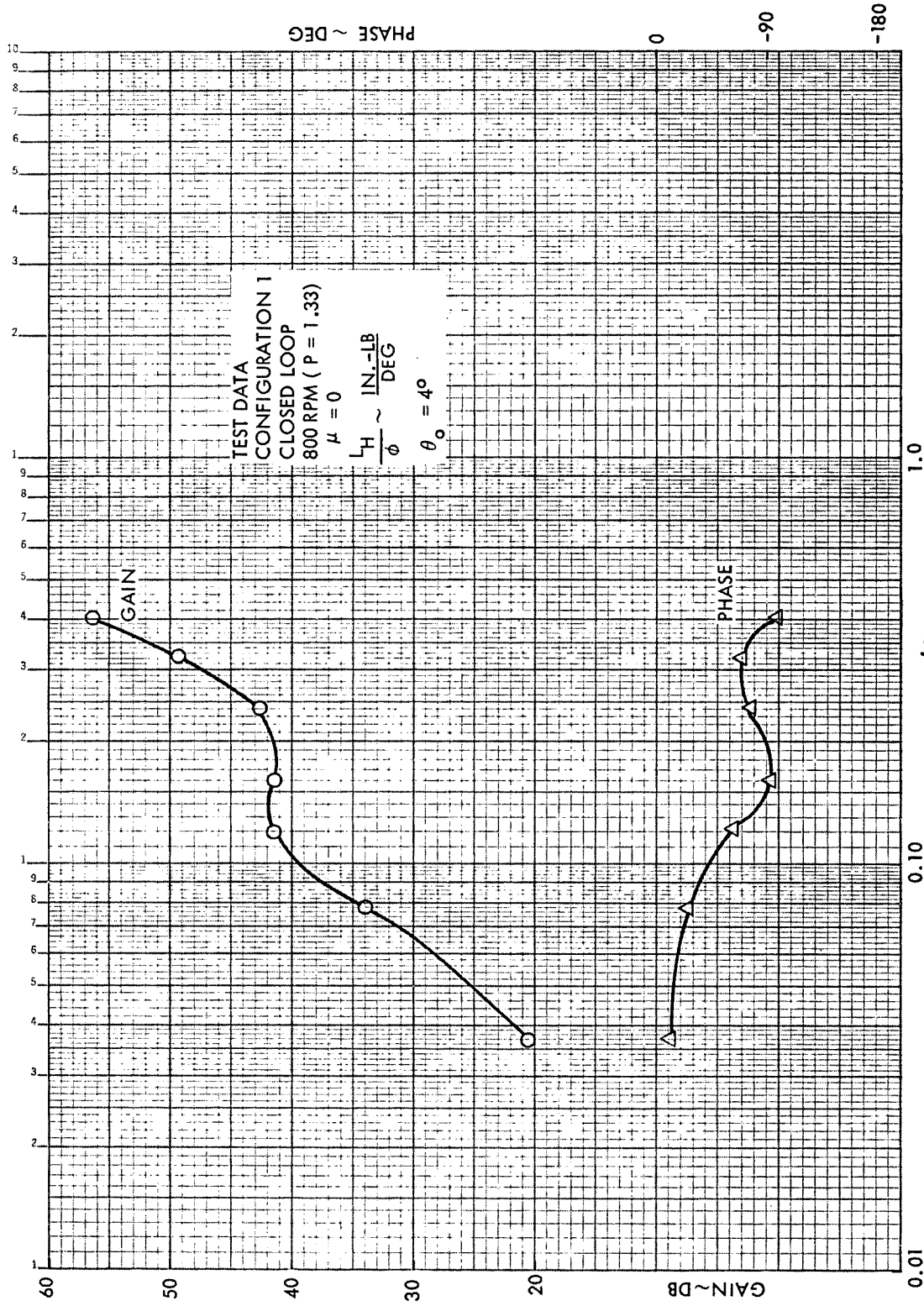

Figure 40. Closed Loop Rotor Hub Roll Moment Frequency Response to Shaft Roll, Configuration 1, μ = 0, 800 RPM (P = 1.33), (A = 0.5, L = 0, $\Delta = \Gamma = 0°$)

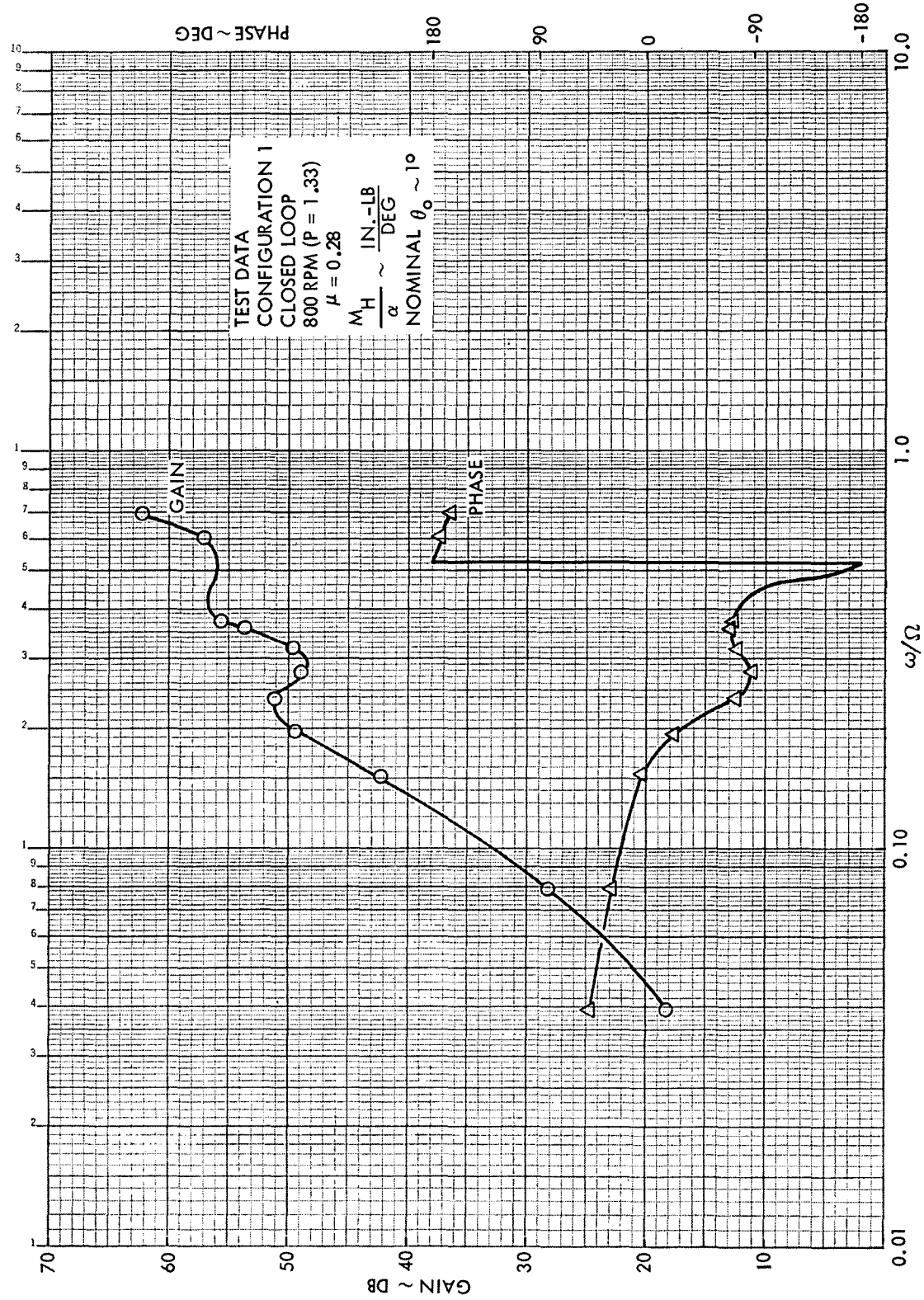

Figure 41. Closed Loop Rotor Hub Pitch Moment Frequency Response to Shaft Pitch, Configuration 1, μ = 0.28, 800 RPM (P = 1.33), (A = 0.5, L = 0, $\Delta = \Gamma = 0°$)

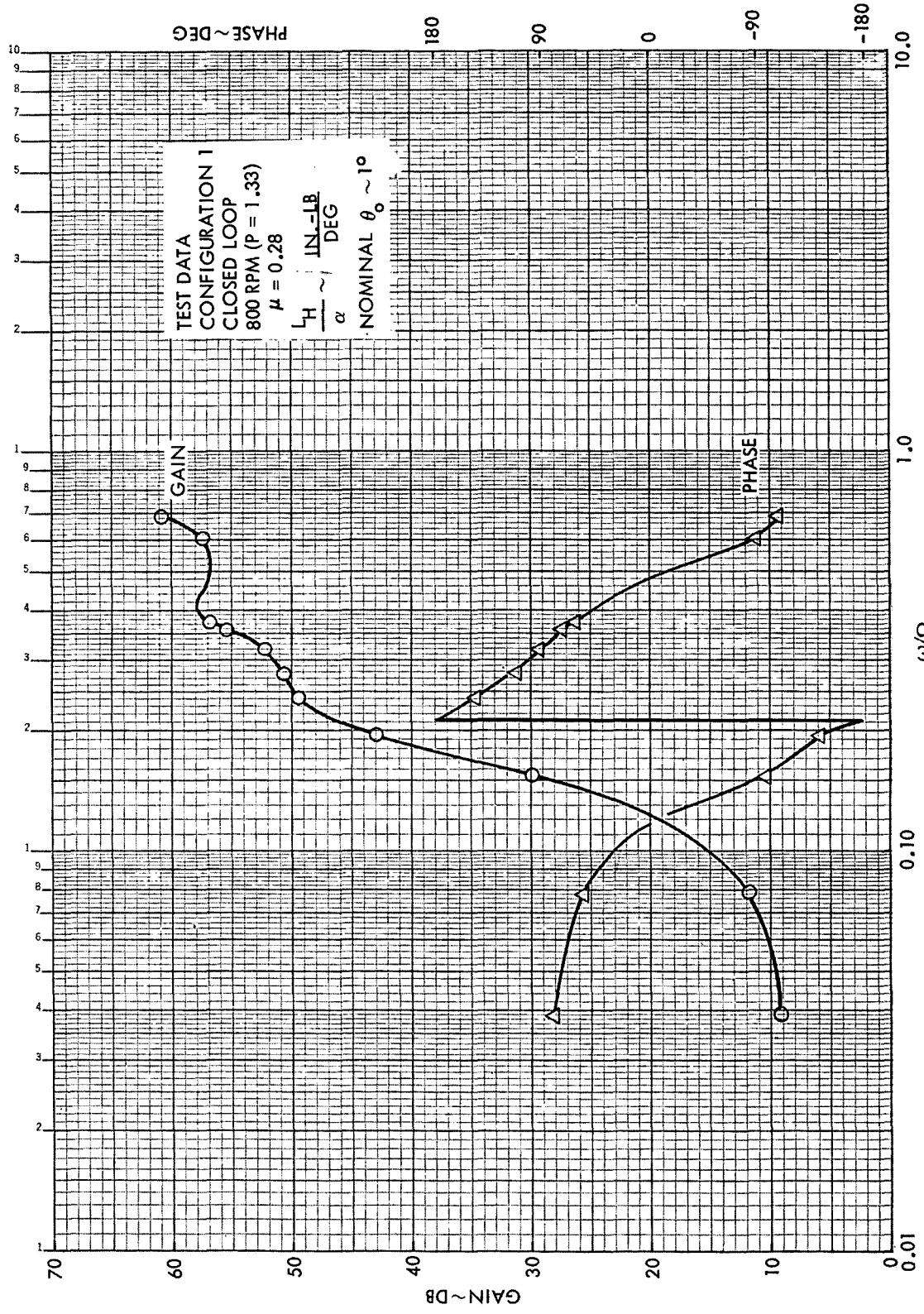

Figure 42. Closed Loop Rotor Hub Roll Moment Frequency Response to Shaft Pitch, Configuration 1, μ = 0.28, 800 RPM (P = 1.33) (A = 0.5, L = 0, $\Delta = \Gamma = 0°$)

SECTION 6

COMPARISON OF THEORETICAL AND EXPERIMENTAL DATA

An important part of the Lockheed/AMRDL High Advance Ratio Research Program has been the evaluation of a simple rotor theory by comparing analytical and experimental data. The correlation effort, previous results of which are reported in References 1 and 2, has been continued during the Phase 3 program. The open loop rotor frequency response to shaft pitch and roll constitute the data which were correlated for the current study.

THEORY

The mathematical rotor model is completely defined in Section 7 of Reference 2. It consists of four untwisted rigid blades which flap individually and inelastically about a centrally arranged flapping hinge. Each blade is restrained by a hypothetical spring which is selected so that the rigid blade flapping frequency is identical to the first flap mode natural frequency of the elastic blade being simulated. Steady state aerodynamic theory is used and the effects of blade stall, Mach number and deviations from a uniform induced velocity field are ignored. Reversed flow is totally accounted for resulting in equations which are valid over the complete advance ratio range, $\mu = 0 \rightarrow \infty$.

The flapping equations of motion in Reference 2 do not include shaft pitch and roll forcing functions. The mass moment acting on the i^{th} blade of a four-bladed rotor due to steady pitch and roll angular rates and accelerations is

$$\frac{M_{Y_i}}{R^4 \rho a \frac{c}{2}} = \frac{2}{\gamma}\left\{\cos\left[\psi + (i-1)\frac{\pi}{2}\right]\ (2\Omega\dot{\phi} + \ddot{\alpha}) + \sin\left[\psi + (i-1)\frac{\pi}{2}\right]\ (-2\Omega\dot{\alpha} + \ddot{\phi})\right\} \qquad (15)$$

The aerodynamic moment is

$$\frac{M_{Y_i}}{R^4 \rho a \frac{c}{2}} = \Omega \dot{\phi} m_{\dot{\phi}} \left[\psi + (i-1)\frac{\pi}{2}\right] + \Omega \dot{\alpha} m_{\dot{\alpha}} \left[\psi + (i-1)\frac{\pi}{2}\right] \tag{16}$$

where $i = 1, 2, 3$ or 4,

$$\left.\begin{aligned} m_{\dot{\alpha}}(\psi) &= \cos(\psi) C(\psi) \\ m_{\dot{\phi}}(\psi) &= \sin(\psi) C(\psi) \end{aligned}\right\} \tag{17}$$

and $C(\psi)$ is the periodic aerodynamic damping of blade flapping. Combining equations (15) and (16) with the flapping equations of motion (i.e., equation (1) of Reference 2) yields

$$\begin{aligned} &\frac{2}{\gamma}\ddot{\beta}_i + \Omega \dot{\beta}_i C\left[\psi + (i-1)\frac{\pi}{2}\right] + \Omega^2 \beta_i \left\{\frac{2}{\gamma} P^2 + K\left[\psi + (i-1)\frac{\pi}{2}\right]\right\} \\ &= \alpha \Omega^2 m_{\alpha}\left[\psi + (i-1)\frac{\pi}{2}\right] + \Omega^2 \left\{\theta_o + \theta_s \sin\left[\psi + (i-1)\frac{\pi}{2}\right] \right. \\ &\left. + \theta_c \cos\left[\psi + (i-1)\frac{\pi}{2}\right]\right\} m_{\theta_o}\left[\psi + (i-1)\frac{\pi}{2}\right] \\ &+ \frac{2}{\gamma}\left\{\cos\left[\psi + (i-1)\frac{\pi}{2}\right](2\Omega\dot{\phi} + \ddot{\alpha}) + \sin\left[\psi + (i-1)\frac{\pi}{2}\right](-2\Omega\dot{\alpha} + \ddot{\phi})\right\} \\ &+ \Omega \dot{\phi} m_{\dot{\phi}}\left[\psi + (i-1)\frac{\pi}{2}\right] + \Omega \dot{\alpha} m_{\dot{\alpha}}\left[\psi + (i-1)\frac{\pi}{2}\right] \end{aligned} \tag{18}$$

Equation (18) was solved using the techniques described in Section 7 of Reference 2 to obtain rotor transfer functions with respect to rotor shaft pitch and roll oscillations.

CORRELATION RESULTS

Only experimental data for configuration 1 have been compared with theoretical data. Typical correlation results are shown in Figures 43 through 48. The measured test derivatives have been nondimensionalized by the rotor stiffness, K_{θ}, in order to obtain data which are compatible with the theoretical

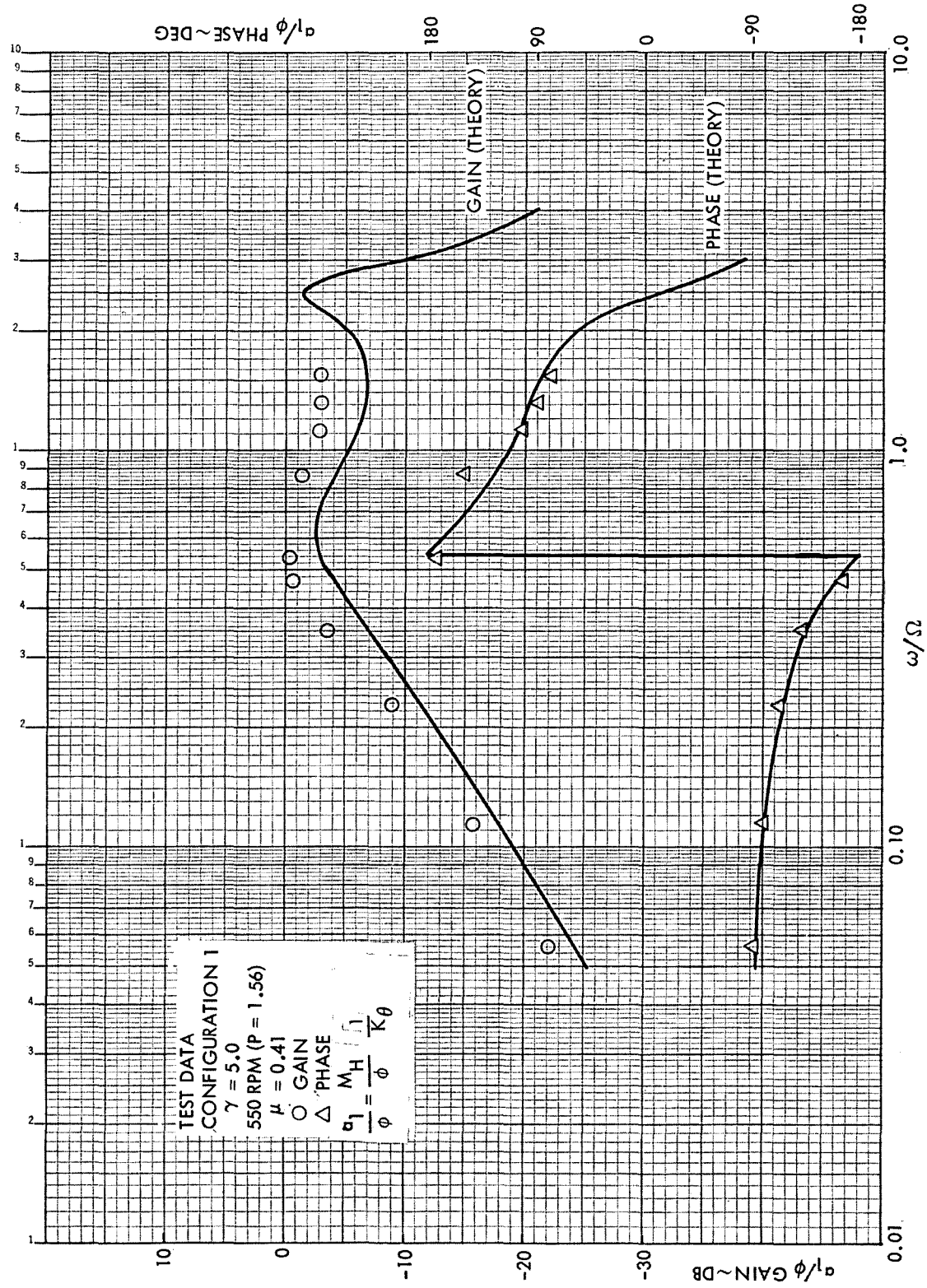

Figure 43. Comparison of Experimental and Theoretical Data, Rotor Longitudinal Frequency Response to ϕ, Configuration 1, μ = 0.41, 550 RPM (P = 1.56)

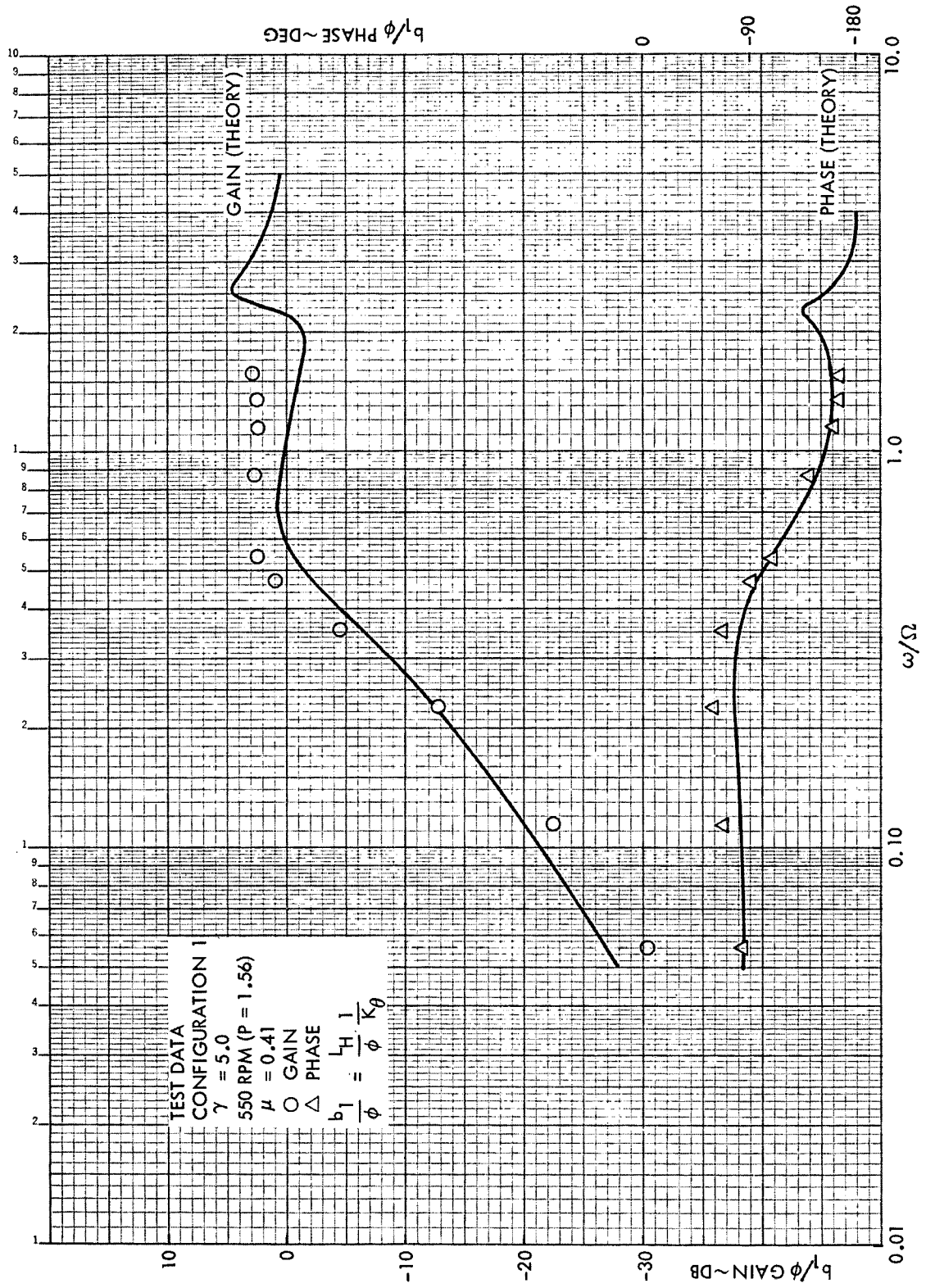

Figure 44. Comparison of Experimental and Theoretical Data, Rotor Lateral Frequency Response to Φ, Configuration 1, μ = 0.41, 550 RPM (P = 1.56)

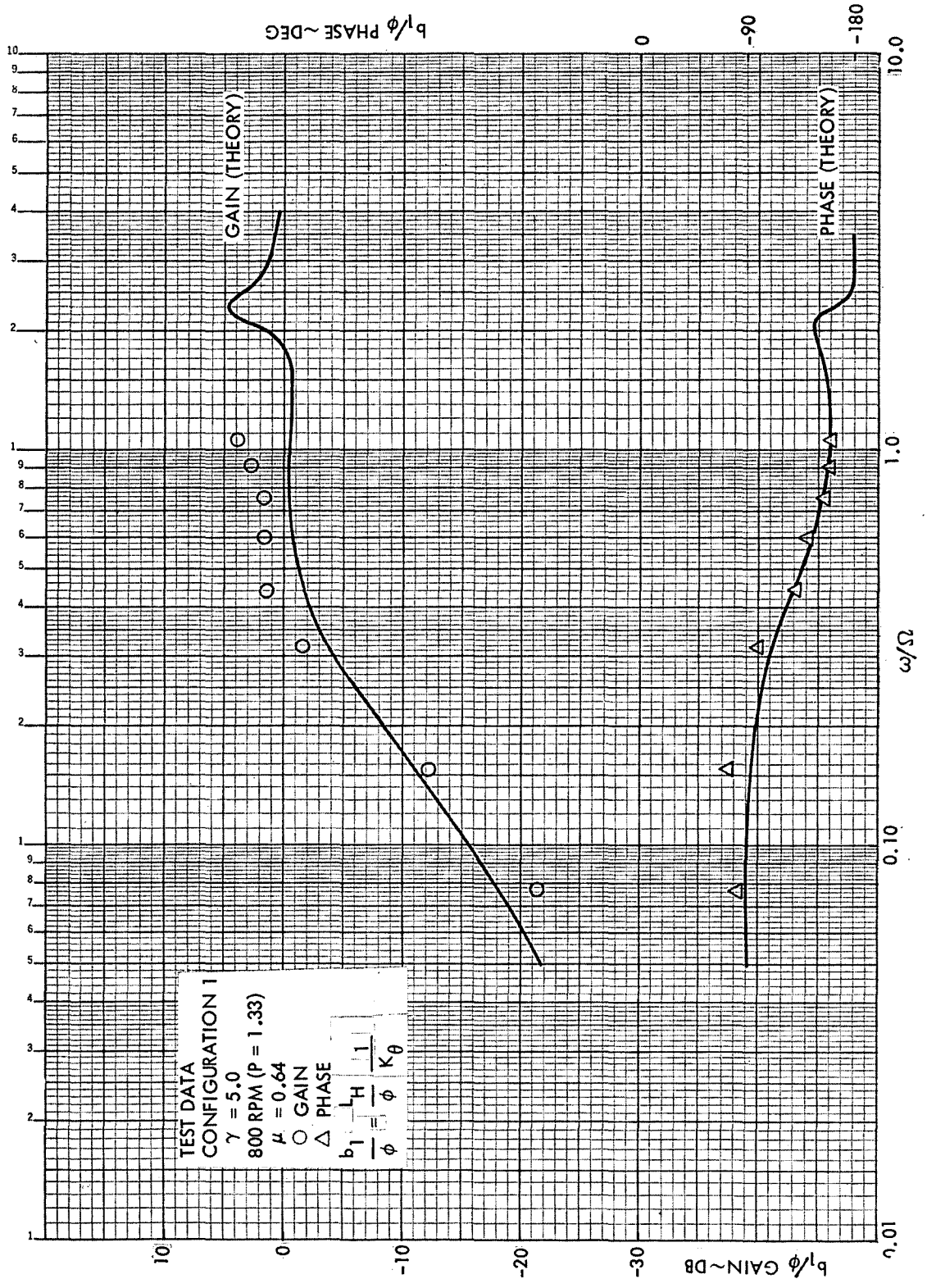

Figure 45. Comparison of Experimental and Theoretical Data, Rotor Lateral Frequency Response to Φ, Configuration 1, μ = 0.64, 800 RPM (P = 1.33)

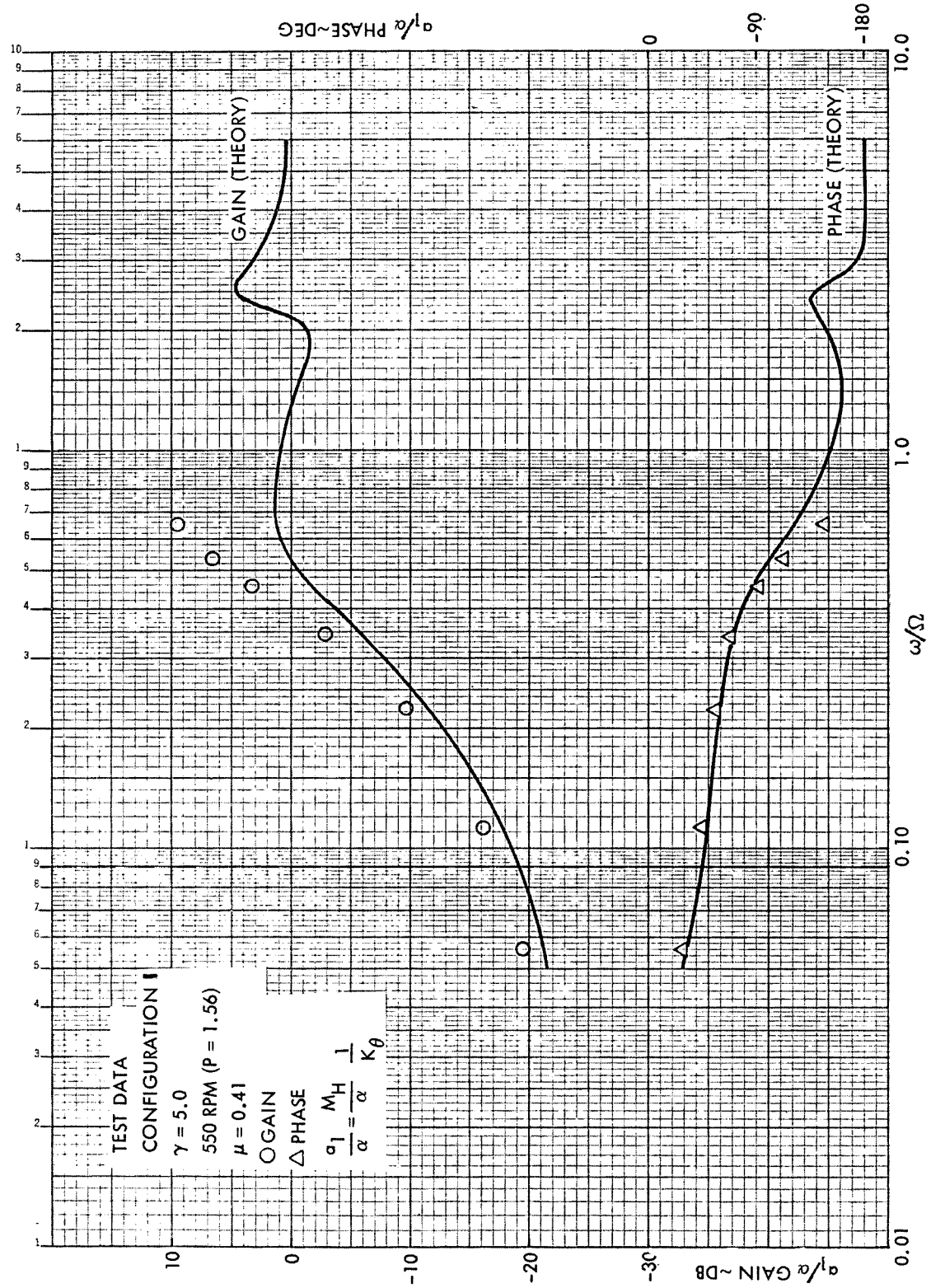

Figure 46. Comparison of Experimental and Theoretical Data, Rotor Longitudinal Frequency Response to α, Configuration 1, μ = 0.41, 550 RPM (P = 1.56)

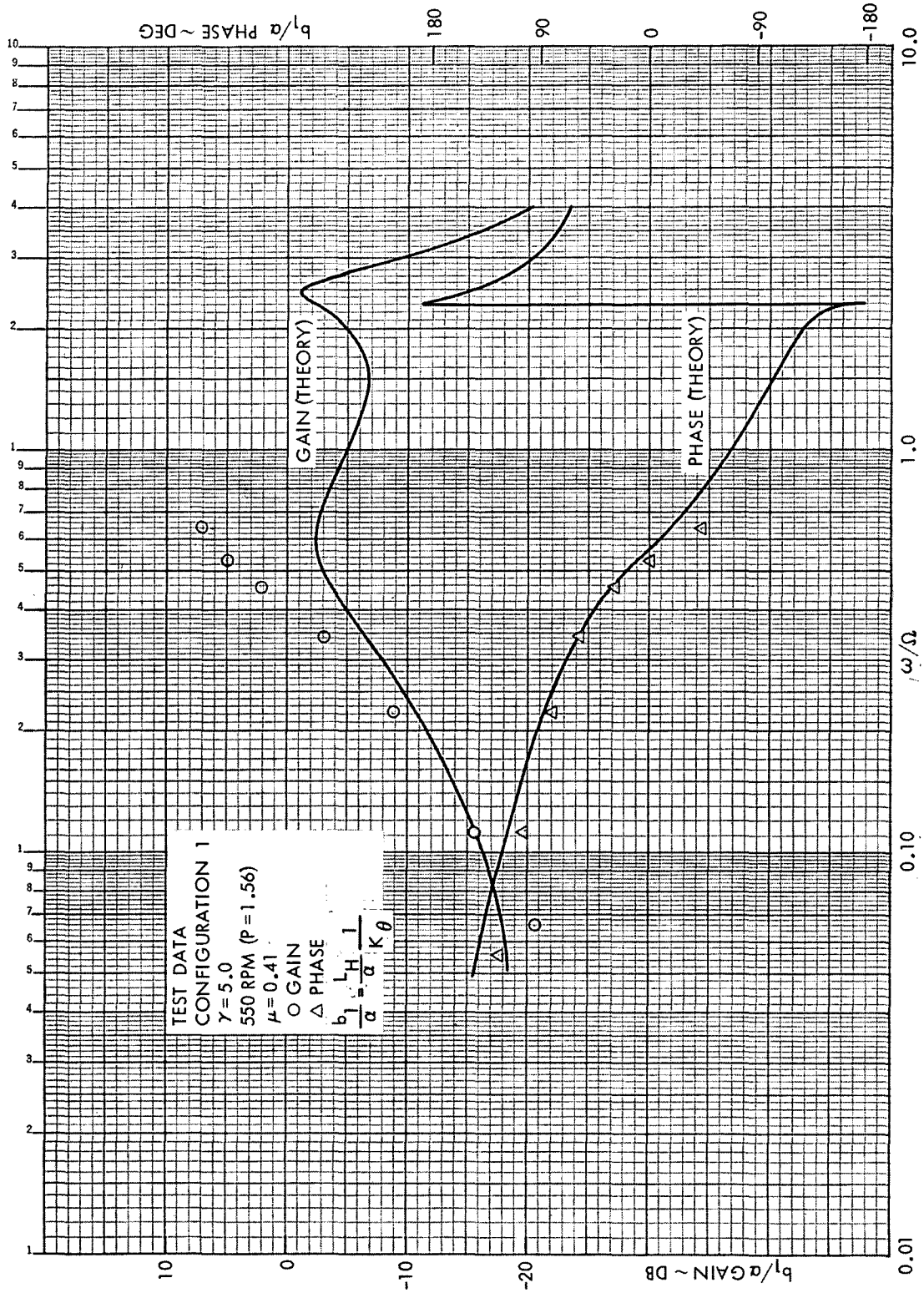

Figure 47. Comparison of Experimental and Theoretical Data, Rotor Lateral Frequency Response to α, Configuration 1, μ = 0.41, 550 RPM (P = 1.56)

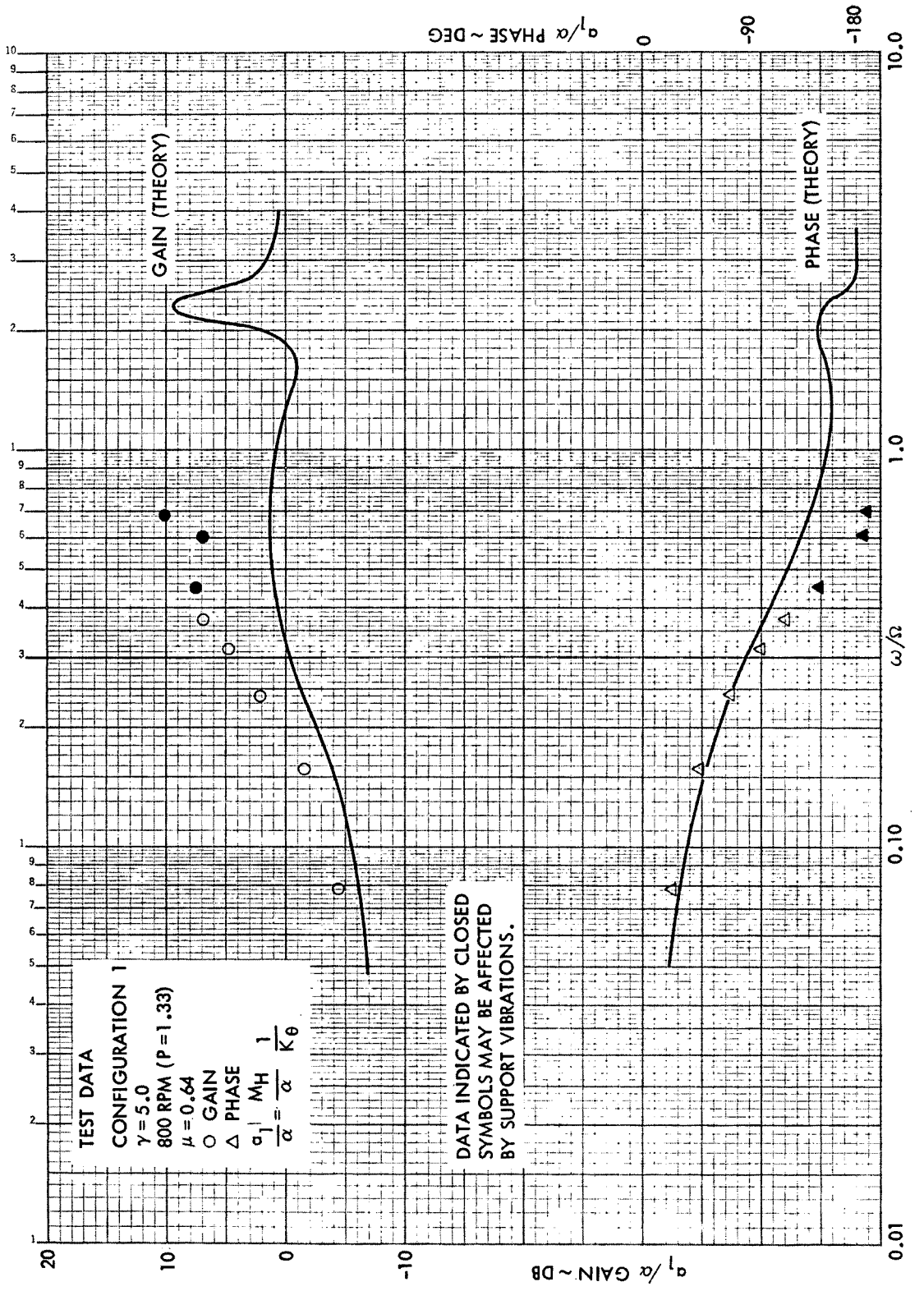

Figure 48. Comparison of Experimental and Theoretical Data, Rotor Longitudinal Frequency Response to α, Configuration 1, $\mu = 0.64$, 800 RPM ($P = 1.33$)

results. K_θ varies with rotor rotational speed and blade structural stiffness (Reference 1). For the data presented, K_θ = 327 in.-lb/deg at 550 rpm and K_θ = 348 in.-lb/deg at 800 rpm.

Without discussing Figures 43 through 48 individually, the following observations are offered concerning the correltation results. With the exception of the absolute gains, good agreement exists between theoretical and experimental frequency response to shaft roll. It is probable that the discrepancies in the magnitudes of the derivatives are due to the procedure by which the test data were nondimensionalized as much as the theory itself. It is highly unlikely that a single value of K_θ (which is based upon the first flap mode response at μ = 0) is valid for all excitation frequencies and forward speeds.

The correlation results for shaft pitch oscillations are not quite as good as for shaft roll. Agreement does exist at low excitation frequencies for both gain and phase data. At higher frequencies, however, the experimental data exhibit greater peaking and more phase lag than the theory. This implies that the actual rotor flap damping is less than that predicted theoretically. The experimental frequency response data for shaft roll excitations also manifest this characteristic to a lesser degree. It is noted that similar correlations of frequency response to swashplate excitations (Reference 2) also suggested that the actual flap damping was less than that predicted analytically.

SECTION 7

CONCLUDING REMARKS

The third phase of the Lockheed/AMRDL "High Advance Ratio Research Program" was primarily an experimental activity. The hingeless rotor data bank establish during the earlier two phases of the program was expanded by testing a larger advance ratio/flap frequency (μ/P) envelope and by determining rotor frequency response to shaft pitch and roll for the first time.

The μ/P envelope for which rotor response data with respect to steady θ_o, θ_s, θ_c, and α excitations are available was extended to include P = 1.125 at $\mu = 0$, P = 1.15 for $\mu = 0 \rightarrow 0.82$ and P = 1.28 for $\mu = 0 \rightarrow 0.92$. The analysis of these steady state data included determining steady rotor hub moment, shaft moment and lift derivatives. The rotor rotating blade flap bending moments at three radial positions (x = 0.073, 0.293, 0.49) were also harmonically analyzed and response derivatives calculated. The characteristics of the data generally agree with previous test results. Variations in the rotor response with changes in flap frequency and advance ratio were as anticipated. Test results at $\mu = 0$ with low and moderate rotor lift levels clearly demonstrate the linear and nonlinear effects of induced inflow.

The rotor frequency response data bank with θ_o, θ_s and θ_c excitations was expanded to include P = 1.15 for $\mu = 0 \rightarrow 0.60$ and P = 1.28 for $\mu = 0 \rightarrow 0.92$. These newly acquired transfer functions have the same characteristics as similar Phase 2 data. The rotor response was a maximum when the excitation frequency was in resonance with the blade first flap bending mode natural frequency. A mild involvement of the blade second flap bending mode in the response was noted at several test conditions. The frequency response characteristics also indicate that the damping of the blade flapping motion increases with advance ratio and that induced inflow is an important consideration only at low excitation frequencies.

Experimental rotor transfer functions with respect to shaft pitching (α) and rolling (ϕ) oscillations were obtained for nondimensional flap frequencies ranging from P = 1.15→1.56 and advance ratios from μ = 0→ to 0.93. The data indicate that the major part of the rotor response is caused by the inertial and gyroscopic excitations. Aerodynamic excitations due to $\dot{\alpha}$ and $\dot{\phi}$ are conparatively weak and the aerodynamic excitation due to α is only a factor at low frequencies.

Several closed loop frequency tests with α and ϕ excitations were also conducted to further evaluate the Phase 2 hub moment feedback control system. The closed loop response characteristics were approximately the same as those previously obtained. That is, the control network was only effective in reducing the rotor response to the shaft excitations at very low frequencies.

Selected experimental rotor transfer functions with α and ϕ excitations were compared with theoretical results in order to assess the validity of the mathematical model. The rigid blade flapping theory agreed reasonably well with the test results, a finding which is consistent with previous correlation efforts.

The hingeless rotor data bank, which has been formed by testing the 7 1/2-foot diameter Lockheed/AMRDL rotor model is characterized by low nominal rotor lift levels. A follow-on effort which is currently in the planning stages will involve testing the model at high rotor lifts. The testing will be open loop and include both steady response and frequency response. These results will greatly compliment the existing data by defining the conditions where the linear rotor derivatives are valid.

SECTION 8

REFERENCES

1. Kuczynski, W. A., and Sissingh, G. J., RESEARCH PROGRAM TO DETERMINE ROTOR RESPONSE CHARACTERISTICS AT HIGH ADVANCE RATIOS, NASA CR 114290, LR 24122, Feb. 1971

2. Kuczynski, W. A., and Sissingh, G. J., CHARACTERISTICS OF HINGELESS ROTORS WITH HUB MOMENT FEEDBACK CONTROLS INCLUDING EXPERIMENTAL ROTOR FREQUENCY RESPONSE, LR 25048, Vol. I NASA CR 114427, Vol. II NASA CR 114428, Jan. 1972

3. Ormiston, R. A., and Peters, D. A., HINGELESS ROTOR RESPONSE WITH NONUNIFORM INFLOW AND ELASTIC BLADE BENDING - THEORY AND EXPERIMENT, AIAA Paper No. 72-65, Presented at the AIAA 10th Aerospace Sciences Meeting, San Diego, California, Jan. 17 - 19, 1972

APPENDIX A

EXPERIMENTAL STEADY STATE ROTOR RESPONSE DATA

The data used to calculate the steady lift and moment derivatives presented in Section 5 of this report are tabulated herein. Measured values of Ω, μ, θ_o, θ_s, θ_c, α, M_H, L_H, M_s, L_s and LIFT are listed in Table IV for each test point. For each data set, where one of the four excitations was varied while the other three were held constant, a linear least squares curve fit of the five responses was used to determine steady derivatives. These are noted in the tabulations as slopes. The deviation of each datum from the statistical line was also calculated and is labeled an error. The errors are useful as a quick check of the linearity of the data.

All of the rotating blade bending moment data are listed in Table V. Derivatives were also determined from these data with a linear least squares curve fit. They are plotted in Figures A1 through A12. The one-per-rev blade bending moment distributions are used in Appendices B and C to transfer hub moment frequency response data to the rotor shaft centerline.

TABLE IV

EXPERIMENTAL STEADY ROTOR RESPONSE TO θ_o, θ_s, θ_c AND α, CONFIGURATION 5

						M_H			L_H			M_S			L_S			LIFT		
Ω rad/sec	μ	θ_o deg	θ_s deg	θ_c deg	α deg	Mag in-lb	Slope in-lb/deg	Error in-lb	Mag in-lb	Slope in-lb/deg	Error in-lb	Mag in-lb	Slope in-lb/deg	Error in-lb	Mag in-lb	Slope in-lb/deg	Error in-lb	Mag lb	Slope lb/deg	Error lb
57.6	0.0	1.98	-0.03	0.23	0.0	-4	*		-5	*		-3	*		-5	*		0	0	-2
57.6	0.0	1.96	2.03	0.22	0.0	6			-64			12			-96			1		1
57.5	0.0	1.98	3.86	0.22	0.0	11			-130			17			-191			3		1
57.5	0.0	1.98	4.88	0.22	0.0	23			-188			38			-275			3		1
57.6	0.0	1.98	-1.85	0.23	0.0	-8			49			-9			81			0		-1
57.5	0.0	1.98	-3.98	0.23	0.0	-21			125			-31			189			2		1
57.5	0.0	1.98	-6.12	0.23	0.0	-47			233			-63			344			3		1
57.4	0.0	3.94	0.03	0.23	0.0	-1	10	-1	-8	-44	6	4	16	4	-14	-64	6	6	0	-2
57.5	0.0	3.94	2.04	0.22	0.0	22		1	-106		-5	32		1	-158		-10	7		-1
57.5	0.0	3.94	3.90	0.22	0.0	43		3	-188		-5	65		5	-273		-6	9		1
57.4	0.0	3.94	4.76	0.22	0.0	52		2	-215		4	71		-3	-316		6	10		2
57.6	0.0	3.94	-2.07	0.23	0.0	-29		-7	81		4	-41		-7	128		13	7		-2
57.5	0.0	3.94	-3.92	0.23	0.0	-52		-11	156		-2	-70		-7	233		1	7		1
57.4	0.0	3.94	-6.31	0.23	0.0	-54		13	260		-2	-92		8	381		-6	11		3
57.4	0.0	5.90	-0.16	0.23	0.0	-4	17	-4	-12	-52	0	-2	26	-6	-15	-76	0	13	0	-2
57.3	0.0	5.90	1.89	0.22	0.0	38		3	-123		-4	59		3	-181		-11	14		1
57.2	0.0	5.90	3.90	0.22	0.0	75		6	-227		-3	121		13	-325		-2	16		1
57.2	0.0	5.90	4.70	0.22	0.0	79		-3	-265		0	121		-6	-383		0	17		1
57.3	0.0	5.90	-2.07	0.22	0.0	-40		-9	98		10	-58		-13	151		21	14		1
57.2	0.0	5.90	-4.16	0.22	0.0	-67		0	204		7	-99		0	299		11	15		0
57.2	0.0	5.90	-6.31	0.22	0.0	-97		6	299		-11	-145		9	432		-19	16		1
57.5	0.0	3.99	-0.10	0.30	0.0	-8	-45	-2	-9	-11	-4	-12	-66	-7	-13	-18	5	6	0	-1
57.4	0.0	3.99	-0.11	2.37	0.0	-105		-7	-33		-4	-155		-13	-45		1	6		-2
57.4	0.0	3.99	-0.10	4.21	0.0	-184		-3	-53		-4	-269		-5	-80		-3	8		0
57.3	0.0	4.00	-0.09	6.24	0.0	-265		7	-67		6	-385		13	-108		5	11		2
57.4	0.0	4.00	-0.09	-1.56	0.0	76		-2	20		3	120		1	26		1	7		0
57.3	0.0	3.99	-0.11	-3.62	0.0	170		1	40		1	252		-3	66		5	8		2
57.4	0.0	3.99	-0.12	-2.59	0.0	132		8	29		1	202		15	41		-2	7		0
89.0	0.0	0.02	-0.05	0.15	0.0	-4	2	0	-6	-3	-3	-2	6	1	-4	-6	-10	-3	*	
88.5	0.0	2.04	-0.05	0.14	0.0	3		2	-7		3	13		3	-6		5	2		
88.2	0.0	4.00	-0.04	0.13	0.0	6		0	-12		4	21		0	-17		6	17		
88.6	0.0	5.96	-0.02	0.12	0.0	3		-8	-28		-5	18		-13	-46		-10	37		
88.3	0.0	6.92	-0.01	0.12	0.0	20		6	-25		1	47		10	-39		3	49		
89.0	0.0	0.01	-0.03	0.14	0.0	-3	*		-7	*		2	*		-8	*		-3	0	1
89.0	0.0	0.01	2.01	0.14	0.0	6			-65			17			-128			-3		1
89.1	0.0	0.01	3.98	0.14	0.0	64			-211			48			-398			-4		1
89.0	0.0	0.01	4.89	0.14	0.0	95			-277			68			-534			-4		1
88.9	0.0	0.01	-2.21	0.15	0.0	-11			66			-8			157			-4		1
88.8	0.0	0.01	-4.14	0.15	0.0	-63			206			-57			400			-5		0
88.6	0.0	0.01	-6.18	0.14	0.0	-147			362			-248			665			-6		1
88.8	0.0	2.00	-0.09	0.14	0.0	-3	*		-5	*		1	*		-1	*		2	0	-6
88.7	0.0	2.00	2.09	0.13	0.0	49			-94			95			-202			7		-1
88.6	0.0	2.00	3.84	0.13	0.0	73			-211			133			-406			11		2
88.5	0.0	2.00	4.87	0.13	0.0	117			-286			209			-539			12		3
88.7	0.0	2.00	-2.23	0.14	0.0	-35			108			-57			224			5		-3
88.6	0.0	2.00	-4.19	0.14	0.0	-63			232			-109			441			10		2
88.4	0.0	2.00	-6.17	0.13	0.0	-160			384			-279			699			11		3

* Nonlinear

TABLE IV

EXPERIMENTAL STEADY ROTOR RESPONSE TO θ_o, θ_s, θ_c AND α, CONFIGURATION 5 (Continued)

Ω rad/sec	μ	θ_o deg	θ_s deg	θ_c deg	α deg	M_H Mag in-lb	M_H Slope in-lb/deg	M_H Error in-lb	L_H Mag in-lb	L_H Slope in-lb/deg	L_H Error in-lb	M_S Mag in-lb	M_S Slope in-lb/deg	M_S Error in-lb	L_S Mag in-lb	L_S Slope in-lb/deg	L_S Error in-lb	LIFT Mag lb	LIFT Slope lb/deg	LIFT Error lb
88.6	0.0	4.00	-0.23	0.12	0.0	-6	40	-9	3	-67	1	-8	70	-20	15	-124	-10	17	0	-3
88.5	0.0	3.99	1.77	0.12	0.0	90		7	-128		6	169		16	-246		-5	18		-2
88.4	0.0	3.99	3.55	0.12	0.0	164		11	-254		1	307		29	-458		4	21		0
88.3	0.0	3.99	4.72	0.12	0.0	194		-6	-335		-2	339		-21	-616		-10	24		4
88.5	0.0	4.00	-2.24	0.13	0.0	-86		-9	134		-3	-141		-12	274		20	18		-3
88.4	0.0	4.00	-4.22	0.13	0.0	-164		-9	264		-6	-274		-6	492		-7	20		0
88.0	0.0	4.00	-5.97	0.13	0.0	-211		14	393		5	-376		15	705		-10	24		4
89.8	0.0	5.92	-0.19	0.12	0.0	-5	56	-17	-11	-75	-4	2	99	-23	-11	-136	-24	38	0	-1
89.0	0.0	5.92	1.76	0.11	0.0	125		5	-148		5	240		21	-276		0	38		-2
88.9	0.0	5.92	3.58	0.11	0.0	230		9	-287		2	430		31	-509		15	40		0
88.7	0.0	5.92	4.70	0.11	0.0	281		-2	-378		-5	481		-29	-701		-24	41		2
89.0	0.0	5.92	-2.24	0.12	0.0	-106		-3	145		1	-185		-7	289		21	37		-2
88.9	0.0	5.92	-4.13	0.13	0.0	-206		2	294		7	-362		3	545		20	39		0
88.7	0.0	5.92	-6.03	0.14	0.0	-309		5	423		-6	-550		3	752		-32	42		3
104.8	0.0	0.01	-0.01	0.14	0.0	-7	3	0	-8	-3	-2	-2	9	2	-9	-7	2	13	*	
104.9	0.0	1.97	-0.01	0.14	0.0	-2		-1	-10		2	12		-3	-11		7	21		
104.9	0.0	3.93	0.0	0.12	0.0	8		2	-16		2	31		0	-33		-1	40		
104.3	0.0	5.92	0.01	0.11	0.0	11		1	-24		0	50		0	-44		2	67		
104.8	0.0	4.95	0.02	0.10	0.0	9		0	-24		-3	42		1	-43		-4	54		
105.3	0.0	0.0	0.02	0.12	0.0	-6	*		-10	*		8	*		-9	*		13	0	1
105.3	0.0	0.0	1.75	0.12	0.0	15			-58			30			-163			15		2
105.4	0.0	0.0	3.58	0.12	0.0	87			-205			178			-454			13		0
105.3	0.0	0.0	4.77	0.07	0.0	139			-289			299			-604			12		-2
105.5	0.0	0.0	-2.24	0.09	0.0	-17			83			-34			226			12		0
105.3	0.0	0.0	-4.23	0.09	0.0	-95			245			-172			541			10		1
105.4	0.0	0.0	-6.29	0.10	0.0	-223			428			-419			850			9		1
105.3	0.0	2.00	-0.08	0.25	0.0	-6	*		-11	*		-7	*		-18	*		20	0	-6
105.4	0.0	2.00	1.66	0.25	0.0	45			-105			106			-246			21		-5
105.2	0.0	2.00	3.53	0.25	0.0	81			-214			154			-469			27		2
105.2	0.0	2.00	4.82	0.25	0.0	147			-337			307			-687			31		6
105.4	0.0	2.00	-2.27	0.27	0.0	-64			117			-128			299			22		-4
105.3	0.0	2.00	-4.27	0.26	0.0	-125			261			-258			564			29		2
105.2	0.0	2.00	-6.17	0.26	0.0	-235			437			-464			865			31		4
105.5	0.0	3.97	-0.07	0.24	0.0	-7	54	-13	-19	-74	0	-4	107	-27	-37	-152	11	40	0	-5
105.6	0.0	3.97	1.75	0.24	0.0	104		1	-146		7	227		10	-331		-17	42		-2
105.5	0.0	3.97	3.54	0.24	0.0	216		15	-286		0	433		24	-606		-20	44		1
105.6	0.0	3.97	4.66	0.24	0.0	262		1	-368		0	519		-8	-746		11	48		5
105.7	0.0	3.97	-2.23	0.26	0.0	-119		-8	131		-10	-225		-17	331		40	42		-4
105.7	0.0	3.97	-4.10	0.26	0.0	-221		-8	273		-6	-406		1	598		23	43		-3
105.5	0.0	3.97	-6.13	0.26	0.0	-306		16	437		9	-608		16	846		-38	54		7
57.6	0.41	0.0	0.03	0.78	0.0	2	69	4	-9	-46	0	-14	107	7	3	-60	-9	4	9	0
57.8	0.41	2.10	0.03	0.78	0.0	139		-4	-104		2	193		-10	-133		-3	22		0
57.8	0.41	4.09	0.03	0.78	0.0	279		-2	-200		-3	416		0	-254		-5	40		0
57.5	0.41	6.15	0.03	0.78	0.0	423		0	-296		-4	635		1	-382		-9	58		0
57.5	0.41	7.21	0.03	0.78	0.0	499		3	-336		4	753		3	-424		12	67		0

* Nonlinear

TABLE IV

EXPERIMENTAL STEADY ROTOR RESPONSE TO θ_o, θ_s, θ_c AND α, CONFIGURATION 5 (Continued)

Ω rad/sec	μ	θ_o deg	θ_s deg	θ_c deg	α deg	M_H Mag in-lb	M_H Slope in-lb/deg	M_H Error in-lb	L_H Mag in-lb	L_H Slope in-lb/deg	L_H Error in-lb	M_s Mag in-lb	M_s Slope in-lb/deg	M_s Error in-lb	L_s Mag in-lb	L_s Slope in-lb/deg	L_s Error in-lb	LIFT Mag lb	LIFT Slope lb/deg	LIFT Error lb
57.8	0.40	0.98	-1.05	0.80	0.0	-16	61	-5	-1	-56	1	-31	89	-2	31	-87	-2	8	4	0
57.6	0.41	0.98	0.94	0.78	0.0	116		5	-106		8	152		4	-144		18	16		0
57.7	0.42	0.98	2.99	0.78	0.0	239		2	-232		-2	311		-20	-368		-27	25		0
57.7	0.42	0.98	5.03	0.78	0.0	359		-2	-350		-4	528		14	-521		-2	34		0
57.5	0.40	0.98	-5.32	0.80	0.0	-275		-4	241		2	-403		7	398		15	-10		1
57.5	0.40	0.98	-7.08	0.80	0.0	-374		4	333		-5	-570		-3	512		-24	-16		1
57.7	0.41	0.98	-1.06	0.80	0.0	-4	-79	8	-1	-39	-7	-24	-116	-2	31	-68	23	6	0	1
57.6	0.41	0.98	-1.06	2.51	0.0	-140		6	-69		-8	-224		-4	-86		-6	7		0
57.6	0.42	0.98	-1.06	4.38	0.0	-301		-8	-144		-9	-444		-7	-227		-20	7		0
57.6	0.42	0.98	-1.06	6.30	0.0	-440		4	-194		17	-645		15	-315		23	6		0
57.8	0.41	0.98	-1.06	-1.42	0.0	150		-13	89		-4	225		-10	186		-3	8		0
57.9	0.41	0.97	-1.06	-3.53	0.0	323		-7	183		6	472		-8	346		13	7		0
57.9	0.41	0.97	-1.06	-5.40	0.0	488		11	254		4	714		17	460		1	8		0
57.9	0.41	0.97	-1.06	0.74	0.0	-21	*		23	*		-54	*		62	*		7	5	1
58.1	0.41	0.97	-1.06	0.74	2.06	41			-7			45			24			17		0
58.2	0.41	0.97	-1.06	0.74	4.22	110			-34			152			-15			27		0
58.0	0.41	0.97	-1.06	0.74	5.05	151			-53			212			-37			32		0
57.7	0.40	0.97	-1.06	0.74	-2.07	-42			15			-90			53			-2		1
57.7	0.40	0.97	-1.06	0.74	-3.11	-78			31			-145			70			-8		0
57.6	0.57	0.01	0.06	1.08	0.0	-6	110	6	-16	-74	-3	-36	170	8	-12	-98	-6	6	10	1
57.8	0.57	2.09	0.06	1.08	0.0	214		-2	-165		2	308		-2	-207		3	25		1
57.9	0.56	4.14	0.06	1.08	0.0	447		5	-323		-4	671		12	-418		-7	48		0
57.9	0.56	4.94	0.06	1.08	0.0	535		6	-380		-3	802		7	-496		-6	57		1
57.9	0.56	3.13	0.06	1.08	0.0	317		-14	-235		9	463		-24	-294		17	36		-1
57.8	0.56	1.15	0.80	0.86	0.0	219	91	27	-156	-72	-10	315	137	33	-201	-108	7	22	6	1
57.9	0.56	1.15	2.85	0.86	0.0	370		-9	-291		3	549		-15	-410		-1	33		-1
58.0	0.56	1.15	3.84	0.86	0.0	463		-6	-361		4	698		-2	-507		9	41		1
57.4	0.55	1.15	-3.40	0.86	0.0	-208		-18	160		3	-325		-30	272		7	-6		1
57.4	0.55	1.15	-5.58	0.86	0.0	-383		6	316		1	-581		14	499		1	-18		0
57.5	0.56	1.15	-1.31	0.86	0.0	0	-89	2	3	-38	-6	-17	-134	-7	46	-66	17	8	0	0
57.5	0.56	1.15	-1.31	2.59	0.0	-151		6	-61		-4	-241		1	-70		-7	8		0
57.5	0.56	1.15	-1.31	4.49	0.0	-339		-13	-128		1	-509		-14	-192		-3	8		0
57.5	0.56	1.15	-1.31	5.49	0.0	-413		3	-157		10	-620		9	-238		17	8		0
57.7	0.55	1.15	-1.31	-1.35	0.0	211		16	70		-23	314		29	173		-25	9		1
57.7	0.55	1.15	-1.31	-3.46	0.0	368		-16	189		15	546		-21	359		21	7		-1
57.7	0.55	1.15	-1.31	-4.40	0.0	469		1	215		6	695		3	403		3	8		0
57.7	0.55	1.14	-1.30	1.08	0.0	0	53	2	-13	-25	-4	-24	83	2	18	-32	7	9	6	0
57.9	0.56	1.14	-1.30	1.08	2.06	112		4	-66		-5	150		6	-53		-12	22		0
58.1	0.55	1.14	-1.30	1.08	4.22	217		-6	-111		3	315		-8	-108		3	37		0
58.2	0.55	1.14	-1.30	1.08	5.05	269		3	-133		2	397		5	-130		7	42		0
57.8	0.55	1.14	-1.30	1.08	-2.06	-120		-8	48		7	-213		-16	98		7	-4		0
57.8	0.55	1.14	-1.30	1.08	-3.11	-162		5	65		-2	-272		12	128		3	-10		0
57.4	0.79	0.08	-0.37	0.99	0.0	-10	179	-5	12	-105	2	-40	263	-7	48	-145	-10	5	14	0
57.6	0.79	1.09	-0.37	0.99	0.0	184		8	-96		0	241		10	-91		1	20		1
57.9	0.78	2.10	-0.37	0.99	0.0	363		7	-207		-5	516		19	-227		12	33		0
57.9	0.79	3.12	-0.37	0.99	0.0	536		-4	-306		4	757		-8	-397		-10	47		0
57.4	0.79	1.75	-0.37	0.99	0.0	288		-6	-167		-2	391		-14	-185		3	27		1

* Nonlinear

TABLE IV

EXPERIMENTAL STEADY ROTOR RESPONSE TO θ_o, θ_s, θ_c AND α, CONFIGURATION 5 (Continued)

Ω rad/sec	μ	θ_o deg	θ_s deg	θ_c deg	α deg	M_H Mag in-lb	M_H Slope in-lb/deg	M_H Error in-lb	L_H Mag in-lb	L_H Slope in-lb/deg	L_H Error in-lb	M_s Mag in-lb	M_s Slope in-lb/deg	M_s Error in-lb	L_s Mag in-lb	L_s Slope in-lb/deg	L_s Error in-lb	LIFT Mag lb	LIFT Slope lb/deg	LIFT Error lb
57.2	0.79	0.56	-0.87	1.29	0.0	-31	160	-7	10	-98	11	-74	235	-27	42	-130	3	10	11	0
57.3	0.79	0.56	0.03	1.29	0.0	139		19	-97		-7	170		6	-104		-29	20		1
58.0	0.79	0.55	1.99	1.29	0.0	426		-7	-283		0	633		9	-312		18	39		1
57.6	0.79	0.55	-2.08	1.29	0.0	-224		-7	115		-3	-334		-4	203		3	-5		-1
57.5	0.79	0.55	-3.10	1.29	0.0	-378		2	217		-2	-553		16	343		10	-14		0
57.7	0.79	0.55	-0.97	1.29	0.0	-14	-104	19	-7	-38	-16	-44	-153	21	34	-64	29	7	0	1
57.5	0.79	0.55	-0.97	2.38	0.0	-156		-10	-35		-4	-252		-20	-26		-8	6		0
57.5	0.80	0.55	-0.97	3.21	0.0	-235		-3	-62		2	-362		-3	-79		-8	6		1
57.5	0.80	0.55	-0.97	4.17	0.0	-340		-9	-83		17	-513		-6	-104		29	4		-1
57.6	0.79	0.55	-0.95	-0.53	0.0	179		23	66		-12	243		29	158		-10	7		0
57.6	0.79	0.55	-0.95	-2.79	0.0	375		-14	163		-1	544		-17	312		1	6		-1
57.7	0.79	0.55	-0.95	-3.87	0.0	496		-5	219		14	721		-6	395		14	9		1
57.6	0.79	0.55	-0.95	1.13	0.0	-4	112	-4	9	-47	-4	-36	164	-8	49	-60	0	7	11	-2
57.9	0.79	0.55	-0.95	1.13	2.05	228		-3	-91		-7	306		-3	-73		-1	29		-3
58.3	0.78	0.55	-0.95	1.13	4.21	477		4	-181		6	671		7	-199		2	59		3
57.7	0.79	0.55	-0.95	1.13	-2.05	-234		-4	113		3	-374		-9	174		0	-13		1
57.8	0.79	0.55	-0.95	1.13	-3.10	-341		7	162		2	-525		13	238		2	-24		2
57.6	0.92	0.04	-0.25	1.35	0.0	-24	231	-6	-2	-116	4	-67	340	-8	27	-150	13	10	17	0
57.7	0.92	0.99	-0.25	1.35	0.0	211		9	-124		-7	275		11	-133		-13	26		0
58.0	0.92	2.15	-0.25	1.34	0.0	462		-8	-247		5	645		-14	-298		-5	45		0
58.0	0.92	1.71	-0.25	1.35	0.0	373		5	-204		-3	520		11	-214		13	38		0
57.8	0.92	0.55	-0.78	1.35	0.0	5	188	-14	-13	-102	6	-21	272	-19	24	-146	-2	11	13	-2
58.0	0.92	0.55	0.15	1.35	0.0	206		12	-124		-10	260		10	-145		-19	26		0
57.9	0.92	0.55	1.46	1.35	0.0	438		-3	-243		4	607		0	-310		7	43		0
57.6	0.92	0.55	-1.82	1.35	0.0	-173		5	86		0	-275		9	159		-2	0		1
57.6	0.93	0.55	-0.81	1.35	0.0	-2	-110	1	-11	-41	4	-33	-163	-9	26	-70	13	10	-1	0
57.6	0.93	0.55	-0.81	2.10	0.0	-64		20	-56		-11	-120		26	-48		-15	11		1
57.5	0.93	0.55	-0.81	3.03	0.0	-200		-14	-80		3	-314		-17	-100		-1	9		0
57.5	0.93	0.55	-0.81	4.00	0.0	-305		-12	-113		10	-462		-7	-154		13	6		-1
57.6	0.92	0.55	-0.78	0.13	0.0	158		25	25		-10	201		26	94		-11	13		1
57.6	0.92	0.55	-0.78	-0.80	0.0	234		-2	64		-9	317		-9	169		-2	14		1
57.5	0.92	0.55	-0.78	-2.83	0.0	442		-16	169		13	648		-9	323		10	15		-1
57.5	0.93	0.55	-0.78	1.44	0.0	-23	152	-32	-10	-55	2	-59	221	-47	21	-65	3	10	15	-5
57.9	0.92	0.55	-0.78	1.44	2.05	316		-5	-125		0	429		-12	-133		-12	45		1
58.2	0.91	0.55	-0.79	1.44	3.16	509		20	-187		1	721		34	-189		5	66		3
57.6	0.92	0.55	-0.78	1.44	-2.05	-305		-3	100		0	-471		-6	150		3	-16		0
57.7	0.92	0.55	-0.78	1.44	-3.12	-445		20	157		-1	-672		30	214		-4	-30		2
88.9	0.27	-0.03	0.15	0.44	0.05	-4	75	4	-1	-16	-1	-38	132	9	-3	-21	-8	0	19	0
88.9	0.27	2.07	0.17	0.44	0.06	145		-4	-30		3	226		-6	-55		3	39		0
88.8	0.27	4.01	0.17	0.44	0.06	292		-2	-66		-3	481		-8	-124		-25	75		0
88.9	0.27	6.17	0.17	0.44	0.07	446		-8	-96		2	769		-6	-153		-8	116		0
88.7	0.27	7.16	0.17	0.44	0.07	538		9	-113		1	917		11	-146		20	135		0
88.8	0.26	1.04	-0.54	0.73	0.06	-20	87	19	-11	-46	4	-89	163	14	-10	-93	29	15	6	0
88.9	0.27	1.04	1.49	0.73	0.07	151		13	-102		7	252		24	-229		-21	27		1
88.9	0.27	1.04	3.59	0.73	0.06	331		12	-217		-11	597		28	-434		-30	39		1
88.9	0.26	1.04	5.66	0.73	0.07	474		-24	-297		4	867		-39	-568		29	48		-2
88.7	0.26	1.04	-2.70	0.74	0.05	-231		-6	78		-6	-473		-19	204		21	2		0
88.8	0.26	1.04	-4.88	0.74	0.04	-429		-14	186		2	-816		-8	380		-7	-11		1

TABLE IV

EXPERIMENTAL STEADY ROTOR RESPONSE TO θ_o, θ_s, θ_c AND α, CONFIGURATION 5 (Continued)

						M_H			L_H			M_s			L_s			LIFT		
$\frac{\Omega}{\text{rad}}$		θ_o	θ_s	θ_c	α	Mag	Slope $\frac{\text{in-lb}}{\text{deg}}$	Error	Mag	Slope $\frac{\text{in-lb}}{\text{deg}}$	Error	Mag	Slope $\frac{\text{in-lb}}{\text{deg}}$	Error	Mag	Slope $\frac{\text{in-lb}}{\text{deg}}$	Error	Mag	Slope $\frac{\text{lb}}{\text{deg}}$	Error
sec	μ	deg	deg	deg	deg	in-lb		in-lb	in-lb		in-lb	in-lb		in-lb	in-lb		in-lb	lb		lb
88.7	0.27	1.04	-0.67	0.73	0.06	-3	-84	37	-4	-75	10	-72	-163	23	8	-155	-24	15	0	0
88.7	0.27	1.04	-0.67	2.78	0.05	-211		3	-164		4	-440		-9	-330		-4	14		0
88.8	0.27	1.04	-0.67	4.70	0.05	-396		-20	-310		2	-744		0	-625		1	13		1
89.0	0.26	1.04	-0.67	-1.34	0.07	126		-8	111		-30	231		-12	289		-24	17		1
89.0	0.26	1.04	-0.67	-3.25	0.07	285		-10	283		1	542		-14	632		23	18		1
88.9	0.26	1.04	-0.67	-4.78	0.07	422		-2	413		15	817		11	837		-10	17		-1
89.0	0.27	1.11	-1.36	0.13	2.10	22	17	-7	16	5	2	9	31	-11	51	8	-9	38	7	-1
89.1	0.27	1.11	-1.36	0.13	4.26	68		3	21		-3	92		5	57		-8	55		0
89.3	0.26	1.10	-1.36	0.13	5.10	80		1	31		3	113		0	78		6	61		1
88.9	0.27	1.10	-1.35	0.13	-2.06	-31		10	-13		-8	-91		18	3		-9	11		1
88.8	0.27	1.10	-1.35	0.13	-3.07	-63		-6	-3		7	-152		-12	11		7	3		0
89.1	0.36	-0.04	-0.56	0.28	0.04	5	106	5	-15	-34	0	-18	193	6	-26	-50	-9	11	21	0
89.1	0.36	2.06	-0.56	0.31	0.05	211		-11	-86		0	367		-12	-129		1	55		1
89.2	0.36	4.07	-0.56	0.31	0.05	440		5	-156		0	773		6	-230		1	98		0
89.0	0.36	1.24	-1.80	0.31	0.04	-22	106	8	-2	-52	-7	-72	196	-6	30	-105	21	27	9	1
89.2	0.36	1.24	0.39	0.31	0.05	222		20	-110		1	399		35	-217		-6	46		0
89.5	0.36	1.24	2.48	0.31	0.05	413		-12	-219		2	766		-7	-439		-7	65		0
89.2	0.36	1.24	-3.76	0.31	0.03	-264		-26	112		3	-510		-59	247		21	7		-2
89.2	0.35	1.24	-6.23	0.30	0.04	-490		10	240		1	-900		36	466		-19	-13		1
89.4	0.36	1.24	-1.67	0.31	0.05	-8	-91	10	-1	-83	1	-66	-170	-15	21	-165	-6	27	-1	0
89.3	0.36	1.24	-1.67	2.19	0.04	-188		1	-151		7	-360		-9	-285		2	25		0
89.2	0.36	1.24	-1.67	4.14	0.04	-374		-8	-321		1	-690		14	-609		2	22		0
89.5	0.36	1.24	-1.67	-1.85	0.05	182		5	159		-18	322		5	377		-6	31		1
89.4	0.36	1.24	-1.66	-4.26	0.05	388		-8	388		10	734		5	788		5	32		1
89.3	0.36	1.24	-1.66	0.43	0.04	-4	34	-5	-8	-2	2	-62	63	-5	20	-3	-17	28	10	0
89.3	0.36	1.24	-1.66	0.43	2.10	69		-3	-14		0	69		-5	-4		1	49		1
89.7	0.36	1.24	-1.66	0.44	4.26	138		-8	-12		6	193		-17	0		11	72		0
90.0	0.36	1.24	-1.66	0.43	5.09	186		12	-25		-6	284		21	-31		-17	82		1
88.9	0.36	1.24	-1.66	0.43	-1.98	-75		-7	-8		-1	-191		-7	5		-2	7		0
88.8	0.36	1.24	-1.66	0.43	-3.07	-95		10	-5		1	-240		13	-2		-12	-3		1
89.0	0.51	0.02	-0.89	0.41	0.04	-4	159	-5	-2	-55	2	-44	274	-11	7	-90	-9	12	23	1
89.1	0.51	1.05	-0.89	0.41	0.05	161		-3	-61		1	241		-9	-90		1	35		-1
89.1	0.51	2.05	-0.89	0.41	0.05	323		1	-113		2	527		3	-171		10	58		0
89.1	0.51	3.14	-0.89	0.43	0.04	498		2	-176		-2	827		5	-288		-9	84		1
88.6	0.51	-0.98	-0.87	0.43	0.04	-153		5	49		-2	-295		12	85		-7	-9		1
88.7	0.51	0.43	-1.20	0.67	0.04	0	155	19	-26	-65	0	-45	279	12	-25	-127	-3	18	14	1
88.9	0.51	0.43	-0.20	0.67	0.04	144		7	-92		1	215		-7	-173		-15	31		0
89.0	0.51	0.43	0.84	0.67	0.05	278		-19	-150		8	488		-24	-285		5	44		-1
89.2	0.51	0.43	1.77	0.66	0.05	443		1	-225		-6	793		21	-410		-3	59		0
88.7	0.51	0.43	-2.21	0.67	0.02	-169		6	39		1	-346		-7	118		20	4		1
88.6	0.50	0.43	-3.43	0.67	0.04	-370		-6	117		-1	-672		8	259		7	-13		1
89.3	0.50	0.43	-3.86	0.67	0.04	-439		-8	147		0	-802		-2	288		-19	-21		-1

TABLE IV

EXPERIMENTAL STEADY ROTOR RESPONSE TO θ_o, θ_s, θ_c AND α, CONFIGURATION 5 (Continued)

						M_H			L_H			M_s			L_s			LIFT		
$\frac{\Omega}{\text{rad}}$ sec	μ	θ_o deg	θ_s deg	θ_c deg	α deg	Mag in-lb	Slope $\frac{\text{in-lb}}{\text{deg}}$	Error in-lb	Mag in-lb	Slope $\frac{\text{in-lb}}{\text{deg}}$	Error in-lb	Mag in-lb	Slope $\frac{\text{in-lb}}{\text{deg}}$	Error in-lb	Mag in-lb	Slope $\frac{\text{in-lb}}{\text{deg}}$	Error in-lb	Mag lb	Slope $\frac{\text{lb}}{\text{deg}}$	Error lb
89.5	0.50	0.43	-1.25	0.67	0.05	11	-89	26	-28	-78	-5	-29	-168	25	-32	-149	36	20	-1	3
89.3	0.51	0.43	-1.25	1.51	0.04	-76		14	-95		-7	-176		20	-159		-20	18		2
89.4	0.51	0.43	-1.25	2.50	0.02	-186		-7	-164		1	-363		1	-294		-8	15		1
89.3	0.51	0.43	-1.25	3.30	0.03	-270		-20	-218		10	-520		-23	-369		36	12		-3
89.5	0.50	0.43	-1.25	-1.39	0.05	168		-1	127		-11	273		-19	283		-11	20		1
89.5	0.50	0.43	-1.24	-3.40	0.05	336		-12	305		11	627		-2	616		22	20		-2
89.4	0.50	0.43	-1.24	0.62	0.03	-7	73	-7	-5	-14	3	-72	127	-20	-14	-20	-4	20	15	-1
89.7	0.50	0.43	-1.22	0.62	2.09	149		-1	-36		1	202		-8	-53		6	48		-3
90.2	0.50	0.42	-1.23	0.62	4.25	306		-3	-61		4	480		-4	-105		-1	84		1
89.5	0.50	0.42	-1.23	0.63	5.08	374		5	-79		-3	605		15	-125		-4	95		1
88.2	0.51	0.42	-1.24	0.63	-2.01	-142		7	13		-7	-299		11	21		-3	-8		1
88.2	0.51	0.42	-1.24	0.63	-3.06	-227		-1	39		5	-438		6	43		-2	-24		1
89.0	0.60	-0.01	-0.98	0.58	0.05	-11	213	-7	3	-70	3	-57	363	-11	7	-119	-25	12	26	1
89.2	0.61	1.01	-0.98	0.58	0.05	202		-13	-67		4	304		-19	-105		10	39		-1
89.4	0.60	2.10	-0.98	0.58	0.05	440		-7	-145		2	717		-2	-218		27	68		0
89.3	0.60	2.44	-0.98	0.58	0.05	527		7	-172		-2	846		4	-310		-25	78		0
88.9	0.61	0.46	-0.98	0.58	0.05	117		20	-39		-6	151		27	-62		-13	28		2
89.3	0.60	0.46	-1.51	0.73	0.05	-8	190	15	-11	-74	-5	-67	351	16	-1	-148	1	17	17	1
89.5	0.60	0.46	-0.51	0.73	0.05	165		-2	-78		3	243		-25	-145		3	30		-3
89.7	0.60	0.46	0.48	0.73	0.05	346		-9	-153		2	604		-12	-290		4	49		-1
90.0	0.60	0.46	1.39	0.73	0.05	527		-2	-222		0	951		15	-430		1	68		2
89.3	0.61	0.46	-2.18	0.73	0.05	-135		15	37		-6	-305		14	90		-11	5		1
89.3	0.60	0.46	-3.50	0.73	0.04	-419		-18	147		6	-790		-7	304		7	-18		0
89.5	0.61	0.46	-1.47	0.73	0.05	-15	-105	9	-2	-73	6	-78	-195	2	21	-148	-28	17	-2	1
89.3	0.61	0.46	-1.47	1.74	0.04	-115		15	-88		-6	-249		28	-171		-29	15		1
89.3	0.61	0.46	-1.47	2.66	0.05	-243		-17	-143		6	-474		-18	-254		24	11		-1
89.5	0.60	0.46	-1.47	-1.22	0.05	176		-4	120		-14	279		-22	267		-28	19		0
89.3	0.60	0.46	-1.47	-3.15	0.05	381		-2	283		8	687		9	599		19	23		0
88.0	0.61	0.47	-1.46	1.60	0.02	26	120	-11	-13	-28	-4	8	201	-21	-12	-32	-10	17	18	-4
98.7	0.61	0.46	-1.44	1.61	2.08	275		-9	-69		-3	428		-17	-77		5	56		-3
89.0	0.61	0.46	-1.44	1.62	3.54	471		11	-100		5	761		22	-133		-4	90		4
88.1	0.61	0.46	-1.46	1.62	-2.03	-203		8	44		-4	-376		8	41		-10	-15		2
88.3	0.61	0.46	-1.46	1.62	-3.08	-336		1	83		6	-586		9	91		6	-34		1
88.8	0.72	0.02	-1.28	1.68	0.03	13	282	12	1	-92	-5	-15	461	19	0	-108	0	18	28	1
89.0	0.72	1.04	-1.28	1.68	0.03	288		1	-88		1	432		-4	-97		3	46		0
89.1	0.72	1.50	-1.28	1.68	0.03	424		6	-130		0	671		22	-147		2	60		1
88.8	0.72	0.62	-1.28	1.68	0.03	153		-17	-45		4	201		-41	-55		0	31		-3
88.7	0.72	-1.09	-1.29	1.69	0.02	-314		-1	110		2	-543		4	135		5	-13		1
88.7	0.72	0.03	-1.28	1.68	0.02	8	250	24	0	-88	-11	-25	457	30	0	-125	-17	16	22	1
89.0	0.72	0.03	-0.12	1.68	0.03	284		9	-96		-4	470		-5	-151		-9	43		1
89.2	0.71	0.03	0.71	1.68	0.03	465		-17	-157		8	847		-7	-237		10	60		0
88.6	0.72	0.03	-2.26	1.70	0.02	-259		2	95		-2	-511		-9	111		-17	-5		0
88.6	0.72	0.03	-2.70	1.70	0.03	-389		-18	144		9	-712		-8	202		19	-15		0

TABLE IV

EXPERIMENTAL STEADY ROTOR RESPONSE TO θ_o, θ_s, θ_c AND α, CONFIGURATION 5 (Continued)

						M_H			L_H			M_s			L_s			LIFT		
$\frac{\Omega}{\text{rad/sec}}$	μ	θ_o deg	θ_s deg	θ_c deg	α deg	Mag in-lb	Slope $\frac{\text{in-lb}}{\text{deg}}$	Error in-lb	Mag in-lb	Slope $\frac{\text{in-lb}}{\text{deg}}$	Error in-lb	Mag in-lb	Slope $\frac{\text{in-lb}}{\text{deg}}$	Error in-lb	Mag in-lb	Slope $\frac{\text{in-lb}}{\text{deg}}$	Error in-lb	Mag lb	Slope $\frac{\text{lb}}{\text{deg}}$	Error lb
88.8	0.72	0.03	-1.31	1.72	0.03	-20	-116	8	9	-70	1	-69	-201	2	13	-144	14	14	-2	0
88.9	0.72	0.03	-1.31	2.78	0.03	-145		5	-73		-6	-275		9	-158		16	13		1
88.8	0.72	0.03	-1.31	3.69	0.02	-279		-22	-124		6	-480		-12	-266		7	9		-1
89.0	0.71	0.03	-1.31	0.78	0.03	94		12	80		6	112		-7	161		14	15		-2
89.0	0.71	0.03	-1.31	-0.30	0.03	235		27	136		-14	358		22	295		-7	22		3
88.9	0.71	0.03	-1.31	-1.74	0.03	345		-30	260		8	612		-15	509		1	20		-2
88.7	0.72	0.03	-1.31	1.85	0.02	-20	168	1	1	-35	-10	-70	278	9	-7	-35	0	15	24	-4
89.3	0.71	0.03	-1.31	1.86	2.07	318		-6	-63		-1	479		-13	-62		13	66		-2
89.6	0.71	0.03	-1.31	1.86	3.09	500		4	-91		6	782		6	-119		-9	95		3
89.0	0.72	0.03	-1.31	1.84	-2.03	-367		1	88		8	-657		-7	67		0	-28		2
88.8	0.72	0.03	-1.31	1.85	-0.99	-189		2	42		-2	-355		5	30		1	-4		1
89.4	0.75	-0.04	0.29	2.17	0.0	-29	297	-21	52	-84	2	-91	543	-41	113	-124	3	0	0	0
89.6	0.75	0.44	0.29	2.17	0.0	148		13	4		-6	230		19	35		-9	0		0
89.9	0.75	0.99	0.29	2.17	0.0	319		21	-37		-2	550		41	-29		-4	0		0
90.3	0.75	1.45	0.29	2.17	0.0	422		-12	-71		3	739		-20	-79		3	0		0
89.8	0.75	-0.52	0.28	2.17	0.0	-170		-19	94		4	-347		-36	171		8	0		0
90.0	0.75	-1.12	0.28	2.17	0.0	-311		18	139		-1	-599		37	229		-8	0		0
88.9	0.75	0.51	-0.59	1.46	0.0	21	259	0	1	-79	1	-1	483	0	38	-140	-26	18	23	1
89.3	0.75	0.51	0.42	1.46	0.0	283		0	-80		-2	492		5	-121		-6	44		2
89.0	0.75	0.51	-1.06	1.46	0.0	-106		-6	46		7	-247		-19	105		12	5		-3
89.0	0.75	0.51	-1.69	1.46	0.0	-251		13	84		-5	-516		17	156		-26	-5		1
89.1	0.75	0.51	-2.18	1.46	0.0	-398		-7	128		1	-772		-3	261		10	-16		1
89.1	0.75	0.51	-0.51	1.62	0.0	-6	-113	-16	-8	-68	-11	-64	-214	-43	5	-134	8	19	-2	1
89.1	0.75	0.51	-0.51	2.68	0.0	-109		1	-71		-1	-245		2	-110		0	15		-1
89.1	0.75	0.51	-0.51	3.33	0.0	-196		-13	-105		9	-392		-6	-180		18	14		-1
89.3	0.75	0.51	-0.51	0.67	0.0	152		35	72		5	229		46	166		8	24		3
89.6	0.74	0.51	-0.51	-0.32	0.0	263		34	122		-13	449		55	264		-26	25		2
89.3	0.74	0.51	-0.51	-1.33	0.0	329		-14	209		6	582		-29	457		32	24		-2
89.2	0.74	0.51	-0.51	-1.33	0.0	315		-27	210		6	586		-25	419		-7	24		-2
89.0	0.81	0.06	-0.13	1.72	0.0	-46	348	-7	-3	-91	1	-138	633	-25	3	-155	-3	17	36	-2
89.2	0.81	0.58	-0.14	1.72	0.0	151		9	-57		-5	228		11	-80		-4	34		-3
89.4	0.80	1.13	-0.14	1.73	0.0	326		-8	-99		3	552		-13	-147		13	57		0
89.6	0.80	1.57	-0.14	1.73	0.0	489		2	-140		2	856		12	-231		-3	75		2
89.0	0.81	-0.45	-0.14	1.73	0.0	-210		7	35		-8	-427		8	62		-22	0		0
89.1	0.81	-1.06	-0.14	1.72	0.0	-434		-4	105		7	-816		6	196		17	-20		2
89.1	0.81	0.51	-0.65	1.74	0.0	-39	290	-26	-4	-84	4	-125	548	-48	26	-162	19	19	28	-4
89.3	0.81	0.51	-0.12	1.73	0.0	150		9	-58		-6	226		12	-86		-3	36		-2
89.5	0.81	0.51	0.40	1.72	0.0	272		-20	-93		3	443		-55	-205		-37	55		2
89.6	0.81	0.51	0.83	1.72	0.0	442		25	-137		-4	798		64	-219		19	67		2
88.7	0.82	0.51	-1.25	1.72	0.0	-180		7	47		5	-400		6	98		-2	4		-2
89.0	0.81	0.51	-1.77	1.73	0.0	-352		-14	99		12	-710		-19	209		24	-8		0
89.1	0.81	0.51	-2.24	1.73	0.0	-454		20	112		-14	-909		39	236		-24	-18		3

TABLE IV

EXPERIMENTAL STEADY ROTOR RESPONSE TO θ_o, θ_s, θ_c AND α, CONFIGURATION 5 (Continued)

						M_H			L_H			M_s			L_s			LIFT		
Ω rad/sec	μ	θ_o deg	θ_s deg	θ_c deg	α deg	Mag in-lb	Slope in-lb/deg	Error in-lb	Mag in-lb	Slope in-lb/deg	Error in-lb	Mag in-lb	Slope in-lb/deg	Error in-lb	Mag in-lb	Slope in-lb/deg	Error in-lb	Mag lb	Slope lb/deg	Error lb
89.1	0.81	0.51	-0.59	1.72	0.0	9	-109	-9	-19	-65	-9	-34	-220	-32	-9	-140	15	24	-4	-1
89.1	0.81	0.51	-0.59	2.24	0.0	-35		4	-50		-7	-125		-9	-83		-28	21		1
89.1	0.81	0.51	-0.59	3.39	0.0	-174		-10	-107		11	-375		-6	-180		36	18		1
89.3	0.81	0.51	-0.59	0.56	0.0	184		39	72		6	330		76	195		15	31		1
89.4	0.81	0.51	-0.59	-0.37	0.0	235		-10	116		-11	479		21	291		-19	35		2
89.1	0.82	0.51	-0.59	-1.19	0.0	321		-13	191		11	587		-51	448		23	36		-1
89.1	0.76	0.49	-0.47	1.56	0.0	55	171	-2	-7	-35	-11	65	354	-10	23	-39	7	21	25	-4
89.4	0.75	0.49	-0.47	1.56	1.05	222		-15	-35		-2	470		23	-31		-17	52		0
89.0	0.75	0.48	-0.47	1.56	1.97	410		15	-60		6	767		-5	-36		14	78		2
87.9	0.76	0.49	-0.47	1.57	-1.04	-130		-10	46		6	-325		-32	76		7	1		0
89.3	0.75	0.49	-0.47	1.57	-1.92	-260		12	72		1	-580		24	104		1	-20		2
89.2	0.82	0.49	-0.69	1.57	0.0	30	202	15	6	-33	-16	8	392	7	52	-53	14	23	29	-2
89.7	0.82	0.49	-0.69	1.57	1.01	204		-15	-13		-1	430		33	-40		-41	53		-2
89.7	0.82	0.49	-0.69	1.56	1.65	355		7	-26		7	628		-21	0		32	77		3
88.1	0.83	0.49	-0.70	1.57	-1.02	-206		-14	64		8	-443		-44	123		14	-4		0
88.2	0.83	0.49	-0.70	1.57	-1.74	-330		7	81		1	-656		25	145		-2	-24		1

TABLE V

HARMONIC CONTENT OF THE BLADE FLAPPING RESPONSE TO θ_o, θ_s, θ_c AND α AT THREE RADIAL POSITIONS, CONFIGURATION 5

						M_β @ r = 22.3 in. in.-lb			M_β @ r = 13.15 in. in.-lb			M_β @ r = 3.3 in. ~ in.-lb						
$\frac{\Omega}{\text{rad}}$ sec	μ	θ_o deg	θ_s deg	θ_c deg	α deg	M_{β_o}	$M_{\beta_{1c}}$	$M_{\beta_{1s}}$	M_{β_o}	$M_{\beta_{1c}}$	$M_{\beta_{1s}}$	M_{β_o}	$M_{\beta_{1c}}$	$M_{\beta_{1s}}$	$M_{\beta_{2c}}$	$M_{\beta_{2s}}$	$M_{\beta_{3c}}$	$M_{\beta_{3s}}$
57.6	0.0	1.98	-0.03	0.23	0.0	34	0	0	54	0	0	-7	0	0	0	0	0	0
57.6	0.0	1.98	2.03	0.22	0.0	35	3	-10	56	5	-18	-4	7	-28	-2	-1	0	0
57.5	0.0	1.98	3.96	0.22	0.0	38	4	-22	59	7	-41	0	10	-62	-4	-2	0	0
57.5	0.0	1.98	6.98	0.22	0.0	36	8	-33	60	13	-60	0	18	-90	-5	-2	1	0
57.6	0.0	1.98	-1.85	0.23	0.0	35	-2	9	56	-3	18	-5	-5	27	-2	0	0	0
57.5	0.0	1.98	-3.98	0.23	0.0	37	-6	23	59	-10	43	0	-14	64	-4	-1	0	0
57.5	0.0	1.98	-6.12	0.23	0.0	38	-12	43	61	-20	79	2	-28	118	-5	-2	-1	0
57.6	0.0	3.94	0.03	0.23	0.0	42	0	0	67	0	0	10	1	-1	0	0	0	0
57.5	0.0	3.94	2.04	0.22	0.0	43	6	-18	68	10	-32	10	15	-50	-1	0	0	0
57.5	0.0	3.94	3.90	0.22	0.0	44	11	-32	70	19	-60	15	28	-90	-6	-4	0	0
57.6	0.0	3.94	4.76	0.22	0.0	45	12	-37	72	21	-69	18	30	-104	-8	-6	0	0
57.6	0.0	3.94	-2.07	0.23	0.0	43	-6	15	67	-11	28	10	-16	42	0	0	0	0
57.5	0.0	3.94	-3.92	0.23	0.0	44	-11	28	69	-20	53	12	-28	79	-6	-5	0	0
57.6	0.0	3.94	-6.31	0.23	0.0	46	-15	47	75	-26	87	22	-38	130	-8	-6	0	-1
57.6	0.0	5.90	-0.16	0.23	0.0	52	0	-1	82	0	-1	30	0	-3	0	-2	0	-1
57.3	0.0	5.90	1.89	0.22	0.0	53	9	-21	84	16	-38	32	24	-58	0	-1	0	1
57.2	0.0	5.90	3.90	0.22	0.0	54	18	-38	86	32	-71	36	48	-108	-2	-3	0	1
57.2	0.0	5.90	4.70	0.22	0.0	54	18	-46	87	32	-85	37	49	-128	-5	-2	0	1
57.3	0.0	5.90	-2.07	0.22	0.0	52	-8	17	83	-14	33	31	-22	50	0	-1	0	0
57.2	0.0	5.90	-4.14	0.22	0.0	53	-14	36	85	-25	68	35	-39	103	-2	-2	0	-2
57.2	0.0	5.90	-6.31	0.22	0.0	53	-22	53	87	-39	99	37	-57	148	-9	-9	0	-1
57.6	0.0	3.99	-0.10	0.30	0.0	43	0	0	67	-1	-1	11	-2	-2	0	0	0	0
57.4	0.0	3.99	-0.11	2.37	0.0	43	-17	-6	67	-33	-11	11	-50	-17	1	0	0	-1
57.5	0.0	3.99	-0.10	4.21	0.0	45	-31	-12	71	-59	-21	16	-89	-31	6	3	1	-1
57.3	0.0	4.00	-0.09	6.24	0.0	47	-46	-17	76	-86	-29	24	-129	-42	6	7	0	-1
57.4	0.0	4.00	-0.09	-1.56	0.0	43	13	4	67	25	9	11	38	13	1	0	0	0
57.3	0.0	3.99	-0.11	-3.62	0.0	44	30	12	70	56	21	15	84	29	5	3	0	1
57.4	0.0	3.99	-0.12	-2.59	0.0	44	23	8	69	43	15	12	65	20	1	2	0	0
89.0	0.0	0.02	-0.05	0.15	0.0	37	0	0	68	0	0	-3	0	0	-2	0	0	0
88.9	0.0	2.04	-0.05	0.14	0.0	41	1	0	73	2	0	2	2	0	-2	0	0	0
88.2	0.0	4.00	-0.04	0.13	0.0	51	2	-1	90	3	-1	22	4	-3	-1	0	0	0
88.5	0.0	5.96	-0.02	0.12	0.0	64	1	-4	113	2	-6	50	3	-10	0	0	-1	0
88.3	0.0	6.92	-0.01	0.12	0.0	71	4	-3	126	7	-5	66	11	-8	-1	-2	-1	0
89.0	0.0	0.01	-0.03	0.14	0.0	38	0	0	68	0	0	-2	0	-1	-2	0	0	0
89.0	0.0	0.01	2.01	0.14	0.0	37	2	-8	65	4	-17	-6	6	-29	-2	0	0	0
89.1	0.0	0.01	3.98	0.14	0.0	36	9	-32	64	15	-64	-7	21	-103	-1	0	1	0
89.0	0.0	0.01	4.89	0.14	0.0	35	12	-42	63	21	-86	-9	30	-139	-1	0	2	0
88.9	0.0	0.01	-2.21	0.15	0.0	37	-2	10	66	-3	22	-6	-4	35	-2	0	-1	0
89.8	0.0	0.01	-4.14	0.15	0.0	36	-13	31	64	-23	64	-8	-35	102	0	0	-3	-1
88.6	0.0	0.01	-6.18	0.14	0.0	35	-29	54	63	-54	110	-9	-83	175	1	1	-3	-2
88.8	0.0	2.00	-0.09	0.14	0.0	41	0	0	74	0	0	2	0	-1	-2	0	0	0
88.7	0.0	2.00	2.09	0.13	0.0	37	9	-14	72	18	-28	11	27	-46	-2	-3	1	0
88.6	0.0	2.00	3.94	0.13	0.0	42	15	-31	77	28	-63	14	42	-102	-4	-4	0	1
88.5	0.0	2.00	4.87	0.13	0.0	43	24	-42	79	44	-85	14	67	-136	-5	-4	3	3
88.7	0.0	2.00	-2.23	0.14	0.0	41	-6	16	75	-11	33	5	-18	54	-2	-2	0	0
88.6	0.0	2.00	-4.19	0.14	0.0	44	-14	34	80	-25	71	12	-37	113	-6	-3	-1	-1
88.4	0.0	2.00	-6.17	0.13	0.0	45	-32	56	82	-60	115	14	-92	184	-3	-5	-2	-5

TABLE V

HARMONIC CONTENT OF THE BLADE FLAPPING RESPONSE TO θ_o, θ_s, θ_c AND α AT THREE RADIAL POSITIONS, CONFIGURATION 5 (Continued)

						M_β @ r = 22.3 in. in.-lb			M_β @ r = 13.15 in. in.-lb			M_β @ r = 3.3 in. ~ in.-lb						
$\frac{\Omega}{\text{rad}}$ sec	μ	θ_o deg	θ_s deg	θ_c deg	α deg	M_{β_o}	$M_{\beta_{1c}}$	$M_{\beta_{1s}}$	M_{β_o}	$M_{\beta_{1c}}$	$M_{\beta_{1s}}$	M_{β_o}	$M_{\beta_{1c}}$	$M_{\beta_{1s}}$	$M_{\beta_{2c}}$	$M_{\beta_{2s}}$	$M_{\beta_{3c}}$	$M_{\beta_{3s}}$
88.6	0.0	4.00	-0.23	0.12	0.0	51	0	1	90	0	2	22	-2	2	-2	-1	0	0
88.5	0.0	3.99	1.77	0.12	0.0	52	16	-17	92	31	-35	24	50	-58	-2	-1	0	1
88.4	0.0	3.99	3.53	0.12	0.0	53	31	-35	95	60	-71	27	94	-115	-2	-4	0	2
88.3	0.0	3.99	4.72	0.12	0.0	55	36	-47	98	68	-97	31	106	-156	-4	-8	0	1
88.5	0.0	4.00	-2.24	0.13	0.0	52	-14	19	91	-27	41	23	-44	66	-2	-2	0	-2
88.4	0.0	4.00	-4.22	0.13	0.0	53	-28	38	95	-55	79	28	-87	125	-4	-6	0	-5
88.0	0.0	4.00	-5.97	0.13	0.0	56	-40	55	100	-77	116	35	-120	184	-1	-12	1	-6
89.8	0.0	5.92	-0.19	0.12	0.0	64	0	-1	113	0	-2	49	0	-4	0	-2	0	0
89.0	0.0	5.92	1.76	0.11	0.0	64	22	-20	114	44	-40	49	69	-65	-1	-2	0	1
88.8	0.0	5.92	3.58	0.11	0.0	66	41	-38	116	81	-80	53	129	-128	-1	-5	0	3
88.7	0.0	5.92	4.70	0.11	0.0	67	47	-55	119	93	-112	55	146	-180	-4	-5	0	4
89.0	0.0	5.92	-2.24	0.12	0.0	63	-16	20	112	-33	45	48	-55	71	-2	-5	-1	-3
88.9	0.0	5.92	-4.13	0.13	0.0	64	-33	42	115	-68	89	52	-110	140	-3	-6	-1	-7
88.7	0.0	5.92	-6.03	0.14	0.0	66	-53	58	119	-107	123	58	-168	196	-2	-9	-2	-9
104.8	0.0	0.01	-0.01	0.16	0.0	38	0	0	78	0	0	-6	0	-1	0	-1	0	0
104.9	0.0	1.97	-0.01	0.14	0.0	41	0	0	84	1	0	0	2	-1	0	0	0	0
104.9	0.0	3.93	0.0	0.12	0.0	52	2	-2	101	3	-2	20	6	-5	-1	0	-2	0
104.8	0.0	5.92	0.01	0.11	0.0	65	3	-2	125	6	-4	48	9	-7	-1	-3	-2	-1
104.8	0.0	4.95	0.02	0.10	0.0	59	2	-2	114	4	-3	35	8	-8	0	-1	-3	0
105.3	0.0	0.0	0.02	0.12	0.0	39	0	0	79	0	0	-5	0	0	0	-1	0	0
105.3	0.0	0.0	1.75	0.12	0.0	32	3	-7	72	6	-17	0	10	-30	0	-1	0	2
105.4	0.0	0.0	3.58	0.12	0.0	34	17	-26	73	33	-57	-4	52	-96	0	-1	5	4
105.3	0.0	0.0	4.77	0.07	0.0	35	27	-36	73	55	-79	-7	85	-132	0	0	8	6
105.5	0.0	0.0	-2.23	0.09	0.0	36	-4	11	75	-7	26	-7	-10	43	-1	-1	-1	-1
105.3	0.0	0.0	-4.23	0.09	0.0	36	-17	33	74	-34	74	-9	-52	120	1	0	-5	-1
105.4	0.0	0.0	-6.29	0.10	0.0	36	-41	55	73	-84	121	-10	-123	202	2	0	-12	-7
105.3	0.0	2.00	-0.08	0.25	0.0	43	0	0	85	0	0	3	0	-2	-1	-1	0	0
105.4	0.0	2.00	1.66	0.25	0.0	43	8	-12	85	17	-27	0	27	-47	0	-3	0	0
105.2	0.0	2.00	3.53	0.25	0.0	46	15	-27	89	30	-60	6	45	-100	-2	-8	3	1
105.2	0.0	2.00	4.82	0.25	0.0	48	29	-42	93	58	-92	11	88	-154	-2	-9	7	7
105.4	0.0	2.00	-2.27	0.27	0.0	44	-10	16	87	-19	36	2	-31	61	-1	-3	0	0
105.3	0.0	2.00	-4.27	0.26	0.0	47	-23	34	92	-47	76	9	-71	126	0	-8	-1	-3
105.2	0.0	2.00	-6.17	0.26	0.0	47	-43	55	94	-88	123	12	-131	206	-1	-8	-7	-9
105.5	0.0	3.97	-0.07	0.24	0.0	53	0	-1	102	0	-2	21	0	-6	0	-1	0	0
105.6	0.0	3.97	1.75	0.24	0.0	53	17	-18	103	35	-39	21	58	-66	0	-2	0	1
105.5	0.0	3.97	3.54	0.24	0.0	55	35	-35	106	72	-78	24	116	-132	0	-6	0	5
105.6	0.0	3.97	4.66	0.24	0.0	56	44	-45	109	91	-100	28	141	-169	0	-12	8	5
105.7	0.0	3.97	-2.23	0.26	0.0	53	-16	17	103	-35	40	21	-58	66	1	-2	0	-2
105.7	0.0	3.97	-4.10	0.26	0.0	54	-33	36	105	-69	81	24	-110	133	-1	-9	-3	-3
105.5	0.0	3.97	-6.13	0.26	0.0	57	-52	53	114	-110	119	35	-167	201	4	-14	-6	-10

TABLE V

HARMONIC CONTENT OF THE BLADE FLAPPING RESPONSE TO θ_o, θ_s, θ_c AND α AT THREE RADIAL POSITIONS, CONFIGURATION 5 (Continued)

						M_β @ r = 22.3 in. in.-lb			M_β @ r = 13.15 in. in.-lb			M_β @ r = 3.3 in. ~ in.-lb						
$\frac{\Omega}{\text{rad}}$ sec	μ	θ_o deg	θ_s deg	θ_c deg	α deg	M_{β_o}	$M_{\beta_{1c}}$	$M_{\beta_{1s}}$	M_{β_o}	$M_{\beta_{1c}}$	$M_{\beta_{1s}}$	M_{β_o}	$M_{\beta_{1c}}$	$M_{\beta_{1s}}$	$M_{\beta_{2c}}$	$M_{\beta_{2s}}$	$M_{\beta_{3c}}$	$M_{\beta_{3s}}$
57.6	0.41	0.0	0.03	0.78	0.0	15	-2	1	36	0	2	0	1	3	0	6	-4	0
57.8	0.41	2.10	0.03	0.78	0.0	30	17	-9	66	40	-22	44	70	-38	0	-9	0	0
57.8	0.41	4.09	0.03	0.78	0.0	45	40	-20	95	86	-47	87	145	-79	3	-24	2	0
57.6	0.41	6.15	0.03	0.78	0.0	60	64	-32	125	133	-73	133	223	-124	5	-37	6	0
57.6	0.41	7.21	0.03	0.78	0.0	68	78	-36	141	160	-83	157	267	-140	13	-44	8	3
57.8	0.40	0.98	-1.05	0.80	0.0	21	-5	2	45	-5	4	11	-4	7	5	6	-3	0
57.6	0.41	0.98	0.94	0.78	0.0	26	15	-11	57	35	-25	29	61	-42	-4	-6	-1	0
57.7	0.42	0.98	2.99	0.78	0.0	31	32	-31	67	69	-67	48	114	-112	-19	-13	-1	-1
57.7	0.42	0.98	5.03	0.78	0.0	36	54	-45	80	114	-96	68	188	-161	-24	-31	2	-3
57.5	0.40	0.98	-5.32	0.80	0.0	9	-48	37	19	-93	76	-30	-145	127	20	35	-7	0
57.5	0.40	0.98	-7.08	0.80	0.0	5	-67	49	9	-131	101	-46	-206	167	27	47	-9	0
57.7	0.41	0.98	-1.06	0.80	0.0	21	-3	2	44	-2	4	7	-1	9	-2	6	-2	-1
57.6	0.41	0.98	-1.06	2.81	0.0	19	-22	-9	43	-42	-19	8	-67	-31	-2	17	-3	-1
57.6	0.42	0.98	-1.06	4.38	0.0	18	-45	-24	41	-89	-50	6	-142	-82	-10	32	-4	0
57.6	0.42	0.98	-1.06	6.30	0.0	16	-66	-34	38	-132	-70	3	-213	-113	-11	45	-5	0
57.8	0.41	0.98	-1.06	-1.42	0.0	22	15	18	46	37	37	10	67	63	9	-5	-2	0
57.9	0.41	0.97	-1.06	-3.53	0.0	23	37	37	47	84	75	10	146	123	19	-16	-2	0
57.9	0.41	0.97	-1.06	-5.40	0.0	25	62	50	48	134	102	12	228	166	20	-30	-1	1
57.9	0.41	0.97	-1.06	0.74	0.0	20	-7	6	43	-9	12	7	-12	21	2	7	-2	-1
58.1	0.41	0.97	-1.06	0.74	2.06	26	1	4	57	10	5	32	20	7	3	1	-2	0
58.2	0.41	0.97	-1.06	0.74	4.22	34	11	2	74	30	-1	57	55	-4	6	-3	-2	0
58.0	0.41	0.97	-1.06	0.74	5.05	36	17	1	80	42	-4	67	75	-11	8	-5	-2	0
57.7	0.40	0.97	-1.06	0.74	-2.07	14	-10	4	31	-15	9	-10	-25	18	2	10	-4	1
57.7	0.40	0.97	-1.06	0.74	-3.11	11	-15	4	23	-28	12	-24	-44	24	-1	16	-4	0
57.6	0.57	0.01	0.06	1.08	0.0	16	-5	2	37	-5	3	1	-8	4	0	13	-5	0
57.8	0.57	2.09	0.06	1.08	0.0	32	28	-14	69	53	-35	50	108	-60	1	-10	-1	-1
57.9	0.56	4.14	0.06	1.08	0.0	49	64	-32	104	137	-77	104	233	-134	7	-36	3	0
57.9	0.56	5.94	0.06	1.08	0.0	55	78	-38	117	166	-93	125	281	-161	12	-44	4	0
57.9	0.56	3.13	0.06	1.08	0.0	41	44	-21	86	96	-53	76	163	-92	5	-23	0	0
57.8	0.56	1.15	0.80	0.86	0.0	29	29	-12	63	66	-31	40	112	-54	-2	-12	-1	-1
57.9	0.56	1.15	2.85	0.86	0.0	36	53	-29	78	115	-70	65	192	-121	-14	-28	0	-2
58.0	0.56	1.15	3.84	0.86	0.0	39	67	-36	87	145	-87	81	244	-151	-15	-38	1	-2
57.4	0.55	1.15	-3.40	0.86	0.0	13	-38	24	26	-74	51	-19	-116	85	16	35	-6	0
57.4	0.55	1.15	-5.58	0.86	0.0	5	-66	44	8	-131	96	-49	-210	162	29	54	-9	2
57.5	0.56	1.15	-1.31	0.86	0.0	21	-3	4	45	-2	7	10	-1	13	5	9	-4	0
57.5	0.56	1.15	-1.31	2.59	0.0	20	-25	-7	43	-47	-15	9	-74	-26	0	25	-5	0
57.6	0.56	1.15	-1.31	4.49	0.0	18	-52	-20	42	-103	-42	8	-167	-70	-8	46	-6	1
57.5	0.56	1.15	-1.31	5.49	0.0	18	-63	-25	41	-127	-52	7	-205	-86	-8	54	-7	2
57.7	0.55	1.15	-1.31	-1.35	0.0	23	24	18	48	56	34	13	99	57	13	-10	-3	0
57.7	0.55	1.15	-1.31	-3.46	0.0	23	44	39	65	98	78	8	169	127	26	-24	-2	1
57.7	0.55	1.15	-1.31	-4.40	0.0	24	58	46	46	128	89	10	219	144	29	-35	-1	2
57.7	0.55	1.14	-1.30	1.08	0.0	21	-4	2	46	-4	3	12	-3	6	5	10	-4	0
57.9	0.56	1.14	-1.30	1.08	2.06	30	11	-1	64	30	-9	43	54	-17	11	0	-3	0
58.1	0.55	1.14	-1.30	1.08	4.22	38	26	-3	84	63	-19	75	110	-35	16	-5	-2	0
58.2	0.55	1.14	-1.30	1.08	5.05	41	33	-3	91	78	-21	88	136	-41	16	-7	-1	1
57.8	0.55	1.14	-1.30	1.08	-2.06	12	-22	7	26	-43	18	-18	-69	33	1	24	-6	0
57.9	0.55	1.14	-1.30	1.08	-3.11	8	-28	9	17	-55	23	-32	-89	43	-2	29	-6	1

TABLE V

HARMONIC CONTENT OF THE BLADE FLAPPING RESPONSE TO θ_o, θ_s, θ_c AND α AT THREE RADIAL POSITIONS, CONFIGURATION 5 (Continued)

						M_β @ r = 22.3 in. in.-lb			M_β @ r = 13.15 in. in.-lb			M_β @ r = 3.3 in. ~ in.-lb						
$\frac{\Omega}{\text{rad}}$ sec	μ	θ_o deg	θ_s deg	θ_c deg	α deg	M_{β_o}	$M_{\beta_{1c}}$	$M_{\beta_{1s}}$	M_{β_o}	$M_{\beta_{1c}}$	$M_{\beta_{1s}}$	M_{β_o}	$M_{\beta_{1c}}$	$M_{\beta_{1s}}$	$M_{\beta_{2c}}$	$M_{\beta_{2s}}$	$M_{\beta_{3c}}$	$M_{\beta_{3s}}$
57.4	0.79	0.08	-0.37	0.99	0.0	16	-6	6	36	-8	12	0	-14	21	2	26	-9	0
57.6	0.79	1.09	-0.37	0.99	0.0	24	21	-3	55	50	-14	32	86	-25	12	0	-5	1
57.9	0.78	2.10	-0.37	0.99	0.0	33	48	-15	74	105	-41	61	181	-70	16	-19	-2	0
57.9	0.79	3.12	-0.37	0.99	0.0	42	72	-29	92	155	-74	93	265	-127	18	-41	1	2
57.4	0.79	1.75	-0.37	0.99	0.0	30	37	-13	67	83	-35	50	141	-59	9	-13	-3	0
57.2	0.79	0.56	-0.87	1.29	0.0	13	-10	6	36	-16	9	9	-24	15	5	27	-8	1
57.3	0.79	0.56	0.03	1.29	0.0	20	15	-5	51	38	-17	30	65	-29	3	11	-8	0
58.0	0.79	0.55	1.99	1.29	0.0	31	60	-19	75	133	-51	69	226	-90	4	-25	-2	0
57.6	0.79	0.55	-2.08	1.29	0.0	12	-38	18	25	-76	39	-22	-123	66	9	47	-10	4
57.5	0.79	0.55	-3.10	1.29	0.0	7	-62	30	13	-125	66	-42	-205	111	13	67	-13	4
57.7	0.79	0.55	-0.97	1.29	0.0	18	-6	5	40	-9	8	4	-13	13	13	20	-6	6
57.5	0.79	0.55	-0.97	2.38	0.0	18	-26	-1	39	-51	-4	0	-84	-8	-1	41	-10	1
57.5	0.80	0.55	-0.97	3.21	0.0	17	-37	-7	39	-73	-16	1	-120	-28	-4	49	-11	2
57.5	0.80	0.55	-0.97	4.17	0.0	17	-52	-10	38	-105	-23	-2	-175	-39	-8	65	-13	4
57.6	0.79	0.55	-0.95	-0.53	0.0	19	19	18	41	45	34	3	78	58	16	-1	-5	0
57.6	0.79	0.55	-0.95	-2.79	0.0	19	44	34	40	98	68	2	171	115	33	-22	-2	2
57.7	0.79	0.55	-0.95	-3.87	0.0	19	60	45	40	133	89	5	229	148	45	-38	0	3
57.6	0.79	0.55	-0.95	1.13	0.0	18	-5	7	40	-7	12	3	-11	21	8	23	-8	2
57.9	0.79	0.55	-0.95	1.13	2.05	29	28	-3	67	64	-14	51	110	-21	19	-1	-5	2
58.3	0.78	0.55	-0.95	1.13	4.21	41	63	-10	100	140	-36	112	239	-61	36	-21	-1	3
57.7	0.79	0.55	-0.95	1.13	-2.05	7	-40	16	14	-81	38	-40	-135	64	-7	48	-12	0
57.8	0.79	0.55	-0.95	1.13	-3.10	2	-56	22	0	-114	52	-65	-191	87	-13	59	-13	1
57.6	0.92	0.04	-0.25	1.35	0.0	17	-9	4	39	-15	8	3	-26	15	1	33	-10	1
57.7	0.92	0.99	-0.25	1.35	0.0	25	23	-8	59	55	-23	39	96	-37	11	1	-6	2
58.0	0.92	2.15	-0.25	1.34	0.0	35	59	-21	83	131	-54	80	225	-91	21	-28	-2	4
58.0	0.92	1.71	-0.25	1.35	0.0	31	47	-14	74	106	-38	65	183	-64	18	-12	-4	2
57.8	0.92	0.55	-0.78	1.35	0.0	18	-5	5	42	-6	7	9	-9	12	14	26	-9	4
58.0	0.92	0.55	0.15	1.35	0.0	24	23	-9	58	55	-25	38	94	-40	5	0	-7	1
57.9	0.92	0.55	1.46	1.35	0.0	31	57	-21	77	125	-53	73	213	-88	3	-22	-4	0
57.6	0.92	0.55	-1.82	1.35	0.0	13	-33	17	29	-63	33	-14	-103	54	11	47	-11	4
57.6	0.93	0.55	-0.81	1.35	0.0	18	-5	4	42	-7	6	8	-11	12	8	29	-9	2
57.6	0.93	0.55	-0.81	2.10	0.0	19	-14	-1	44	-24	-8	10	-39	-15	2	34	-10	3
57.5	0.93	0.55	-0.81	3.03	0.0	19	-32	-7	41	-63	-19	6	-106	-34	-5	49	-13	2
57.5	0.93	0.55	-0.81	4.00	0.0	18	-46	-14	40	-93	-32	1	-156	-55	-12	63	-14	4
57.6	0.92	0.55	-0.78	0.13	0.0	19	15	11	45	38	20	14	65	37	17	5	-6	2
57.6	0.92	0.55	-0.78	-0.80	0.0	19	25	19	45	58	36	15	101	61	26	-4	-5	3
57.5	0.92	0.55	-0.78	-2.83	0.0	20	53	34	45	118	69	17	205	117	42	-32	-2	5
57.5	0.93	0.55	-0.78	1.44	0.0	18	-7	4	42	-11	5	7	-18	9	9	29	-9	3
57.9	0.92	0.55	-0.78	1.44	2.05	32	39	-8	80	89	-26	78	155	-42	27	-9	-5	6
58.2	0.91	0.55	-0.78	1.44	3.16	41	67	-11	104	149	-36	122	258	-59	38	-24	-2	5
57.6	0.92	0.55	-0.78	1.44	-2.05	7	-50	16	10	-101	36	-80	-170	56	-5	61	-14	3
57.7	0.92	0.55	-0.78	1.44	-3.12	0	-70	22	-8	-145	50	-94	-246	80	-9	76	-16	5
88.9	0.27	-0.03	0.15	0.44	0.05	20	-5	1	52	-3	4	-8	-3	6	-2	2	-3	0
88.9	0.27	2.07	0.17	0.44	0.06	34	15	1	84	37	0	38	67	0	1	-3	0	1
88.8	0.27	4.01	0.17	0.44	0.06	50	35	-1	117	79	-9	74	146	-18	-14	-6	-3	4
88.9	0.27	6.17	0.17	0.44	0.07	68	57	0	157	125	-11	150	218	-24	8	-13	2	4
88.7	0.27	7.16	0.17	0.44	0.07	77	68	2	175	150	-6	177	260	-17	12	-15	2	4

TABLE V

HARMONIC CONTENT OF THE BLADE FLAPPING RESPONSE TO θ_o, θ_s, θ_c AND α AT THREE RADIAL POSITIONS, CONFIGURATION 5 (Continued)

						M_β @ r = 22.3 in. in.-lb			M_β @ r = 13.15 in. in.-lb			M_β @ r = 3.3 in. ~ in.-lb						
$\frac{\Omega}{\text{rad}}$ sec	μ	θ_o deg	θ_s deg	θ_c deg	α deg	M_{β_o}	$M_{\beta_{1c}}$	$M_{\beta_{1s}}$	M_{β_o}	$M_{\beta_{1c}}$	$M_{\beta_{1s}}$	M_{β_o}	$M_{\beta_{1c}}$	$M_{\beta_{1s}}$	$M_{\beta_{2c}}$	$M_{\beta_{2s}}$	$M_{\beta_{3c}}$	$M_{\beta_{3s}}$
88.8	0.26	1.04	-0.54	0.73	0.06	27	-5	0	66	-7	0	17	-9	1	-1	2	0	0
88.9	0.27	1.04	1.49	0.73	0.07	31	17	-9	76	44	-23	28	77	-41	-5	-3	1	1
88.9	0.27	1.04	3.59	0.73	0.06	34	42	-22	84	97	-51	47	170	-89	-5	-12	3	3
88.9	0.26	1.04	5.66	0.73	0.07	37	61	-28	91	140	-66	58	246	-120	-6	-18	4	4
88.7	0.26	1.04	-2.70	0.74	0.05	22	-34	9	55	-70	20	3	-117	38	0	10	-3	-1
88.8	0.26	1.04	-4.88	0.74	0.04	18	-63	19	45	-133	44	-14	-224	80	0	18	-3	-4
88.7	0.27	1.04	-0.67	0.73	0.06	26	-3	2	65	-3	4	16	-3	8	0	1	0	1
88.7	0.27	1.04	-0.67	2.78	0.05	24	-26	-22	63	-56	-50	12	-96	-87	-4	1	0	0
88.8	0.27	1.04	-0.67	4.70	0.05	21	-46	-43	59	-103	-100	12	-179	-175	-8	2	0	-2
89.0	0.26	1.04	-0.67	-1.36	0.07	29	10	17	69	31	39	18	58	70	1	0	-1	0
89.0	0.26	1.04	-0.67	-3.25	0.07	30	24	42	71	65	97	20	123	169	8	0	-2	3
88.9	0.26	1.04	-0.67	-4.78	0.07	32	41	60	72	104	136	21	194	236	8	0	0	3
89.0	0.27	1.11	-1.36	0.13	2.10	34	0	6	86	4	11	41	11	16	3	2	0	0
89.1	0.27	1.11	-1.36	0.13	4.26	39	5	9	100	17	14	63	35	19	1	0	1	1
89.3	0.26	1.10	-1.36	0.13	5.10	41	6	10	105	20	17	71	40	24	4	0	0	0
88.9	0.27	1.10	-1.35	0.13	-2.06	28	-6	0	65	-9	0	6	-12	0	2	3	-1	2
88.8	0.27	1.10	-1.35	0.13	-3.07	25	-11	0	59	-19	1	-2	-29	3	0	4	-2	0
89.1	0.36	-0.04	-0.56	0.28	0.04	24	-5	2	60	-3	1	3	2	2	-1	4	-2	0
89.1	0.36	2.06	-0.56	0.31	0.05	42	21	-2	102	58	-13	63	113	-25	5	-4	1	0
89.2	0.36	4.07	-0.56	0.31	0.05	59	50	-4	141	122	-23	121	228	-47	13	-12	2	5
89.0	0.36	1.24	-1.80	0.31	0.04	31	-9	4	76	-11	7	25	-11	7	5	4	0	1
89.2	0.36	1.24	0.39	0.31	0.05	37	22	-7	92	60	-21	50	116	-41	1	-6	1	1
89.5	0.36	1.24	2.48	0.31	0.05	42	46	-19	106	114	-51	73	213	-95	0	-14	4	1
89.2	0.36	1.24	-3.76	0.31	0.03	26	-41	16	61	-84	35	0	-138	57	6	17	-3	0
89.2	0.35	1.24	-6.23	0.30	0.04	20	-70	28	46	-151	65	-24	-256	114	11	28	-5	-1
89.4	0.36	1.24	-1.67	0.31	0.05	32	-7	4	77	-7	6	25	-5	7	4	4	0	1
89.3	0.36	1.24	-1.67	2.19	0.04	29	-27	-17	73	-57	-41	22	-90	-76	1	10	-1	0
89.2	0.36	1.24	-1.67	4.14	0.04	27	-47	-39	68	-104	-94	16	-174	-171	-5	14	-2	0
89.5	0.36	1.24	-1.67	-1.85	0.05	34	15	26	82	46	56	32	92	98	8	0	-1	0
89.4	0.36	1.24	-1.66	-4.26	0.05	36	36	58	85	98	129	35	187	222	18	-3	-1	3
89.3	0.36	1.24	-1.66	0.43	0.04	32	-6	4	78	-5	5	27	-1	5	6	1	0	0
89.3	0.36	1.24	-1.66	0.43	2.10	38	0	5	94	12	5	54	33	4	4	1	0	0
89.7	0.36	1.24	-1.66	0.44	4.26	44	6	9	111	28	9	83	64	8	8	0	0	0
90.0	0.36	1.24	-1.65	0.43	5.09	46	12	9	119	42	6	95	89	0	7	-1	0	0
88.9	0.36	1.24	-1.66	0.43	-1.98	26	-14	0	62	-27	0	1	-36	2	2	8	-1	0
88.8	0.36	1.24	-1.66	0.43	-3.07	23	-16	0	52	-30	0	-11	-49	2	-1	9	-2	0
89.0	0.51	0.02	-0.89	0.41	0.04	24	-8	5	61	-7	7	4	-6	10	1	11	-4	0
89.1	0.51	1.05	-0.89	0.41	0.05	33	12	3	82	41	-4	35	83	-14	6	1	-1	0
89.1	0.51	2.05	-0.89	0.41	0.05	42	31	0	103	87	-16	67	169	-36	12	-5	0	0
89.1	0.51	3.14	-0.89	0.43	0.04	51	52	-2	125	136	-31	100	259	-67	20	-12	1	2
88.6	0.51	-0.98	-0.87	0.43	0.04	15	-26	7	40	-52	18	-25	-86	30	-5	20	-6	0
88.7	0.51	0.43	-1.20	0.67	0.04	26	-8	3	66	-6	2	11	-2	0	3	10	-3	0
88.9	0.51	0.43	-0.20	0.67	0.04	30	9	-1	76	34	-14	28	70	-31	2	3	-1	0
89.0	0.51	0.43	0.84	0.67	0.05	33	26	-5	86	75	-27	45	146	-55	2	-3	0	-2
89.2	0.51	0.43	1.77	0.66	0.05	37	45	-10	96	121	-42	61	229	-84	2	-11	1	-1
88.7	0.51	0.43	-2.21	0.67	0.02	21	-29	9	54	-57	19	-7	-93	31	5	18	-4	3
88.6	0.50	0.43	-3.43	0.67	0.04	17	-53	13	41	-114	34	-28	-195	61	6	29	-5	3

TABLE V

HARMONIC CONTENT OF THE BLADE FLAPPING RESPONSE TO θ_o, θ_s, θ_c AND α AT THREE RADIAL POSITIONS, CONFIGURATION 5 (Continued)

						M_β @ r = 22.3 in. in.-lb			M_β @ r = 13.15 in. in.-lb			M_β @ r = 3.3 in. - in.-lb						
$\frac{\Omega}{\text{rad}}$ sec	μ	θ_o deg	θ_s deg	θ_c deg	α deg	M_{β_o}	$M_{\beta_{1c}}$	$M_{\beta_{1s}}$	M_{β_o}	$M_{\beta_{1c}}$	$M_{\beta_{1s}}$	M_{β_o}	$M_{\beta_{1c}}$	$M_{\beta_{1s}}$	$M_{\beta_{2c}}$	$M_{\beta_{2s}}$	$M_{\beta_{3c}}$	$M_{\beta_{3s}}$
89.3	0.50	0.43	-3.86	0.67	0.04	15	-61	12	36	-135	37	-38	-234	68	0	33	-7	3
89.5	0.50	0.43	-1.25	0.67	0.05	26	-7	3	66	-5	1	11	0	0	3	9	-2	2
89.3	0.51	0.43	-1.25	1.51	0.04	25	-16	-6	64	-27	-23	11	-39	-40	0	14	-4	1
89.4	0.51	0.43	-1.25	2.50	0.02	24	-27	-18	62	-56	-43	6	-92	-80	-3	19	-3	3
89.3	0.51	0.43	-1.25	3.30	0.03	23	-37	-25	60	-81	-58	3	-137	-104	-6	23	-3	4
89.5	0.50	0.43	-1.25	-1.39	0.05	29	10	25	69	39	49	16	80	83	12	3	-1	-1
89.5	0.50	0.43	-1.24	-3.40	0.05	30	28	50	72	85	105	17	165	179	22	-1	-1	0
89.4	0.50	0.43	-1.24	0.62	0.03	21	-9	4	61	-10	5	16	-10	5	2	10	-2	1
89.7	0.50	0.43	-1.22	0.62	2.09	33	6	8	83	35	6	51	66	2	9	14	13	2
90.2	0.50	0.42	-1.23	0.62	4.25	42	23	13	112	76	3	91	154	-11	18	1	-1	0
89.5	0.50	0.42	-1.23	0.63	5.08	45	31	14	121	95	1	107	188	-15	22	1	0	1
88.2	0.51	0.42	-1.24	0.63	-2.01	18	-22	0	44	-46	6	-22	-77	13	-1	17	-4	2
88.2	0.51	0.42	-1.24	0.63	-3.06	13	-32	0	32	-69	7	-39	-123	11	-5	20	-7	2
89.0	0.50	-0.01	-0.98	0.58	0.05	24	-10	6	59	-11	9	2	-12	13	2	15	-2	0
89.2	0.51	1.01	-0.98	0.58	0.05	32	13	5	81	48	-3	36	98	-13	14	5	0	0
89.4	0.60	2.10	-0.98	0.58	0.05	43	40	2	106	115	-17	75	223	-41	25	-6	4	0
89.3	0.60	2.44	-0.98	0.58	0.05	47	51	-1	114	138	-30	87	264	-65	28	-12	3	0
88.9	0.61	0.46	-0.98	0.58	0.05	28	2	5	70	21	2	20	48	0	11	8	-2	1
89.3	0.60	0.46	-1.51	0.73	0.05	26	-11	5	64	-13	7	9	-14	8	5	15	-2	1
89.5	0.60	0.46	-0.51	0.73	0.05	31	9	0	75	36	-9	33	74	-8	24	6	0	0
89.7	0.60	0.46	0.48	0.73	0.05	34	30	-2	87	90	-25	49	175	-52	8	-1	1	0
90.0	0.60	0.46	1.39	0.73	0.05	38	52	-6	100	144	-40	71	274	-83	11	-10	2	-1
89.3	0.61	0.46	-2.18	0.73	0.05	23	-26	7	56	-49	16	-5	-80	25	4	21	-4	2
89.3	0.60	0.46	-3.50	0.73	0.04	16	-61	15	37	-132	43	-36	-229	76	5	35	-6	5
89.5	0.61	0.46	-1.47	0.73	0.05	25	-11	8	63	-13	11	8	-15	14	12	12	-2	2
89.3	0.61	0.46	-1.47	1.74	0.04	25	-22	-6	62	-41	-19	24	-61	-37	-1	21	-3	1
89.3	0.61	0.46	-1.47	2.66	0.05	23	-36	-15	58	-76	-35	14	-130	-69	-2	32	-3	2
89.5	0.60	0.46	-1.47	-1.22	0.05	28	9	26	68	40	48	49	86	81	10	18	-1	0
89.3	0.60	0.46	-1.47	-3.15	0.05	30	30	51	71	93	103	21	185	174	31	-2	1	0
88.0	0.61	0.47	-1.46	1.60	0.02	26	-6	5	65	-1	6	7	6	10	7	17	-3	2
88.7	0.61	0.46	-1.44	1.61	2.08	36	19	8	92	64	-1	58	142	-10	21	6	3	0
89.0	0.61	0.46	-1.44	1.62	3.54	41	39	11	112	113	-6	100	244	-27	38	0	4	1
89.1	0.61	0.46	-1.46	1.62	-2.03	16	-31	3	38	-65	14	-40	-126	34	-6	27	-11	5
89.3	0.61	0.46	-1.46	1.62	-3.08	10	-44	3	24	-98	20	-67	-196	49	-17	33	-12	5
88.8	0.72	0.02	-1.28	1.68	0.03	22	-6	9	58	-5	10	0	-4	19	20	16	-3	6
89.0	0.72	1.04	-1.28	1.68	0.03	31	21	6	81	66	-3	39	145	-13	25	11	0	-1
89.1	0.72	1.50	-1.28	1.68	0.03	36	37	3	93	104	-13	60	225	-31	32	3	5	0
88.8	0.72	0.62	-1.28	1.68	0.03	27	6	6	69	27	2	18	65	2	17	16	-2	0
88.7	0.72	-1.09	-1.29	1.69	0.02	11	-45	12	32	-98	31	-46	-193	64	-12	45	-19	6
88.7	0.72	0.03	-1.29	1.68	0.02	22	-8	7	58	-8	9	-1	-11	19	4	26	-6	1
89.0	0.72	0.03	-0.12	1.68	0.03	27	22	4	74	68	-8	33	146	-24	16	13	-4	-2
89.2	0.71	0.03	0.71	1.68	0.03	31	44	0	87	120	-22	57	254	-51	19	6	2	-8
88.6	0.72	0.03	-2.26	1.70	0.02	17	-42	9	42	-90	24	-32	-175	52	-6	42	-12	2
88.6	0.72	0.03	-2.70	1.70	0.03	13	-56	15	35	-124	37	-46	-243	77	0	49	-16	11
88.8	0.72	0.03	-1.31	1.72	0.03	22	-12	8	56	-18	12	-4	-30	23	5	27	-5	0
88.9	0.72	0.03	-1.31	2.78	0.03	21	-26	-3	55	-52	-11	-7	-100	-25	-2	36	-9	3
88.9	0.72	0.03	-1.31	3.69	0.02	19	-40	-12	52	-87	-29	-13	-172	-60	-10	45	-14	5

TABLE V

HARMONIC CONTENT OF THE BLADE FLAPPING RESPONSE TO θ_o, θ_s, θ_c AND α AT THREE RADIAL POSITIONS, CONFIGURATION 5 (Continued)

						M_β @ r = 22.3 in. in.-lb			M_β @ r = 13.15 in. in.-lb			M_β @ r = 3.3 in. ~ in.-lb						
$\frac{\Omega}{\text{rad/sec}}$	μ	θ_o deg	θ_s deg	θ_c deg	α deg	M_{β_o}	$M_{\beta_{1c}}$	$M_{\beta_{1s}}$	M_{β_o}	$M_{\beta_{1c}}$	$M_{\beta_{1s}}$	M_{β_o}	$M_{\beta_{1c}}$	$M_{\beta_{1s}}$	$M_{\beta_{2c}}$	$M_{\beta_{2s}}$	$M_{\beta_{3c}}$	$M_{\beta_{3s}}$
89.0	0.71	0.03	-1.31	0.78	0.03	23	0	17	58	12	33	-2	33	65	12	21	-4	-1
89.0	0.71	0.03	-1.31	-0.30	0.03	24	15	28	63	52	52	7	119	99	23	13	-1	-1
88.9	0.71	0.03	-1.31	-1.74	0.03	24	29	43	61	87	86	5	196	159	39	-2	0	0
88.7	0.72	0.03	-1.31	1.85	0.02	21	-12	6	57	-18	10	-3	-29	18	4	27	-7	1
89.3	0.71	0.03	-1.31	1.86	2.07	30	21	12	87	69	4	60	152	-1	35	16	2	-1
89.6	0.71	0.03	-1.31	1.86	3.09	36	40	12	105	116	-2	97	250	-15	45	8	6	-1
89.0	0.72	0.03	-1.31	1.84	-2.03	11	-50	5	26	-114	21	-63	-228	45	-20	43	-21	10
88.8	0.72	0.03	-1.31	1.85	-0.99	17	-30	5	43	-64	14	-31	-125	33	-5	34	-13	6
89.4	0.75	-0.04	0.29	2.17	0.0	18	-8	12	43	-8	20	-11	-7	30	1	19	-6	0
89.6	0.75	0.44	0.29	2.17	0.0	24	11	9	58	41	9	10	82	11	9	11	-2	0
89.9	0.75	0.99	0.29	2.17	0.0	29	30	10	72	88	3	33	170	-2	18	5	0	0
90.3	0.75	1.45	0.29	2.17	0.0	34	42	6	82	117	-5	47	222	-15	22	0	2	0
89.8	0.75	-0.52	0.28	2.17	0.0	15	-24	12	33	-48	27	-28	-80	45	-6	28	-11	0
90.0	0.75	-1.12	0.28	2.17	0.0	10	-41	13	21	-90	34	-47	-156	61	-13	34	-14	2
88.9	0.75	0.51	-0.59	1.46	0.0	23	-2	6	51	5	6	0	18	7	7	18	-5	1
89.3	0.75	0.51	0.42	1.46	0.0	27	27	2	67	79	-11	28	153	-25	13	7	-1	0
89.0	0.75	0.51	-1.06	1.46	0.0	19	-19	10	43	-34	18	-14	-50	26	1	25	-9	1
89.0	0.75	0.51	-1.69	1.46	0.0	19	-35	7	36	-74	19	-28	-125	34	-6	31	-11	2
89.1	0.75	0.51	-2.18	1.46	0.0	15	-53	12	28	-116	33	-41	-200	57	-4	38	-12	5
89.1	0.75	0.51	-0.51	1.62	0.0	22	-5	5	50	-2	3	-1	3	1	2	20	-5	0
89.1	0.75	0.51	-0.51	2.68	0.0	21	-17	-3	49	-30	-16	-2	-46	-33	-3	26	-7	0
89.1	0.75	0.51	-0.51	3.33	0.0	21	-26	-9	47	-53	-29	-7	-86	-55	-9	29	-9	1
89.3	0.75	0.51	-0.51	0.67	0.0	23	10	18	54	40	29	7	81	47	14	12	-4	0
89.6	0.74	0.51	-0.51	-0.32	0.0	24	23	25	56	71	43	11	138	72	18	5	0	0
89.3	0.74	0.51	-0.51	-1.33	0.0	26	27	36	57	83	71	9	161	123	26	5	-1	0
89.2	0.74	0.51	-0.51	-1.33	0.0	25	28	34	56	83	67	7	163	112	25	2	0	-1
89.0	0.81	0.06	-0.13	1.72	0.0	21	-9	4	47	-12	1	-5	-15	1	0	25	-8	0
89.2	0.81	0.58	-0.14	1.72	0.0	26	12	2	62	43	-9	17	86	-19	10	15	-3	0
89.4	0.80	1.13	-0.14	1.73	0.0	30	30	2	75	89	-15	41	173	-34	21	7	0	0
89.6	0.80	1.57	-0.14	1.73	0.0	35	49	0	88	135	-27	63	257	-56	29	-2	3	-1
89.0	0.81	-0.45	-0.14	1.73	0.0	17	-27	4	35	-57	8	-26	-98	14	-11	30	-10	0
89.1	0.81	-1.06	-0.14	1.72	0.0	10	-54	8	19	-122	25	-51	-217	47	-19	45	-17	4
89.1	0.81	0.51	-0.65	1.74	0.0	23	-9	4	50	-11	2	-3	-11	2	4	21	-7	0
89.3	0.81	0.51	-0.12	1.73	0.0	25	11	2	60	42	-10	18	86	-22	12	16	-5	0
89.5	0.81	0.51	0.40	1.72	0.0	27	26	-2	68	75	-25	33	146	-51	17	4	-3	-1
89.6	0.81	0.51	0.83	1.72	0.0	29	45	0	78	125	-24	54	238	-48	19	4	0	-2
88.7	0.82	0.51	-1.25	1.72	0.0	20	-26	7	41	-54	13	-18	-90	21	-1	33	-11	2
89.0	0.81	0.51	-1.77	1.73	0.0	18	-46	10	31	-101	29	-35	-179	46	-6	39	-13	5
89.1	0.81	0.51	-2.24	1.73	0.0	21	-57	11	38	-129	27	-58	-242	45	-14	42	-16	4
89.1	0.81	0.51	-0.59	1.72	0.0	23	-3	3	52	3	0	2	14	-2	5	22	-7	1
89.1	0.81	0.51	-0.59	2.24	0.0	23	-8	0	52	-10	-10	0	-9	-22	-2	23	-7	0
89.1	0.81	0.51	-0.59	3.39	0.0	22	-23	-9	49	-48	-29	-3	-78	-55	-6	30	-11	2
89.3	0.81	0.51	-0.59	0.56	0.0	24	16	20	57	56	32	14	111	54	19	13	-2	0
89.4	0.81	0.51	-0.59	-0.37	0.0	24	24	25	58	75	46	15	146	78	25	7	-1	-1
89.1	0.82	0.51	-0.59	-1.19	0.0	26	29	31	58	85	66	12	165	119	23	7	2	-2

TABLE V

HARMONIC CONTENT OF THE BLADE FLAPPING RESPONSE TO θ_o, θ_s, θ_c AND α AT THREE RADIAL POSITIONS, CONFIGURATION 5 (Continued)

						M_β @ r = 22.3 in. in.-lb			M_β @ r = 13.15 in. in.-lb			M_β @ r = 3.3 in. ~ in.-lb						
$\frac{\Omega}{\text{rad}}$ sec	μ	θ_o deg	θ_s deg	θ_c deg	α deg	M_{β_o}	$M_{\beta_{1c}}$	$M_{\beta_{1s}}$	M_{β_o}	$M_{\beta_{1c}}$	$M_{\beta_{1s}}$	M_{β_o}	$M_{\beta_{1c}}$	$M_{\beta_{1s}}$	$M_{\beta_{2c}}$	$M_{\beta_{2s}}$	$M_{\beta_{3c}}$	$M_{\beta_{3s}}$
89.1	0.76	0.49	-0.47	1.56	0.0	23	1	7	53	16	6	9	38	6	8	18	-5	0
89.4	0.75	0.49	-0.47	1.56	1.05	29	25	10	72	77	1	45	150	-4	22	10	-2	0
89.0	0.75	0.48	-0.47	1.56	1.97	33	42	11	88	121	2	75	231	-3	28	7	2	-1
87.9	0.76	0.49	-0.47	1.57	-1.04	19	-22	6	37	-43	13	-20	-72	21	-7	26	-10	1
89.3	0.75	0.49	-0.47	1.57	-1.92	14	-36	4	23	-81	17	-45	-145	30	-18	28	-13	2
89.2	0.82	0.49	-0.69	1.57	0.0	23	-1	9	51	8	10	7	24	15	10	19	-5	0
89.7	0.82	0.49	-0.69	1.57	1.01	28	24	6	71	72	-2	44	140	-9	25	4	-1	-1
89.7	0.82	0.49	-0.69	1.56	1.65	29	33	12	81	100	6	68	194	5	36	9	1	-1
88.1	0.83	0.49	-0.70	1.57	-1.02	18	-29	9	34	-61	19	-25	-104	30	-7	32	-13	2
88.2	0.83	0.49	-0.70	1.57	-1.74	15	-42	7	22	-95	21	-48	-167	36	-17	35	-17	6

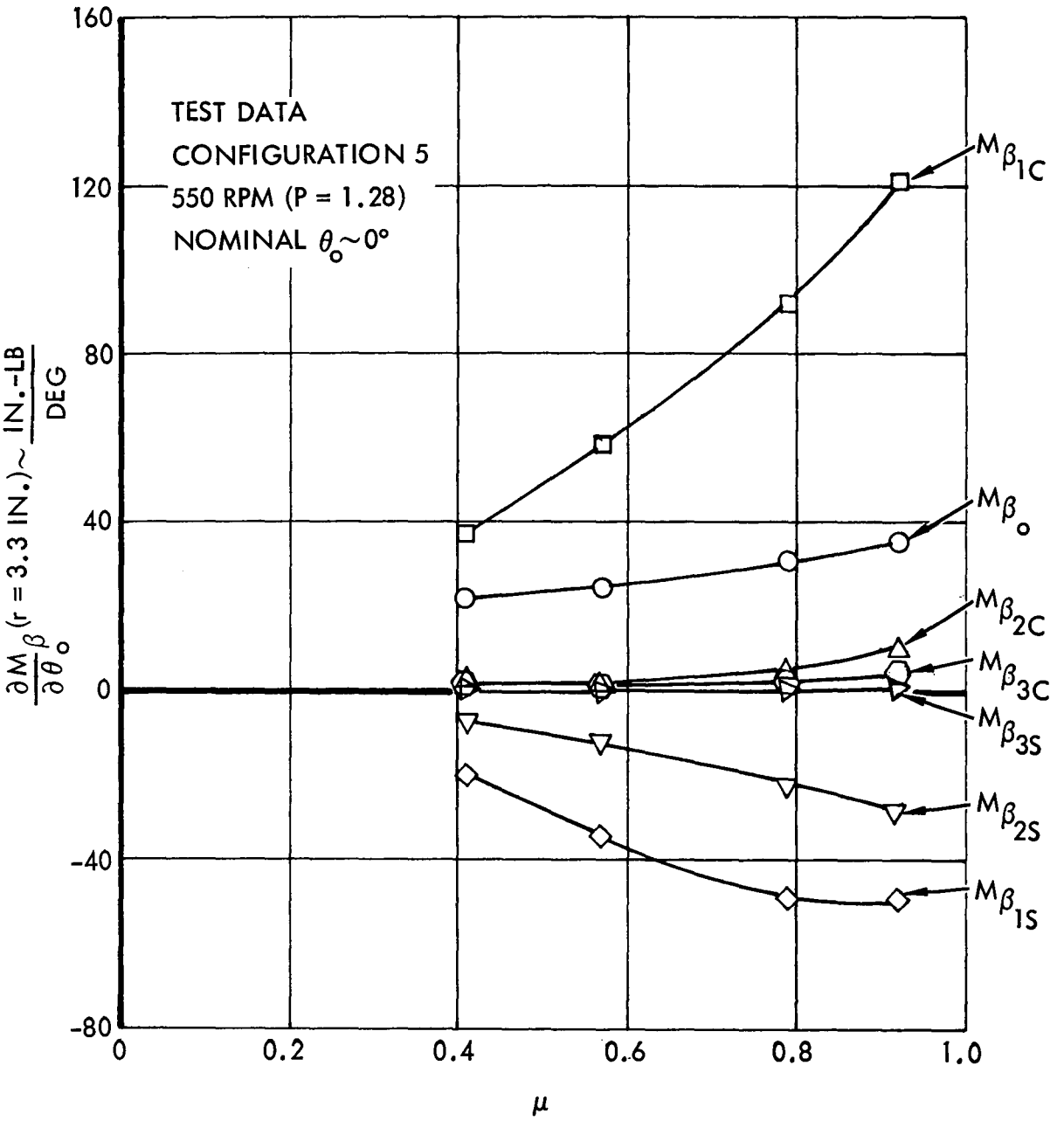

Figure A1. Harmonic Content of Blade Flapping, Configuration 5, 550 RPM (P = 1.28), Steady θ_o Excitation

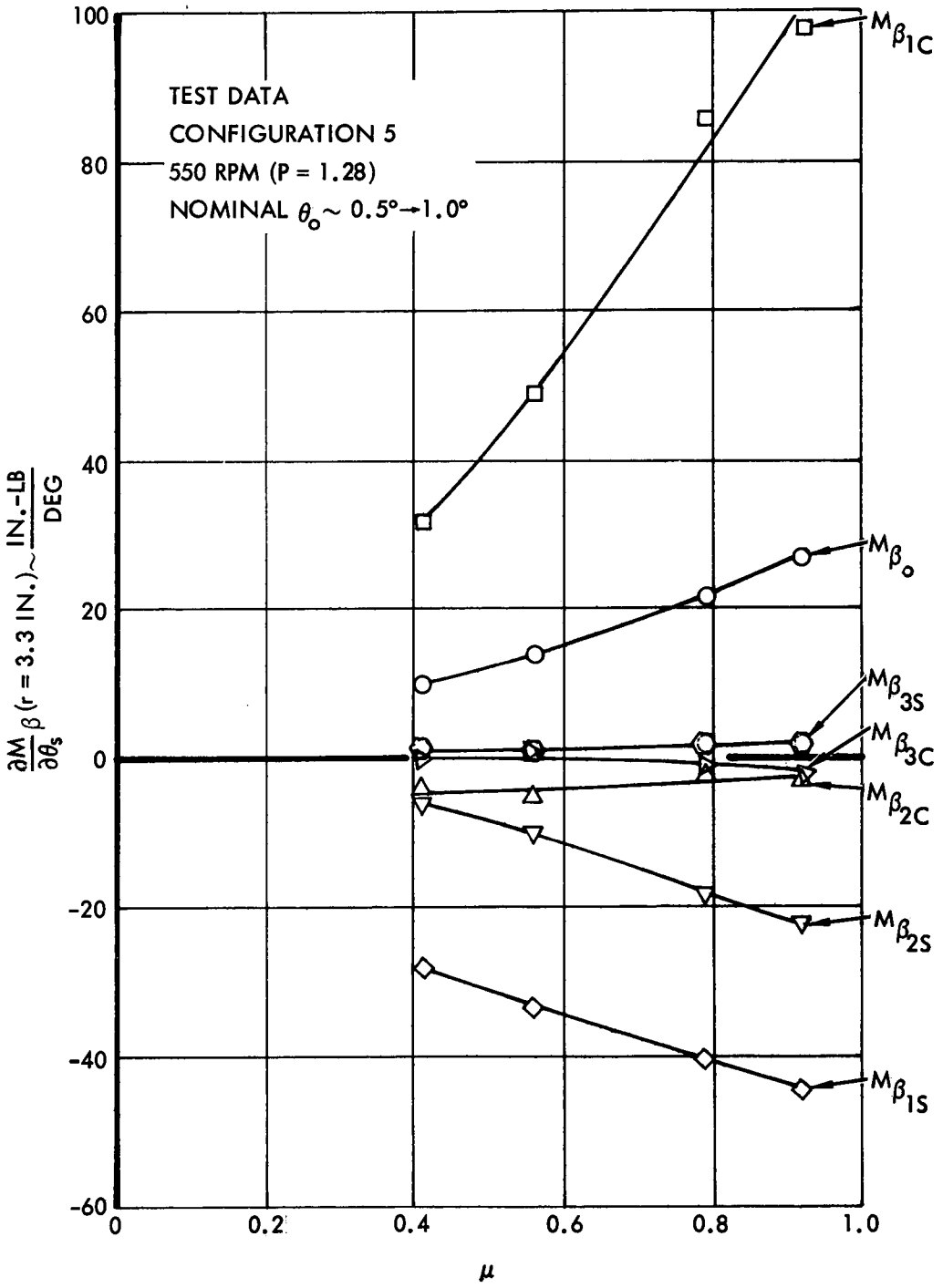

Figure A2. Harmonic Content of Blade Flapping, Configuration 5, 550 RPM (P = 1.28), Steady θ_s Excitation

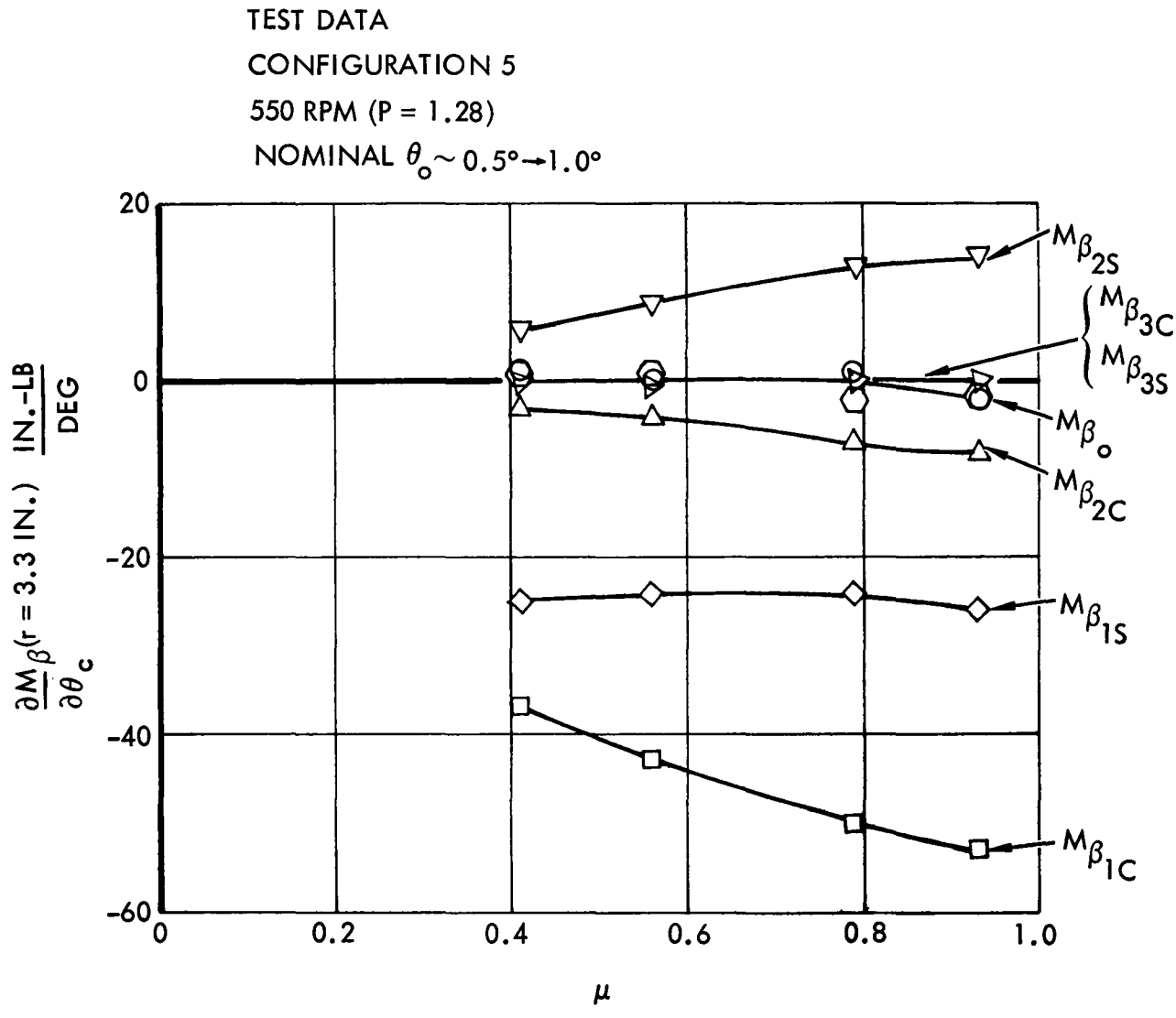

Figure A3. Harmonic Content of Blade Flapping, Configuration 5, 550 RPM (P = 1.28), Steady θ_c Excitation

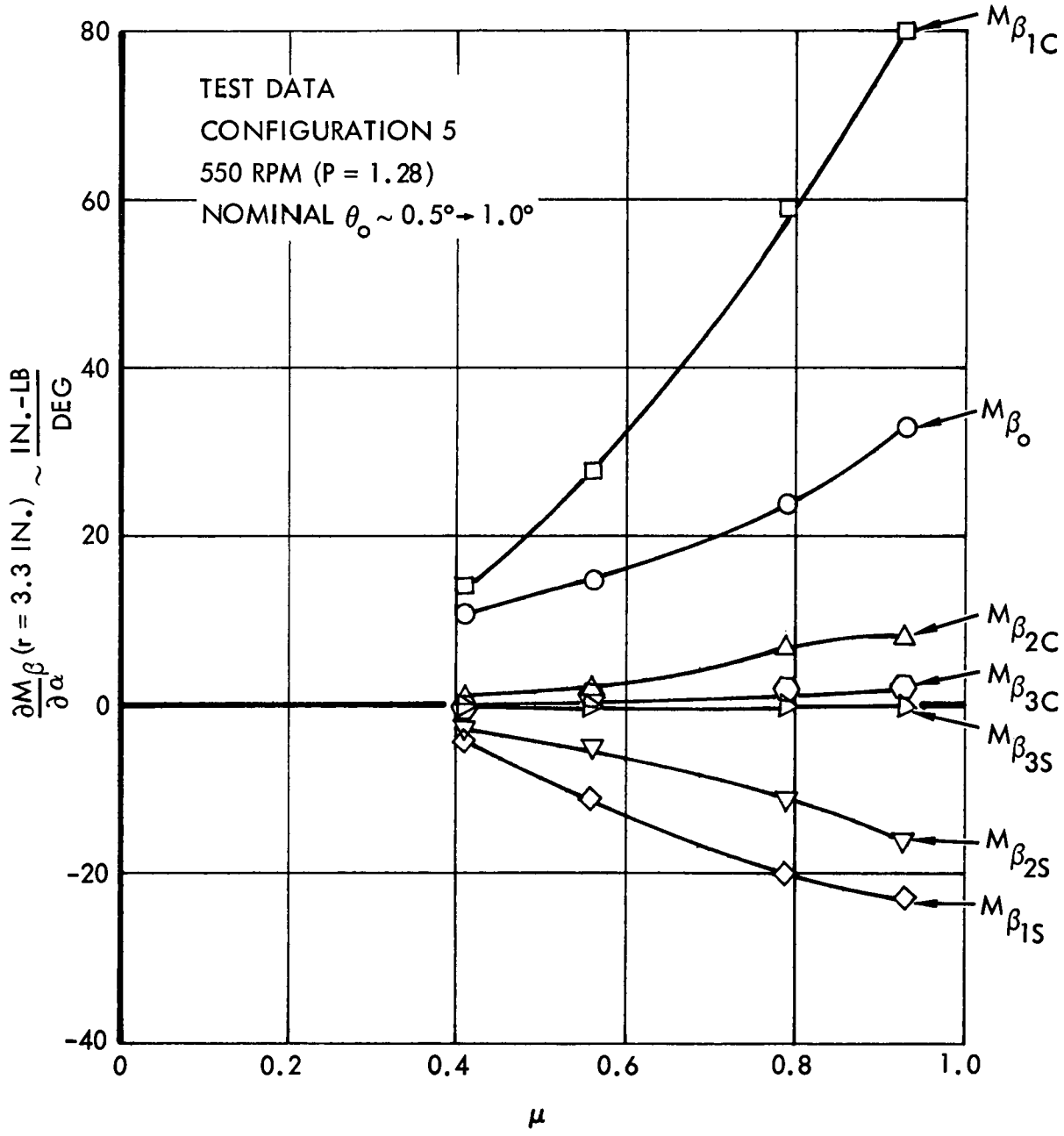

Figure A4. Harmonic Content of Blade Flapping, Configuration 5, 550 RPM (P = 1.28), Steady α Excitation

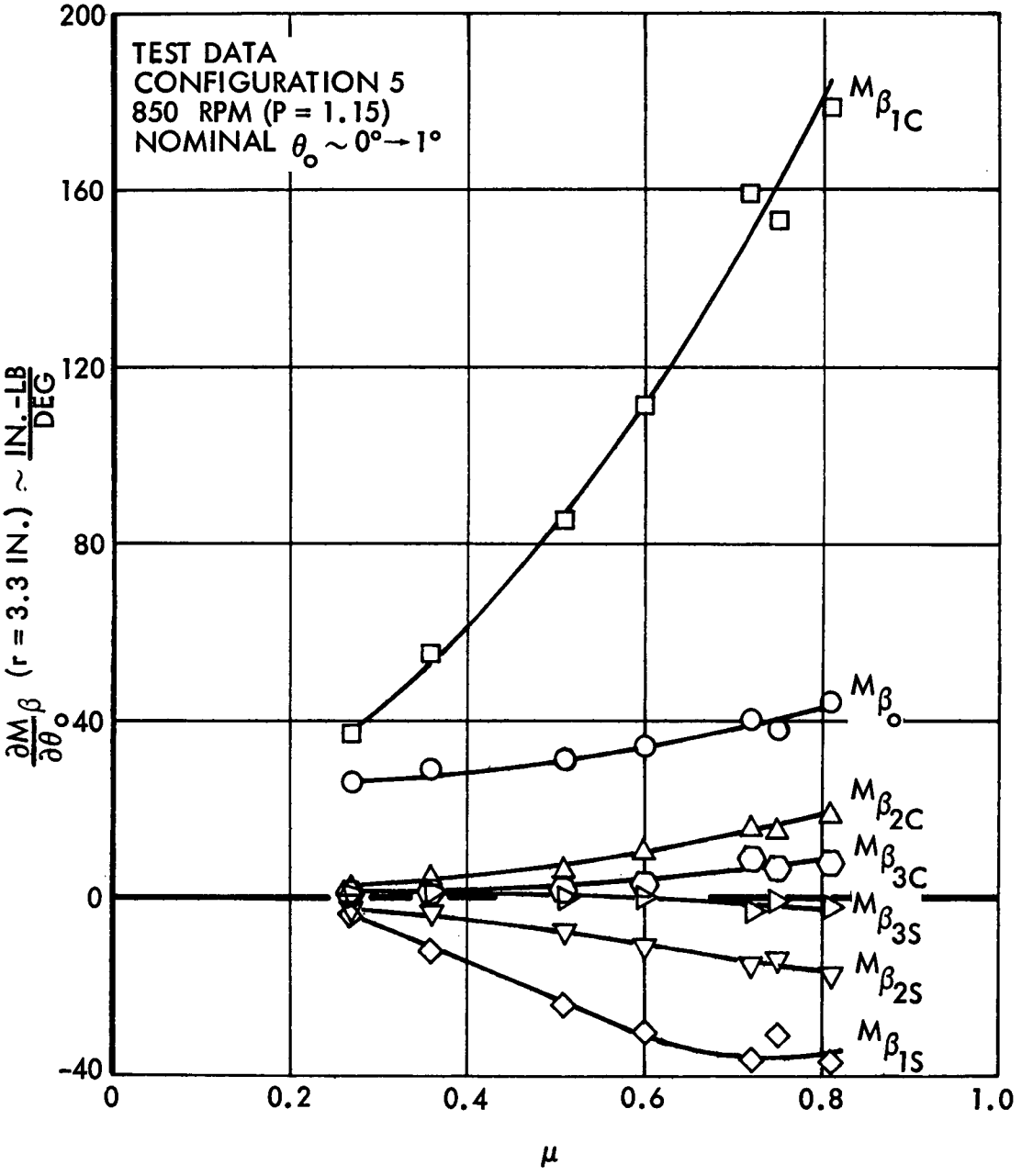

Figure A5. Harmonic Content of Blade Flapping, Configuration 5, 550 RPM (P = 1.15), Steady θ_o Excitation

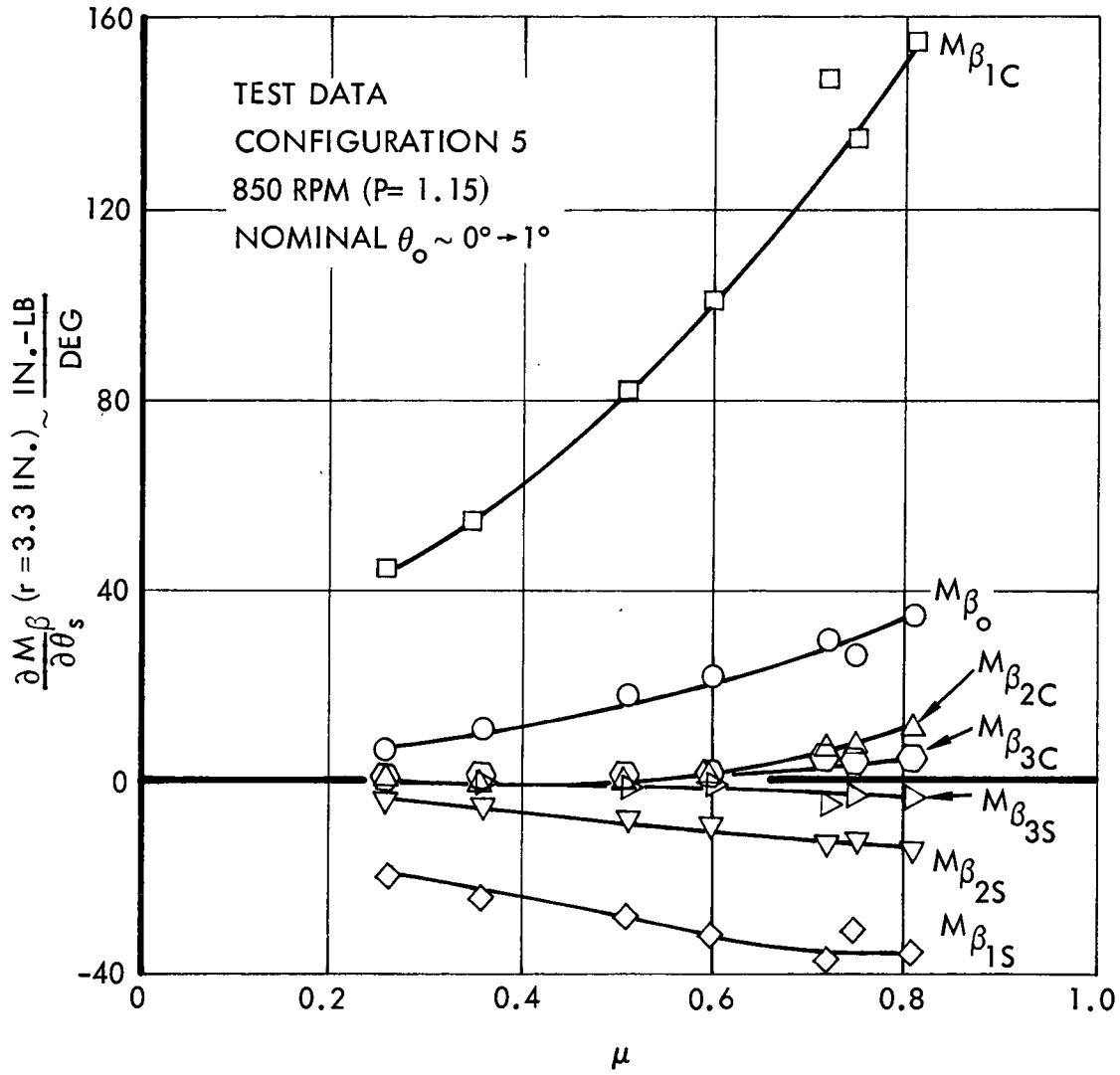

Figure A6. Harmonic Content of Blade Flapping, Configuration 5, 850 RPM (P = 1.15), Steady θ_s Excitation

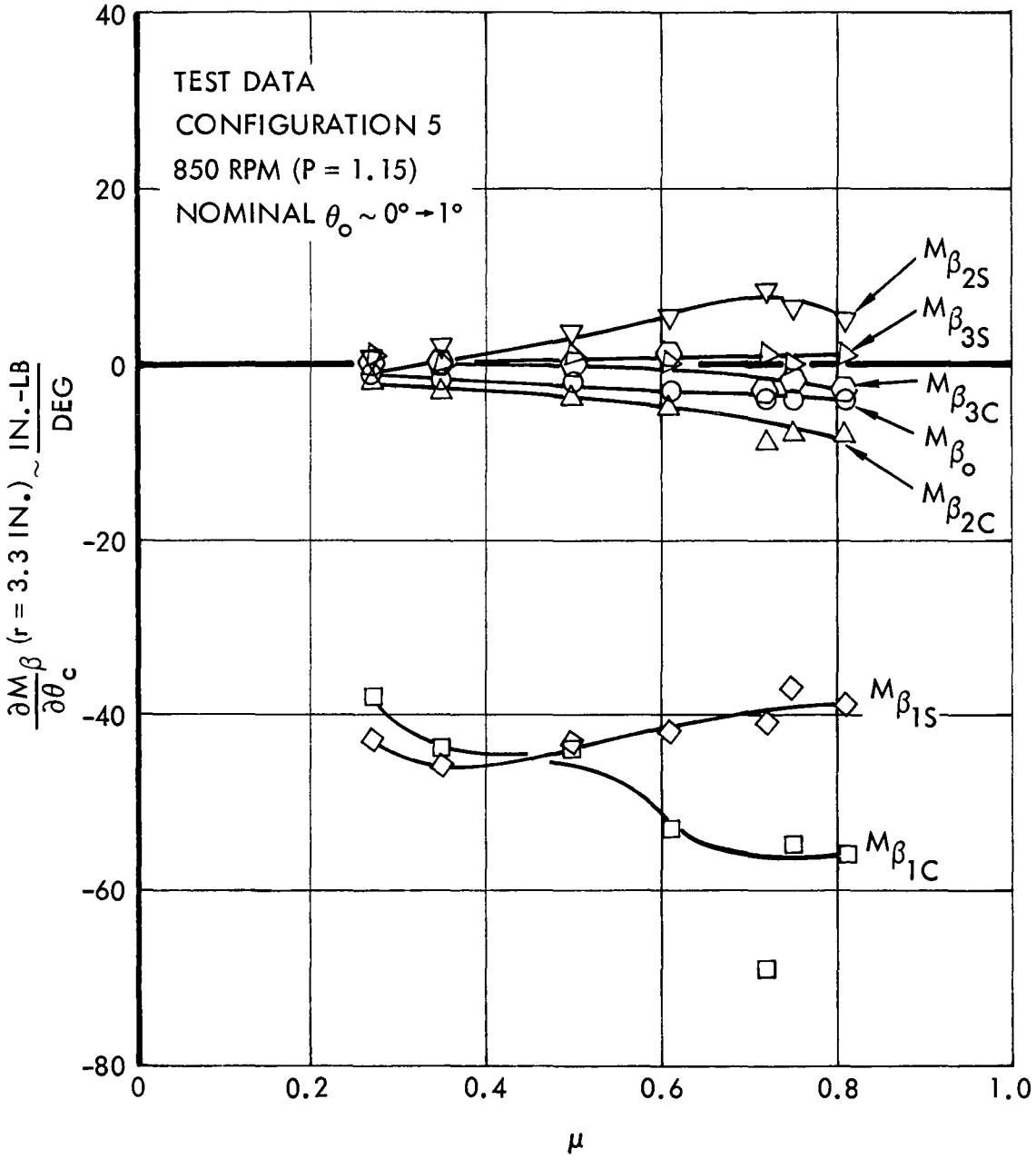

Figure A7. Harmonic Content of Blade Flapping, Configuration 5, 850 RPM (P = 1.15), Steady θ_c Excitation

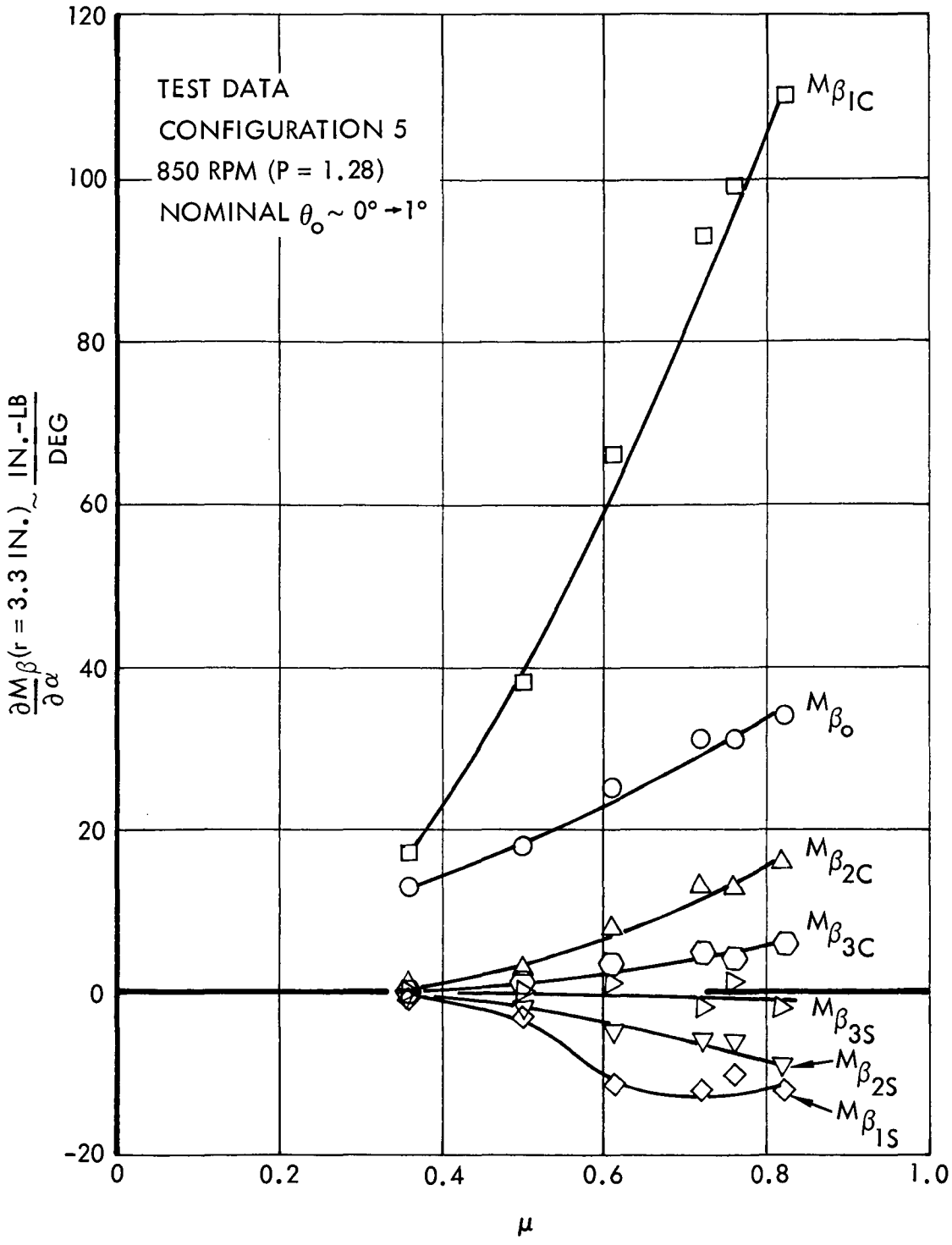

Figure A8. Harmonic Content of Blade Flapping, Configuration 5, 850 RPM (P = 1.15), Steady α Excitation

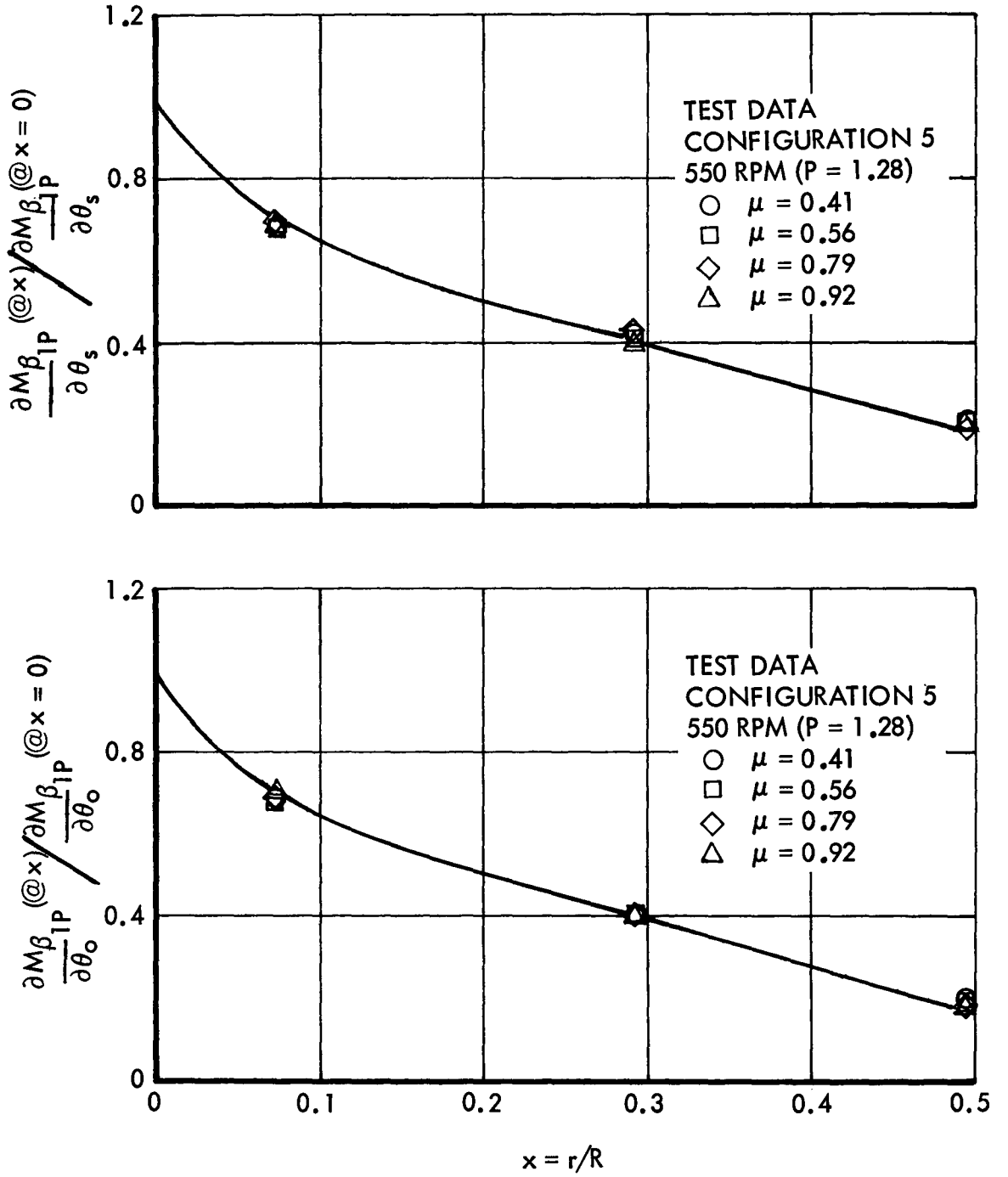

Figure A9. One-Per-Rev Blade Radial Flap Bending Moment Distribution Configuration 5, 550 RPM (P = 1.28), θ_o and θ_s Excitations

c

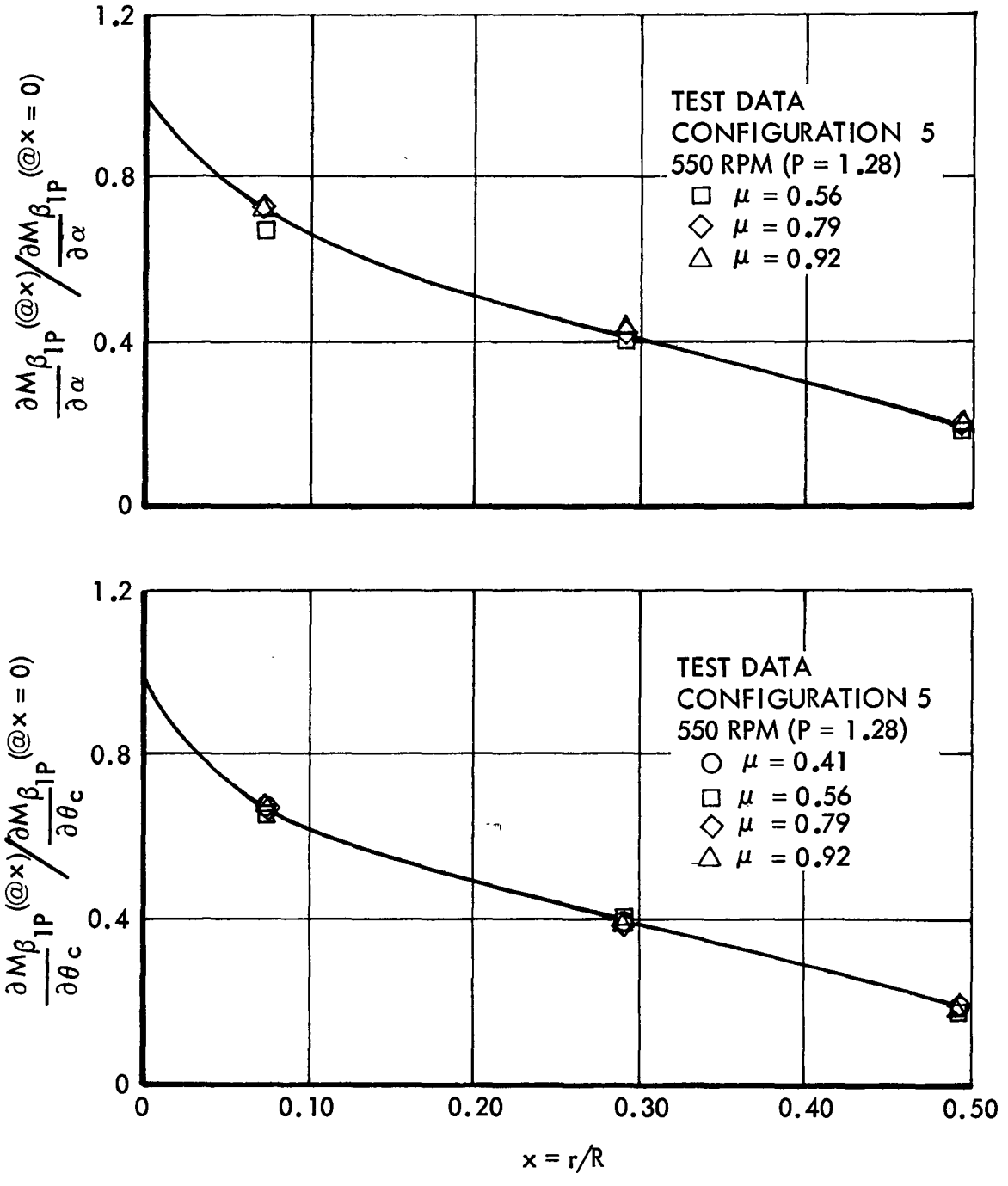

Figure A10. One-Per-Rev Blade Radial Flap Bending Moment Distribution Configuration 5, 550 RPM (P = 1.28), θ_c and α Excitations

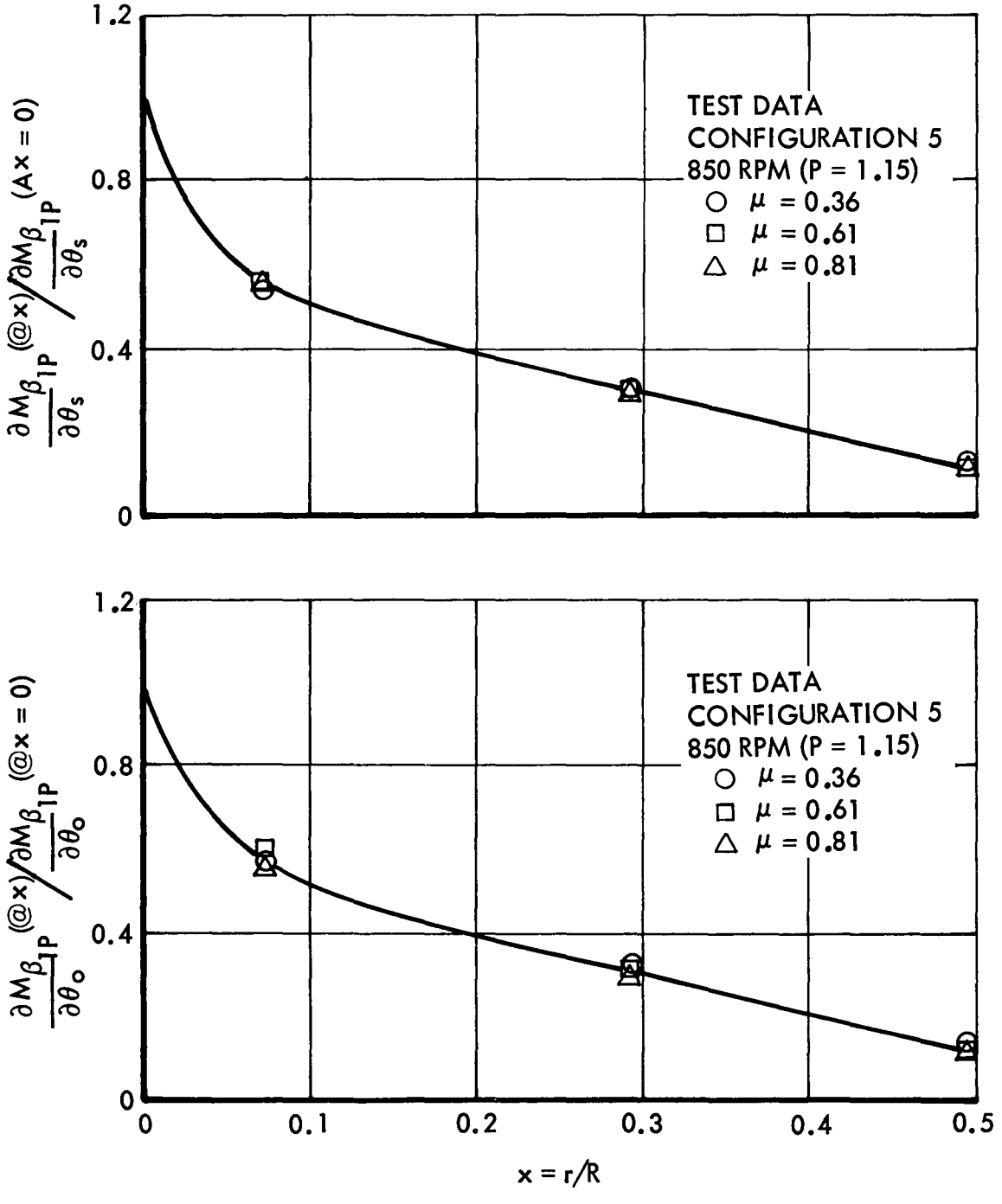

Figure A11. One-Per-Rev Blade Radial Flap Bending Moment Distribution Configuration 5, 850 RPM (P = 1.15), θ_o and θ_s Excitations

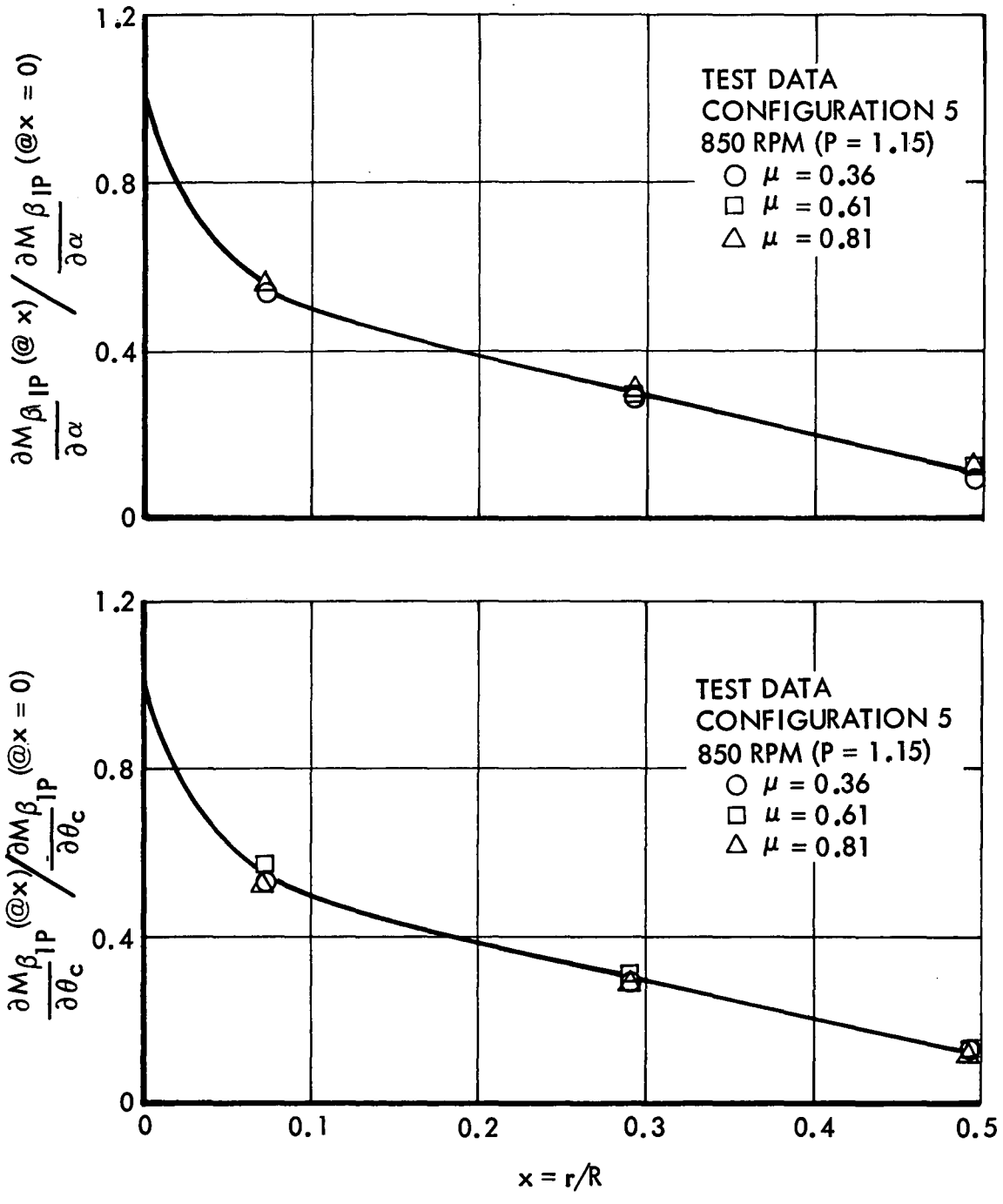

Figure A12. One-Per-Rev Blade Radial Flap Bending Moment Distribution Configuration 5, 850 RPM (P = 1.15), θ_c and α Excitations

APPENDIX B

EXPERIMENTAL ROTOR FREQUENCY RESPONSE DATA (θ_o, θ_s AND θ_c EXCITATIONS)

All of the Phase 3 rotor transfer functions with respect to θ_o, θ_s and θ_c are contained in this appendix. The hub moment frequency response is plotted (in Figures B1 through B46) as it was in the main body of this report. The hub moment data have also been transferred to the shaft centerline, nondimensionalized and tabulated (Tables VI, VII and VIII). The procedure by which this was accomplished is fully described in Appendix C. The reader is reminded that the nominal rotor lift is approximately zero for all of these data.

TABLE VI

ROTOR MOMENT FREQUENCY RESPONSE TO COLLECTIVE PITCH, CONFIGURATION 5

rpm/P	μ	ω (rad/sec)	$\frac{\omega}{\Omega}$	$\frac{c_m}{\theta_o a\, \sigma}$	c_m Phase (rad)	$\frac{c_l}{\theta_o a\, \sigma}$	c_l Phase (rad)
850/1.15	0.27	3.26	0.037	0.0200	-0.152	0.0033	-3.499
		6.63	0.075	0.0192	-0.304	0.0032	-3.836
		13.14	0.148	0.0178	-0.601	0.0020	-4.847
		26.96	0.304	0.0120	-1.072	0.0029	-1.275
		20.16	0.227	0.0151	-0.890	0.0020	-0.316
		33.78	0.381	0.0098	-1.204	0.0037	-1.752
		38.70	0.436	0.0077	-1.430	0.0046	-1.970
		50.72	0.571	0.0069	-1.314	0.0043	-2.467
		64.23	0.725	0.0086	-0.994	0.0032	-2.835
		77.98	0.880	0.0085	-0.874	0.0031	-2.839
		101.60	1.145	0.0070	-1.411	0.0061	-3.003
		114.16	1.287	0.0068	-1.366	0.0065	-3.191
		127.04	1.434	0.0079	-1.369	0.0072	-3.269
		153.10	1.727	0.0121	-1.661	0.0115	-3.473
		141.58	1.598	0.0100	-1.516	0.0094	-3.368
		180.35	2.037	0.0241	-2.597	0.0272	-4.309
	0.36	3.25	0.036	0.0303	-0.139	0.0085	-3.414
		6.58	0.074	0.0296	-0.271	0.0080	-3.697
		13.16	0.147	0.0283	-0.551	0.0063	-4.314
		20.22	0.226	0.0250	-0.836	0.0038	-5.101
		26.83	0.300	0.0210	-1.057	0.0023	-0.040
		33.50	0.374	0.0171	-1.226	0.0028	-1.182
		37.78	0.421	0.0148	-1.343	0.0039	-1.567
		50.67	0.565	0.0137	-1.010	0.0040	-2.525
		57.51	0.641	0.0123	-1.194	0.0047	-2.515
		63.49	0.714	0.0097	-1.226	0.0055	-2.678
		76.61	0.859	0.0102	-1.083	0.0056	-2.862
		102.90	1.154	0.0089	-1.441	0.0086	-3.109
		113.29	1.270	0.0087	-1.403	0.0087	-3.239
		127.20	1.427	0.0108	-1.386	0.0097	-3.273
		140.44	1.574	0.0136	-1.532	0.0115	-3.337
		153.10	1.714	0.0160	-1.672	0.0157	-3.326
		166.58	1.865	0.0218	-1.975	0.0227	-3.625
		180.14	2.016	0.0283	-2.435	0.0301	-4.046
		196.35	2.199	0.0307	-3.464	0.0316	-4.888
		207.64	2.323	0.0215	-4.302	0.0206	-5.059

TABLE VI

ROTOR MOMENT FREQUENCY RESPONSE TO COLLECTIVE PITCH, CONFIGURATION 5 (Continued)

rpm/P	μ	ω (rad/sec)	$\frac{\omega}{\Omega}$	$\frac{c_m}{\theta_o a \sigma}$	c_m Phase (rad)	$\frac{c_l}{\theta_o a \sigma}$	c_l Phase (rad)
850/1.15	0.51	3.26	0.037	0.0443	-0.164	0.0116	-3.472
		6.55	0.073	0.0433	-0.310	0.0110	-3.765
		13.01	0.146	0.0414	-0.601	0.0092	-4.397
		26.48	0.297	0.0305	-1.154	0.0048	-6.197
		50.56	0.566	0.0159	-1.042	0.0050	-2.259
		63.45	0.710	0.0153	-1.338	0.0069	-2.342
		76.85	0.860	0.0145	-1.297	0.0077	-2.608
		101.57	1.138	0.0109	-1.550	0.0120	-3.099
		114.91	1.288	0.0135	-1.424	0.0131	-3.324
		126.17	1.412	0.0167	-1.576	0.0143	-3.463
		139.26	1.558	0.0206	-1.801	0.0171	-3.589
		152.73	1.708	0.0259	-2.034	0.0232	-3.718
		179.01	2.003	0.0403	-2.879	0.0424	-4.518
		164.66	1.838	0.0351	-2.245	0.0343	-3.917
		206.41	2.302	0.0173	-4.293	0.0252	-5.685
		194.17	2.179	0.0351	-3.893	0.0404	-5.472
	0.60	3.26	0.037	0.0556	-0.175	0.0156	-3.466
		6.54	0.074	0.0553	-0.323	0.0151	-3.758
		12.96	0.146	0.0520	-0.626	0.0125	-4.361
		13.00	0.146	0.0512	-0.632	0.0124	-4.365
		26.59	0.299	0.0368	-1.216	0.0057	-6.032
		37.60	0.422	0.0225	-1.622	0.0058	-1.345
		50.33	0.566	0.0168	-1.587	0.0069	-2.055
		19.85	0.223	0.0452	-0.948	0.0085	-5.101
		63.40	0.712	0.0173	-1.441	0.0076	-2.321
		76.57	0.860	0.0162	-1.386	0.0090	-2.538
		88.42	0.992	0.0152	-1.620	0.0127	-2.747
		101.61	1.140	0.0124	-1.489	0.0152	-3.092
		113.87	1.278	0.0159	-1.416	0.0160	-3.356
		126.48	1.420	0.0204	-1.571	0.0171	-3.474
		139.82	1.569	0.0251	-1.808	0.0206	-3.587
		152.80	1.716	0.0310	-2.034	0.0277	-3.740
		179.32	2.012	0.0608	-3.012	0.0621	-4.646
		194.89	2.188	0.0397	-3.982	0.0454	-5.572

TABLE VI

ROTOR MOMENT FREQUENCY RESPONSE TO COLLECTIVE PITCH, CONFIGURATION 5 (Continued)

rpm/P	μ	ω (rad/sec)	$\frac{\omega}{\Omega}$	$\frac{c_m}{\theta_o a \sigma}$	c_m Phase (rad)	$\frac{c_l}{\theta_o a \sigma}$	c_l Phase (rad)
550/1.28	0.41	3.27	0.056	0.0356	-0.067	0.0230	-3.337
		6.62	0.114	0.0370	-0.147	0.0223	-3.553
		13.08	0.225	0.0408	-0.398	0.0201	-4.065
		26.53	0.455	0.0330	-1.105	0.0054	-5.584
		20.09	0.344	0.0399	-0.803	0.0132	-4.797
		38.29	0.659	0.0204	-1.493	0.0049	-2.133
		50.87	0.879	0.0145	-1.628	0.0090	-2.652
		63.65	1.099	0.0154	-1.437	0.0100	-2.858
		77.57	1.336	0.0137	-1.190	0.0123	-3.226
		88.72	1.528	0.0170	-1.239	0.0136	-3.310
		101.44	1.744	0.0213	-1.455	0.0171	-3.361
		114.83	1.973	0.0282	-1.808	0.0254	-3.578
		127.35	2.187	0.0378	-2.426	0.0370	-4.119
		142.93	2.453	0.0283	-3.562	0.0300	-5.109
		133.24	2.285	0.0383	-2.865	0.0387	-4.509
		154.30	2.646	0.0180	-4.049	0.0206	-5.462
	0.79	6.61	0.115	0.0974	-0.228	0.0544	-3.620
		13.07	0.227	0.1022	-0.546	0.0484	-4.200
		20.18	0.351	0.0933	-0.992	0.0320	-4.955
		26.74	0.465	0.0725	-1.327	0.0154	-5.661
		38.02	0.661	0.0431	-1.749	0.0091	-1.606
		50.25	0.873	0.0254	-1.810	0.0173	-2.416
		63.30	1.100	0.0233	-1.571	0.0224	-2.677
		77.30	1.343	0.0247	-1.193	0.0286	-3.170
		89.05	1.550	0.0334	-1.302	0.0281	-3.325
		100.60	1.748	0.0416	-1.522	0.0343	-3.378
		114.24	1.986	0.0541	-1.968	0.0497	-3.692
		127.04	2.209	0.0703	-2.608	0.0684	-4.263
		132.62	2.309	0.0668	-3.024	0.0671	-4.643
		140.44	2.443	0.0511	-3.501	0.0533	-5.055
		153.10	2.664	0.0318	-4.023	0.0355	-5.483
		179.73	3.127	0.0117	-4.879	0.0126	-6.111

TABLE VI

ROTOR MOMENT FREQUENCY RESPONSE TO COLLECTIVE PITCH, CONFIGURATION 5 (Continued)

rpm/P	μ	ω (rad/sec)	$\frac{\omega}{\Omega}$	$\frac{c_m}{\theta_o a\, \sigma}$	c_m Phase (rad)	$\frac{c_l}{\theta_o a\, \sigma}$	c_l Phase (rad)
550/1.28	0.92	3.26	0.056	0.1307	-0.123	0.0621	-3.385
		6.62	0.114	0.1294	-0.262	0.0597	-3.652
		12.97	0.224	0.1302	-0.587	0.0519	-4.231
		19.92	0.344	0.1177	-1.009	0.0340	-4.967
		26.44	0.457	0.0935	-1.331	0.0173	-5.753
		31.26	0.540	0.0763	-1.501	0.0102	-0.235
		37.96	0.657	0.0530	-1.716	0.0118	-1.655
		50.52	0.871	0.0312	-1.662	0.0204	-2.453
		63.47	1.094	0.0290	-1.582	0.0291	-2.651
		76.23	1.314	0.0299	-1.196	0.0364	-3.132
		88.75	1.530	0.0411	-1.337	0.0353	-3.373
		101.51	1.751	0.0510	-1.592	0.0414	-3.438
		114.49	1.977	0.0653	-1.940	0.0567	-3.662
		127.45	2.202	0.0806	-2.631	0.0764	-4.274
		132.84	2.295	0.0774	-3.001	0.0755	-4.606
		120.33	2.077	0.0742	-2.199	0.0673	-3.880
		152.51	2.634	0.0404	-3.960	0.0443	-5.428
		179.52	3.099	0.0151	-4.845	0.0156	-6.051

TABLE VII

ROTOR MOMENT FREQUENCY RESPONSE TO LONGITUDINAL CYCLIC PITCH, CONFIGURATION 5

rpm/P	μ	ω (rad/sec)	$\frac{\omega}{\Omega}$	$\frac{C_m}{\theta_s a \sigma}$	C_m Phase (rad)	$\frac{C_l}{\theta_s a \sigma}$	C_l Phase (rad)
850/1.15	0	3.52	0.040	0.0130	-6.108	0.0168	-3.331
		6.55	0.074	0.0161	-6.080	0.0171	-3.549
		9.73	0.111	0.0196	-6.190	0.0173	-3.844
		13.02	0.149	0.0213	-0.146	0.0154	-4.214
		16.37	0.188	0.0211	-0.380	0.0121	-4.547
		19.94	0.229	0.0192	-0.549	0.0086	-4.786
		23.13	0.262	0.0179	-0.625	0.0069	-4.847
		26.49	0.298	0.0167	-0.697	0.0051	-4.936
		33.03	0.372	0.0146	-0.792	0.0030	-4.961
		37.76	0.424	0.0138	-0.844	0.0020	-4.900
		50.25	0.565	0.0129	-0.908	0.0011	-3.991
		57.27	0.643	0.0121	-0.995	0.0013	-3.354
		63.11	0.709	0.0115	-1.051	0.0017	-3.190
		76.51	0.858	0.0102	-1.148	0.0028	-3.108
		88.30	0.991	0.0112	-1.033	0.0030	-3.252
		101.02	1.132	0.0116	-1.236	0.0037	-3.151
		113.70	1.274	0.0117	-1.365	0.0046	-3.150
		126.17	1.414	0.0123	-1.473	0.0053	-3.113
		139.69	1.565	0.0134	-1.629	0.0083	-3.153
		152.51	1.723	0.0143	-1.799	0.0115	-3.454
		165.26	1.862	0.0172	-2.009	0.0141	-3.835
	0.27	3.50	0.039	0.0231	-0.091	0.0123	-3.317
		6.65	0.075	0.0231	-0.189	0.0122	-3.515
		13.05	0.147	0.0228	-0.406	0.0108	-3.897
		26.57	0.300	0.0183	-0.835	0.0053	-4.573
		38.03	0.429	0.0136	-1.067	0.0015	-4.589
		50.74	0.572	0.0112	-1.120	0.0015	-3.387
		63.75	0.719	0.0116	-1.124	0.0017	-3.249
		76.66	0.864	0.0112	-1.036	0.0021	-3.139
		89.45	1.009	0.0108	-1.251	0.0033	-2.907
		101.11	1.141	0.0106	-1.383	0.0044	-3.111
		114.95	1.298	0.0102	-1.470	0.0051	-3.251
		126.94	1.433	0.0107	-1.536	0.0057	-3.304
		152.58	1.723	0.0139	-1.737	0.0107	-3.443
		180.97	2.043	0.0207	-2.342	0.0179	-4.058

TABLE VII

ROTOR MOMENT FREQUENCY RESPONSE TO LONGITUDINAL CYCLIC PITCH, CONFIGURATION 5 (Continued)

rpm/P	μ	ω (rad/sec)	$\frac{\omega}{\Omega}$	$\frac{C_m}{\theta_s a \sigma}$	C_m Phase (rad)	$\frac{C_l}{\theta_s a \sigma}$	C_l Phase (rad)
850/1.15	0.36	3.54	0.040	0.0285	-0.080	0.0142	-3.312
		6.59	0.074	0.0279	-0.217	0.0135	-3.538
		13.09	0.147	0.0272	-0.439	0.0116	-3.938
		26.90	0.302	0.0216	-0.909	0.0053	-4.641
		37.19	0.417	0.0154	-1.182	0.0010	-4.810
		50.74	0.569	0.0152	-1.082	0.0014	-3.512
		69.58	0.778	0.0123	-1.284	0.0027	-2.854
		83.38	0.928	0.0110	-1.343	0.0037	-2.854
		95.17	1.060	0.0104	-1.435	0.0049	-2.964
		109.16	1.215	0.0100	-1.463	0.0059	-3.163
		120.05	1.335	0.0099	-1.493	0.0061	-3.134
		127.45	1.425	0.0106	-1.501	0.0069	-3.150
		159.80	1.792	0.0165	-1.799	0.0135	-3.597
	0.51	3.53	0.039	0.0370	-0.099	0.0155	-3.342
		6.55	0.073	0.0361	-0.236	0.0146	-3.584
		13.07	0.146	0.0352	-0.495	0.0126	-4.022
		26.50	0.296	0.0277	-1.007	0.0057	-4.949
		38.00	0.425	0.0175	-1.366	0.0009	-0.767
		50.61	0.566	0.0139	-1.341	0.0022	-2.410
		64.00	0.715	0.0142	-1.321	0.0027	-2.536
		77.25	0.862	0.0129	-1.272	0.0037	-2.692
		88.90	0.992	0.0118	-1.404	0.0052	-2.718
		100.72	1.122	0.0104	-1.419	0.0066	-2.998
		114.28	1.273	0.0107	-1.350	0.0071	-3.142
		126.27	1.407	0.0124	-1.383	0.0077	-3.219
		139.57	1.571	0.0149	-1.527	0.0101	-3.175
		152.06	1.710	0.0174	-1.645	0.0140	-3.335
		179.52	2.017	0.0287	-2.265	0.0257	-3.973
		206.68	2.322	0.0245	-3.457	0.0227	-5.185
	0.60	3.28	0.037	0.0453	-0.143	0.0173	-3.387
		6.55	0.073	0.0449	-0.271	0.0167	-3.619
		13.02	0.146	0.0433	-0.545	0.0143	-4.079
		26.30	0.295	0.0326	-1.072	0.0061	-5.085
		33.21	0.372	0.0253	-1.271	0.0023	-5.664
		38.00	0.425	0.0197	-1.411	0.0010	-1.115
		50.61	0.566	0.0138	-1.319	0.0030	-2.528

TABLE VII

ROTOR MOMENT FREQUENCY RESPONSE TO LONGITUDINAL CYCLIC PITCH, CONFIGURATION 5 (Continued)

rpm/P	μ	ω (rad/sec)	$\frac{\omega}{\Omega}$	$\frac{C_m}{\theta_s a \sigma}$	C_m Phase (rad)	$\frac{C_l}{\theta_s a \sigma}$	C_l Phase (rad)
850/1.15	0.60	63.96	0.716	0.0154	-1.395	0.0035	-2.428
		76.27	0.854	0.0138	-1.306	0.0045	-2.574
		88.47	0.991	0.0122	-1.456	0.0067	-2.683
		101.21	1.134	0.0106	-1.406	0.0085	-3.005
		113.58	1.276	0.0119	-1.318	0.0086	-3.174
		126.42	1.417	0.0139	-1.364	0.0090	-3.210
		139.32	1.562	0.0160	-1.503	0.0114	-3.158
		152.21	1.707	0.0187	-1.642	0.0153	-3.335
		178.81	2.006	0.0299	-2.172	0.0271	-3.849
550/1.28	0	3.25	0.057	0.0085	-5.778	0.0235	-3.163
		6.52	0.113	0.0149	-5.570	0.0274	-3.244
		9.79	0.169	0.0250	-5.657	0.0329	-3.491
		13.03	0.225	0.0339	-6.010	0.0347	-3.904
		16.47	0.284	0.0361	-0.141	0.0285	-4.345
		19.95	0.343	0.0331	-0.429	0.0203	-4.624
		26.52	0.456	0.0270	-0.699	0.0109	-4.797
		33.14	0.568	0.0234	-0.847	0.0063	-4.717
		37.67	0.645	0.0217	-0.929	0.0044	-4.531
		50.09	0.859	0.0204	-1.046	0.0036	-3.931
		57.21	0.979	0.0188	-1.159	0.0045	-3.506
		63.06	1.107	0.0179	-1.247	0.0056	-3.393
		76.33	1.426	0.0171	-1.456	0.0086	-3.394
		88.50	1.650	0.0174	-1.507	0.0102	-3.600
		100.56	1.873	0.0214	-1.840	0.0144	-3.710
		114.08	2.051	0.0258	-2.198	0.0197	-3.995
		126.27	2.221	0.0272	-2.669	0.0227	-4.434
		140.38	2.469	0.0213	-3.312	0.0206	-4.935
		152.66	2.683	0.0146	-3.937	0.0162	-5.517
	0.41	3.28	0.056	0.0346	-0.036	0.0294	-3.305
		6.55	0.113	0.0364	-0.085	0.0295	-3.484
		13.16	0.227	0.0417	-0.295	0.0285	-3.932
		26.50	0.457	0.0364	-1.010	0.0115	-4.570
		19.80	0.341	0.0429	-0.668	0.0215	-4.499
		38.18	0.657	0.0234	-1.307	0.0007	-3.491
		44.60	0.775	0.0218	-1.273	0.0027	-3.167
		50.62	0.869	0.0179	-1.346	0.0054	-2.844
		62.92	1.080	0.0188	-1.367	0.0070	-2.989
		77.42	1.327	0.0182	-1.349	0.0102	-3.221

TABLE VII

ROTOR MOMENT FREQUENCY RESPONSE TO LONGITUDINAL CYCLIC PITCH, CONFIGURATION 5 (Continued)

rpm/P	μ	ω (rad/sec)	$\frac{\omega}{\Omega}$	$\frac{c_m}{\theta_s a \sigma}$	c_m Phase (rad)	$\frac{c_l}{\theta_s a \sigma}$	c_l Phase (rad)
550/1.28	0.41	89.18	1.527	0.0197	-1.431	0.0125	-3.317
		102.37	1.753	0.0235	-1.616	0.0164	-3.465
		114.41	1.957	0.0287	-1.880	0.0226	-3.676
		127.19	2.221	0.0414	-2.585	0.0378	-4.324
		140.00	2.438	0.0313	-3.459	0.0316	-5.185
		133.12	2.316	0.0396	-2.995	0.0379	-4.726
		153.70	2.674	0.0165	-3.972	0.0187	-5.628
		179.01	3.113	0.0050	-4.226	0.0089	-5.964
	0.79	6.60	0.114	0.0761	-0.204	0.0461	-3.596
		13.01	0.226	0.0822	-0.504	0.0425	-4.132
		20.09	0.349	0.0759	-0.939	0.0293	-4.818
		26.38	0.458	0.0615	-1.260	0.0158	-5.377
		31.23	0.542	0.0513	-1.424	0.0083	-5.904
		37.87	0.658	0.0379	-1.619	0.0047	-1.130
		50.54	0.877	0.0216	-1.639	0.0118	-2.452
		63.30	1.100	0.0217	-1.557	0.0164	-2.704
		76.53	1.329	0.0224	-1.286	0.0206	-3.166
		88.50	1.537	0.0295	-1.368	0.0214	-3.302
		101.51	1.763	0.0374	-1.623	0.0284	-3.418
		113.74	1.974	0.0450	-1.977	0.0377	-3.726
		127.14	2.207	0.0595	-2.657	0.0555	-4.352
		132.17	2.295	0.0575	-3.025	0.0559	-4.708
		139.69	2.427	0.0460	-3.510	0.0470	-5.173
		152.58	2.650	0.0269	-3.989	0.0301	-5.585
		179.52	3.118	0.0072	-4.549	0.0114	-6.108
	0.92	6.60	0.114	0.0984	-0.252	0.0492	-3.632
		12.91	0.222	0.1024	-0.557	0.0439	-4.166
		20.08	0.346	0.0916	-0.985	0.0295	-4.877
		26.37	0.454	0.0738	-1.293	0.0155	-5.521
		31.26	0.539	0.0619	-1.447	0.0087	-6.129
		37.97	0.654	0.0432	-1.671	0.0069	-1.380
		50.96	0.877	0.0275	-1.606	0.0138	-2.419
		63.22	1.089	0.0245	-1.600	0.0208	-2.658
		76.59	1.317	0.0254	-1.283	0.0262	-3.165
		88.15	1.517	0.0327	-1.392	0.0251	-3.380
		100.98	1.739	0.0416	-1.640	0.0311	-3.463
		114.74	1.976	0.0519	-2.053	0.0427	-3.793
		126.43	2.178	0.0629	-2.647	0.0567	-4.333
		140.94	2.425	0.0477	-3.509	0.0466	-5.106
		152.66	2.626	0.0322	-3.963	0.0354	-5.507
		180.35	3.103	0.0075	-4.727	0.0119	-6.128

TABLE VIII

ROTOR MOMENT FREQUENCY RESPONSE TO LATERAL CYCLIC PITCH, CONFIGURATION 5

rpm/P	μ	ω (rad/sec)	$\frac{\omega}{\Omega}$	$\frac{C_m}{\theta_c a \sigma}$	C_m Phase (rad)	$\frac{C_l}{\theta_c a \sigma}$	C_l Phase (rad)
850/1.15	0.27	3.26	0.037	0.0202	-3.361	0.0201	-3.162
		6.60	0.074	0.0197	-3.594	0.0213	-3.207
		13.02	0.146	0.0170	-4.045	0.0237	-3.388
		26.49	0.298	0.0079	-4.845	0.0226	-3.938
		37.75	0.425	0.0026	-4.966	0.0175	-4.271
		50.37	0.567	0.0015	-4.152	0.0136	-4.465
		63.62	0.715	0.0022	-3.714	0.0107	-4.553
		76.72	0.863	0.0035	-3.447	0.0093	-4.545
		101.41	1.140	0.0036	-3.448	0.0095	-4.680
		114.91	1.292	0.0044	-3.405	0.0099	-4.780
		126.73	1.424	0.0055	-3.457	0.0102	-4.862
		153.10	1.722	0.0083	-3.693	0.0113	-5.089
		182.02	2.048	0.0148	-4.221	0.0176	-5.604
	0.36	3.26	0.037	0.0218	-3.357	0.0203	-3.159
		6.65	0.075	0.0210	-3.562	0.0212	-3.200
		12.94	0.146	0.0184	-3.982	0.0233	-3.362
		26.33	0.297	0.0093	-4.773	0.0231	-3.873
		37.95	0.427	0.0032	-4.997	0.0186	-4.209
		50.77	0.571	0.0015	-4.238	0.0152	-4.440
		63.98	0.720	0.0025	-3.764	0.0123	-4.577
		77.28	0.870	0.0039	-3.542	0.0103	-4.634
		101.83	1.146	0.0037	-3.526	0.0095	-4.771
		115.33	1.298	0.0046	-3.504	0.0095	-4.831
		127.14	1.430	0.0056	-3.577	0.0100	-4.884
		152.80	1.719	0.0085	-3.769	0.0118	-5.138
	0.51	3.24	0.036	0.0228	-3.372	0.0203	-3.144
		6.57	0.074	0.0223	-3.575	0.0212	-3.184
		13.11	0.147	0.0194	-4.016	0.0236	-3.342
		26.52	0.297	0.0099	-4.800	0.0236	-3.842
		37.62	0.422	0.0036	-4.948	0.0193	-4.130
		50.46	0.565	0.0015	-4.380	0.0160	-4.364

TABLE VIII

ROTOR MOMENT FREQUENCY RESPONSE TO LATERAL CYCLIC PITCH, CONFIGURATION (Continued)

rpm/P	μ	ω (rad/sec)	$\frac{\omega}{\Omega}$	$\frac{C_m}{\theta_c a \sigma}$	C_m Phase (rad)	$\frac{C_l}{\theta_c a \sigma}$	C_l Phase (rad)
850/1.15	0.51	64.09	0.716	0.0022	-3.824	0.0133	-4.507
		76.81	0.858	0.0037	-3.549	0.0116	-4.590
		88.75	0.992	0.0034	-3.553	0.0112	-4.676
		100.89	1.126	0.0038	-3.554	0.0104	-4.788
		114.07	1.280	0.0049	-3.511	0.0100	-4.857
		126.38	1.417	0.0060	-3.614	0.0101	-4.928
		140.00	1.568	0.0070	-3.680	0.0110	-5.021
		152.73	1.709	0.0085	-3.850	0.0115	-5.105
		178.91	2.001	0.0147	-4.341	0.0182	-5.616
		206.96	2.314	0.0125	-5.679	0.0117	-0.285
	0.60	3.26	0.036	0.0271	-3.357	0.0189	-3.134
		6.58	0.074	0.0257	-3.581	0.0205	-3.146
		12.88	0.144	0.0228	-3.999	0.0234	-3.281
		26.41	0.296	0.0118	-4.782	0.0242	-3.806
		33.27	0.373	0.0069	-5.008	0.0215	-4.010
		37.94	0.425	0.0042	-4.985	0.0197	-4.106
		50.13	0.561	0.0020	-4.670	0.0164	-4.324
		63.39	0.709	0.0024	-3.972	0.0140	-4.454
		76.85	0.860	0.0037	-3.685	0.0124	-4.540
		101.74	1.139	0.0040	-3.436	0.0110	-4.777
		113.83	1.274	0.0054	-3.452	0.0107	-4.857
		127.09	1.422	0.0065	-3.586	0.0106	-4.929
		140.00	1.566	0.0075	-3.672	0.0112	-5.029
		152.80	1.711	0.0090	-3.874	0.0117	-5.126
		172.71	1.933	0.0142	-4.256	0.0165	-5.535
550/1.28	0.41	3.26	0.056	0.0360	-3.311	0.0216	-3.074
		6.55	0.113	0.0361	-3.505	0.0243	-3.041
		12.99	0.225	0.0349	-3.953	0.0327	-3.194
		26.58	0.460	0.0150	-4.964	0.0345	-4.032
		20.07	0.347	0.0264	-4.561	0.0386	-3.641
		38.12	0.660	0.0042	-4.862	0.0242	-4.389
		43.87	0.759	0.0041	-4.399	0.0220	-4.446
		50.96	0.882	0.0035	-3.848	0.0187	-4.566
		64.10	1.109	0.0053	-3.648	0.0157	-4.664
		76.79	1.329	0.0077	-3.448	0.0146	-4.735
		89.30	1.545	0.0097	-3.517	0.0154	-4.821
		101.64	1.758	0.0129	-3.611	0.0175	-4.958
		114.20	1.975	0.0181	-3.804	0.0212	-5.192

TABLE VIII

ROTOR MOMENT FREQUENCY RESPONSE TO LATERAL CYCLIC PITCH, CONFIGURATION 5 (Continued)

rpm/P	μ	ω (rad/sec)	$\frac{\omega}{\Omega}$	$\frac{c_m}{a\sigma}$	c_m Phase (rad)	$\frac{c_l}{a\sigma}$	c_l Phase (rad)
550/1.28	0.41	128.44	2.220	0.0293	-4.475	0.0291	-5.861
		140.69	2.434	0.0264	-5.272	0.0223	-0.347
		134.09	2.315	0.0306	-4.849	0.0282	-6.237
		153.33	2.646	0.0185	-5.666	0.0167	-0.637
		180.24	3.108	0.0085	-6.234	0.0051	-1.292
	0.79	6.50	0.113	0.0524	-3.536	0.0251	-2.909
		13.05	0.227	0.0490	-4.002	0.0362	-3.091
		20.10	0.349	0.0360	-4.564	0.0429	-3.546
		26.41	0.459	0.0219	-4.897	0.0390	-3.903
		31.25	0.543	0.0144	-4.998	0.0343	-4.092
		37.68	0.655	0.0088	-4.997	0.0294	-4.251
		50.54	0.880	0.0033	-4.658	0.0248	-4.452
		63.49	1.103	0.0044	-3.458	0.0218	-4.620
		76.66	1.332	0.0100	-3.269	0.0196	-4.780
		89.15	1.549	0.0136	-3.492	0.0209	-4.870
		101.41	1.760	0.0188	-3.667	0.0236	-5.042
		113.83	1.974	0.0253	-3.996	0.0277	-5.355
		126.78	2.199	0.0379	-4.627	0.0358	-6.005
		132.73	2.302	0.0395	-5.021	0.0344	-0.120
		140.25	2.434	0.0327	-5.486	0.0259	-0.570
		152.36	2.643	0.0217	-5.909	0.0175	-0.927
		178.91	3.107	0.0084	-0.436	0.0040	-2.226
	0.92	6.50	0.112	0.0575	-3.553	0.0253	-2.901
		13.07	0.225	0.0524	-4.020	0.0365	-3.096
		20.00	0.343	0.0376	-4.543	0.0420	-3.530
		26.67	0.458	0.0228	-4.876	0.0386	-3.883
		31.26	0.535	0.0155	-4.964	0.0350	-4.054
		37.74	0.648	0.0095	-4.848	0.0300	-4.197
		50.78	0.872	0.0043	-4.595	0.0262	-4.427
		63.42	1.091	0.0046	-3.617	0.0234	-4.623
		76.66	1.321	0.0103	-3.361	0.0206	-4.774
		88.77	1.528	0.0139	-3.521	0.0209	-4.870
		100.44	1.730	0.0190	-3.674	0.0239	-5.025
		114.20	1.967	0.0289	-4.038	0.0304	-5.362
		126.32	2.176	0.0378	-4.663	0.0348	-6.006
		140.69	2.425	0.0330	-5.610	0.0249	-0.662
		152.51	2.626	0.0236	-6.035	0.0188	-1.064
		179.83	3.098	0.0089	-0.568	0.0052	-2.478

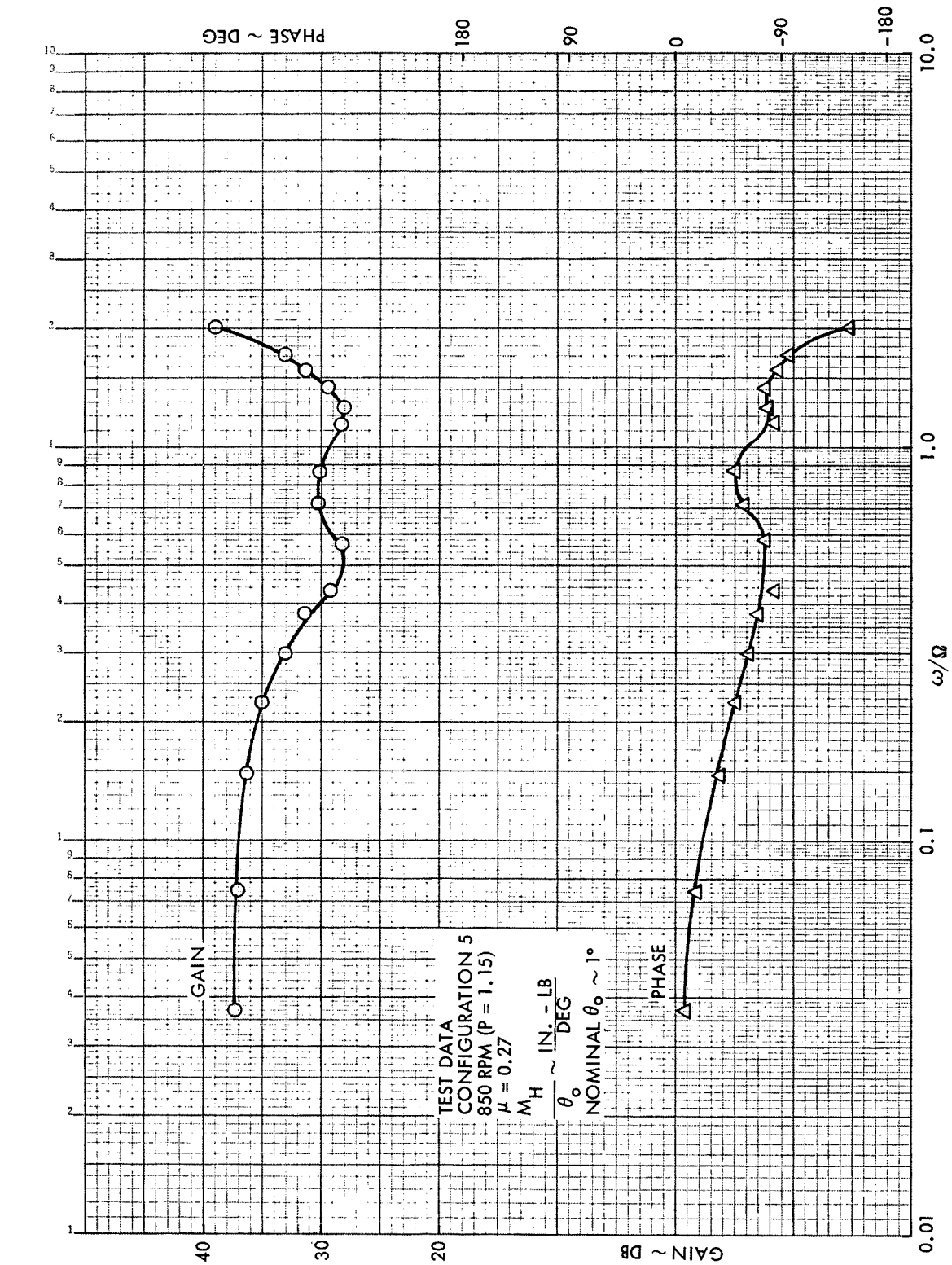

Figure B1. Rotor Hub Pitch Moment Frequency Response to Collective Pitch, Configuration 5, μ = 0.27, 850 RPM (P = 1.15)

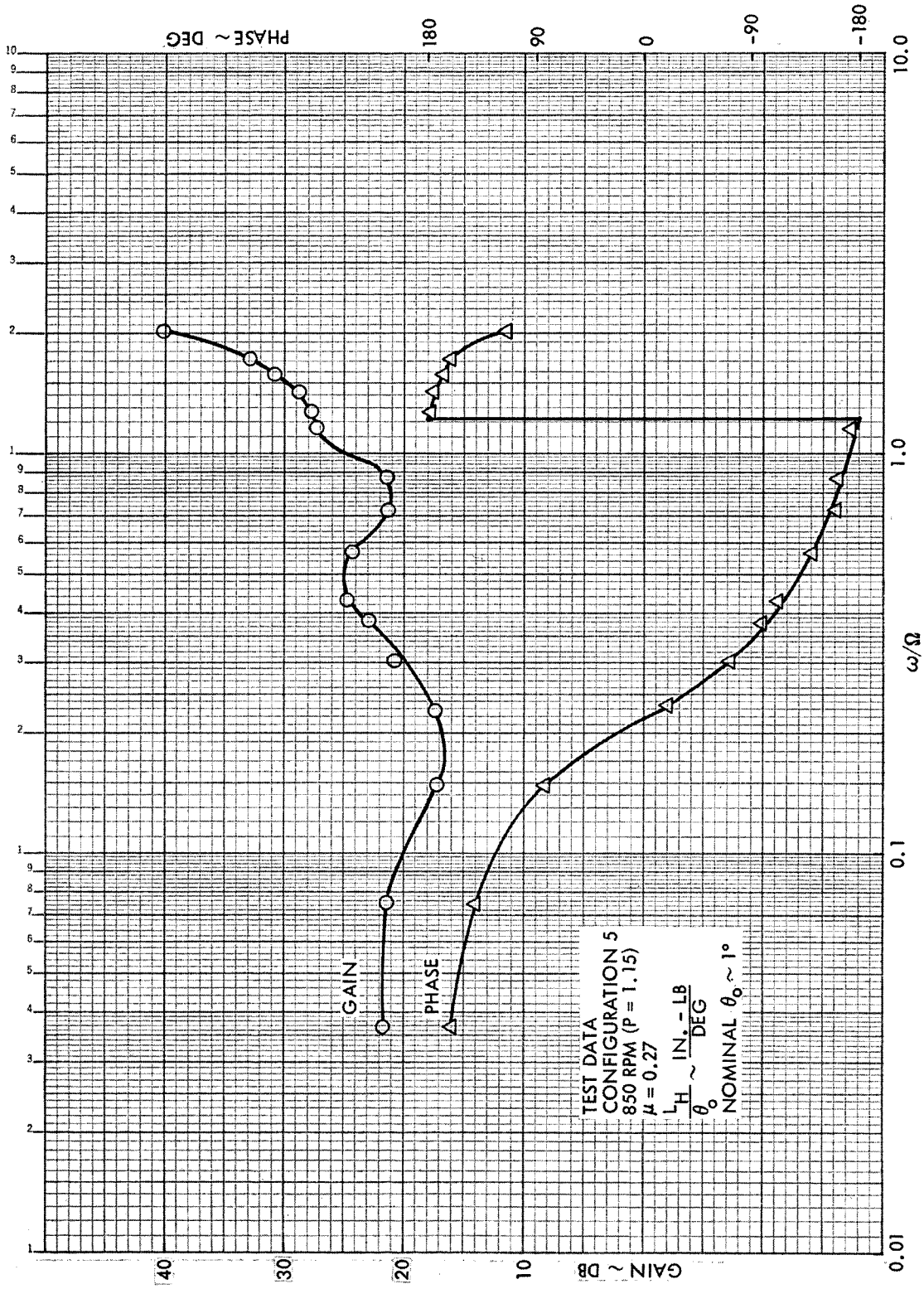

Figure B2. Rotor Hub Roll Moment Frequency Response to Collective Pitch, Configuration 5, μ = 0.27, 850 RPM (P = 1.15)

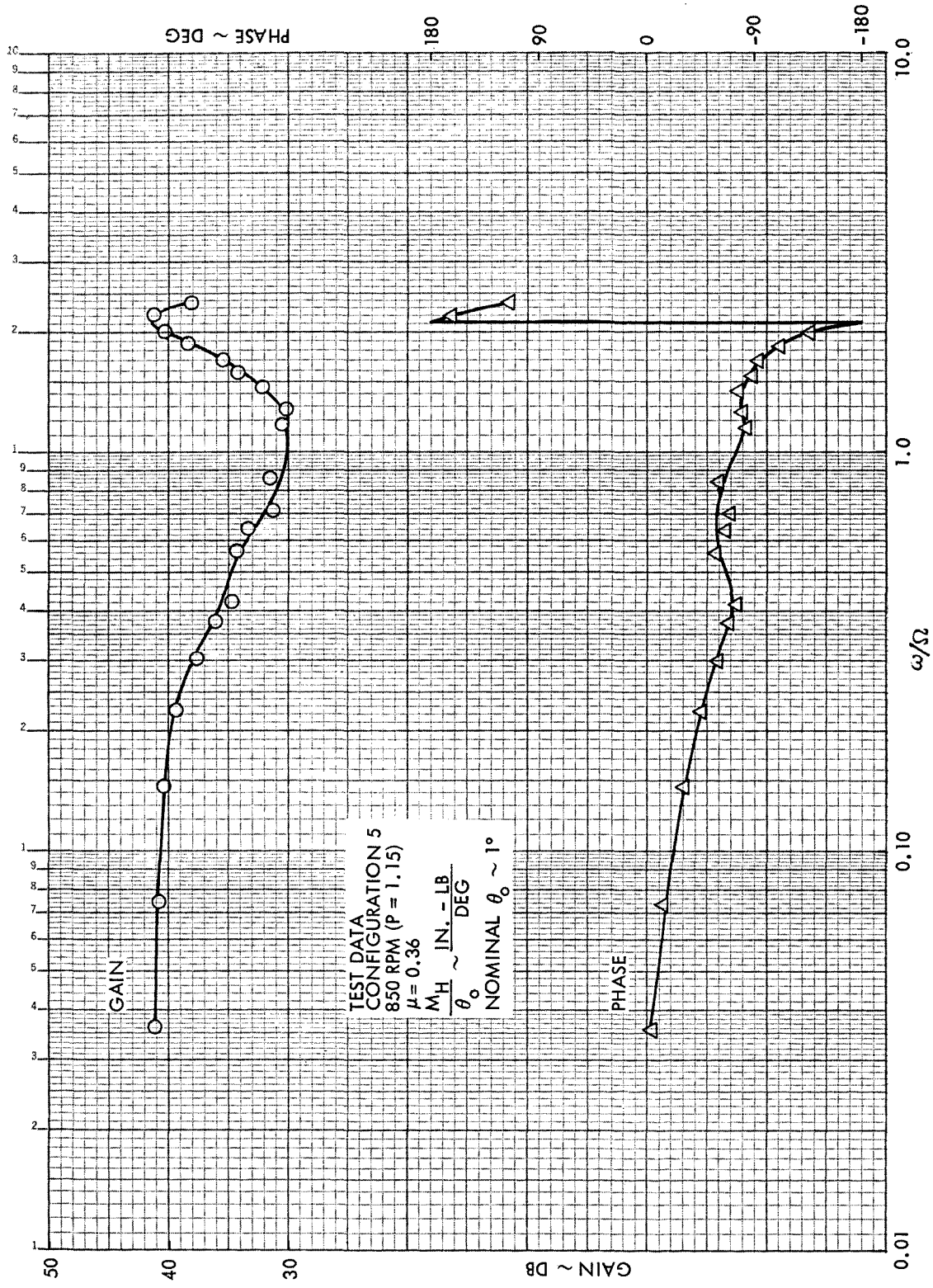

Figure B3. Rotor Hub Pitch Moment Frequency Response to Collective Pitch, Configuration 5, μ = 0.36, 850 RPM (P = 1.15)

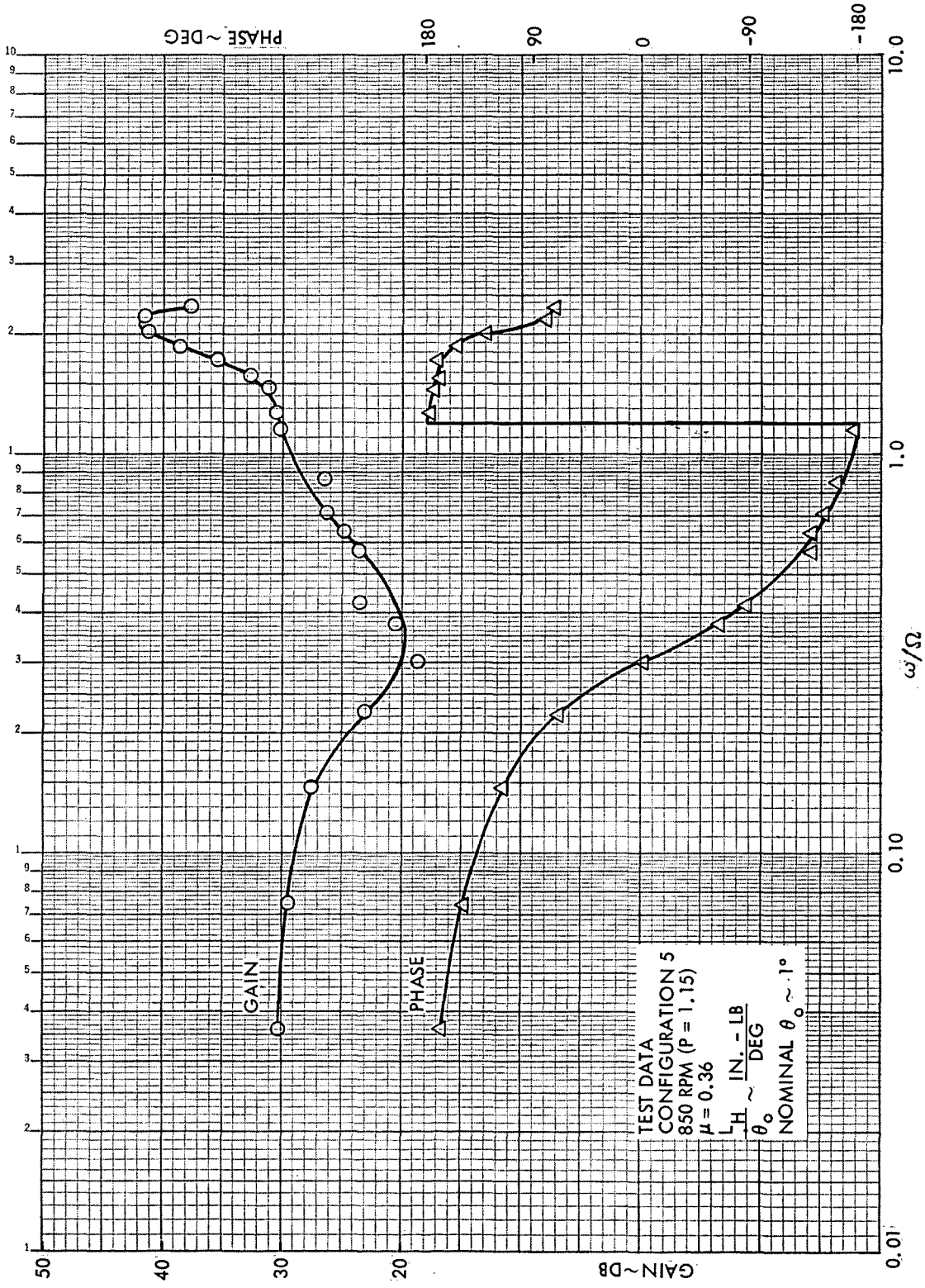

Figure B4. Rotor Hub Roll Moment Frequency Response to Collective Pitch, Configuration 5, $\mu = 0.36$, 850 RPM (P = 1.15)

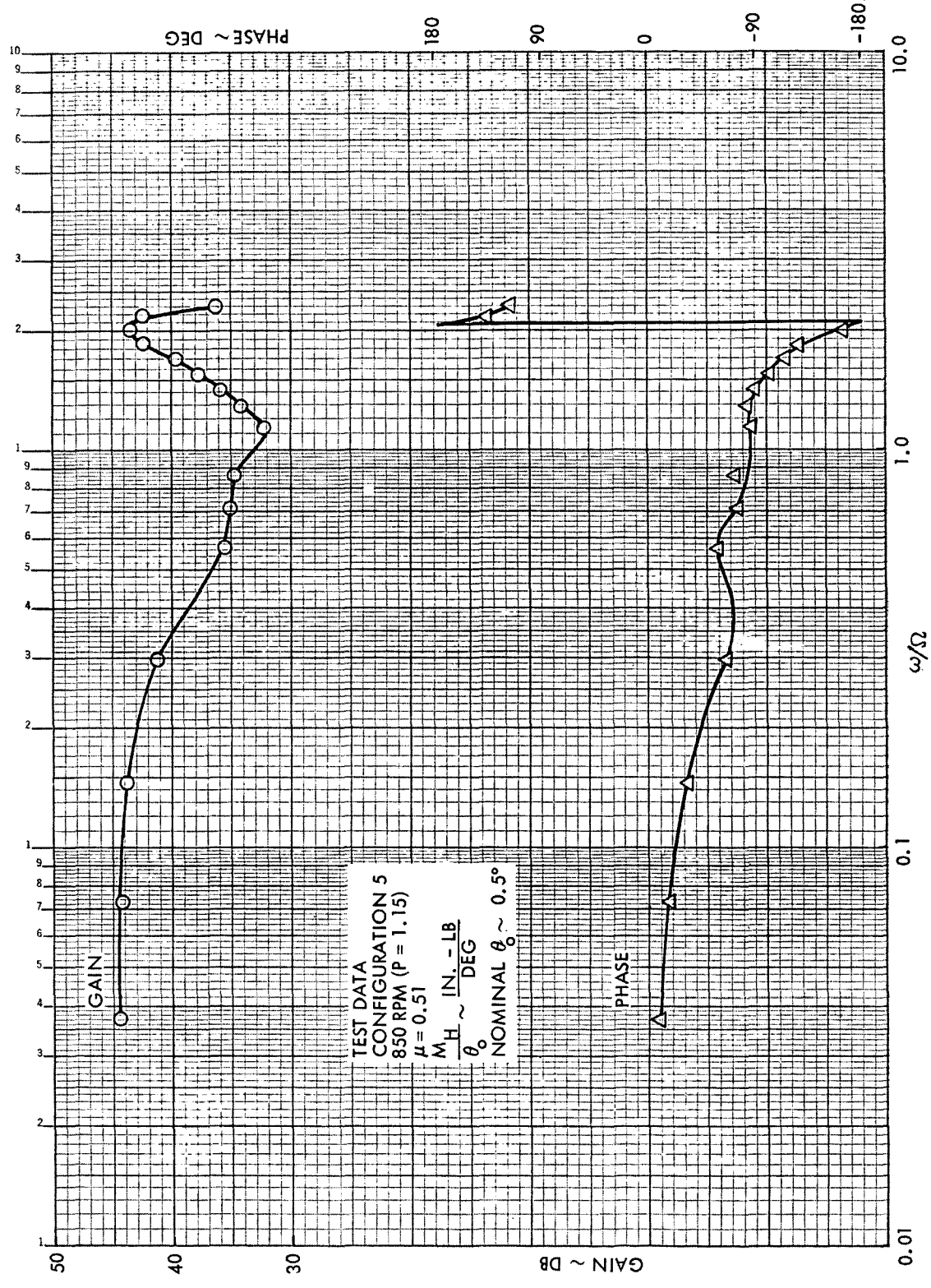

Figure B5. Rotor Hub Pitch Moment Frequency Response to Collective Pitch, Configuration 5, μ = 0.51, 850 RPM (P = 1.15)

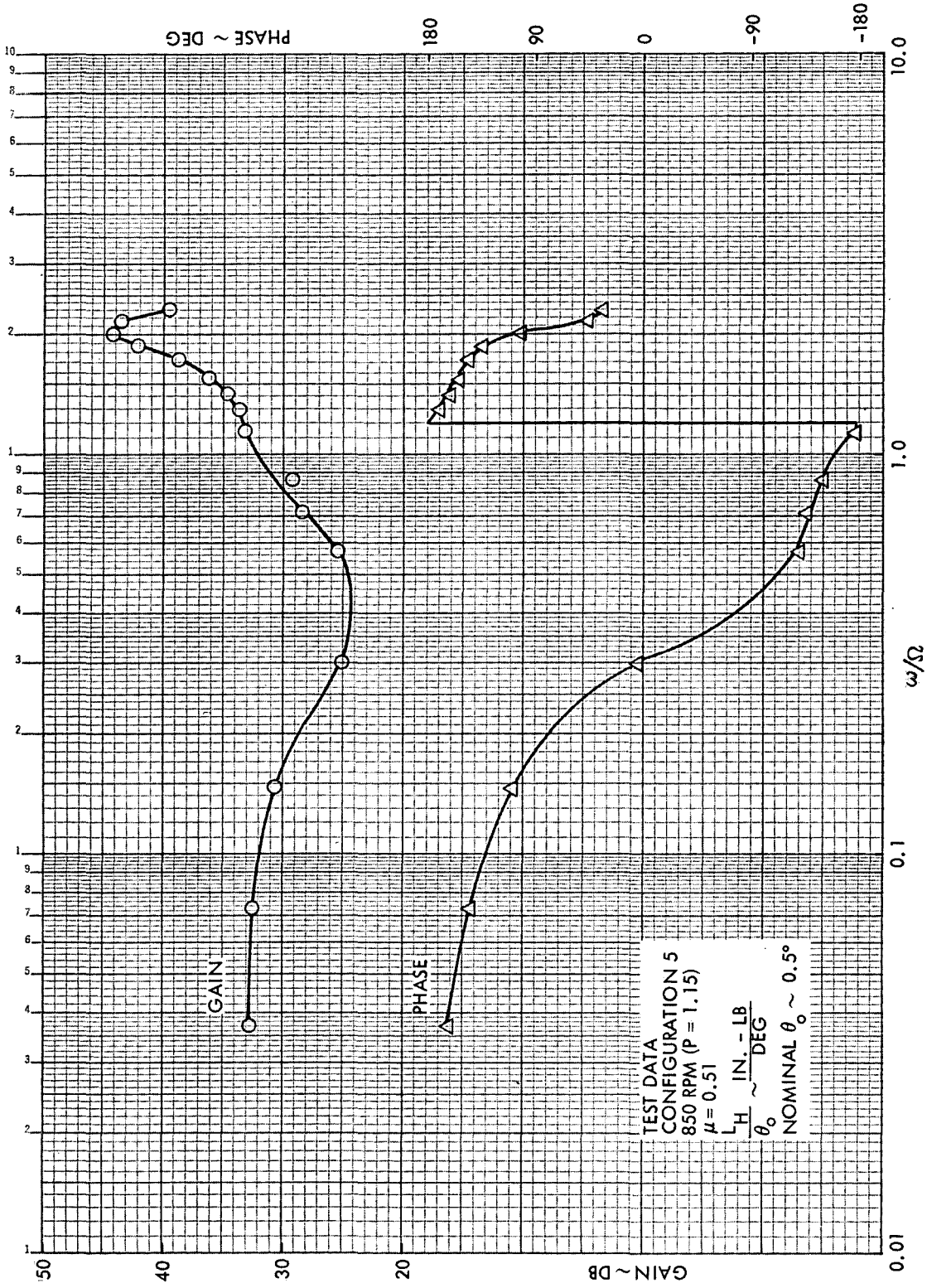

Figure B6. Rotor Hub Roll Moment Frequency Response to Collective Pitch, Configuration 5, μ = 0.51, 850 RPM (P = 1.15)

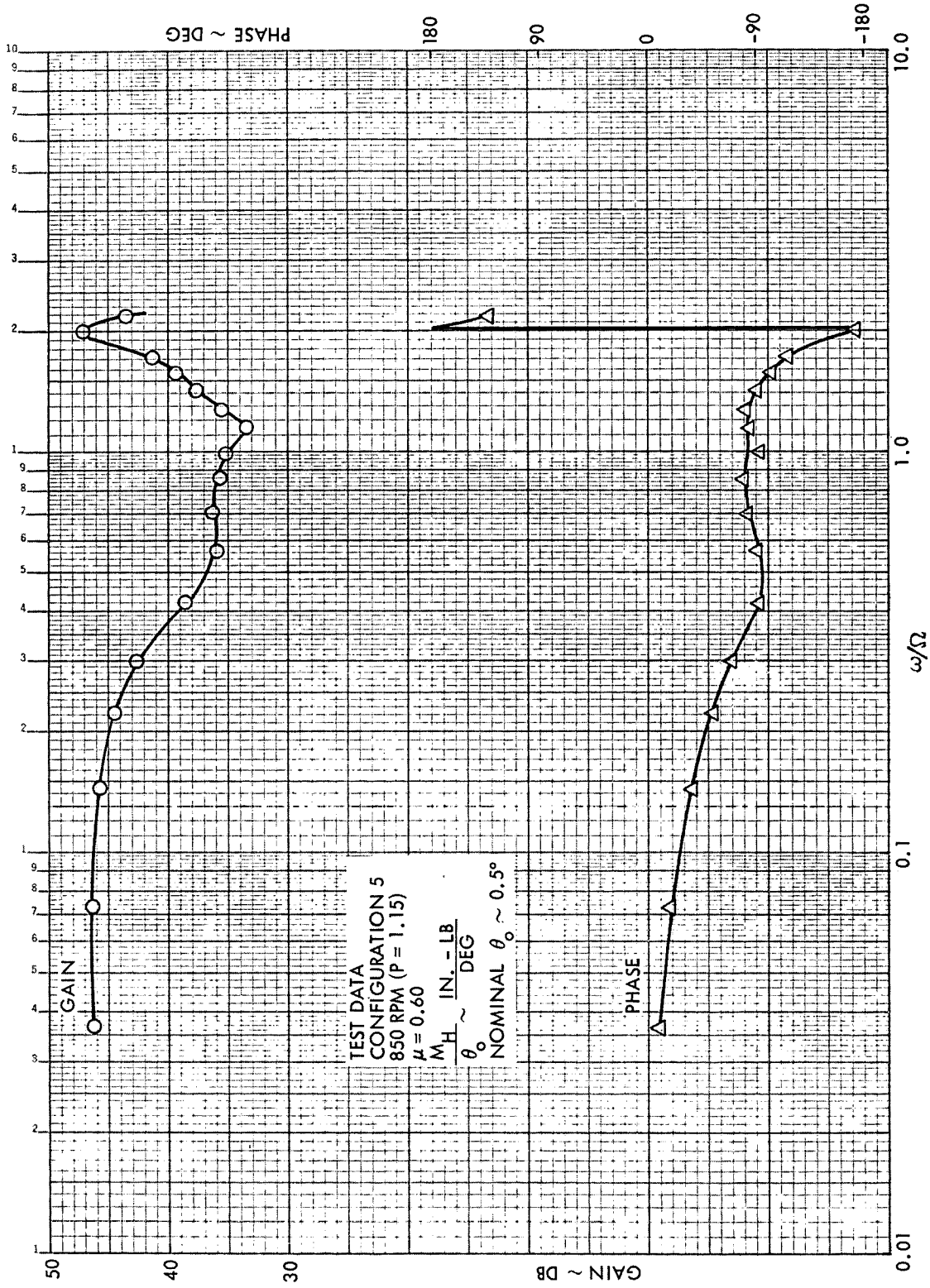

Figure B7. Rotor Hub Pitch Moment Frequency Response to Collective Pitch, Configuration 5, μ = 0.60, 850 RPM (P = 1.15)

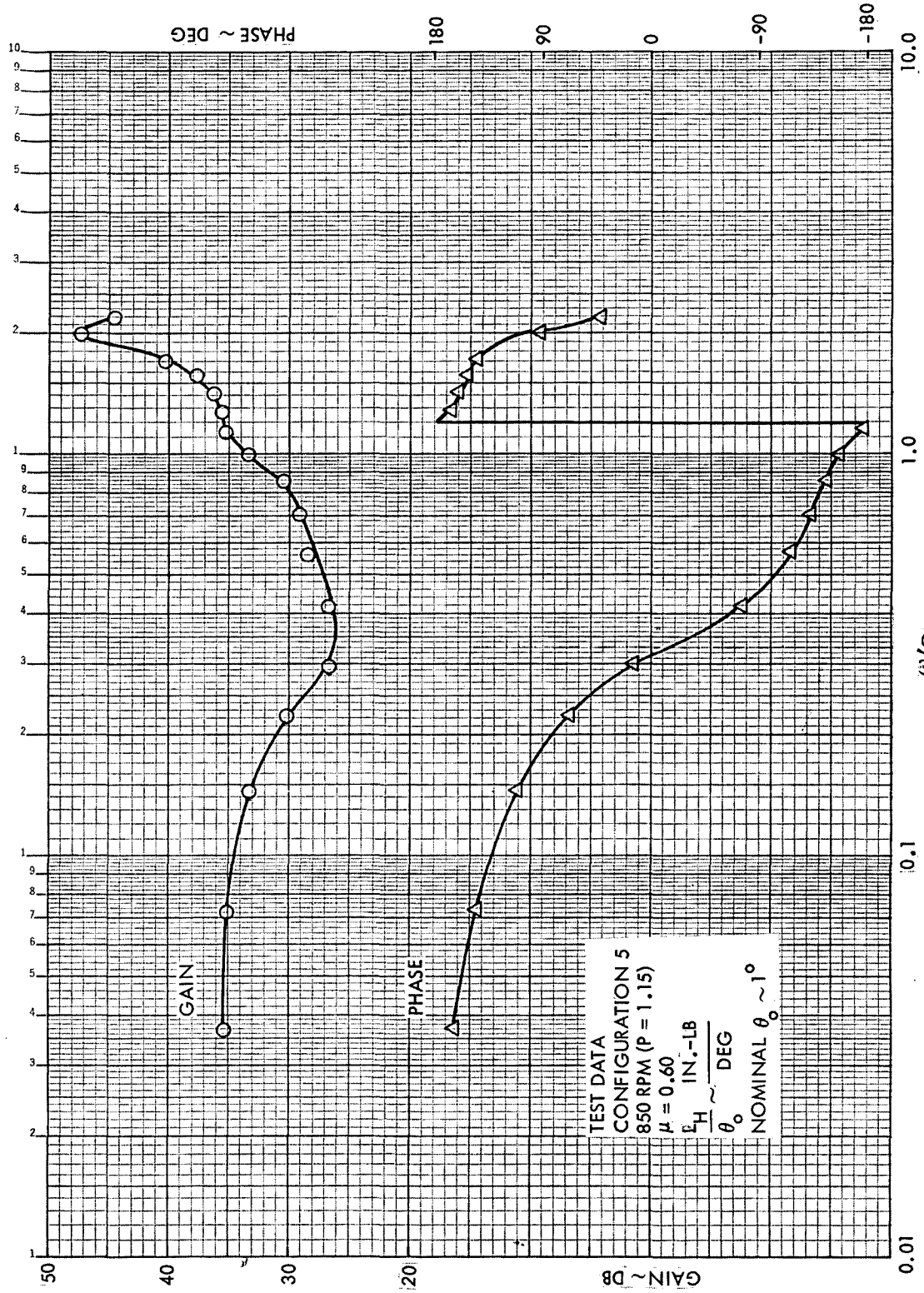

Figure B8. Rotor Hub Roll Moment Frequency Response to Collective Pitch, Configuration 5, μ = 0.60, 850 RPM (P = 1.15)

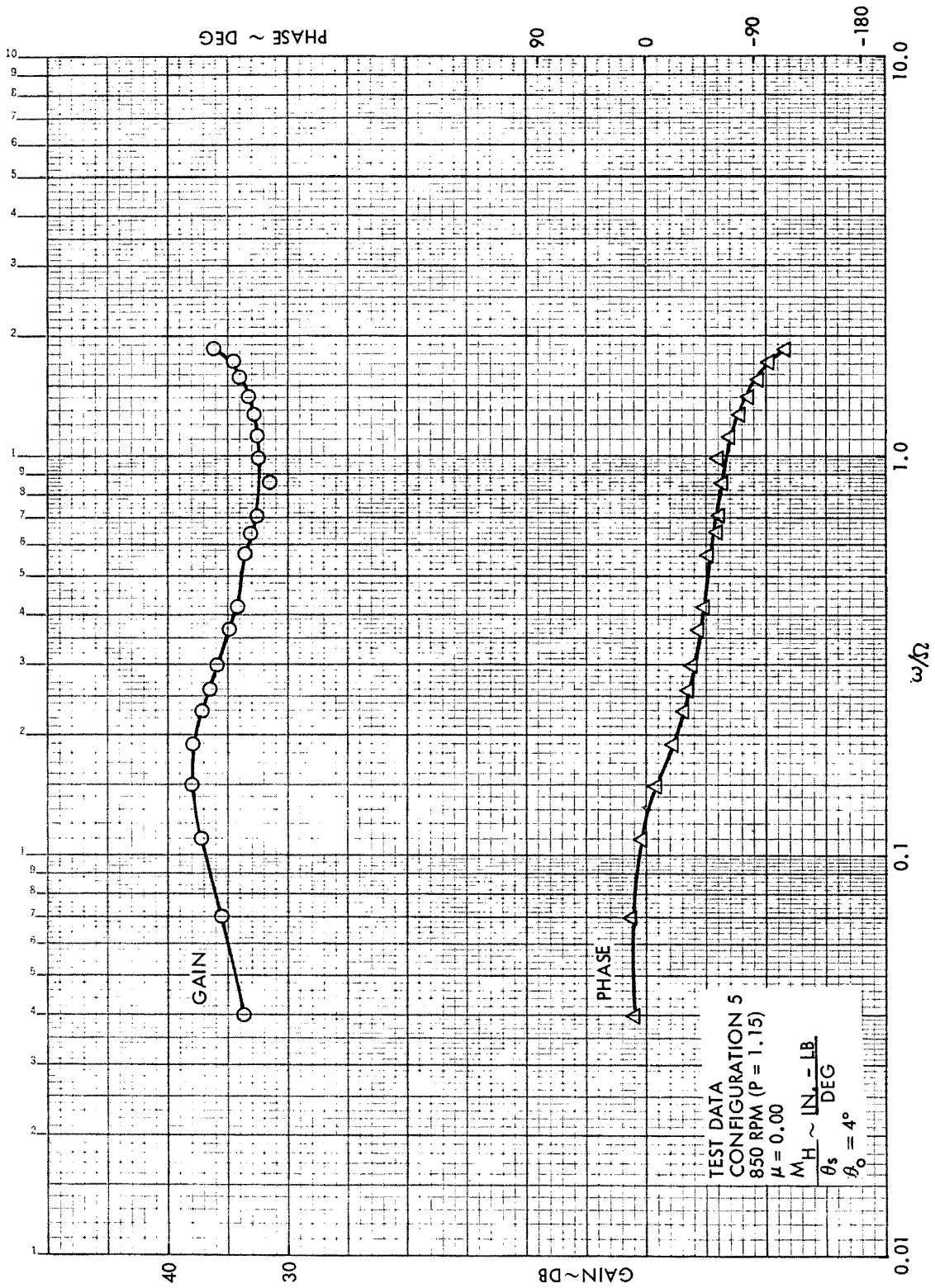

Figure B9. Rotor Hub Pitch Moment Frequency Response to Longitudinal Cyclic Pitch, Configuration 5, $\mu = 0.0$, 850 RPM (P = 1.15)

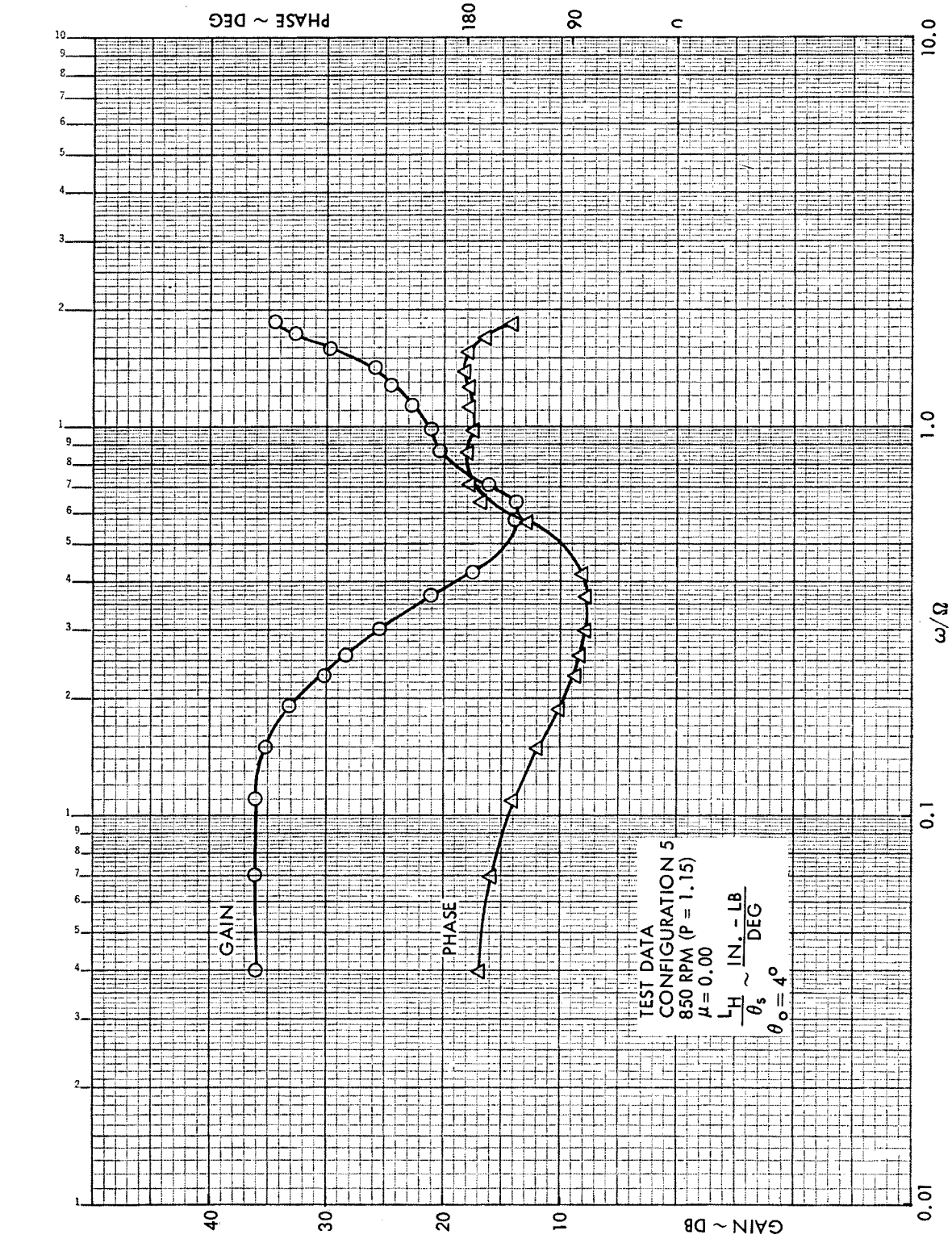

Figure B10. Rotor Hub Roll Moment Frequency Response to Longitudinal Cyclic Pitch, Configuration 5, μ = 0.0, 850 RPM (P = 1.15)

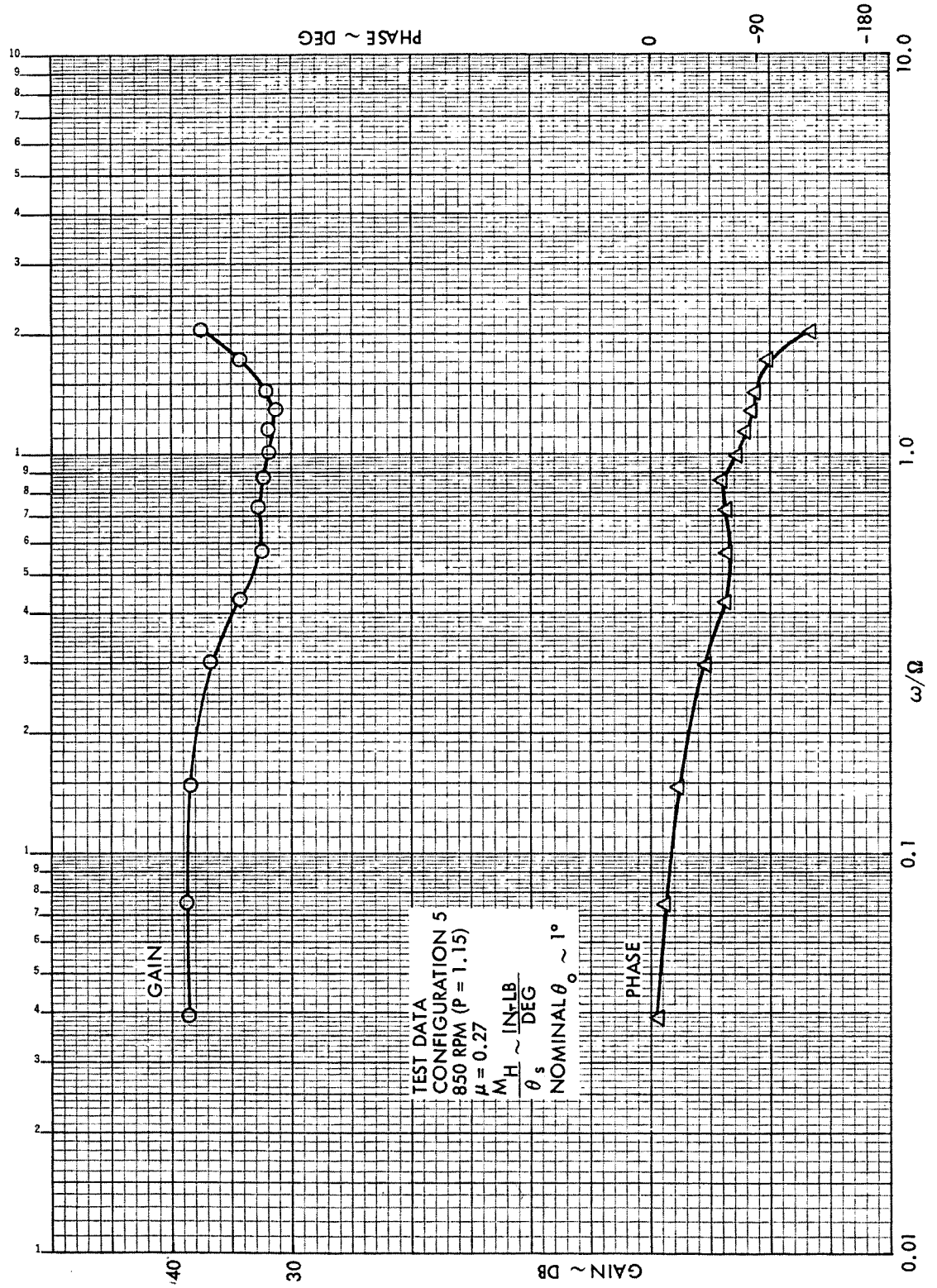

Figure B11. Rotor Hub Pitch Moment Frequency Response to Longitudinal Cyclic Pitch, Configuration 5, $\mu = 0.27$, 850 RPM (P = 1.15)

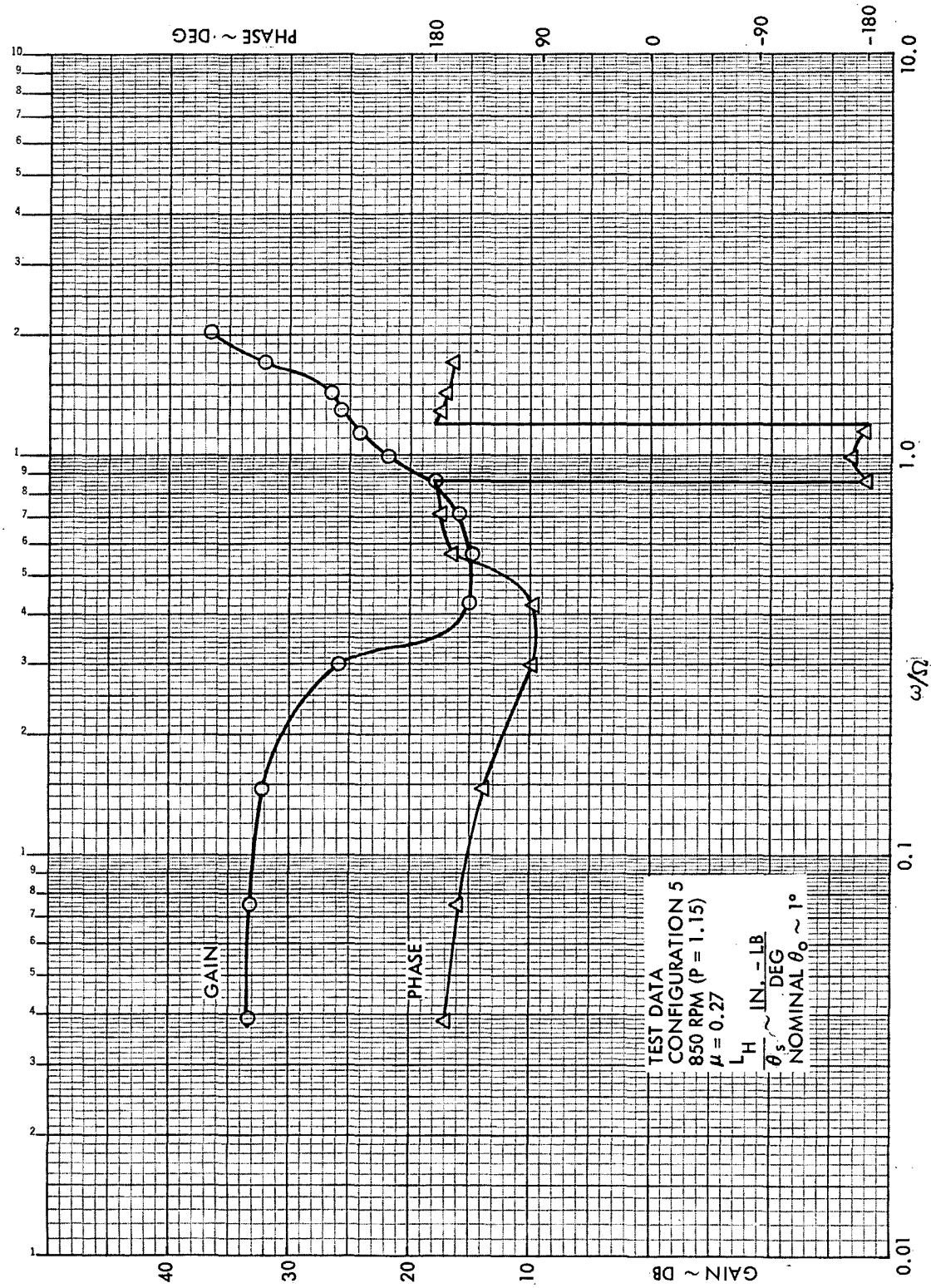

Figure B12. Rotor Hub Roll Moment Frequency Response to Longitudinal Cyclic Pitch, Configuration 5, μ = 0.27, 850 RPM (P = 1.15)

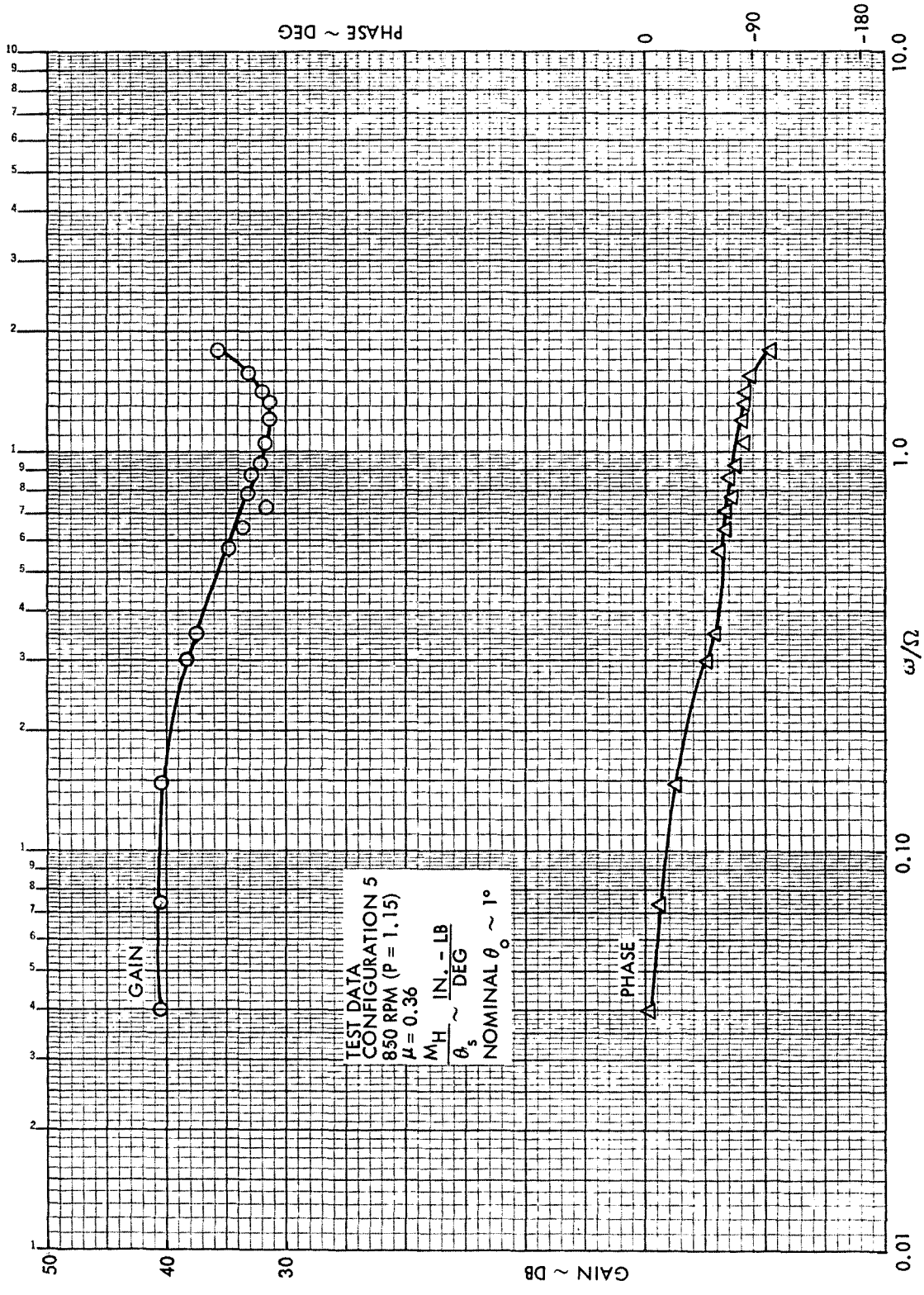

Figure B13. Rotor Hub Pitch Moment Frequency Response to Longitudinal Cyclic Pitch, Configuration 5, μ = 0.36, 850 RPM (P = 1.15)

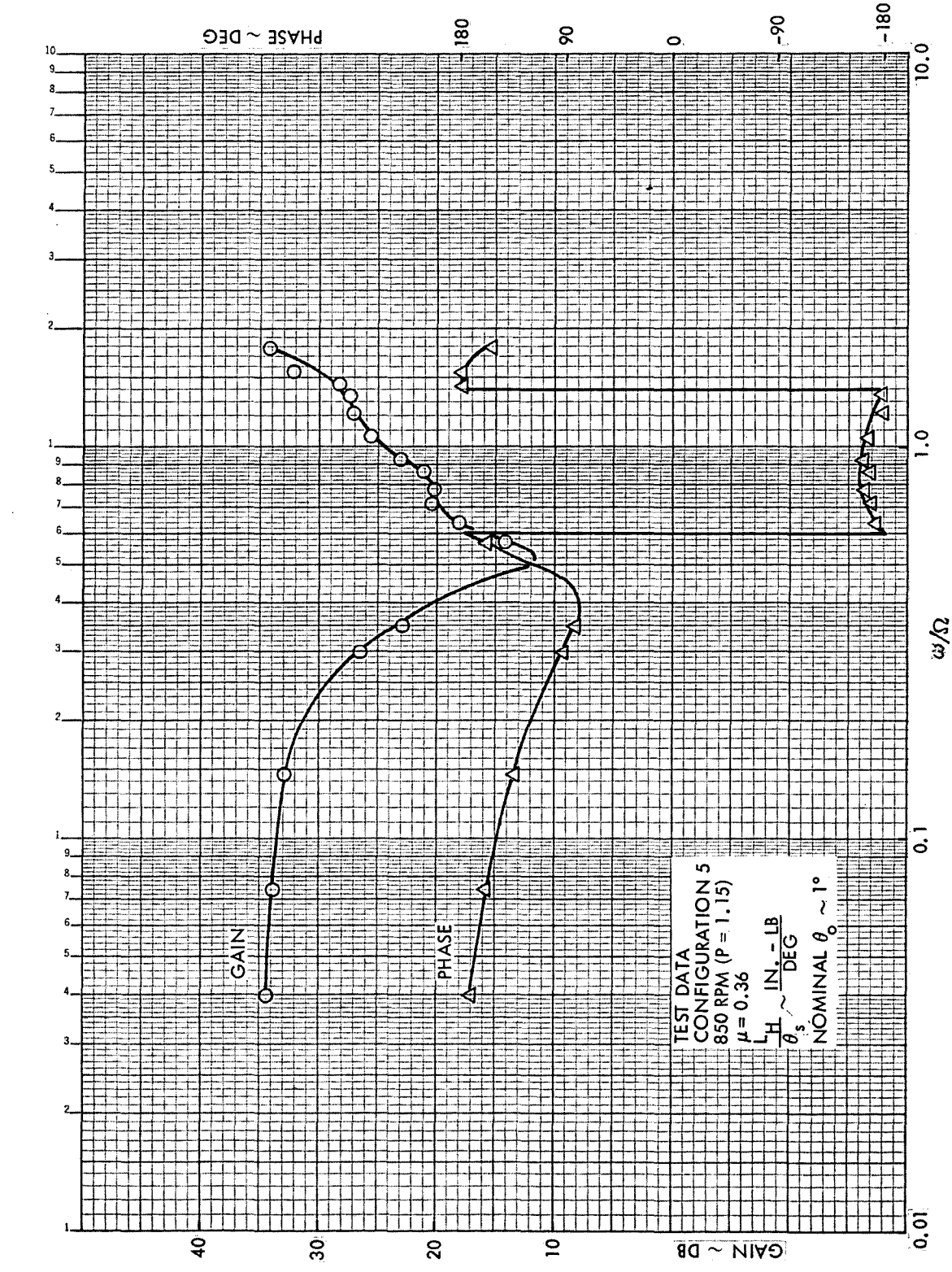

Figure B14. Rotor Hub Roll Moment Frequency Response to Longitudinal Cyclic Pitch, Configuration 5, μ = 0.36, 850 RPM (P = 1.15)

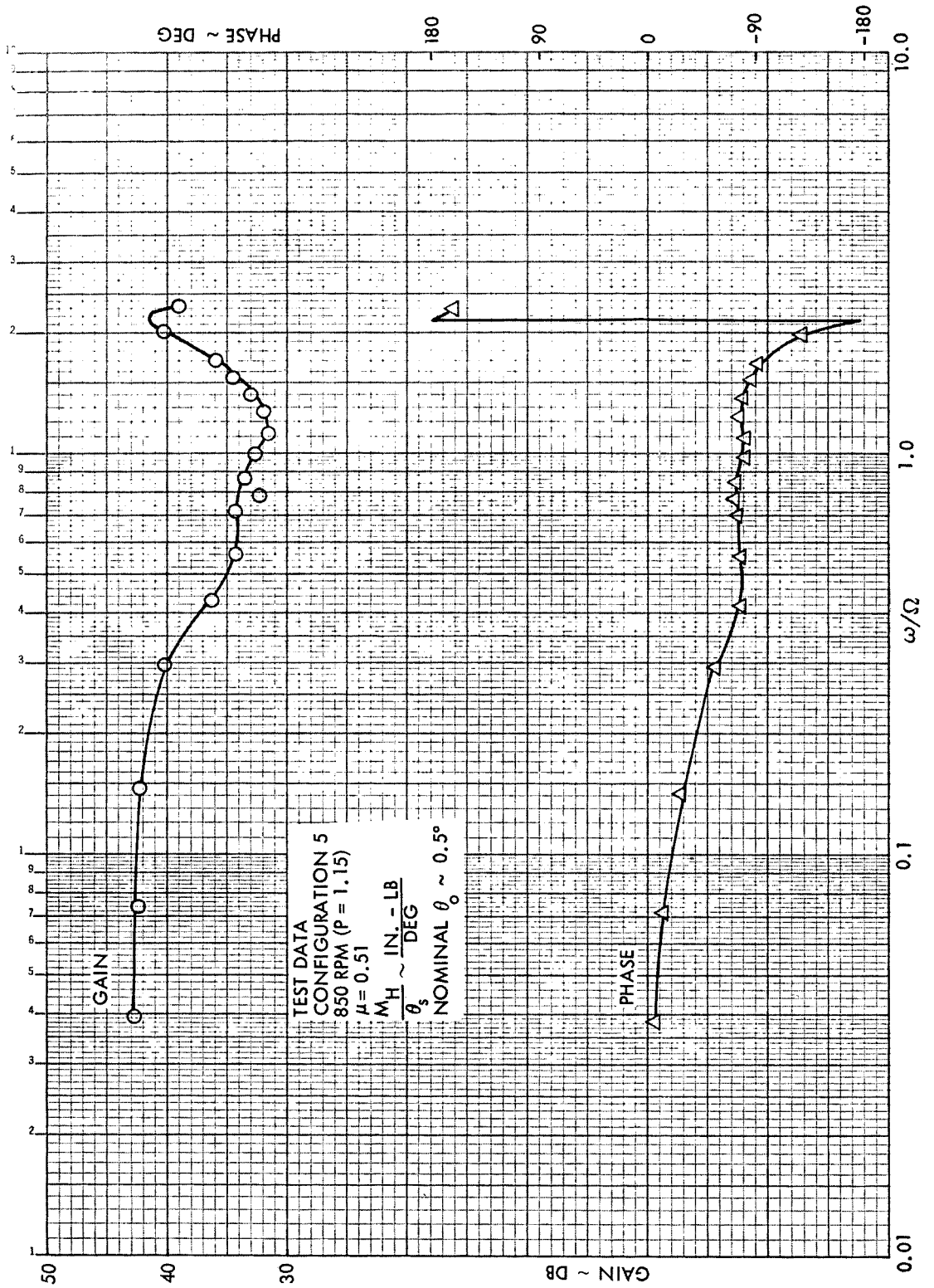

Figure B15. Rotor Hub Pitch Moment Frequency Response to Longitudinal Cyclic Pitch, Configuration 5, μ = 0.51, 850 RPM (P = 1.15)

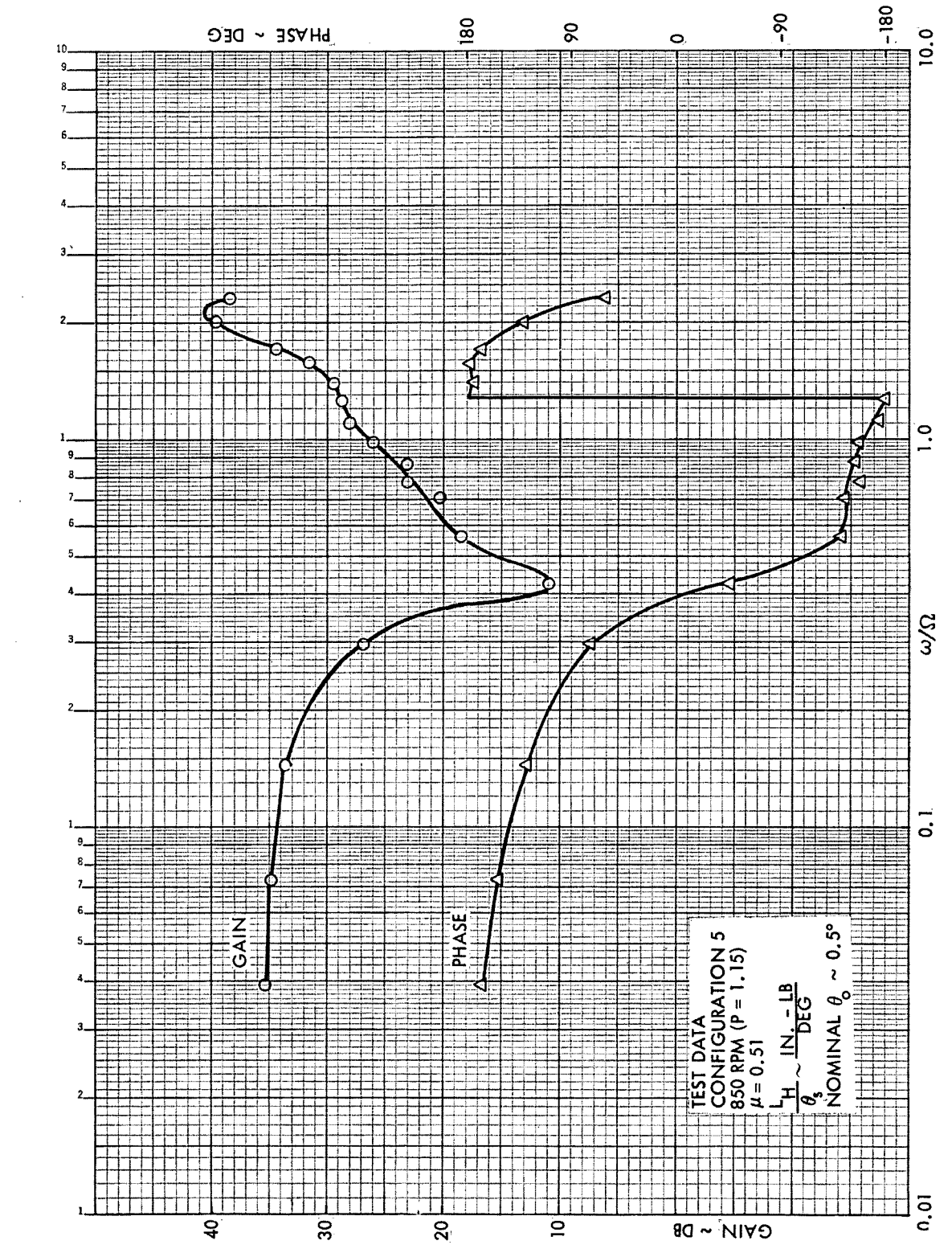

Figure B16. Rotor Hub Roll Moment Frequency Response to Longitudinal Cyclic Pitch, Configuration 5, μ = 0.51, 850 RPM (P = 1.15)

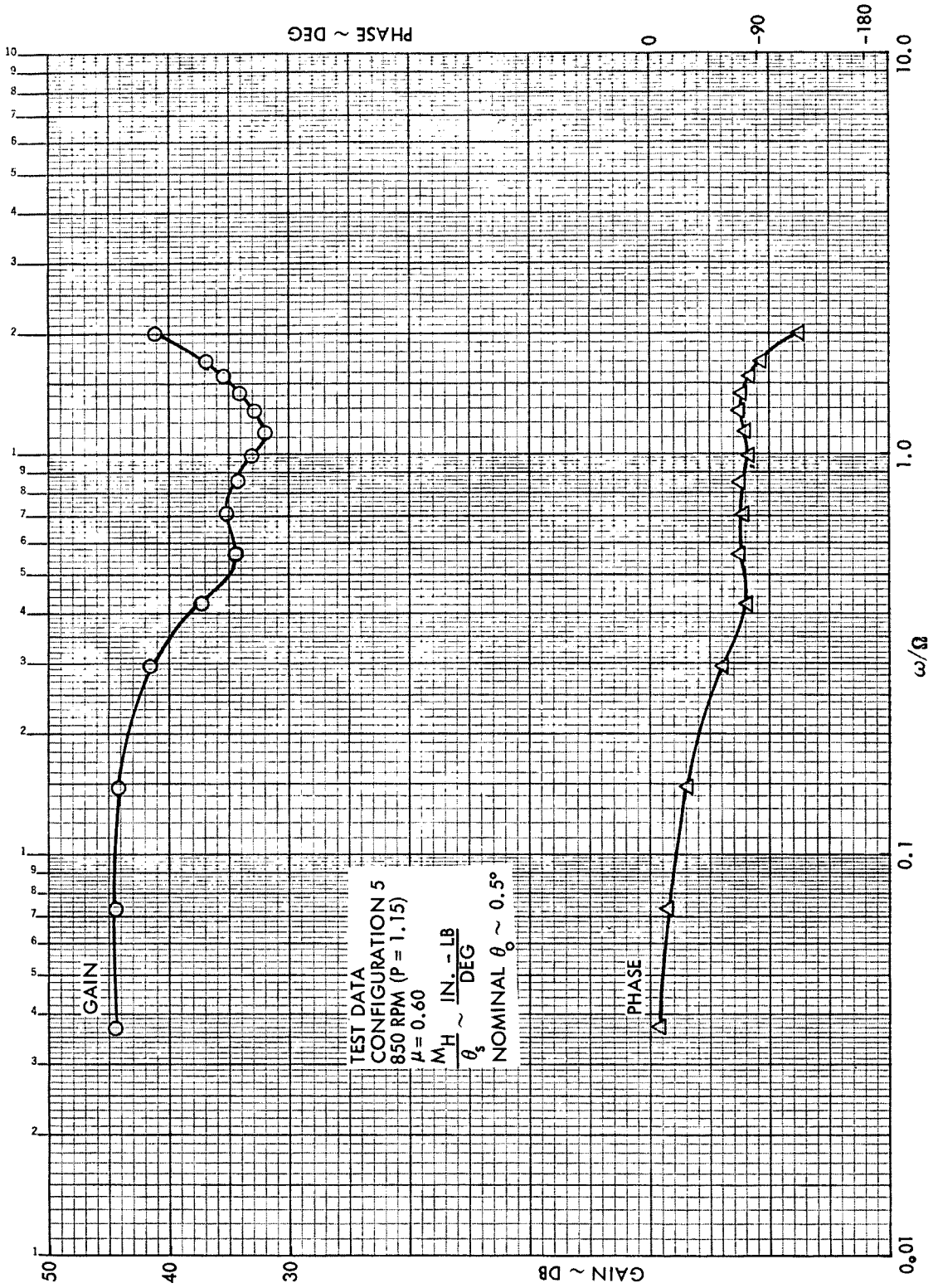

Figure B17. Rotor Hub Pitch Moment Frequency Response to Longitudinal Cyclic Pitch, Configuration 5, $\mu = 0.60$, 850 RPM (P = 1.15)

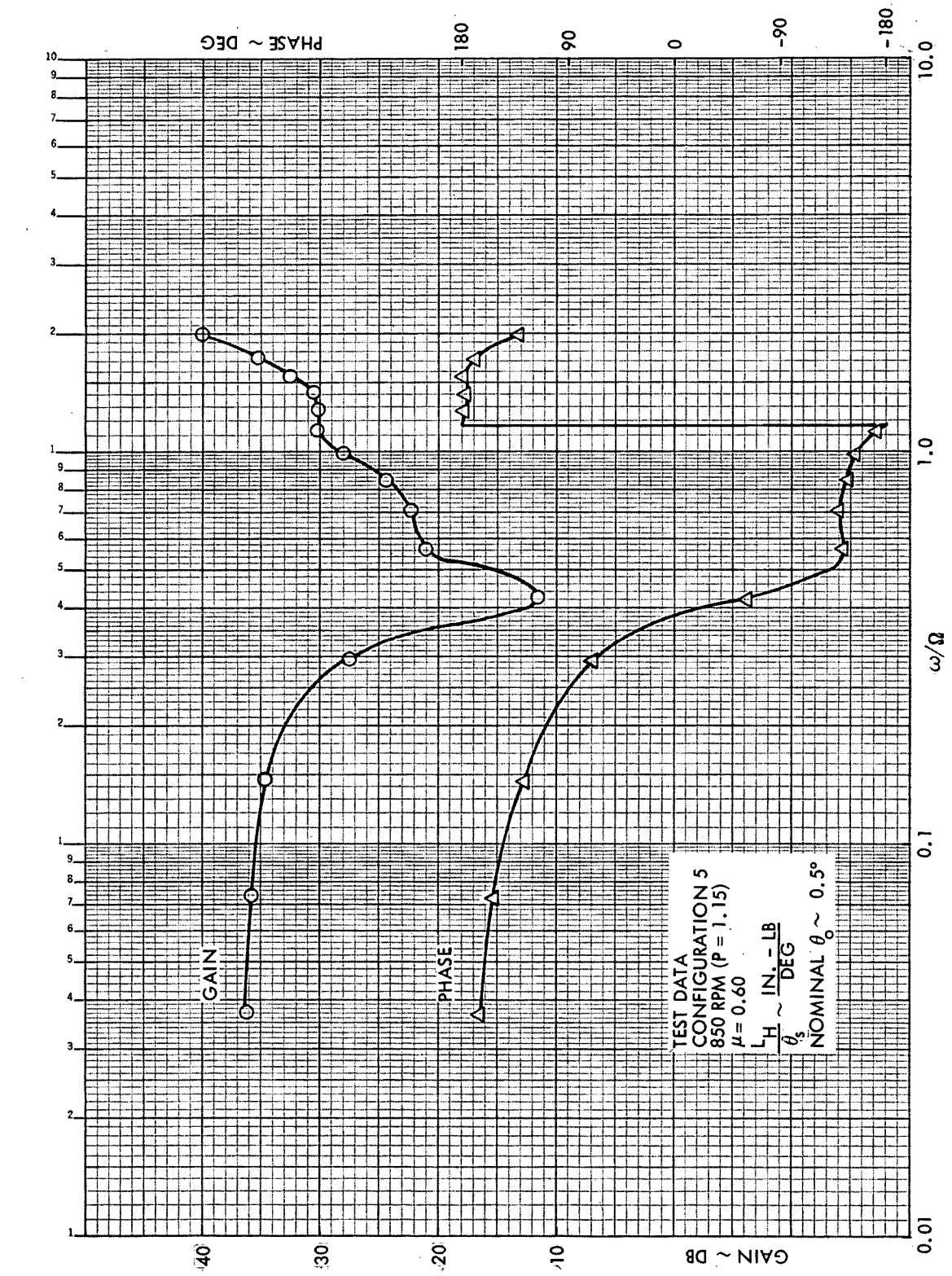

Figure B18. Rotor Hub Roll Moment Frequency Response to Longitudinal Cyclic Pitch, Configuration 5, μ = 0.60, 850 RPM (P = 1.15)

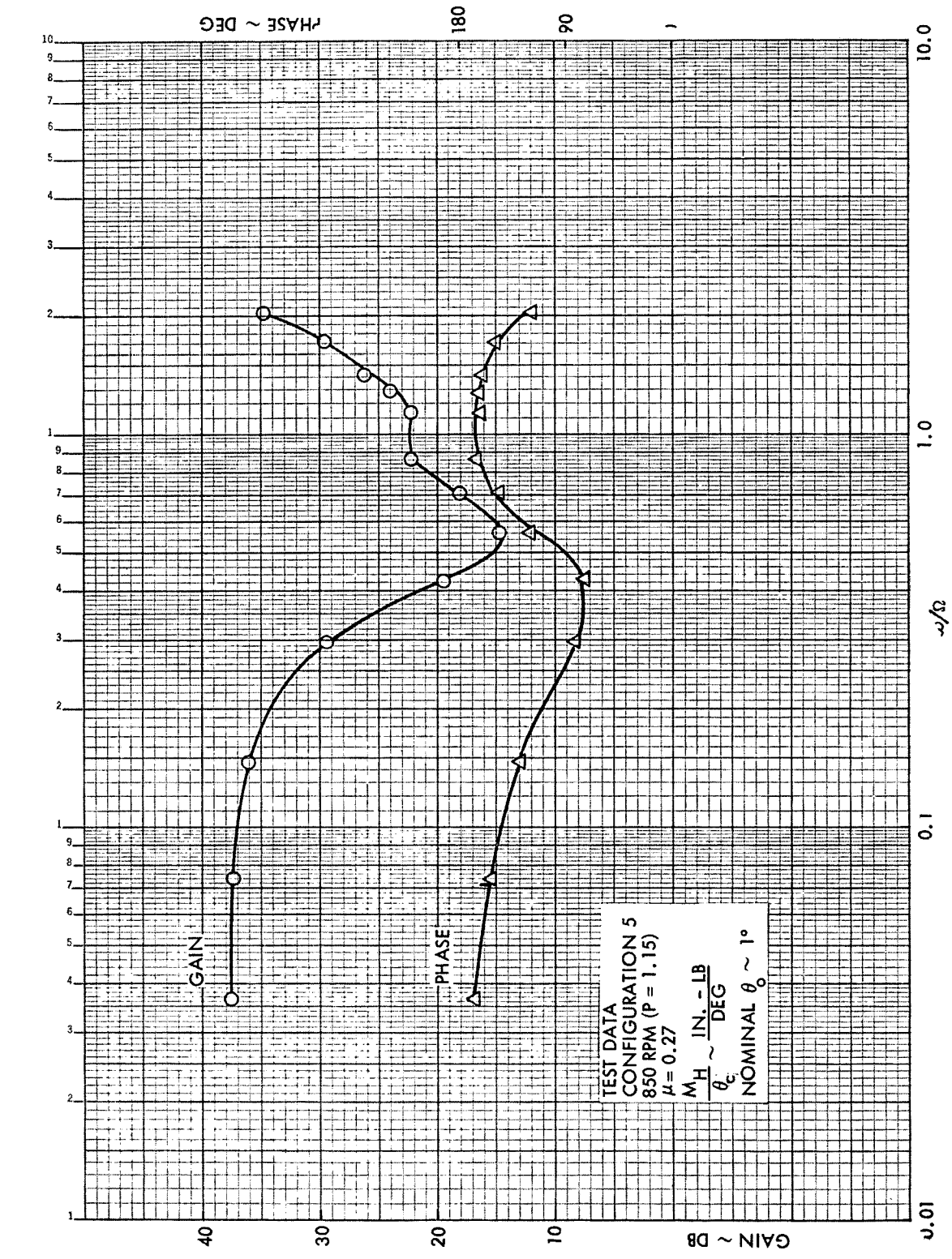

Figure B19. Rotor Hub Pitch Moment Frequency Response to Lateral Cyclic Pitch, Configuration 5, μ = 0.27, 850 RPM (P = 1.15)

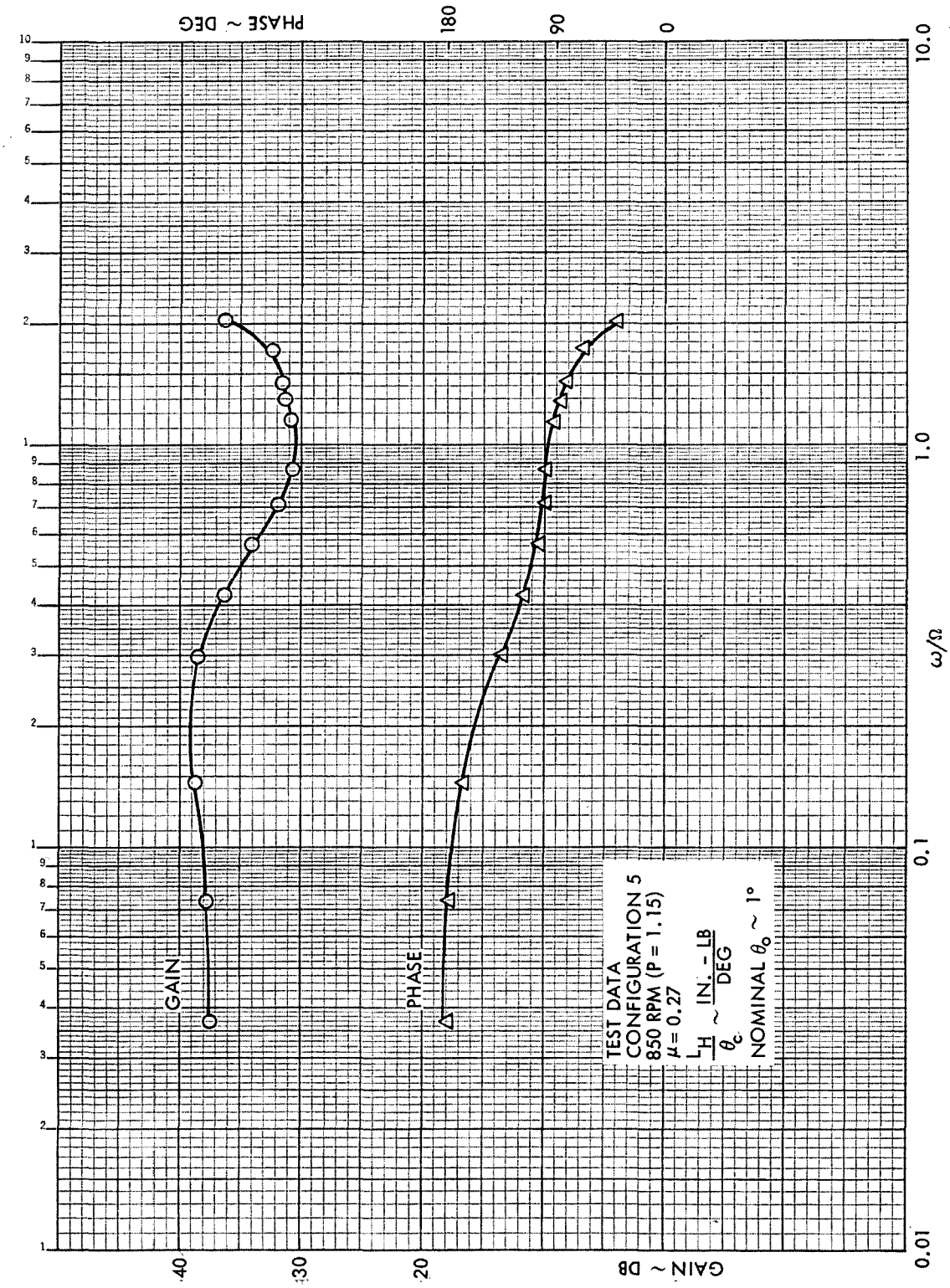

Figure B20. Rotor Hub Roll Moment Frequency Response to Lateral Cyclic Pitch, Configuration 5, μ = 0.27, 850 RPM (P = 1.15)

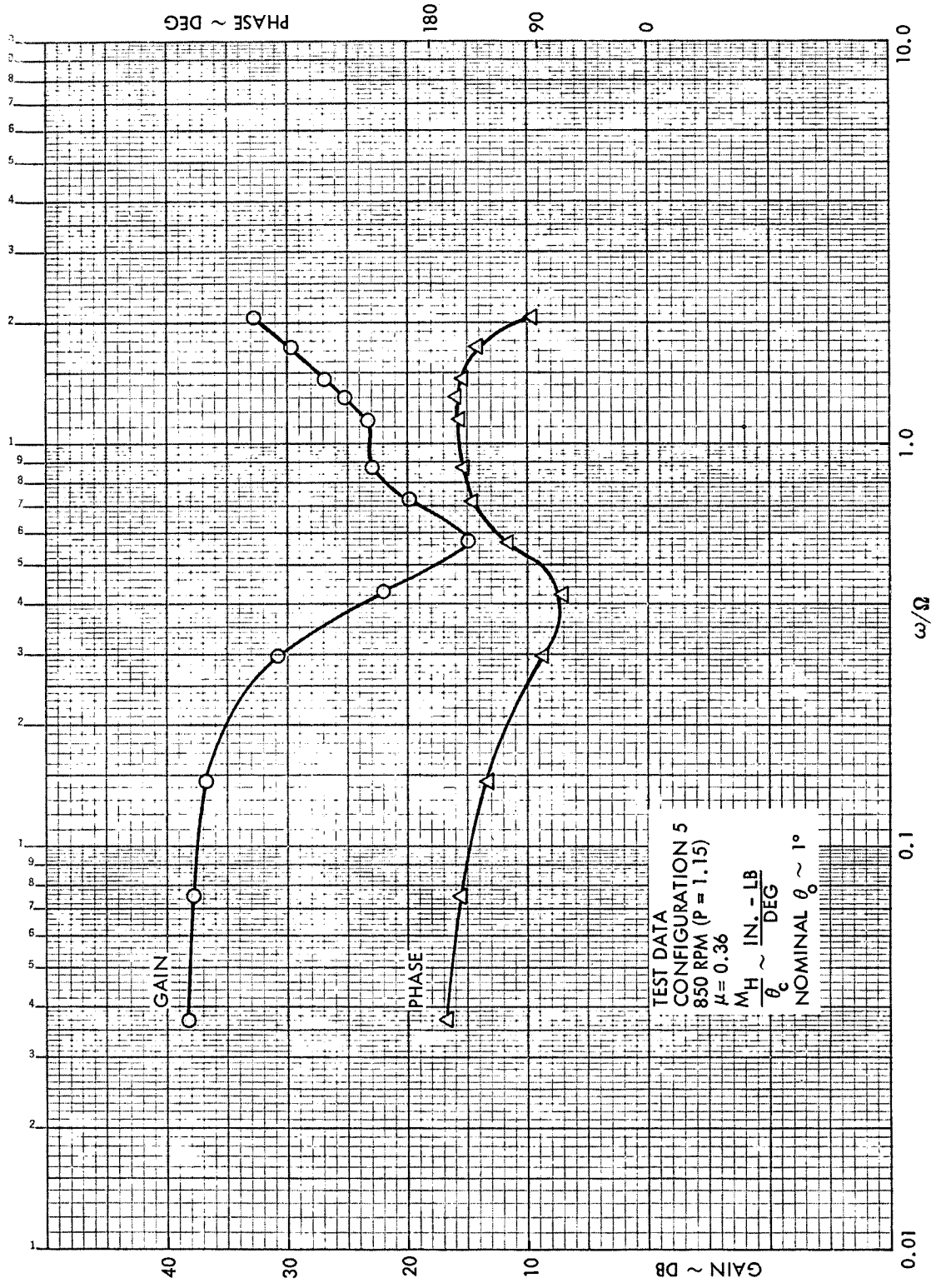

Figure B21. Rotor Hub Pitch Moment Frequency Response to Lateral Cyclic Pitch, Configuration 5, μ = 0.36, 850 RPM (P = 1.15)

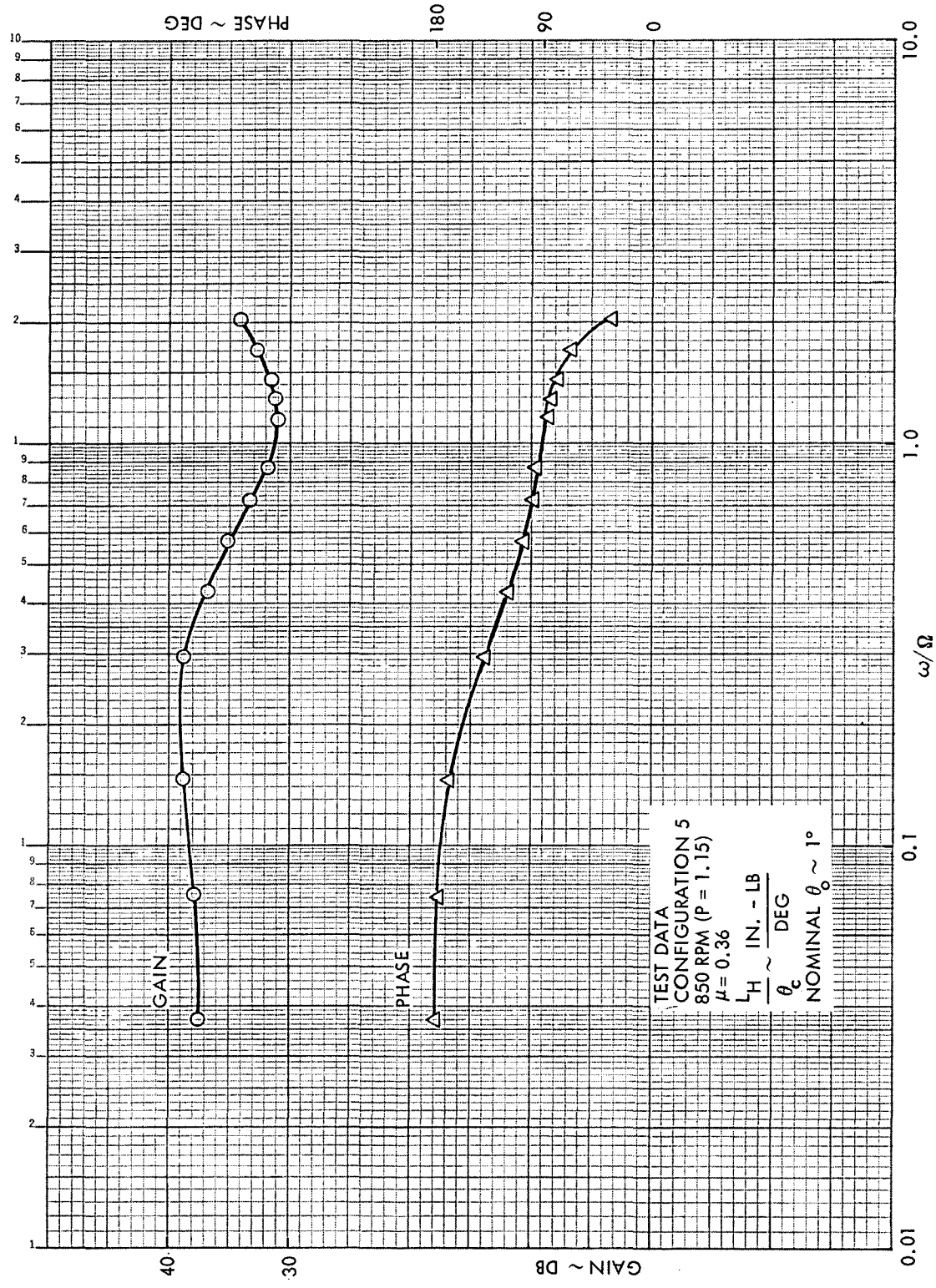

Figure B22. Rotor Hub Roll Moment Frequency Response to Lateral Cyclic Pitch, Configuration 5, $\mu = 0.36$, 850 RPM (P = 1.15)

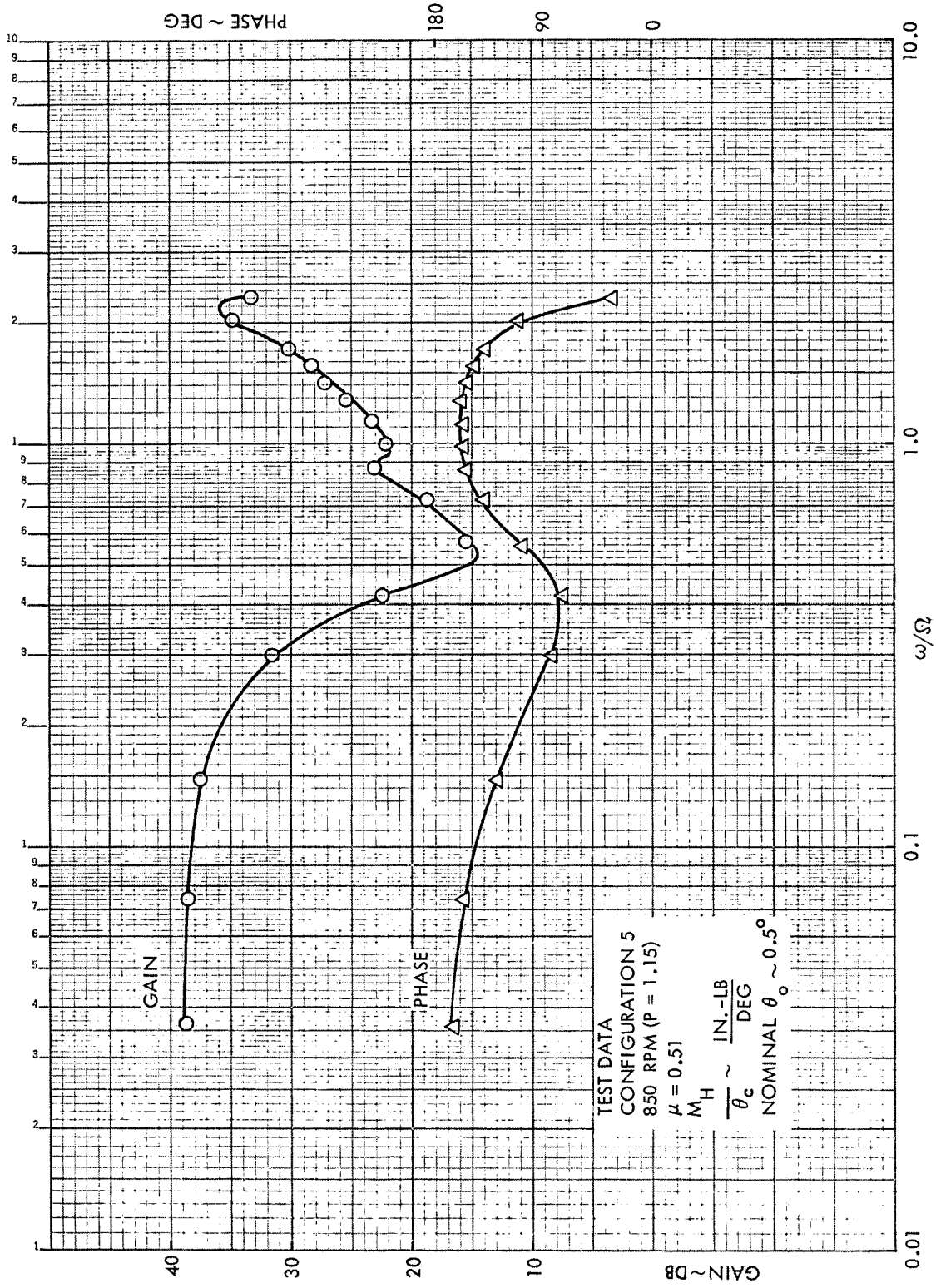

Figure B23. Rotor Hub Pitch Moment Frequency Response to Lateral Cyclic Pitch, Configuration 5, μ = 0.51, 850 RPM (P = 1.15)

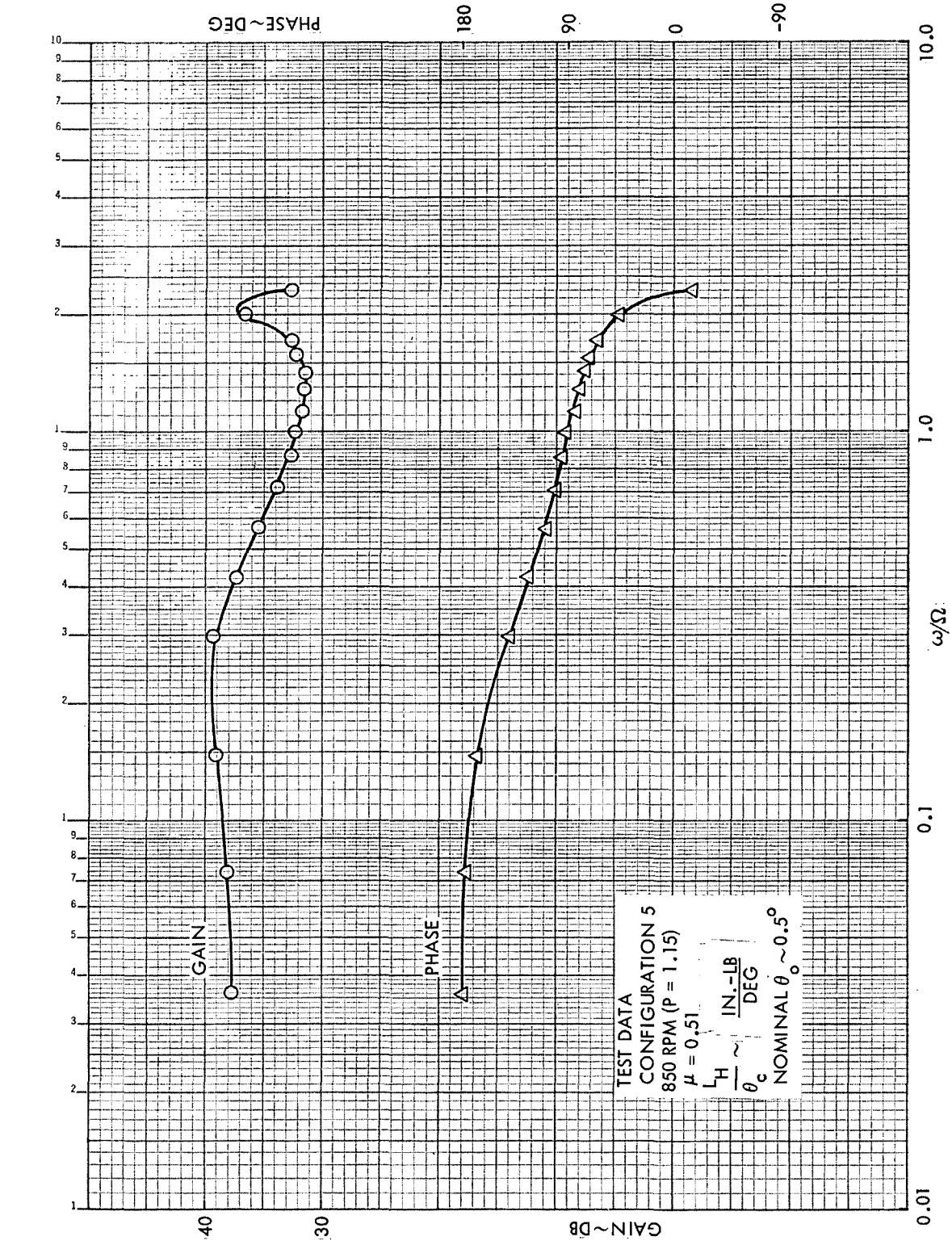

Figure B24. Rotor Hub Roll Moment Frequency Response to Lateral Cyclic Pitch, Configuration 5, μ = 0.51, 850 RPM (P = 1.15)

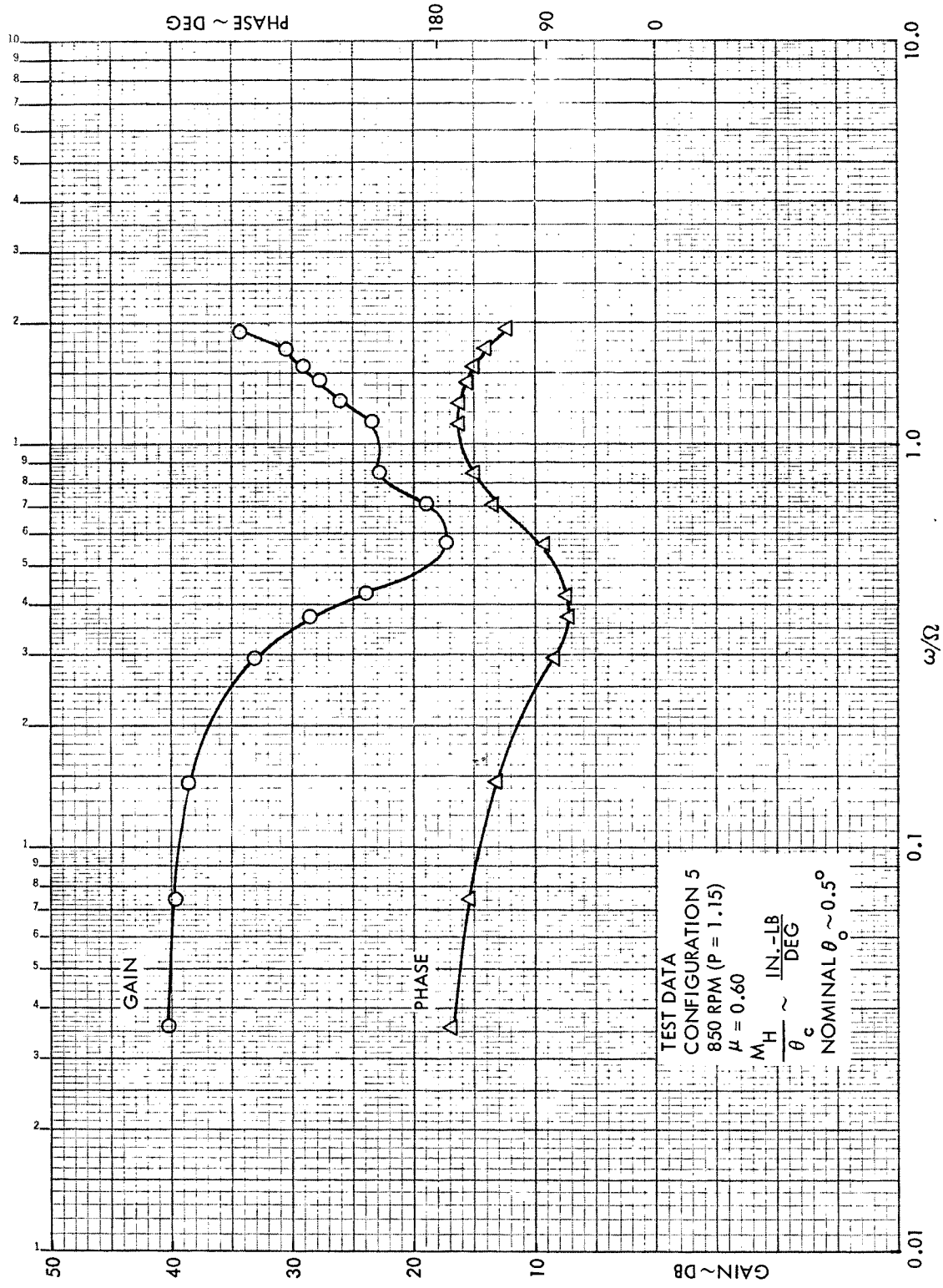

Figure B25. Rotor Hub Pitch Moment Frequency Response to Lateral Cyclic Pitch, Configuration 5, μ = 0.60, 850 RPM (P = 1.15)

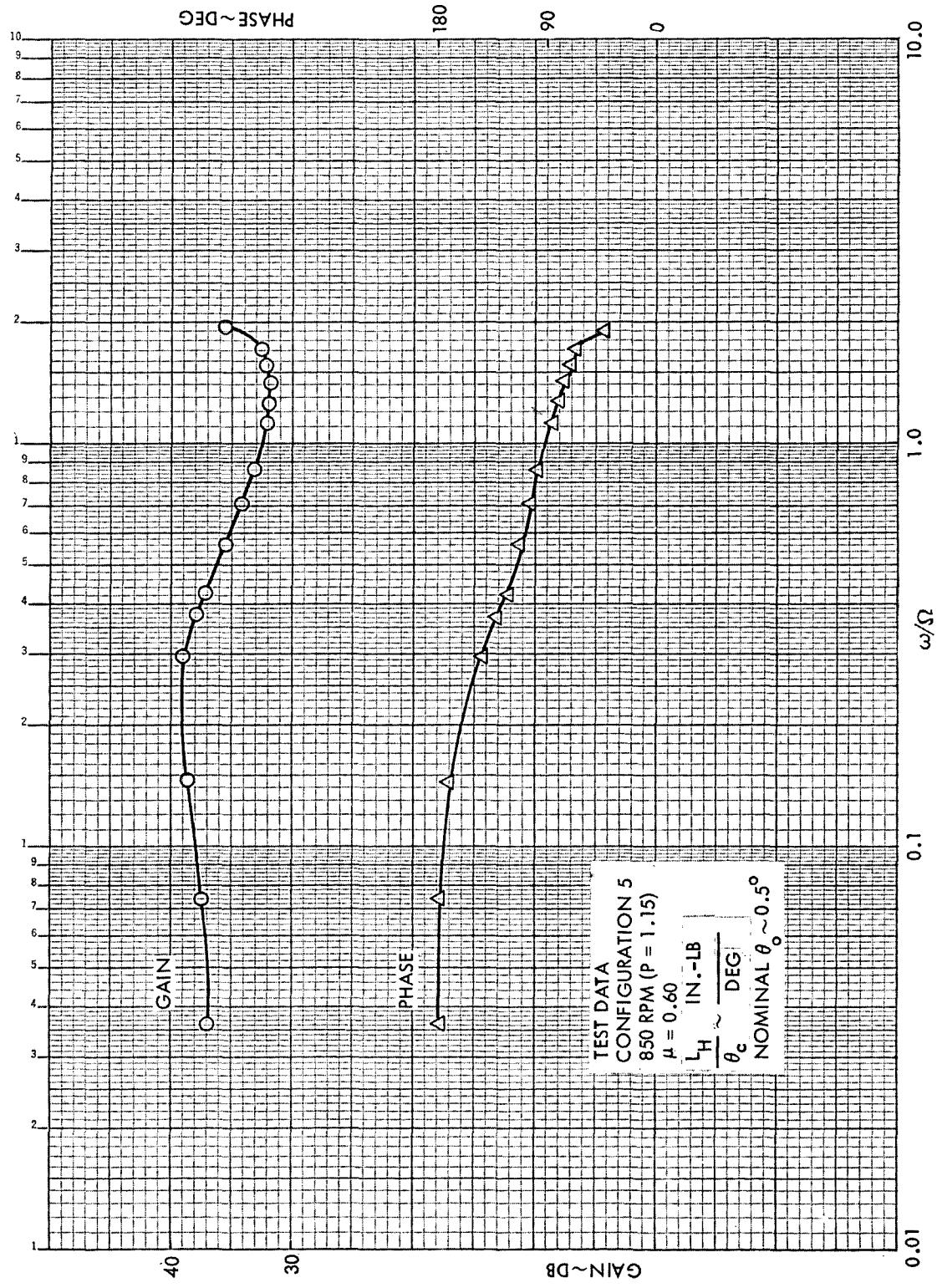

Figure B26. Rotor Hub Roll Moment Frequency Response to Lateral Cyclic Pitch, Configuration 5, μ = 0.60, 850 RPM (P = 1.15)

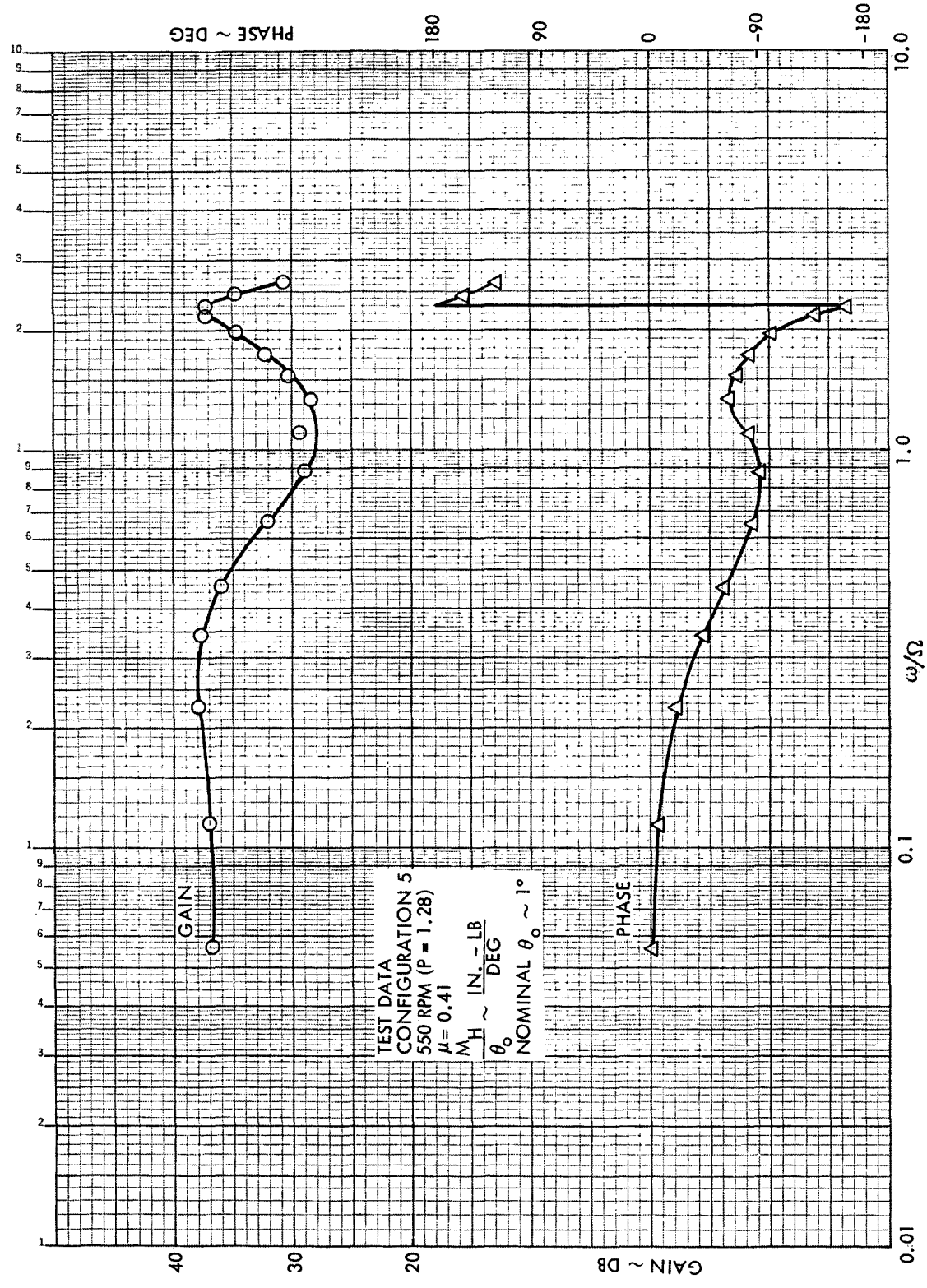

Figure B27. Rotor Hub Pitch Moment Frequency Response to Collective Pitch, Configuration 5, μ = 0.41, 550 RPM (P = 1.28)

LOCKHEED
CALIFORNIA COMPANY

F

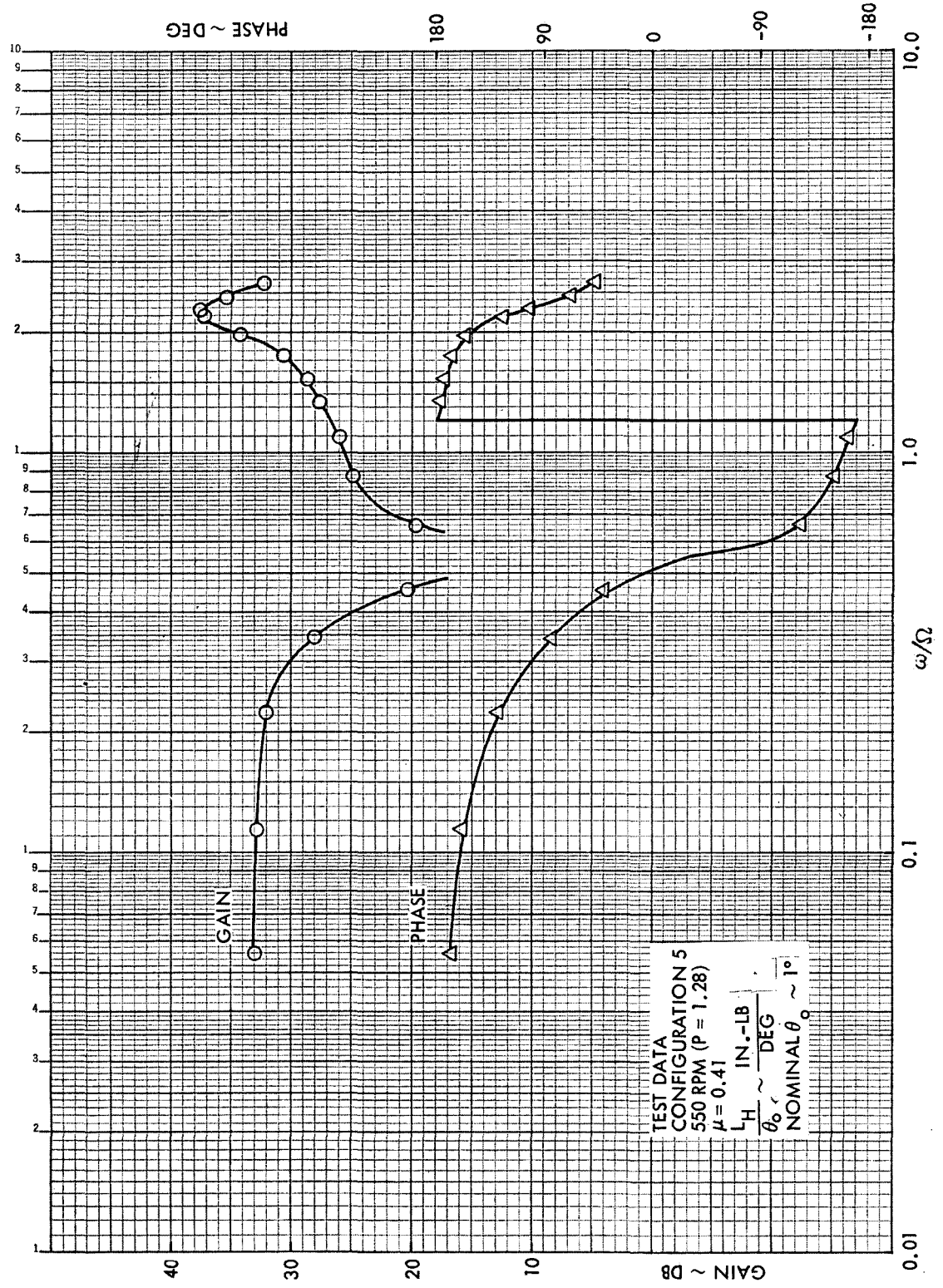

Figure B28. Rotor Hub Roll Moment Frequency Response to Collective Pitch, Configuration 5, $\mu = 0.41$, 550 RPM (P = 1.28)

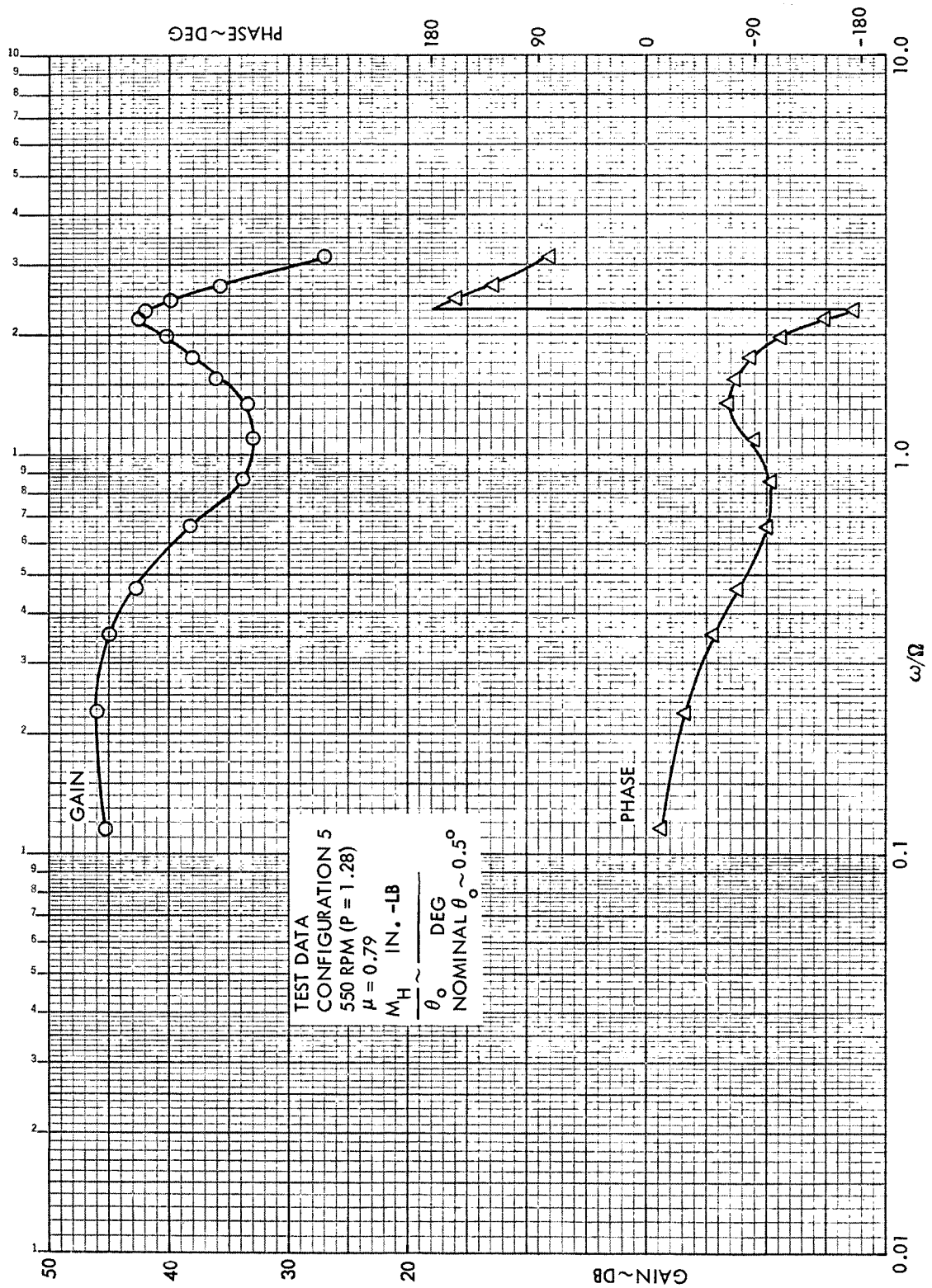

Figure B29. Rotor Hub Pitch Moment Frequency Response to Collective Pitch, Configuration 5, $\mu = 0.79$, 550 RPM (P = 1.28)

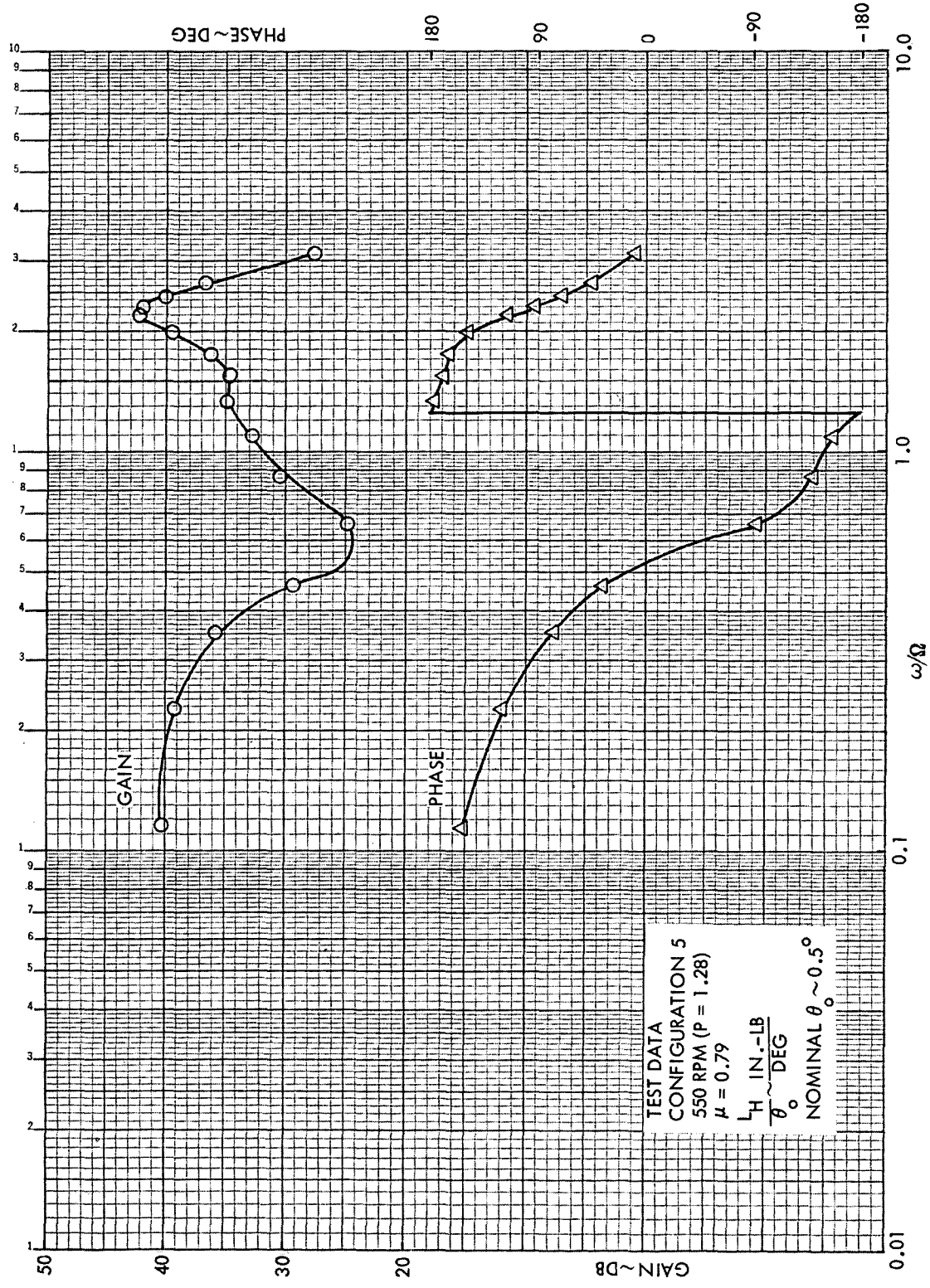

Figure B30. Rotor Hub Roll Moment Frequency Response to Collective Pitch, Configuration 5, μ = 0.79, 550 RPM (P = 1.28)

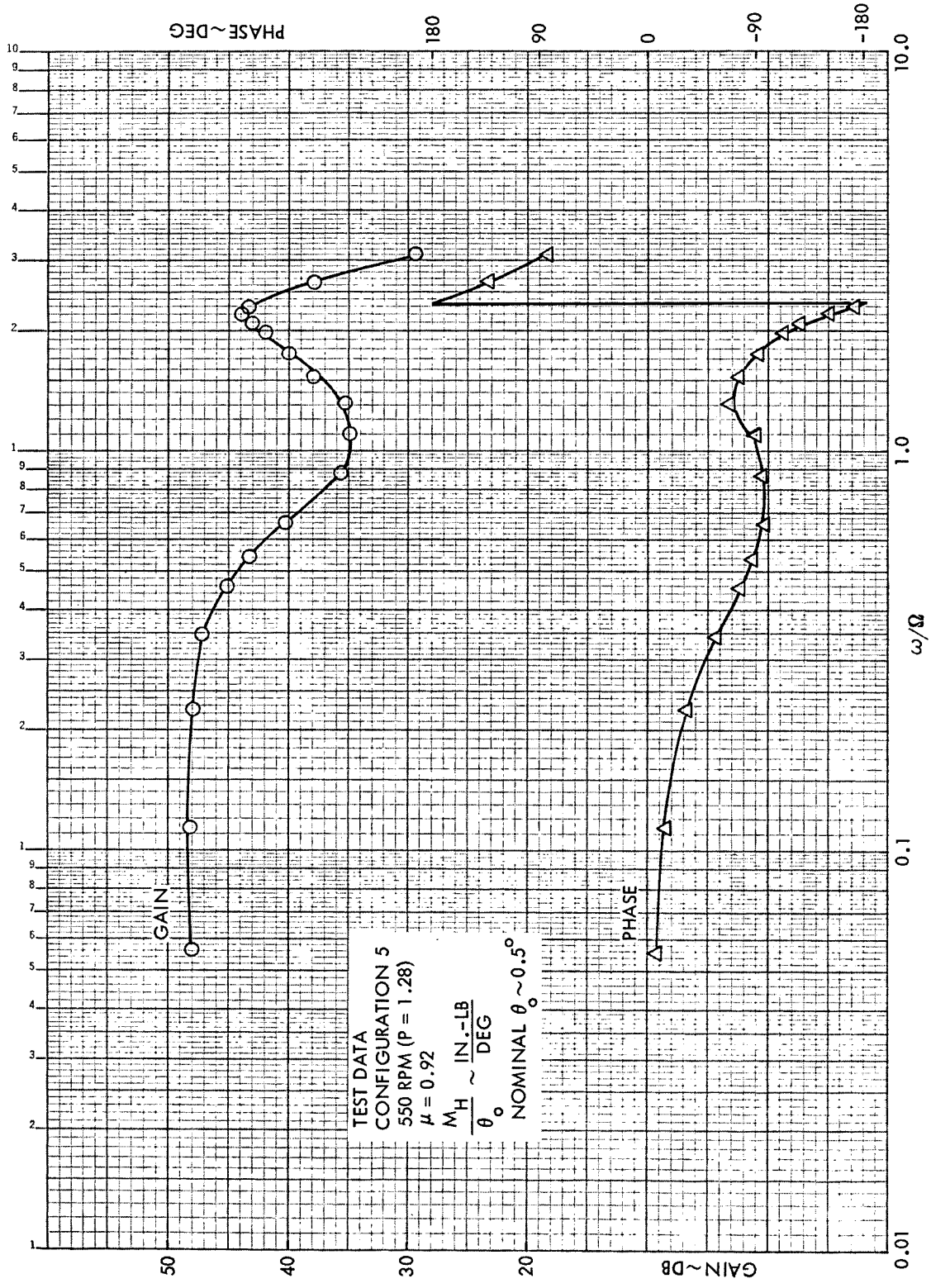

Figure B31. Rotor Hub Pitch Moment Frequency Response to Collective Pitch, Configuration 5, $\mu = 0.92$, 550 RPM (P = 1.28)

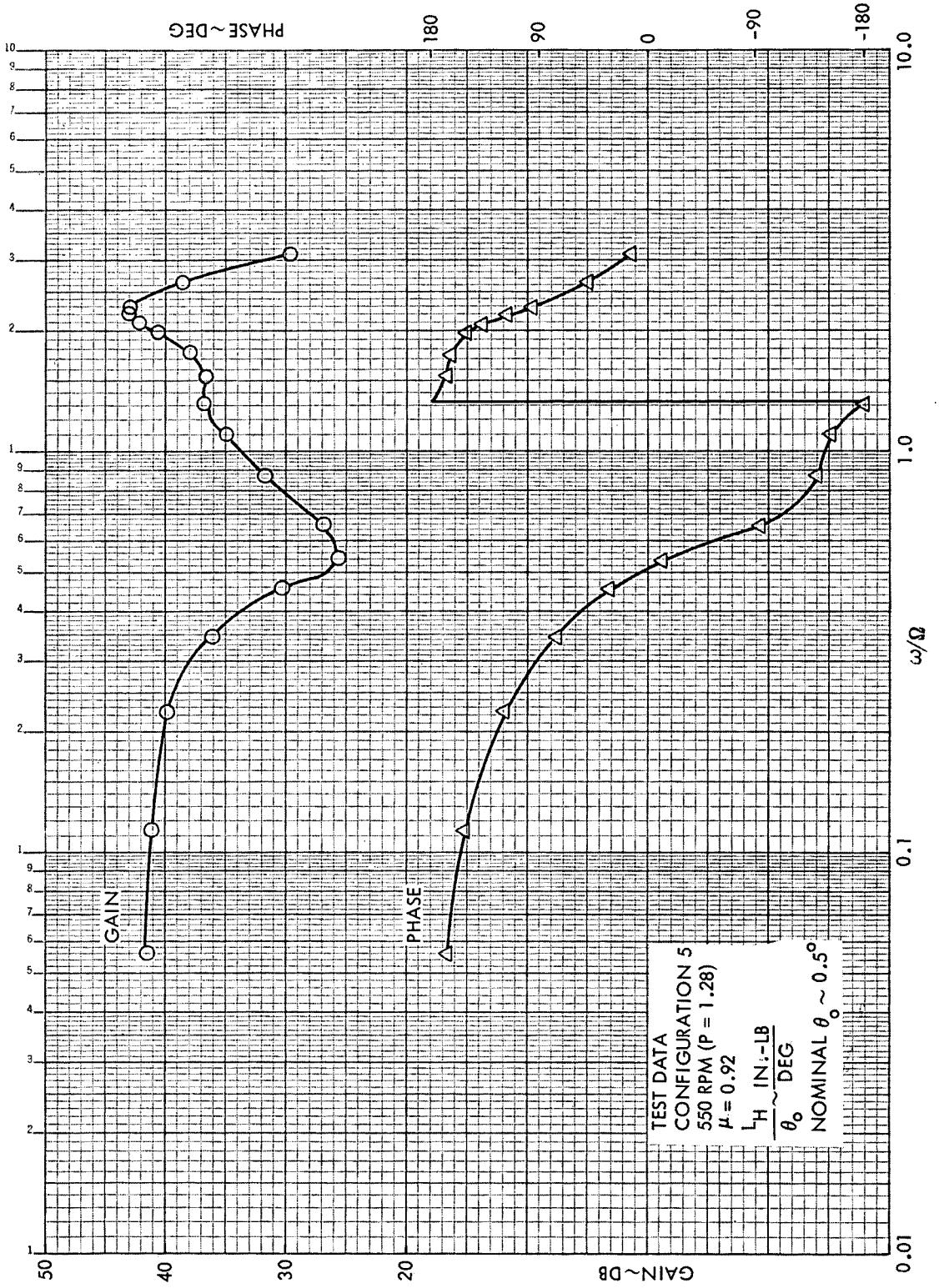

Figure B32. Rotor Hub Roll Moment Frequency Response to Collective Pitch, Configuration 5, μ = 0.92, 550 RPM (P = 1.28)

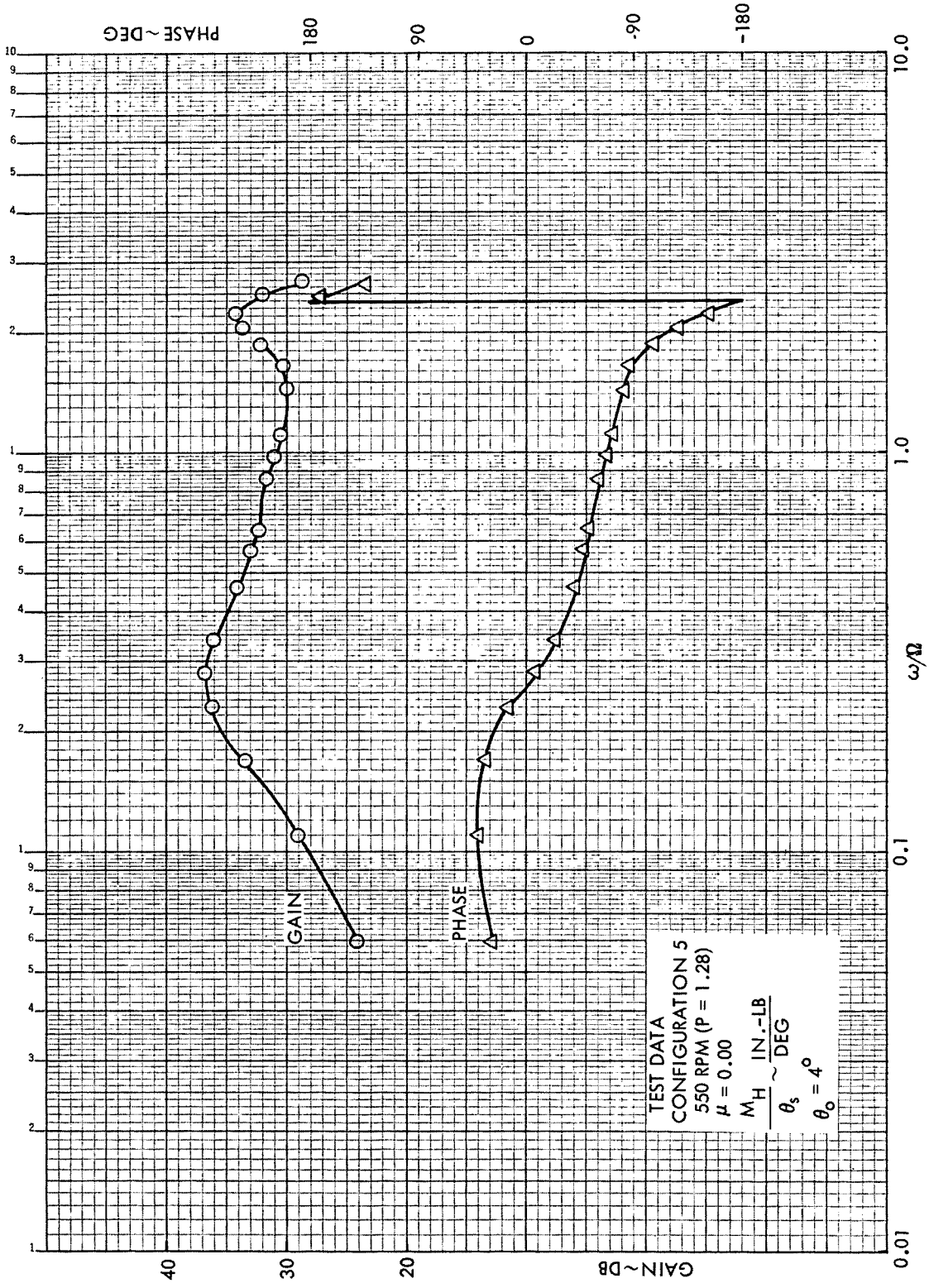

Figure B33. Rotor Hub Pitch Moment Frequency Response to Longitudinal Cyclic Pitch, Configuration 5, μ = 0.0, 550 RPM (P = 1.28)

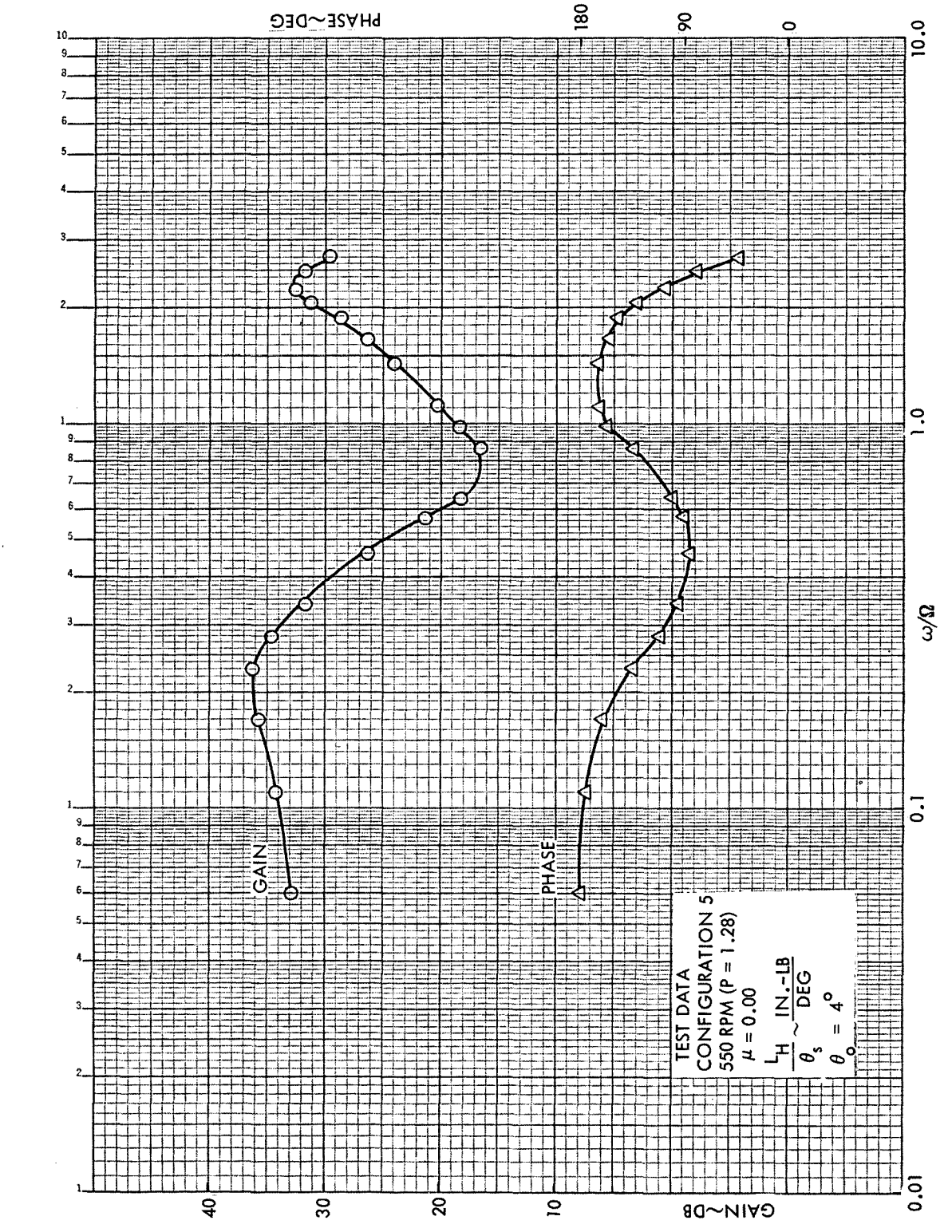

Figure B34. Rotor Hub Roll Moment Frequency Response to Longitudinal Cyclic Pitch, Configuration 5, μ = 0.0, 550 RPM (P = 1.28)

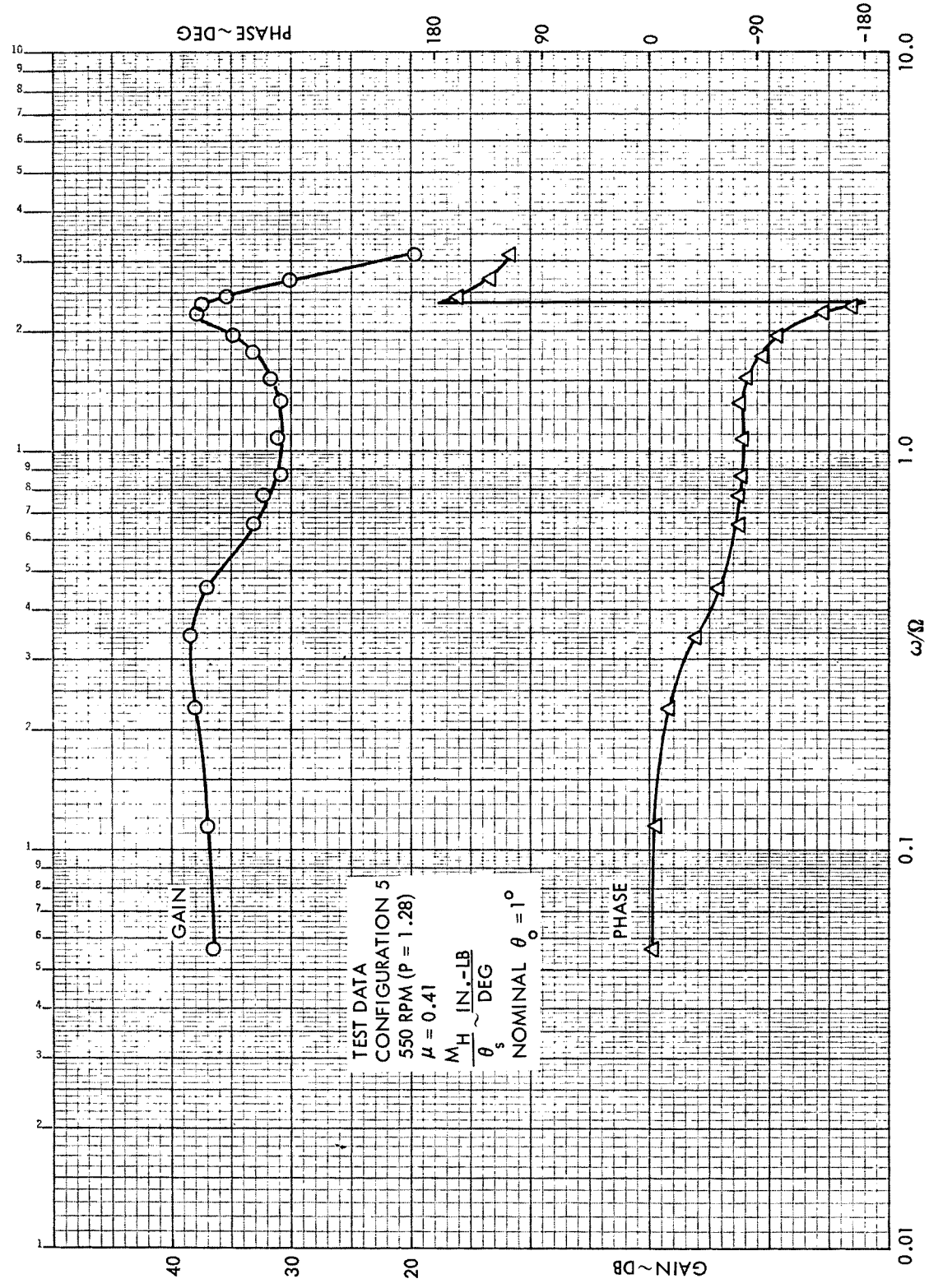

Figure B35. Rotor Hub Pitch Moment Frequency Response to Longitudinal Cyclic Pitch, Configuration 5, μ = 0.41, 550 RPM (P = 1.28)

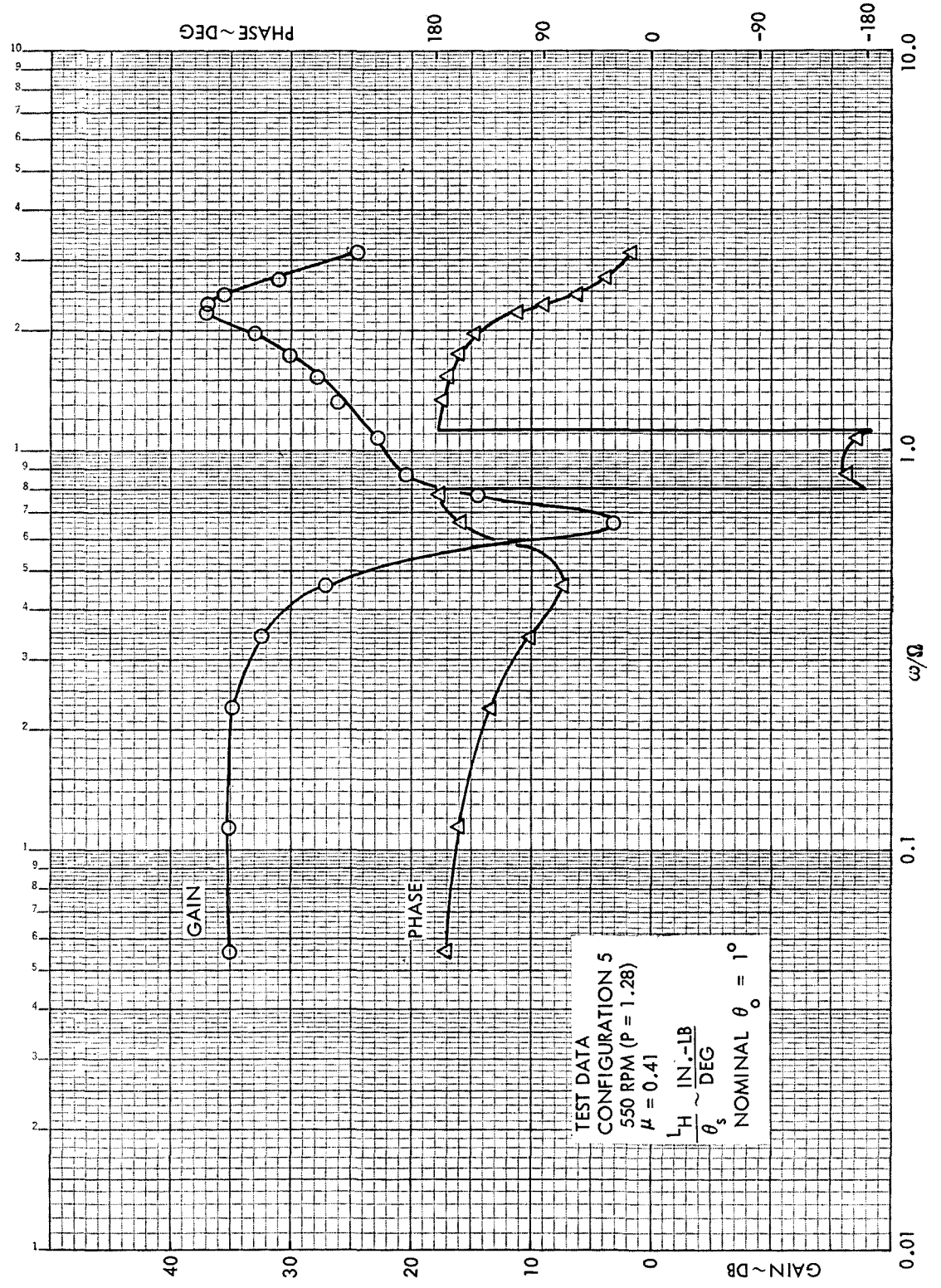

Figure B36. Rotor Hub Roll Moment Frequency Response to Longitudinal Cyclic Pitch, Configuration 5, μ = 0.41, 550 RPM (P = 1.28)

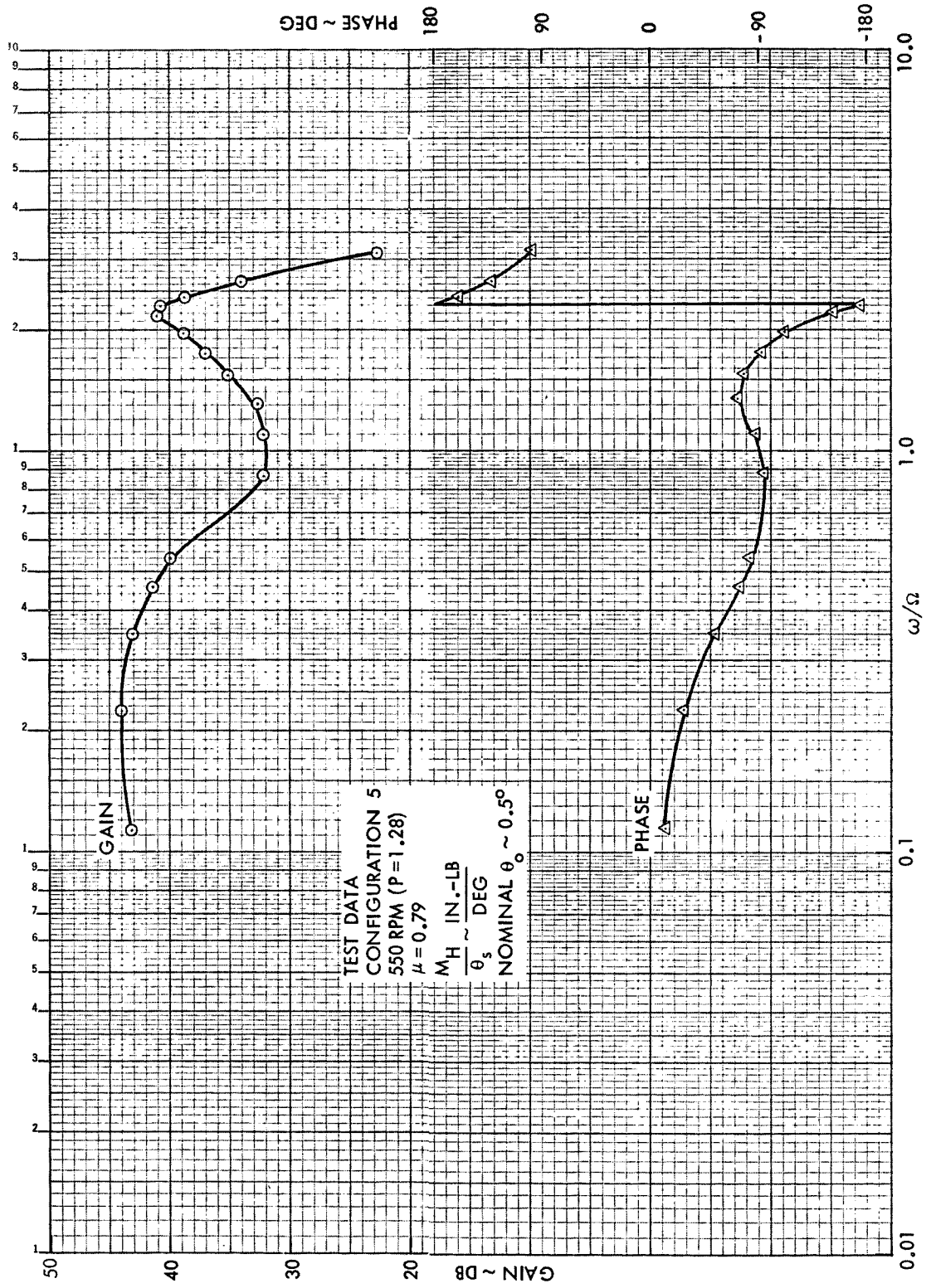

Figure B37. Rotor Hub Pitch Moment Frequency Response to Longitudinal Cyclic Pitch, Configuration 5, μ = 0.79, 550 RPM (P = 1.28)

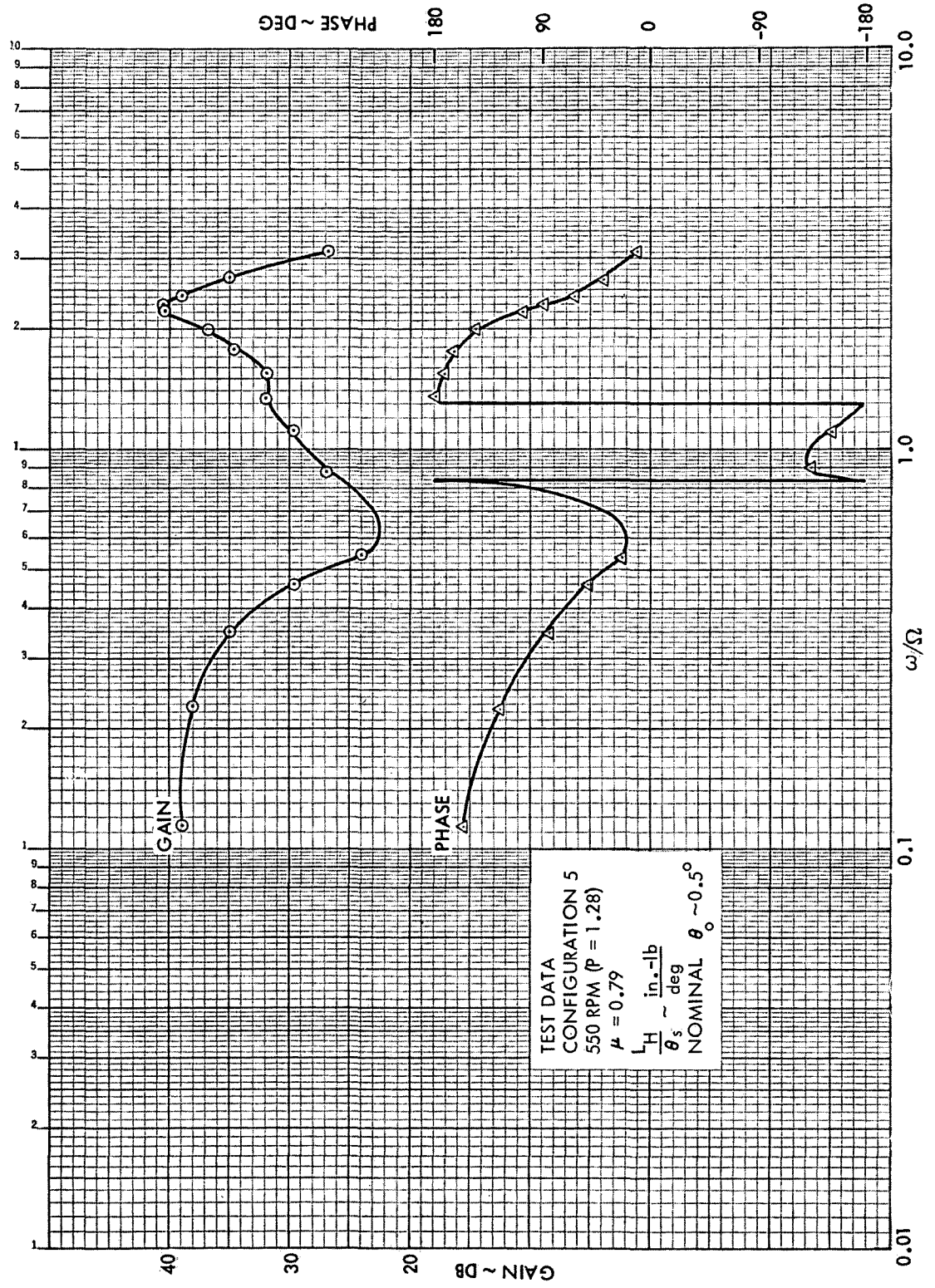

Figure B38. Rotor Hub Roll Moment Frequency Response to Longitudinal Cyclic Pitch, Configuration 5, μ = 0.79, 550 RPM (P = 1.28)

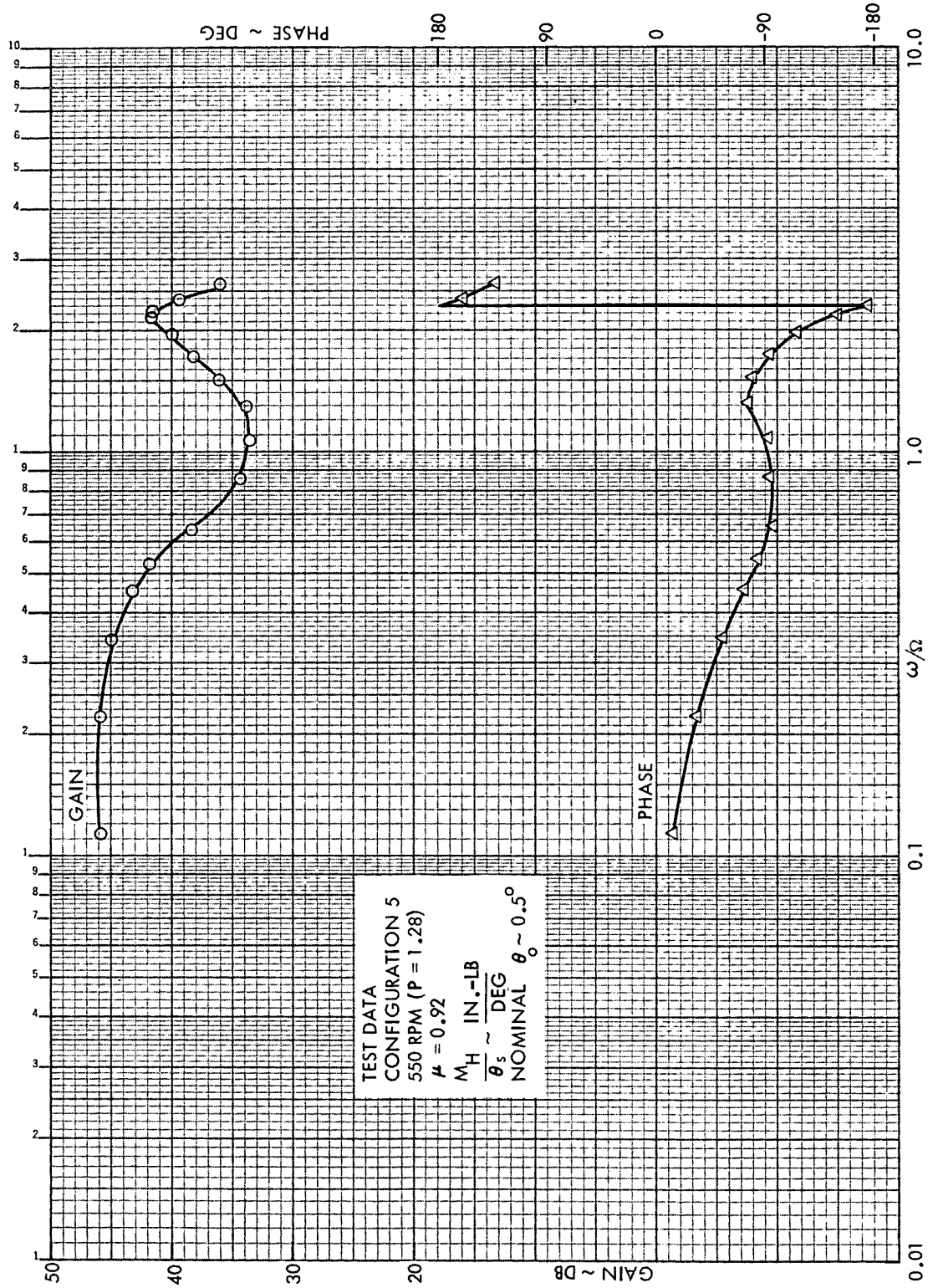

Figure B39. Rotor Hub Pitch Moment Frequency Response to Longitudinal Cyclic Pitch, Configuration 5, μ = 0.92, 550 RPM (P = 1.28)

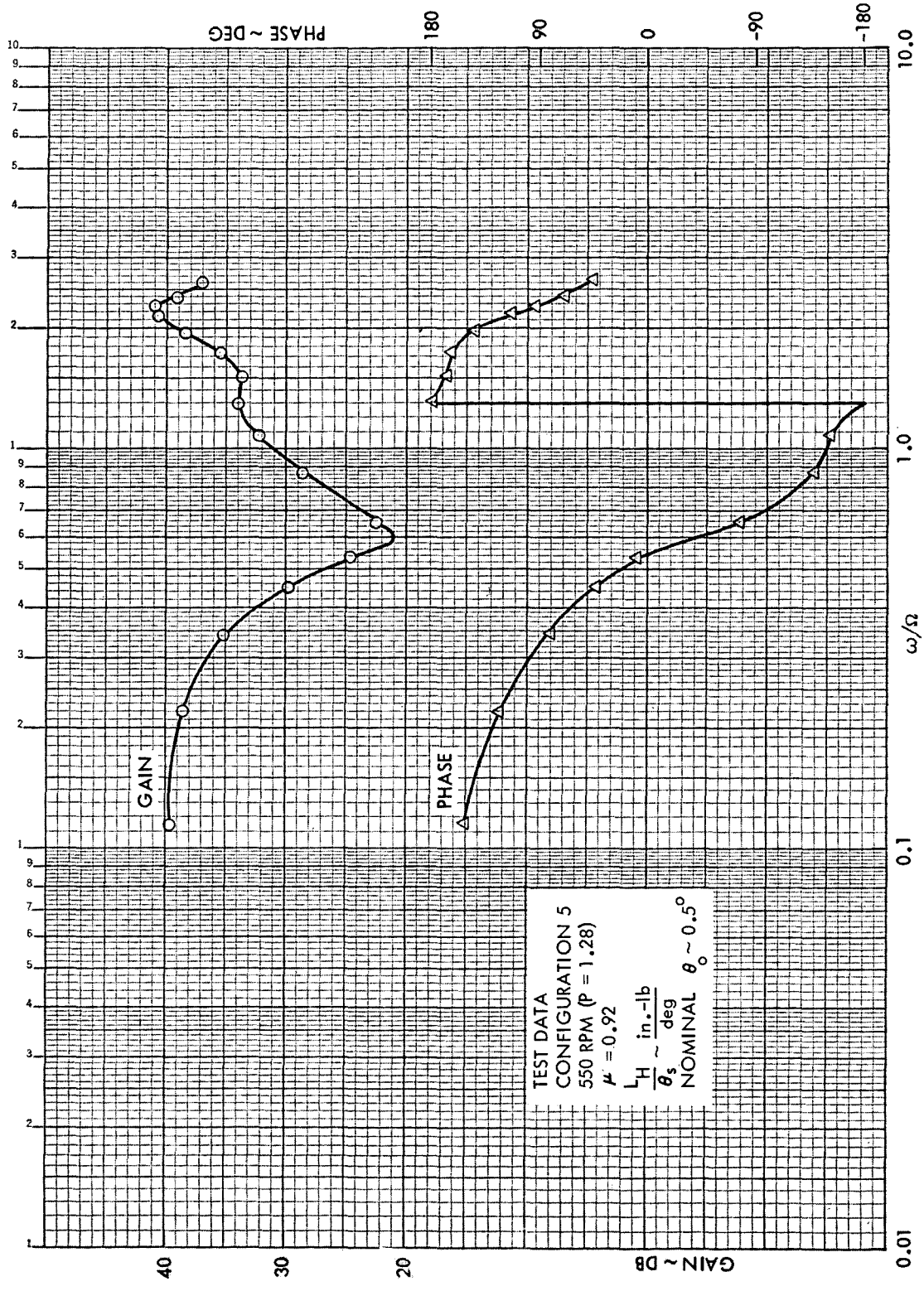

Figure B40. Rotor Hub Roll Moment Frequency Response to Longitudinal Cyclic Pitch, Configuration 5, μ = 0.92, 550 RPM (P = 1.28)

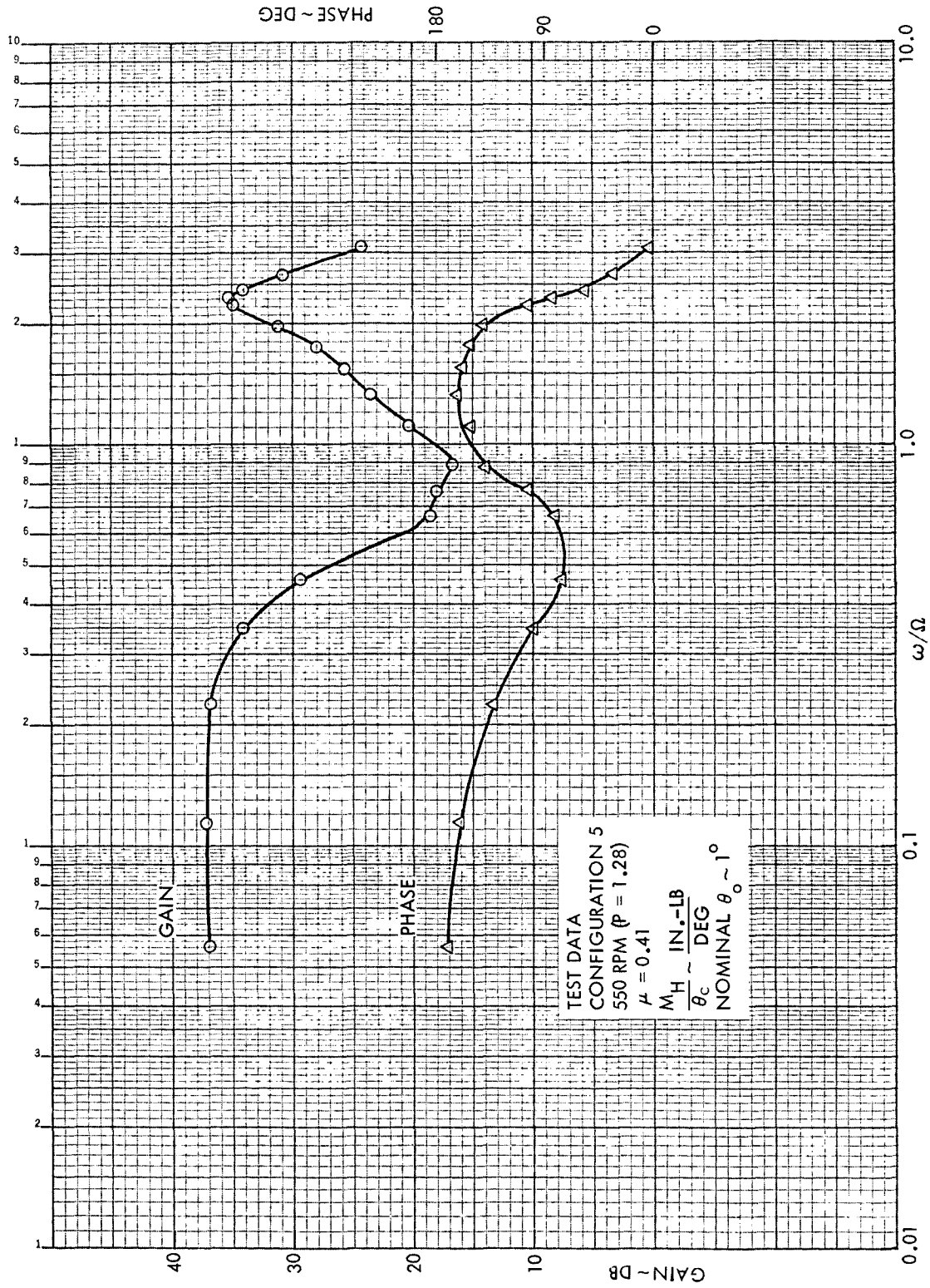

Figure B41. Rotor Hub Pitch Moment Frequency Response to Lateral Cyclic Pitch, Configuration 5, μ = 0.41, 550 RPM (P = 1.28)

LOCKHEED
CALIFORNIA COMPANY

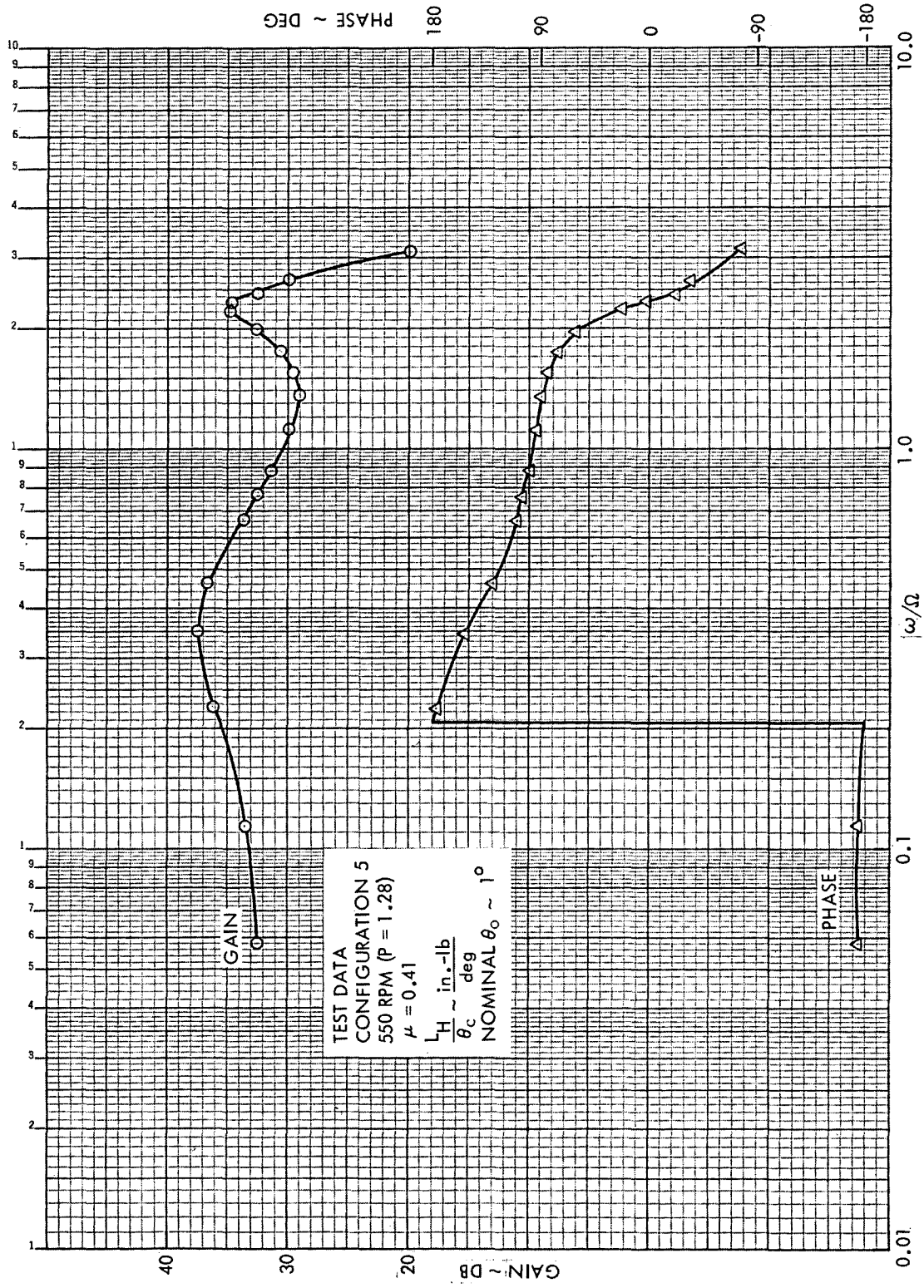

Figure B42. Rotor Hub Roll Moment Frequency Response to Lateral Cyclic Pitch, Configuration 5, μ = 0.41, 550 RPM (P = 1.28)

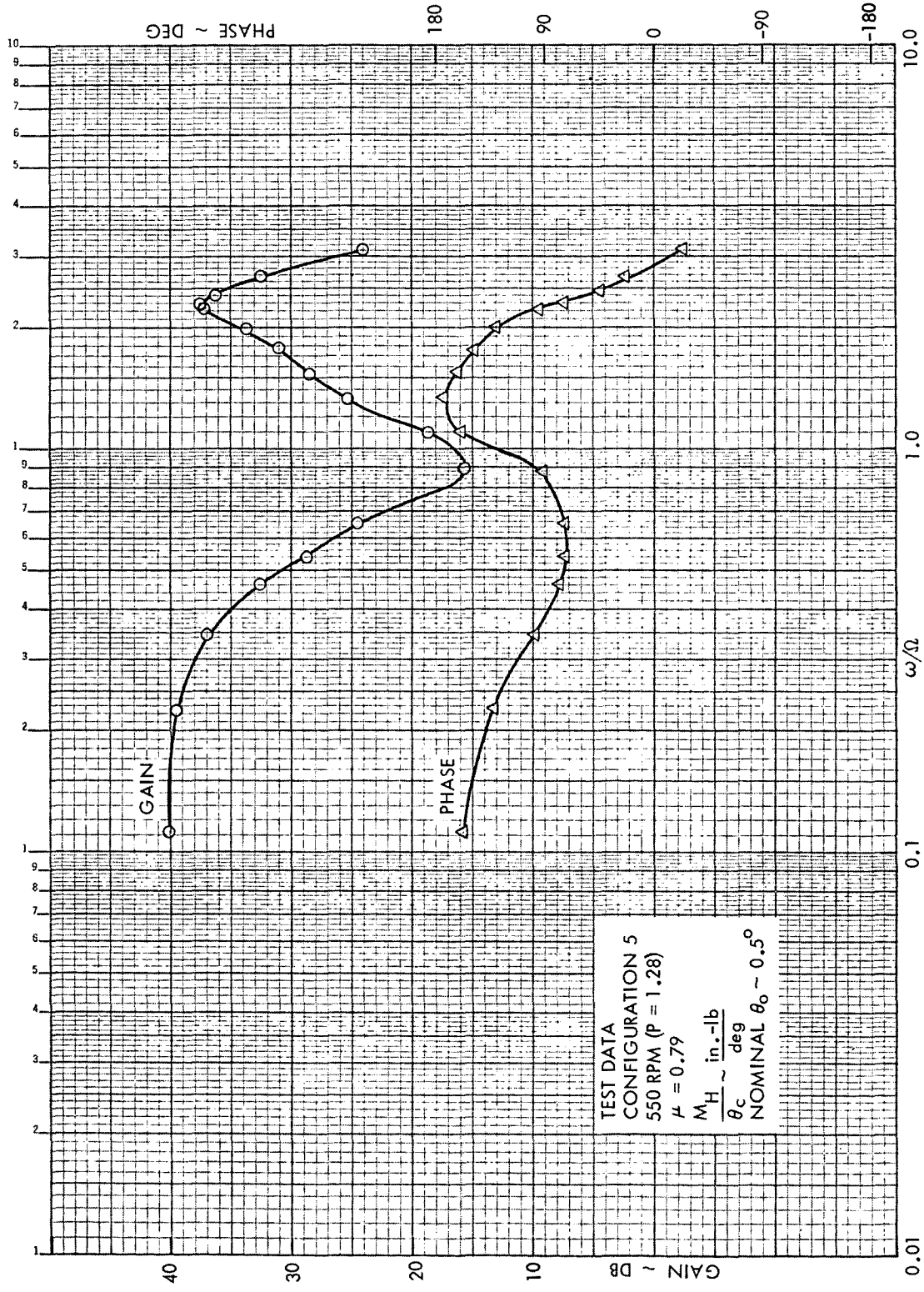

Figure B43. Rotor Hub Pitch Moment Frequency Response to Lateral Cyclic Pitch, Configuration 5, μ = 0.79, 550 RPM (P = 1.28)

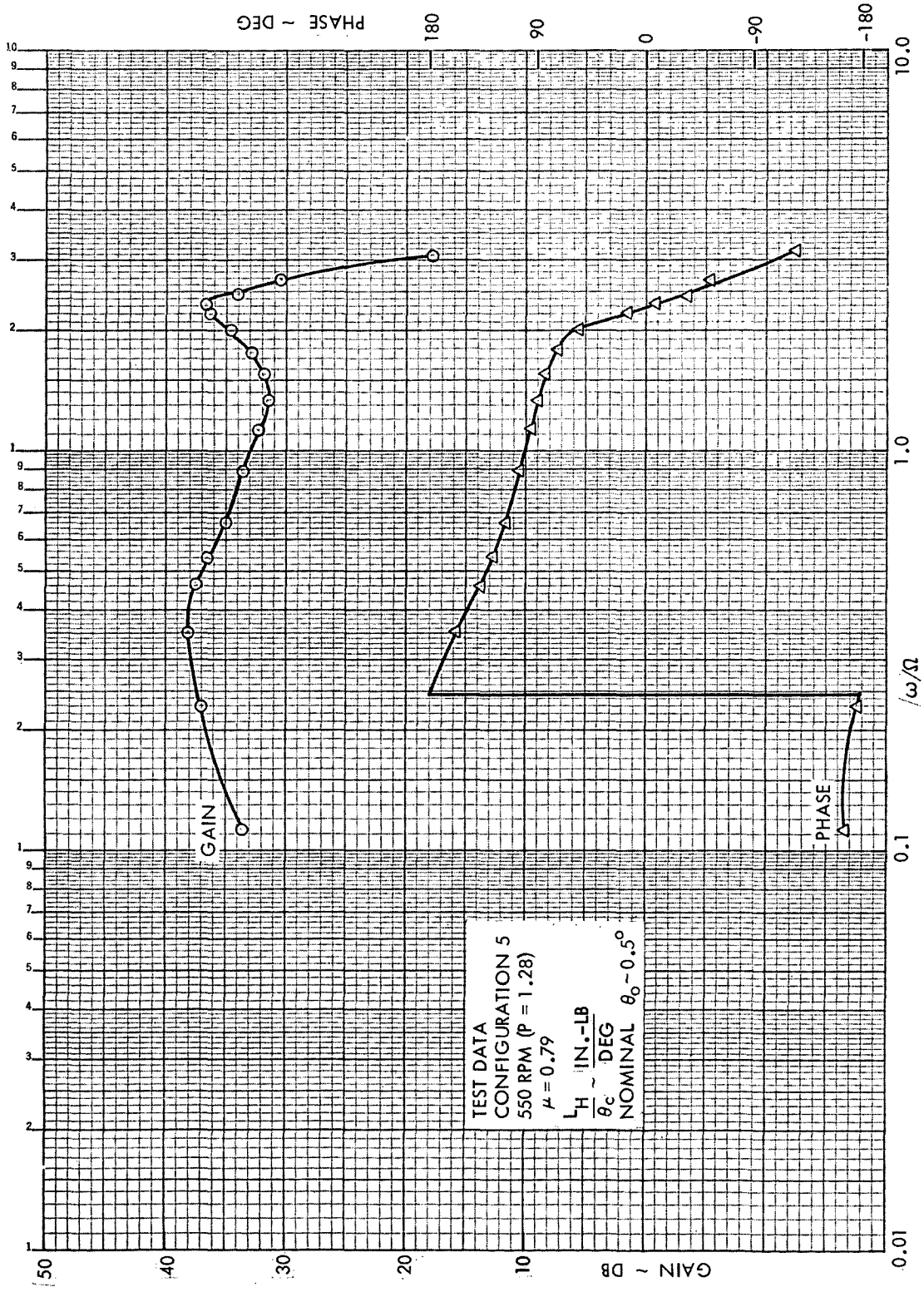

Figure B44. Rotor Hub Roll Moment Frequency Response to Lateral Cyclic Pitch, Configuration 5, μ = 0.79, 550 RPM (P = 1.28)

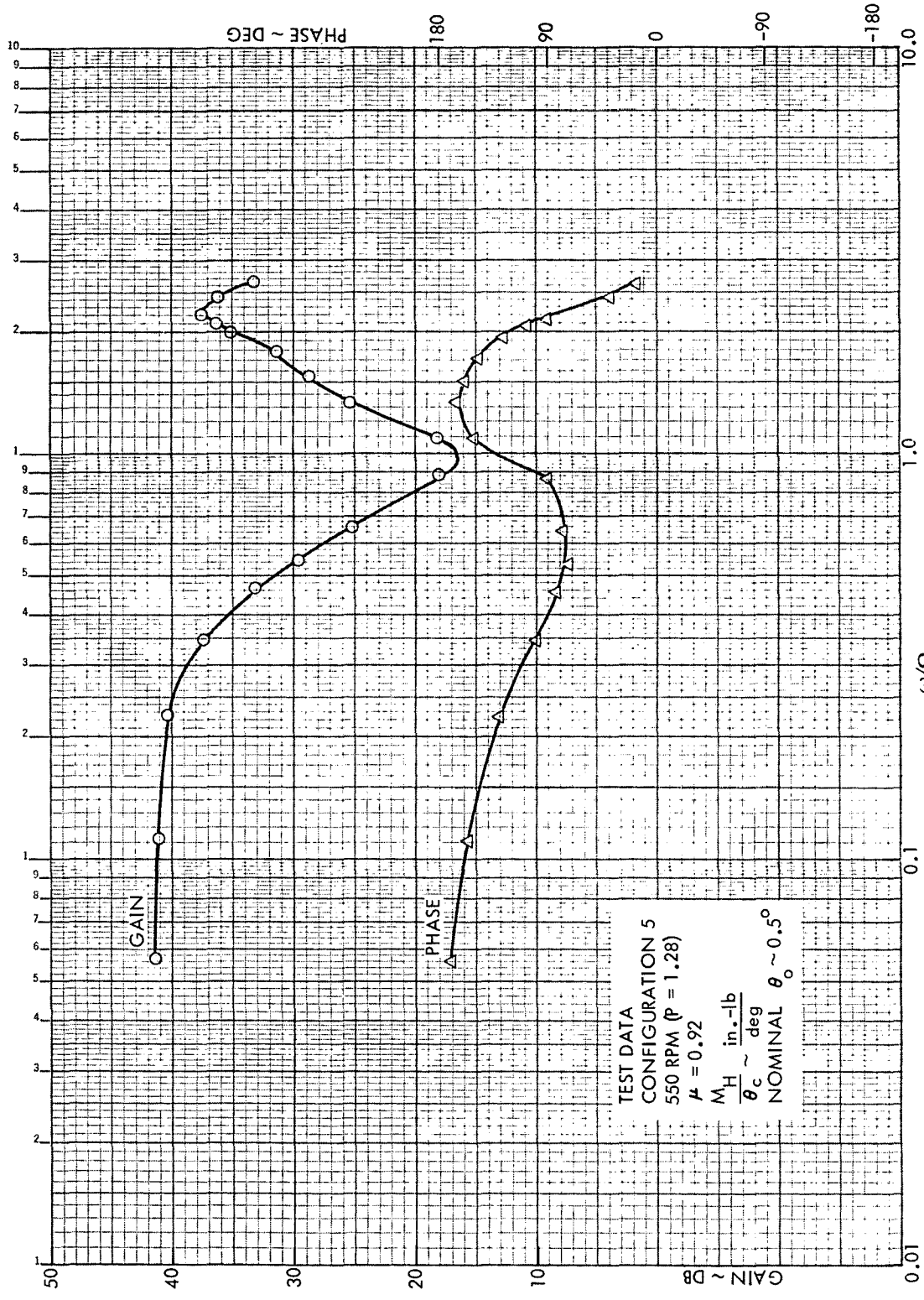

Figure B45. Rotor Hub Pitch Moment Frequency Response to Lateral Cyclic Pitch, Configuration 5, μ = 0.92, 550 RPM (P = 1.28)

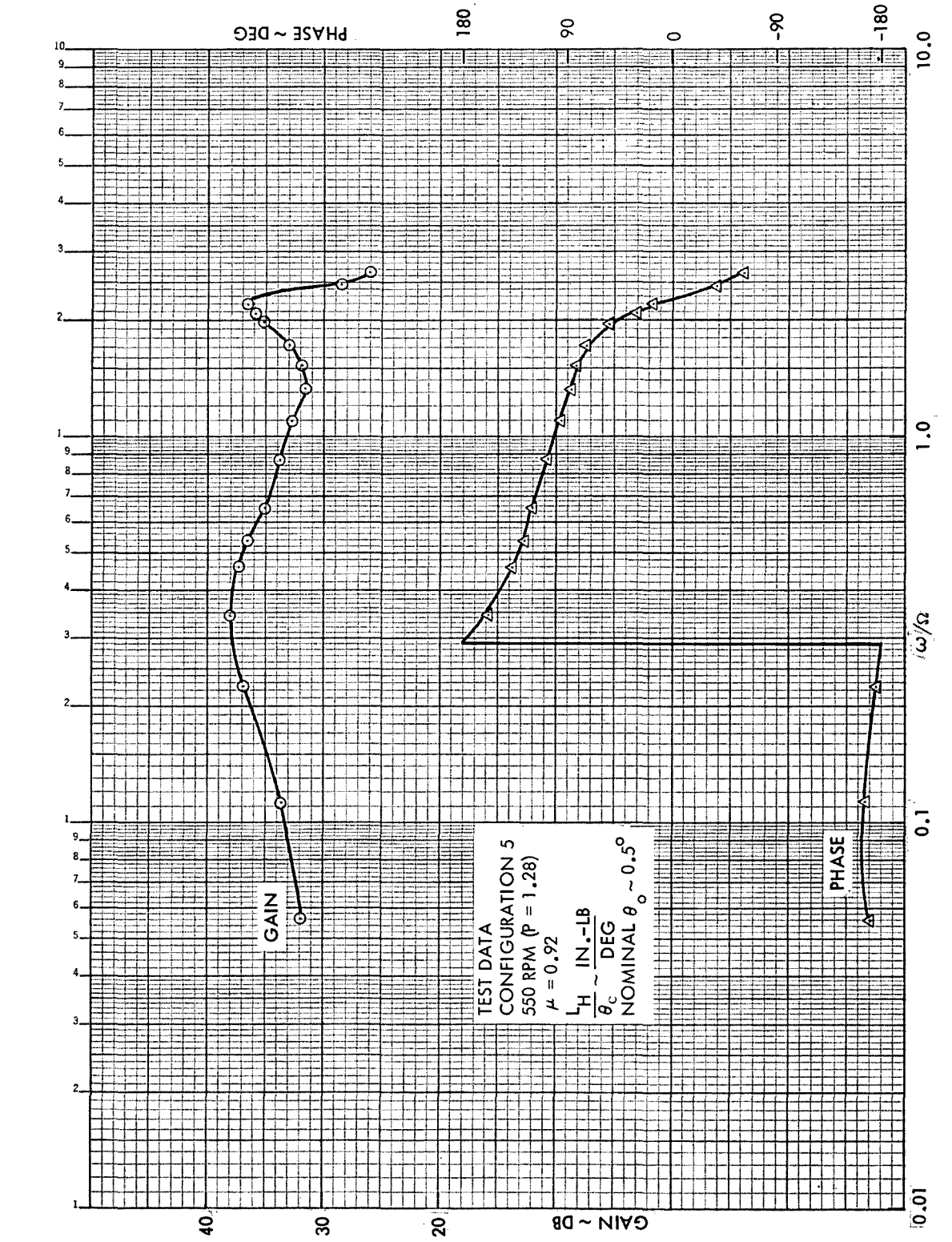

Figure B46. Rotor Hub Roll Moment Frequency Response to Lateral Cyclic Pitch, Configuration 5, μ = 0.92, 550 RPM (P = 1.28)

APPENDIX C

EXPERIMENTAL ROTOR FREQUENCY RESPONSE DATA (ROTOR SHAFT EXCITATIONS)

All of the rotor transfer functions with respect to shaft pitch (α) and roll (ϕ), which were acquired during the Phase 3 test, are contained in this appendix. The hub moment frequency response data, with the dimensions, in.-lb/deg, are plotted in Figures C1 through C54. These derivatives have also been transferred to the center of rotation, converted to coefficient form and tabulated (Tables IX through XII). The amplification factors (k) used to transfer the configuration 5 hub moment derivatives to the shaft centerline are based on the experimental one-per-rev blade bending moment distributions plotted in Appendix A. The amplification factors for configuration 1 are analytically determined as described in Reference 1 (page 84). The values of k used are summarized below:

Configuration	RPM	k
1	800	1.235
	550	1.17
5	850	1.785
	550	1.43

The equations used to nondimensionalize the data are:

$$\frac{c_m}{a\sigma} = \frac{kM_H}{\pi R^3 \rho (\Omega R)^2 a\sigma}$$

$$\frac{c_l}{a\sigma} = \frac{kL_H}{\pi R^3 \rho (\Omega R)^2 a\sigma}$$

where $a = 5.73$ and $\rho = 0.002324$ slugs/ft^3 are assumed.

The tabulated phase lags are expressed in radians in the range $0 \rightarrow -2\pi$. It is noted that the nominal rotor lift is approximately zero for all of the data presented herein.

TABLE IX

ROTOR MOMENT FREQUENCY RESPONSE TO SHAFT PITCH
CONFIGURATION 5

rpm/P	μ	ω (rad/sec)	$\frac{\omega}{\Omega}$	$\frac{c_m}{\alpha a \sigma}$	c_m Phase (rad)	$\frac{c_l}{\alpha a \sigma}$	c_l Phase (rad)
850/1.15	0	3.26	0.037	0.0048	-1.448	0.0064	-5.005
		6.52	0.073	0.0122	-1.474	0.0136	-5.346
		9.70	0.109	0.0226	-1.674	0.0208	-5.761
		13.08	0.147	0.0320	-2.045	0.0239	-6.266
		16.31	0.184	0.0364	-2.294	0.0234	-0.323
		19.87	0.223	0.0387	-2.495	0.0217	-0.605
		23.02	0.258	0.0397	-2.605	0.0199	-0.774
		26.37	0.296	0.0422	-2.679	0.0189	-0.900
		33.03	0.371	0.0485	-2.801	0.0187	-1.128
		*37.61	0.422	0.0571	-2.913	0.0194	-1.336
		*50.29	0.564	0.0626	-3.150	0.0191	-1.670
		*57.01	0.641	0.0675	-3.050	0.0199	-1.674
		*63.21	0.712	0.1068	-3.174	0.0299	-1.877
	0.27	3.31	0.037	0.0078	-0.997	0.0038	-5.395
		6.57	0.074	0.0135	-1.421	0.0070	-5.443
		20.01	0.224	0.0387	-2.133	0.0219	-0.002
		26.39	0.296	0.0502	-2.388	0.0266	-0.367
		31.23	0.350	0.0604	-2.567	0.0297	-0.653
		*38.23	0.429	0.0937	-2.781	0.0402	-1.066
		*57.73	0.647	0.1109	-3.404	0.0369	-2.098
		*63.74	0.715	0.1199	-4.513	0.0385	-3.205
	0.36	3.26	0.037	0.0099	-0.677	0.0032	-4.986
		6.61	0.074	0.0141	-1.204	0.0056	-5.124
		20.07	0.225	0.0397	-2.000	0.0216	-6.153
		26.53	0.298	0.0526	-2.293	0.0266	-0.312
		31.24	0.351	0.0638	-2.495	0.0308	-0.598
		*37.96	0.427	0.0979	-2.727	0.0424	-1.024
		*57.68	0.648	0.1147	-3.382	0.0411	-2.077
		*63.44	0.713	0.1256	-4.441	0.0428	-3.141

*These data may be affected by support vibrations.

TABLE IX

ROTOR MOMENT FREQUENCY RESPONSE TO SHAFT PITCH,
CONFIGURATION 5 (Continued)

rpm/P	μ	ω (rad/sec)	$\frac{\omega}{\Omega}$	$\frac{c_m}{\alpha a \sigma}$	c_m Phase (rad)	$\frac{c_l}{\alpha a \sigma}$	c_l Phase (rad)
850/1.15	0.51	3.26	0.037	0.0206	-0.382	0.0049	-4.157
		6.55	0.074	0.0235	-0.752	0.0084	-4.740
		12.98	0.146	0.0339	-1.310	0.0161	-5.425
		19.82	0.223	0.0476	-1.793	0.0236	-6.027
		26.80	0.301	0.0617	-2.184	0.0296	-0.267
		31.26	0.351	0.0729	-2.397	0.0330	-0.565
		*38.12	0.429	0.1094	-2.661	0.0449	-1.005
		*58.35	0.657	0.1372	-3.487	0.0483	-2.195
		*64.23	0.722	0.1227	-4.041	0.0441	-2.806
	0.60	3.26	0.037	0.0306	-0.323	0.0072	-3.922
		6.58	0.074	0.0340	-0.673	0.0103	-4.540
		12.81	0.144	0.0420	-1.229	0.0157	-5.212
		20.20	0.228	0.0566	-1.737	0.0239	-5.998
		26.64	0.300	0.0691	-2.107	0.0291	-0.230
		33.07	0.373	0.0876	-2.386	0.0348	-0.653
		*37.74	0.425	0.1167	-2.602	0.0452	-0.993
		*58.17	0.654	0.1359	-3.676	0.0459	-2.438
		*64.04	0.721	0.1335	-3.876	0.0438	-2.701
550/1.28	0	3.28	0.057	0.0058	-1.191	0.0125	-4.898
		6.54	0.113	0.0182	-1.080	0.0282	-5.119
		9.73	0.169	0.0407	-1.256	0.0489	-5.483
		12.97	0.225	0.0748	-1.688	0.0732	-6.043
		16.31	0.284	0.0873	-2.153	0.0722	-0.288
		19.80	0.344	0.0896	-2.453	0.0624	-0.546
		23.02	0.401	0.0902	-2.604	0.0558	-0.857
		26.46	0.461	0.0915	-2.701	0.0510	-1.015
		*33.00	0.574	0.1010	-2.823	0.0482	-1.236
		*37.52	0.653	0.1185	-2.922	0.0512	-1.438
		*44.02	0.766	0.0908	-3.197	0.0385	-1.749
		*50.30	0.875	0.1043	-3.178	0.0436	-1.823
		*57.27	0.996	0.1346	-3.049	0.0511	-1.899
		*63.00	1.099	0.2000	-3.178	0.0743	-2.062

*These data may be affected by support vibrations.

TABLE X

ROTOR MOMENT FREQUENCY RESPONSE TO SHAFT ROLL,
CONFIGURATION 5

rpm/P	μ	ω (rad/sec)	$\frac{\omega}{\Omega}$	$\frac{c_m}{\phi a \sigma}$	c_m Phase (rad)	$\frac{c_l}{\phi a \sigma}$	c_l Phase (rad)
850/1.15	0	3.26	0.037	0.0056	-1.844	0.0044	-1.426
		6.54	0.074	0.0122	-2.154	0.0110	-1.445
		9.74	0.110	0.0184	-2.554	0.0202	-1.638
		12.87	0.145	0.0219	-2.989	0.0289	-1.933
		16.31	0.184	0.0214	-3.402	0.0337	-2.245
		19.93	0.225	0.0191	-3.648	0.0349	-2.429
		26.52	0.299	0.0162	-3.974	0.0363	-2.631
		32.97	0.371	0.0152	-4.173	0.0385	-2.726
		37.48	0.421	0.0154	-4.292	0.0423	-2.814
		*50.31	0.566	0.0108	-4.378	0.0366	-2.806
		*57.41	0.646	0.0112	-4.454	0.0390	-2.815
		63.00	0.709	0.0134	-4.516	0.0416	-2.832
	0.27	3.26	0.037	0.0038	-1.722	0.0036	-1.599
		6.63	0.074	0.0067	-1.953	0.0074	-1.572
		13.02	0.146	0.0125	-2.462	0.0174	-1.695
		26.73	0.299	0.0164	-3.420	0.0382	-2.218
		37.83	0.423	0.0160	-3.979	0.0475	-2.564
		*50.64	0.569	0.0099	-4.205	0.0447	-2.746
		63.54	0.713	0.0161	-4.247	0.0487	-2.876
		77.06	0.864	0.0258	-4.730	0.0559	-2.984
		89.02	0.997	0.0184	-5.848	0.0594	-2.854
		20.17	0.227	0.0158	-3.003	0.0293	-1.963
		31.25	0.351	0.0159	-3.700	0.0429	-2.382
		*44.07	0.496	0.0134	-4.380	0.0436	-2.763
		*57.60	0.650	0.0117	-4.229	0.0489	-2.826
	0.36	3.26	0.037	0.0034	-1.652	0.0034	-1.641
		6.56	0.074	0.0064	-1.932	0.0067	-1.603
		13.04	0.147	0.0115	-2.365	0.0158	-1.729
		20.25	0.228	0.0157	-2.929	0.0277	-1.945
		26.64	0.300	0.0165	-3.313	0.0361	-2.175
		31.26	0.352	0.0146	-3.550	0.0396	-2.319
		38.02	0.427	0.0140	-3.946	0.0452	-2.525
		*44.17	0.496	0.0125	-4.274	0.0409	-2.695
		*50.82	0.570	0.0103	-4.172	0.0441	-2.696
		*57.76	0.648	0.0097	-4.160	0.0468	-2.768
		63.76	0.715	0.0160	-4.273	0.0504	-2.829
		77.40	0.868	0.0238	-4.792	0.0549	-2.958

*These data may be affected by support vibrations.

TABLE X

ROTOR MOMENT FREQUENCY RESPONSE TO SHAFT ROLL,
CONFIGURATION 5 (Continued)

rpm/P	μ	ω (rad/sec)	$\frac{\omega}{\Omega}$	$\frac{c_m}{\phi a \sigma}$	c_m Phase (rad)	$\frac{c_l}{\phi a \sigma}$	c_l Phase (rad)
850/1.15	0.51	3.26	0.037	0.0033	-1.630	0.0031	-1.651
		6.60	0.074	0.0057	-1.873	0.0055	-1.630
		12.93	0.145	0.0113	-2.370	0.0141	-1.702
		20.05	0.224	0.0161	-2.888	0.0263	-1.902
		31.23	0.350	0.0155	-3.585	0.0379	-2.279
		*44.21	0.495	0.0172	-4.342	0.0445	-2.650
		*50.76	0.567	0.0122	-4.122	0.0467	-2.651
		76.85	0.855	0.0252	-4.807	0.0585	-2.935
		89.02	1.000	0.0259	-5.718	0.0572	-2.728
	0.60	3.26	0.036	0.0034	-1.285	0.0030	-1.865
		6.53	0.073	0.0061	-1.861	0.0065	-1.647
		12.98	0.145	0.0131	-2.385	0.0150	-1.684
		20.08	0.224	0.0176	-2.909	0.0258	-1.896
		26.86	0.300	0.0195	-3.364	0.0348	-2.132
		31.24	0.348	0.0194	-3.678	0.0398	-2.292
		31.26	0.348	0.0194	-3.652	0.0395	-2.285
		38.03	0.427	0.0195	-4.124	0.0459	-2.517
		*44.22	0.496	0.0132	-4.754	0.0404	-2.683
		*50.35	0.564	0.0118	-4.118	0.0452	-2.644
		*57.42	0.643	0.0149	-4.247	0.0495	-2.731
		63.26	0.707	0.0183	-5.199	0.0473	-2.840
		76.76	0.856	0.0110	-5.200	0.0542	-2.843
		88.80	0.990	0.0107	-5.325	0.0642	-2.859
550/1.28	0	3.26	0.056	0.0123	-1.755	0.0056	-1.158
		6.52	0.112	0.0278	-1.971	0.0178	-1.017
		9.70	0.167	0.0506	-2.335	0.0432	-1.191
		13.03	0.224	0.0711	-2.961	0.0779	-1.702
		16.26	0.278	0.0655	-3.490	0.0861	-2.176
		19.83	0.340	0.0550	-3.803	0.0829	-2.452
		26.55	0.453	0.0413	-4.111	0.0777	-2.672
		33.07	0.563	0.0366	-4.285	0.0788	-2.765
		37.73	0.641	0.0365	-4.458	0.0862	-2.865
		*43.92	0.758	0.0253	-4.530	0.0640	-2.869
		*50.23	0.865	0.0261	-4.550	0.0721	-2.832
		*57.22	0.984	0.0262	-4.621	0.0761	-2.836
		62.96	1.081	0.0284	-4.609	0.0801	-2.831

*These data may be affected by support vibrations.

TABLE XI

ROTOR MOMENT FREQUENCY RESPONSE TO SHAFT PITCH,
CONFIGURATION 1

rpm/P	μ	ω (rad/sec)	$\frac{\omega}{\Omega}$	$\frac{c_m}{\alpha a \sigma}$	c_m Phase (rad)	$\frac{c_l}{\alpha a \sigma}$	c_l Phase (rad)
800/1.33	0.28	3.27	0.039	0.0087	-0.777	0.0058	-4.320
		6.54	0.078	0.0140	-1.127	0.0119	-4.967
		13.05	0.155	0.0299	-1.409	0.0260	-5.254
		19.92	0.236	0.0557	-1.684	0.0454	-5.651
		26.50	0.314	0.0896	-2.008	0.0669	-6.117
		31.23	0.371	0.1196	-2.279	0.0830	-0.206
		*37.92	0.450	0.1871	-2.740	0.1134	-0.800
		*50.48	0.599	0.1684	-3.443	0.0904	-1.737
		*63.49	0.752	0.2140	-3.922	0.0948	-2.355
	0.38	3.26	0.039	0.0129	-0.517	0.0069	-4.278
		6.60	0.078	0.0176	-0.846	0.0125	-4.660
		13.07	0.155	0.0329	-1.229	0.0262	-5.108
		19.95	0.237	0.0601	-1.554	0.0458	-5.562
		26.55	0.316	0.0959	-1.928	0.0675	-6.055
		31.23	0.373	0.1271	-2.208	0.0835	-0.140
		*38.25	0.458	0.1435	-2.747	0.0856	-0.768
		*50.51	0.604	0.1526	-3.505	0.0802	-1.757
	0.54	3.26	0.039	0.0278	-0.312	0.0149	-3.742
		6.61	0.079	0.0312	-0.558	0.0185	-4.182
		13.04	0.155	0.0472	-0.979	0.0320	-4.809
		20.01	0.239	0.0770	-1.383	0.0522	-5.373
		26.60	0.317	0.1141	-1.809	0.0726	-5.926
		31.26	0.373	0.1461	-2.120	0.0878	-0.044
		*38.10	0.454	0.1650	-2.654	0.0907	-0.687
		*50.42	0.601	0.1557	-3.449	0.0788	-1.711
		*57.59	0.687	0.2083	-4.009	0.0952	-2.391
	0.64	3.26	0.039	0.0398	-0.221	0.0210	-3.590
		6.56	0.078	0.0444	-0.438	0.0249	-3.978
		13.09	0.156	0.0619	-0.852	0.0377	-4.638
		20.05	0.239	0.0943	-1.310	0.0576	-5.280
		26.31	0.314	0.1291	-1.749	0.0760	-5.849
		31.29	0.373	0.1635	-2.092	0.0918	-0.004
		*37.86	0.451	0.1750	-2.578	0.0918	-0.590
		*50.37	0.601	0.1631	-3.281	0.0807	-1.536
		*57.73	0.689	0.2329	-3.285	0.1043	-1.660
		*64.66	0.771	0.2814	-4.111	0.1253	-2.564

*These data may be affected by support vibrations.

TABLE XI

ROTOR MOMENT FREQUENCY RESPONSE TO SHAFT PITCH,
CONFIGURATION 1 (Continued)

rpm/P	μ	ω (rad/sec)	$\frac{\omega}{\Omega}$	$\frac{c_m}{\alpha a \sigma}$	c_m Phase (rad)	$\frac{c_l}{\alpha a \sigma}$	c_l Phase (rad)
550/1.56	0.41	3.26	0.056	0.0146	-0.482	0.0130	-4.122
		6.57	0.113	0.0213	-0.768	0.0230	-4.502
		13.05	0.224	0.0454	-1.002	0.0507	-4.887
		20.01	0.344	0.0982	-1.211	0.0991	-5.274
		26.76	0.459	0.2017	-1.593	0.1798	-5.812
		31.26	0.535	0.2950	-1.984	0.2438	-0.001
		38.00	0.649	0.4241	-2.583	0.3107	-0.744
	0.56	3.27	0.056	0.0258	-0.292	0.0232	-3.720
		6.57	0.113	0.0320	-0.531	0.0312	-4.137
		13.08	0.226	0.0575	-0.835	0.0582	-4.678
		20.11	0.347	0.1169	-1.126	0.1108	-5.164
		26.67	0.460	0.2226	-1.542	0.1896	-5.738
		31.23	0.539	0.3165	-1.958	0.2503	-6.251
		37.84	0.654	0.4455	-2.548	0.3167	-0.686
		58.13	1.011	0.4227	-3.372	0.2491	-1.861
	0.78	3.26	0.056	0.0511	-0.201	0.0445	-3.513
		6.60	0.114	0.0593	-0.359	0.0524	-3.830
		13.05	0.226	0.0889	-0.654	0.0782	-4.393
		19.96	0.345	0.1602	-0.999	0.1332	-4.964
		26.55	0.459	0.2798	-1.499	0.2141	-5.653
		31.26	0.540	0.3752	-1.952	0.2684	-6.215
		38.08	0.657	0.4970	-2.569	0.3217	-0.688
		57.90	0.998	0.4644	-3.393	0.2631	-1.836
	0.93	3.27	0.056	0.0742	-0.164	0.0594	-3.471
		6.60	0.114	0.0835	-0.293	0.0668	-3.733
		12.93	0.224	0.1132	-0.551	0.0896	-4.246
		20.08	0.347	0.1991	-0.949	0.1494	-4.900
		26.60	0.460	0.3234	-1.486	0.2267	-5.630
		31.24	0.540	0.4125	-1.949	0.2732	-6.204
		37.92	0.656	0.5500	-2.555	0.3409	-0.655

TABLE XII

ROTOR MOMENT FREQUENCY RESPONSE TO SHAFT ROLL,
CONFIGURATION 1

rpm/P	μ	ω (rad/sec)	$\frac{\omega}{\Omega}$	$\frac{c_m}{\phi a \sigma}$	c_m Phase (rad)	$\frac{c_l}{\phi a \sigma}$	c_l Phase (rad)
800/1.33	0	3.27	0.039	0.0079	-1.675	0.0033	-1.236
		6.50	0.078	0.0159	-1.776	0.0082	-1.043
		12.88	0.154	0.0397	-2.081	0.0299	-1.023
		19.72	0.235	0.0723	-2.762	0.0767	-1.550
		22.99	0.274	0.0784	-3.163	0.0931	-1.894
		26.31	0.313	0.0733	-3.481	0.0978	-2.184
		30.05	0.358	0.0658	-3.755	0.0974	-2.407
		33.10	0.394	0.0591	-3.934	0.0958	-2.539
		37.49	0.447	0.0542	-4.125	0.0969	-2.709
		49.88	0.596	0.0397	-4.200	0.0809	-2.745
		57.02	0.681	0.0357	-4.334	0.0827	-2.790
		63.20	0.755	0.0349	-4.384	0.0852	-2.809
	0.28	3.26	0.039	0.0058	-1.680	0.0038	-1.534
		6.80	0.081	0.0122	-1.802	0.0079	-1.365
		12.98	0.155	0.0256	-2.132	0.0200	-1.325
		26.61	0.319	0.0549	-2.993	0.0699	-1.759
		38.09	0.457	0.0548	-3.841	0.1010	-2.379
		50.78	0.609	0.0485	-3.944	0.0982	-2.589
		63.49	0.758	0.0407	-4.548	0.0962	-2.849
		77.28	0.924	0.0315	-4.723	0.1010	-2.880
		89.00	1.063	0.0305	-4.830	0.1124	-2.891
	0.64	6.54	0.078	0.0131	-1.806	0.0063	-1.415
		13.18	0.157	0.0281	-2.151	0.0181	-1.278
		26.70	0.319	0.0566	-3.059	0.0631	-1.731
		37.19	0.444	0.0552	-3.852	0.0883	-2.282
		50.79	0.605	0.0487	-3.887	0.0904	-2.468
		63.78	0.761	0.0401	-4.574	0.0904	-2.720
		76.59	0.914	0.0367	-4.799	0.1011	-2.779
		88.84	1.059	0.0346	-4.970	0.1164	-2.814
550/1.56	0	3.26	0.057	0.0119	-1.615	0.0035	-1.038
		12.92	0.224	0.0635	-1.866	0.0401	-0.699
		16.30	0.283	0.0953	-2.035	0.0711	-0.803
		19.83	0.344	0.1380	-2.305	0.1211	-1.024
		22.94	0.398	0.1820	-2.638	0.1781	-1.316
		26.27	0.456	0.2093	-3.099	0.2286	-1.737
		32.93	0.572	0.1761	-3.743	0.2288	-2.331

TABLE XII

ROTOR MOMENT FREQUENCY RESPONSE TO SHAFT ROLL,
CONFIGURATION 1 (Continued)

rpm/P	μ	ω (rad/sec)	$\frac{\omega}{\Omega}$	$\frac{c_m}{\phi a \sigma}$	c_m Phase (rad)	$\frac{c_l}{\phi a \sigma}$	c_l Phase (rad)
550/1.56	0	37.67	0.654	0.1509	-4.077	0.2204	-2.620
		50.07	0.869	0.1064	-4.223	0.1728	-2.709
		57.18	0.991	0.0943	-4.364	0.1691	-2.771
		63.25	1.096	0.0832	-4.408	0.1661	-2.775
	0.41	3.26	0.056	0.0108	-1.653	0.0042	-1.462
		6.66	0.115	0.0225	-1.760	0.0103	-1.199
		13.29	0.228	0.0499	-1.993	0.0319	-1.029
		20.54	0.352	0.0921	-2.365	0.0820	-1.159
		27.25	0.467	0.1322	-2.923	0.1541	-1.586
		31.27	0.535	0.1341	-3.298	0.1828	-1.919
		50.80	0.866	0.1198	-3.692	0.1894	-2.459
		64.40	1.115	0.1004	-4.535	0.1815	-2.834
		76.94	1.331	0.0991	-4.782	0.1850	-2.905
		89.15	1.546	0.1000	-4.947	0.1939	-2.891
	0.56	3.26	0.057	0.0109	-1.663	0.0038	-1.476
		6.61	0.115	0.0232	-1.775	0.0094	-1.145
		13.18	0.228	0.0512	-2.014	0.0303	-0.977
		20.16	0.349	0.0927	-2.405	0.0791	-1.133
		26.86	0.465	0.1297	-2.967	0.1457	-1.573
		31.27	0.543	0.1305	-3.369	0.1738	-1.921
		50.74	0.880	0.1176	-3.679	0.1845	-2.406
		64.09	1.111	0.1053	-4.549	0.1839	-2.790
		77.21	1.337	0.1032	-4.814	0.1902	-2.881
		89.10	1.541	0.1010	-4.977	0.2006	-2.875
	0.93	3.26	0.057	0.0112	-1.476	0.0041	-2.143
		6.57	0.114	0.0245	-1.704	0.0067	-1.283
		13.12	0.228	0.0555	-2.006	0.0259	-0.888
		20.03	0.348	0.0996	-2.492	0.0767	-1.095
		26.70	0.463	0.1286	-3.098	0.1358	-1.594
		31.25	0.541	0.1254	-3.485	0.1571	-1.923
		50.68	0.878	0.0964	-3.736	0.1660	-2.358
		64.17	1.112	0.1053	-4.553	0.1750	-2.685
		77.06	1.334	0.1099	-4.899	0.1841	-2.782
		89.07	1.542	0.1090	-5.111	0.2073	-2.739

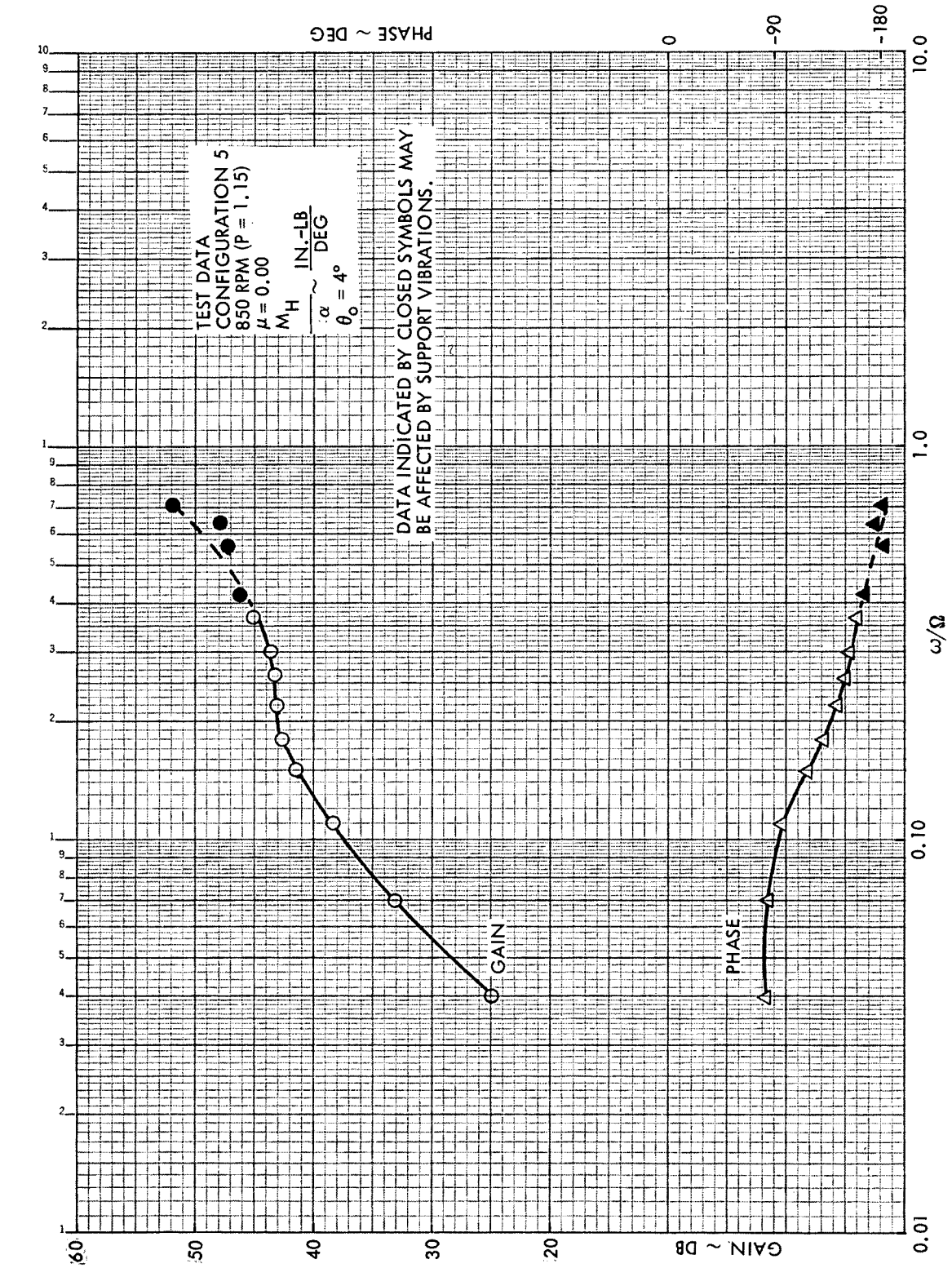

Figure C1. Rotor Hub Pitch Moment Frequency Response to Shaft Pitch, Configuration 5, μ = 0.0, 850 RPM (P = 1.15)

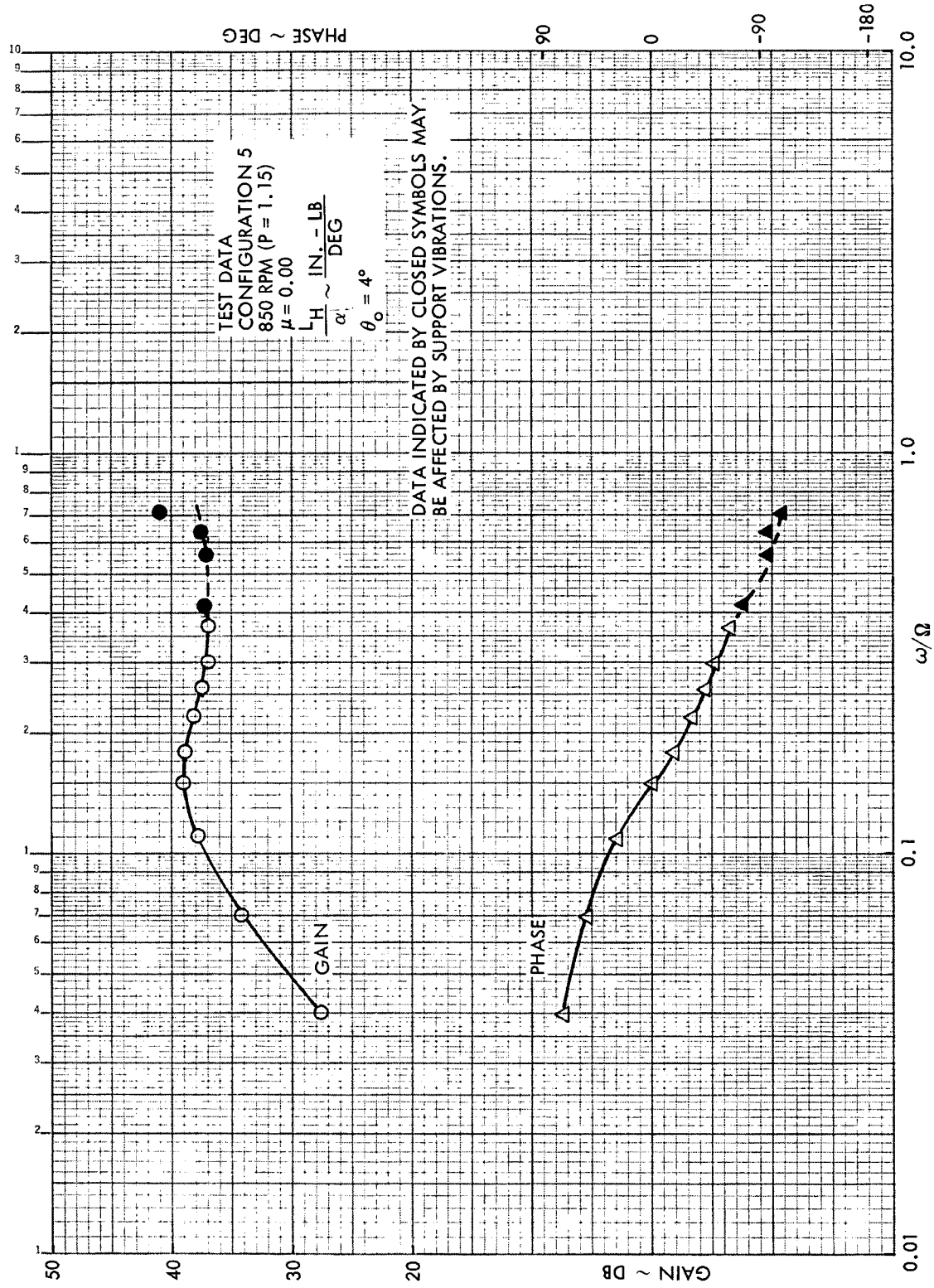

Figure C2. Rotor Hub Roll Moment Frequency Response to Shaft Pitch, Configuration 5, μ = 0.0, 850 RPM (P = 1.15)

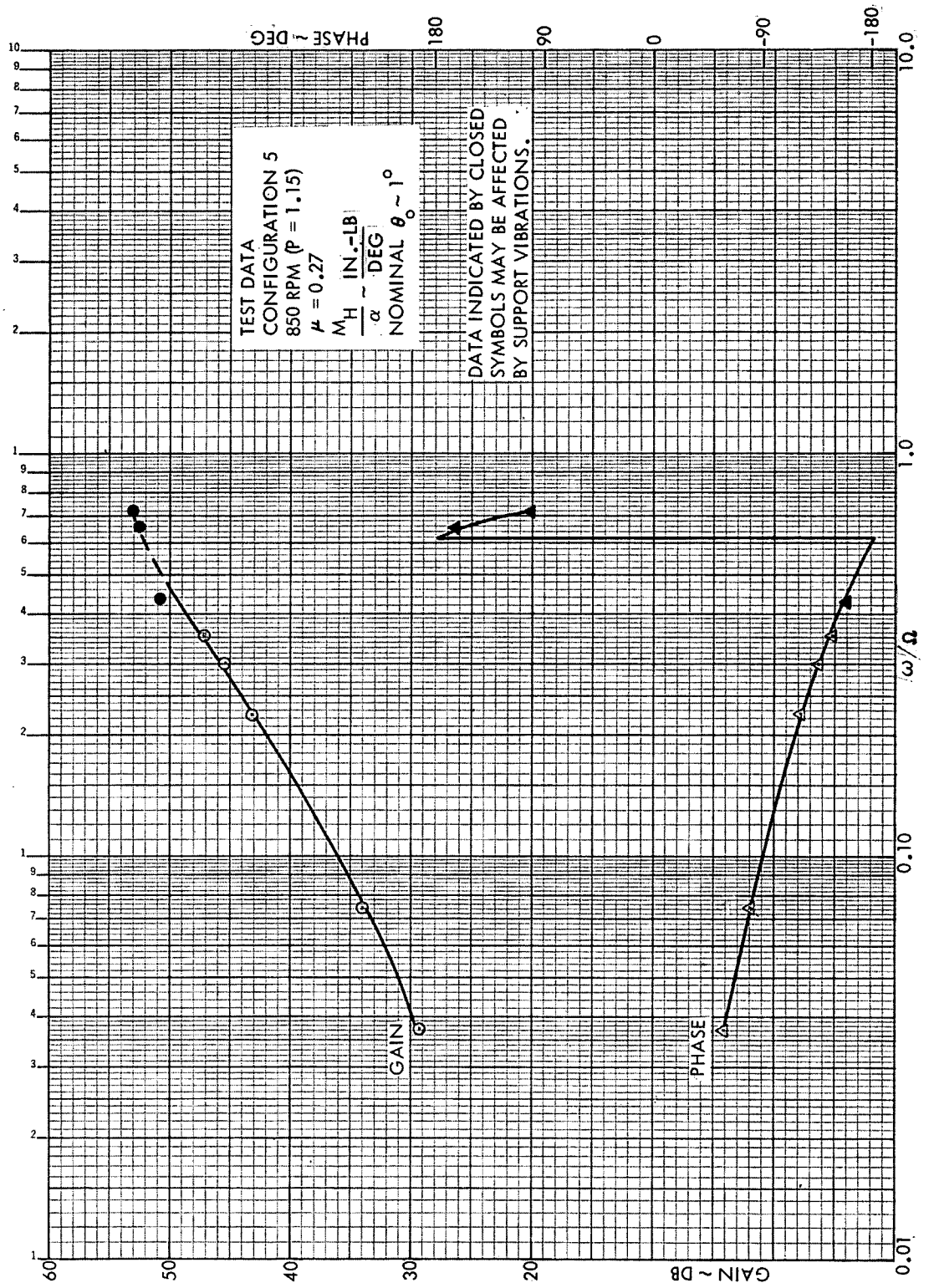

Figure C3. Rotor Hub Pitch Moment Frequency Response to Shaft Pitch, Configuration 5, μ = 0.27, 850 RPM (P = 1.15)

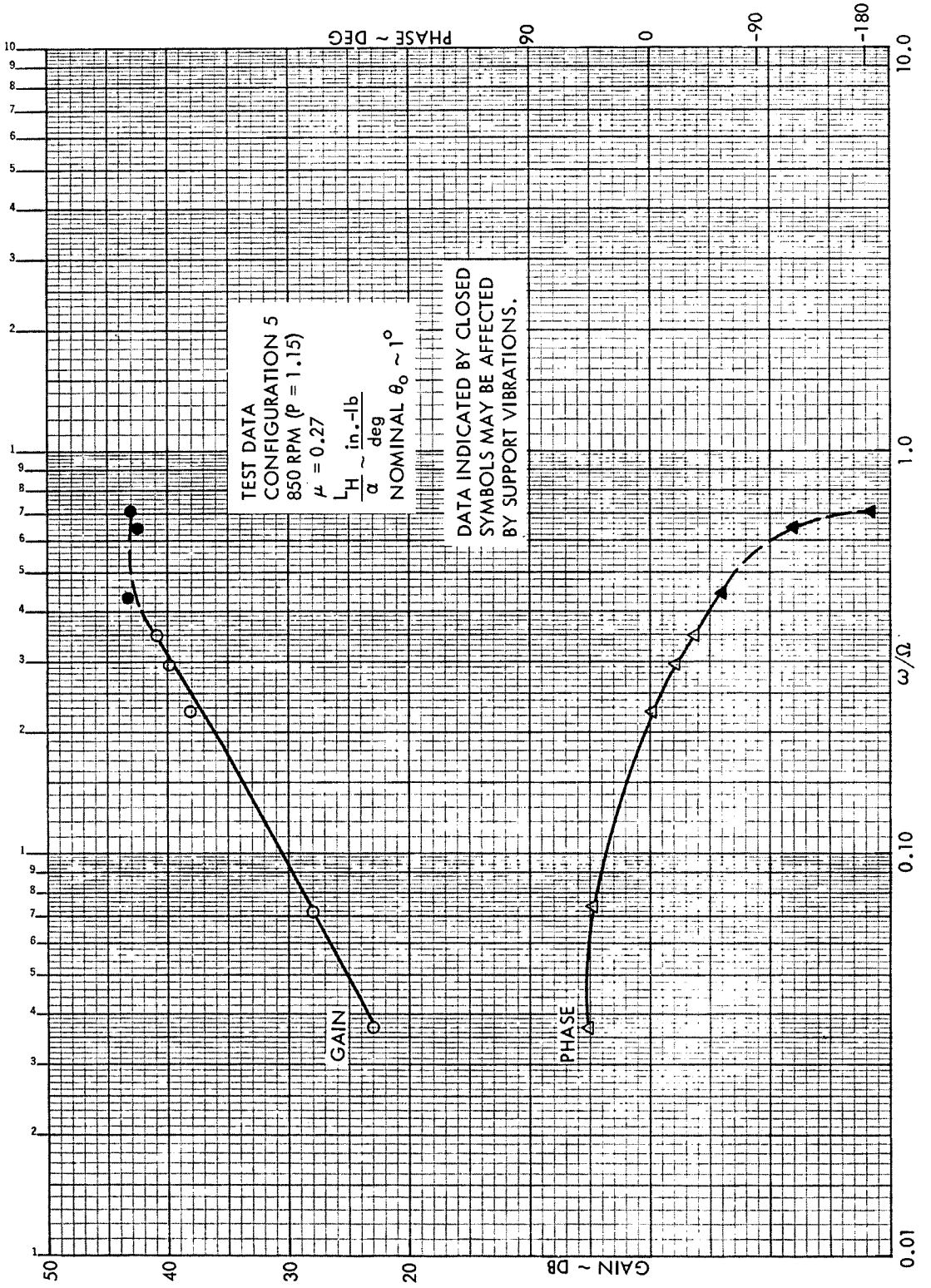

Figure C4. Rotor Hub Roll Moment Frequency Response to Shaft Pitch, Configuration 5, μ = 0.27, 850 RPM (P = 1.15)

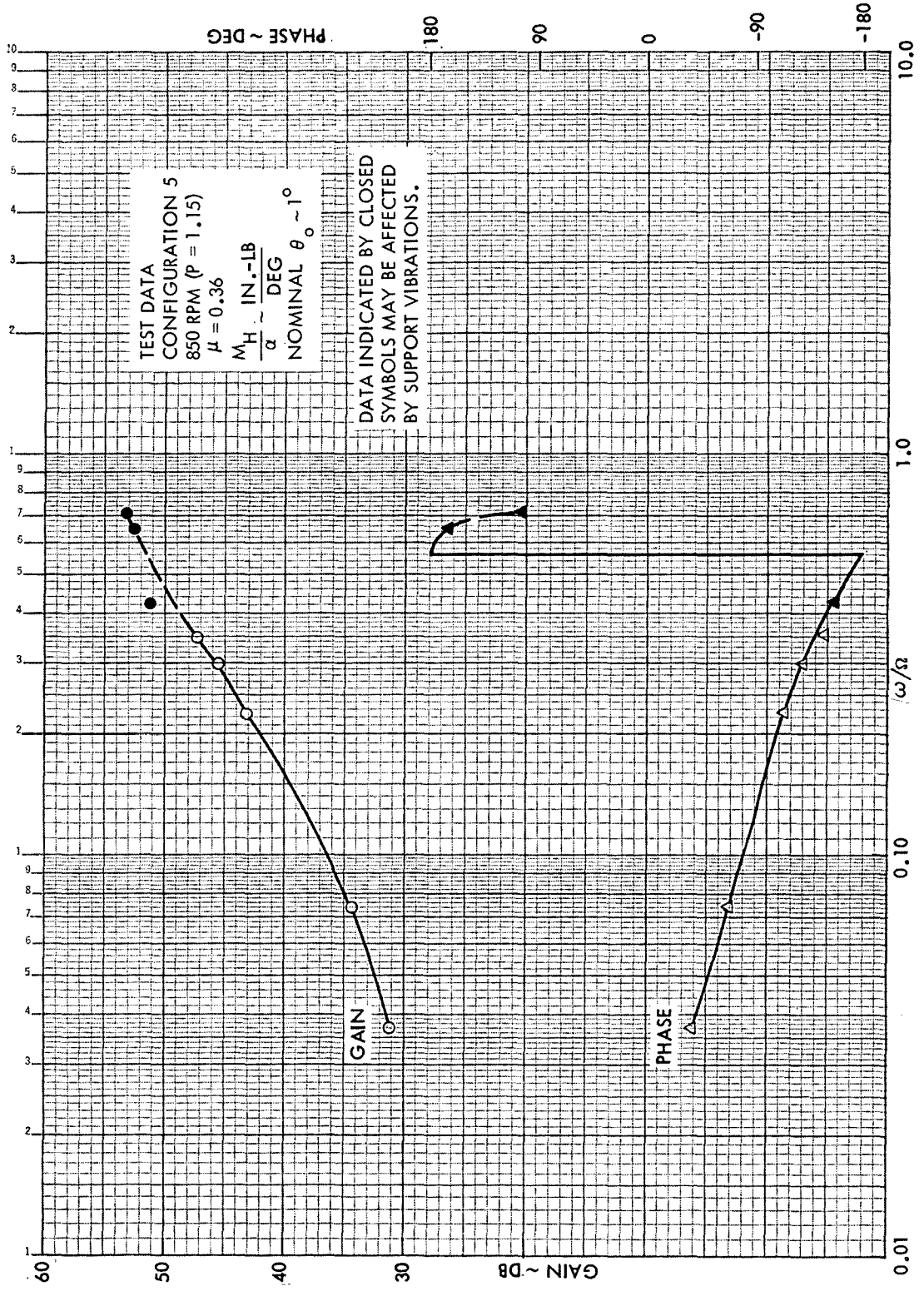

Figure C5. Rotor Hub Pitch Moment Frequency Response to Shaft Pitch, Configuration 5, μ = 0.36, 850 RPM (P = 1.15)

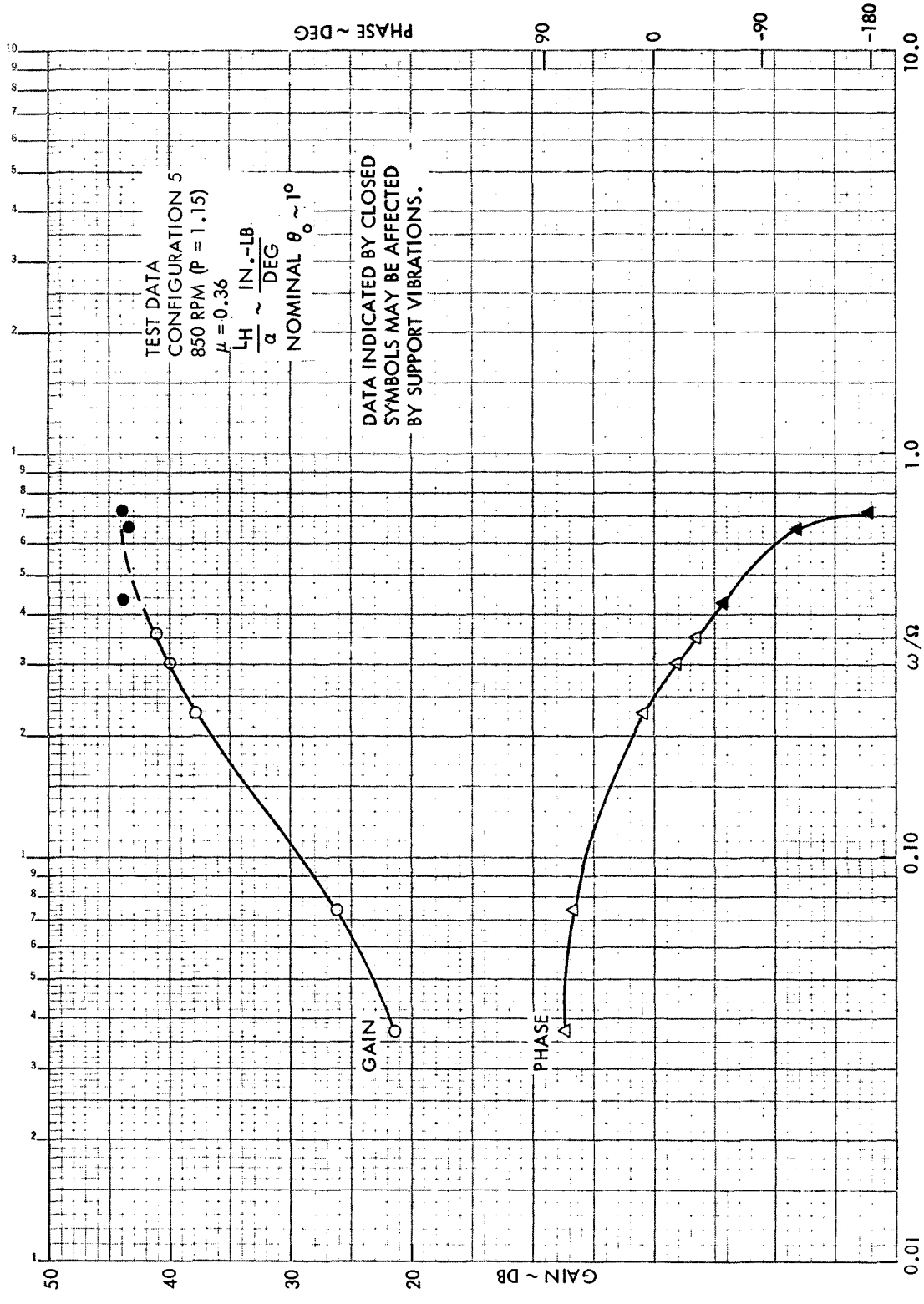

Figure C6. Rotor Hub Roll Moment Frequency Response to Shaft Pitch, Configuration 5, μ = 0.36, 850 RPM (P = 1.15)

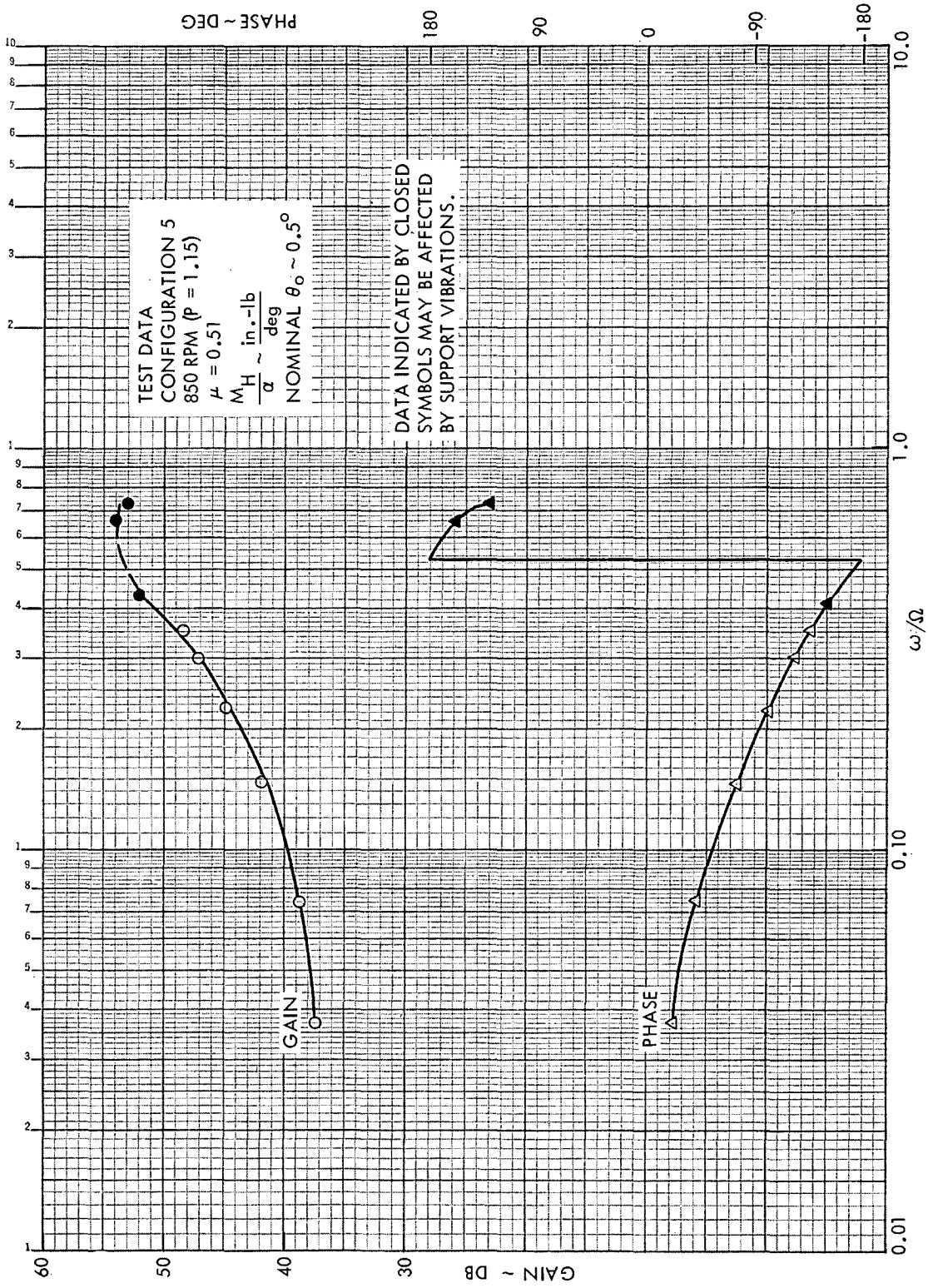

Figure C7. Rotor Hub Pitch Moment Frequency Response to Shaft Pitch, Configuration 5, μ = 0.51, 850 RPM (P = 1.15)

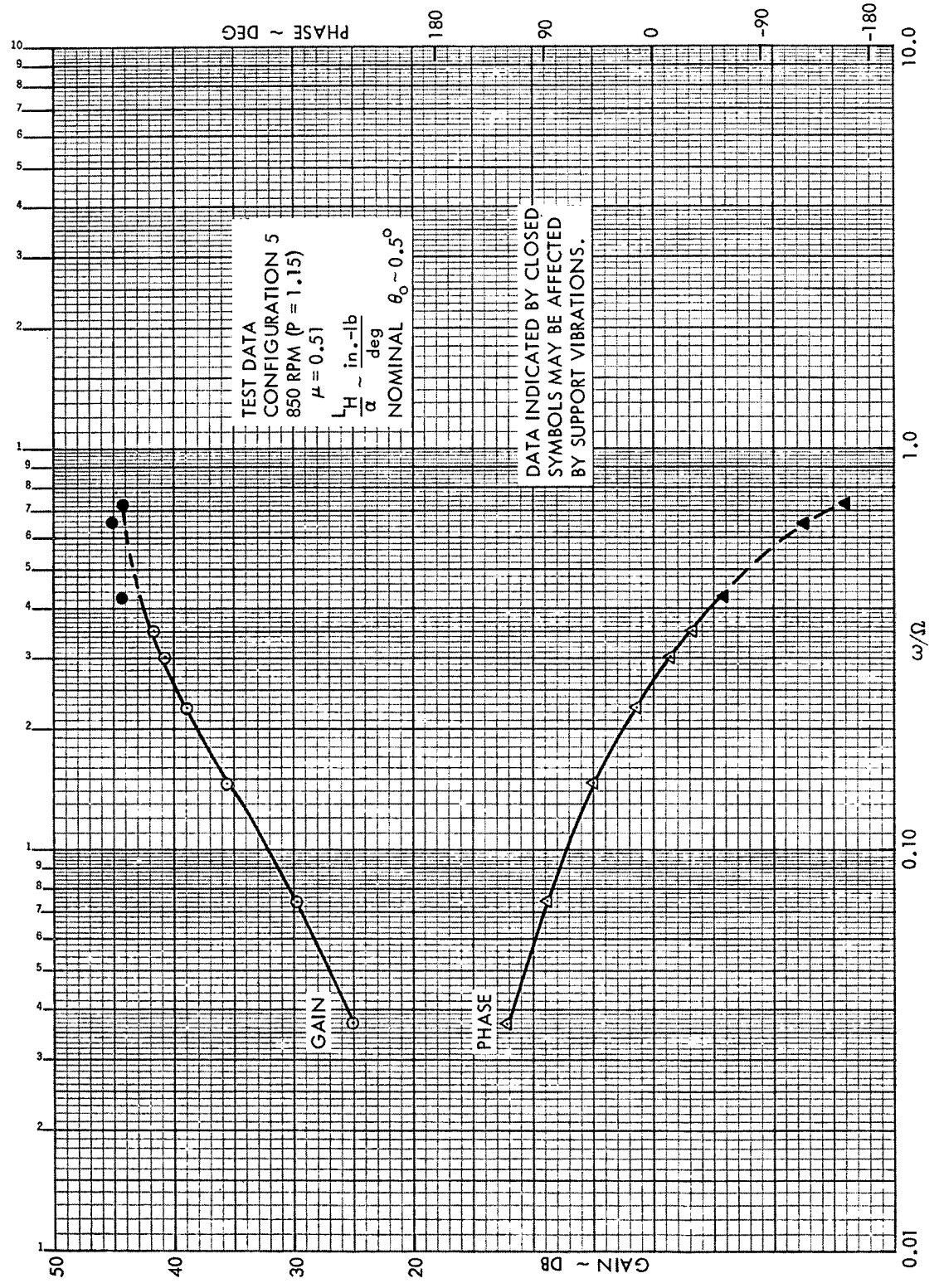

Figure C8. Rotor Hub Roll Moment Frequency Response to Shaft Pitch, Configuration 5, μ = 0.51, 850 RPM (P = 1.15)

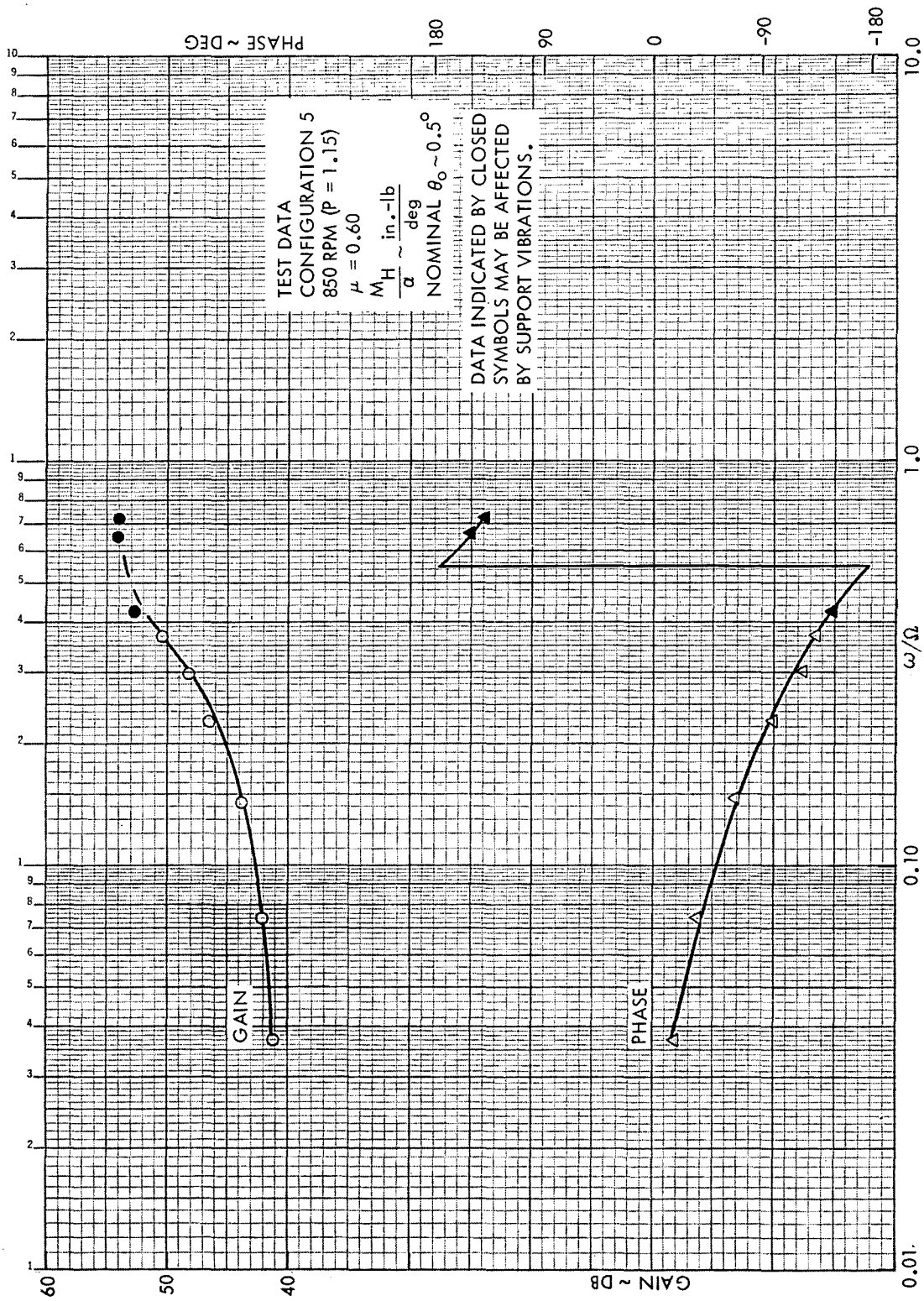

Figure C9. Rotor Hub Pitch Moment Frequency Response to Shaft Pitch, Configuration 5, μ = 0.60, 850 RPM (P = 1.15)

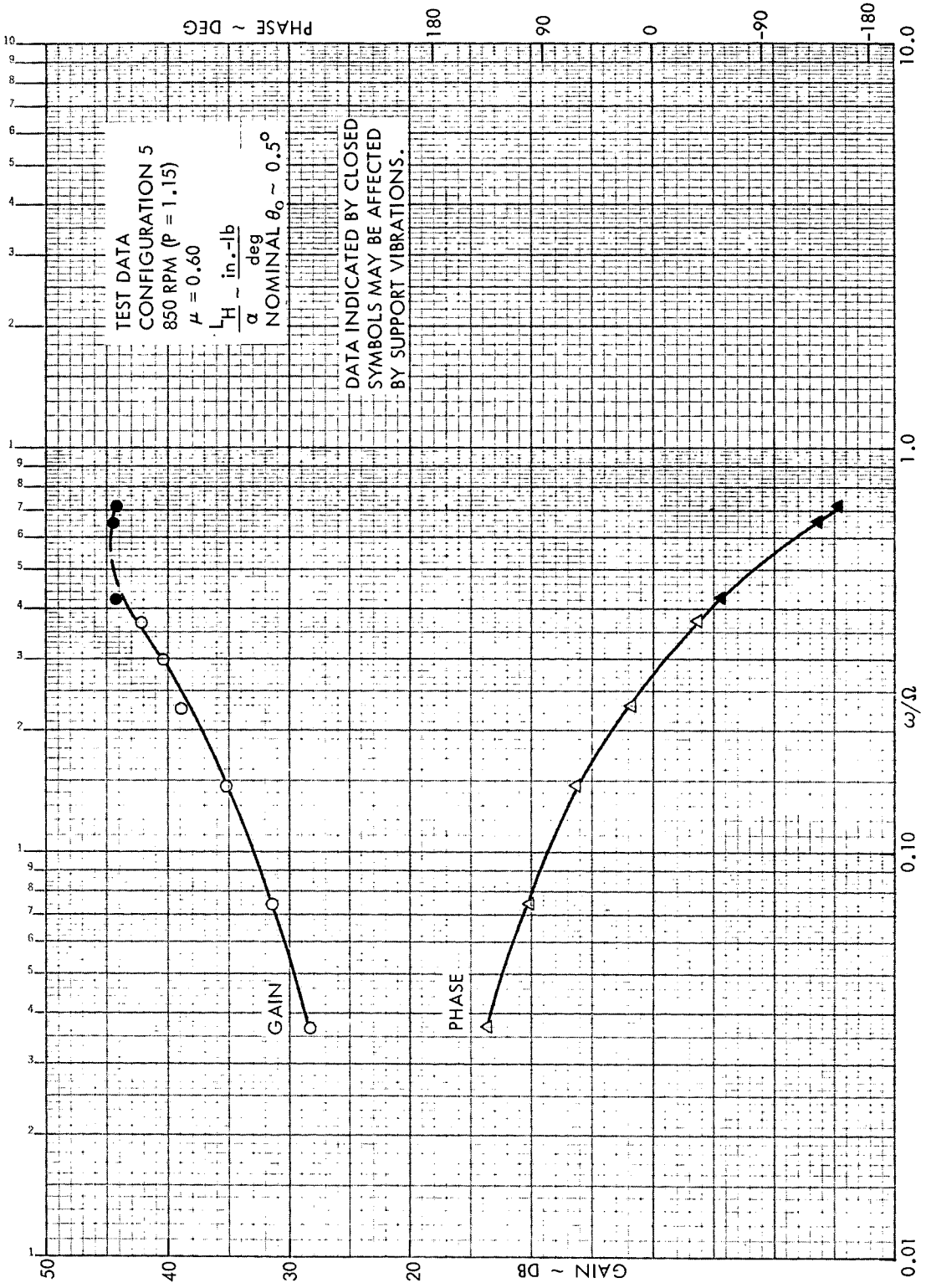

Figure C10. Rotor Hub Roll Moment Frequency Response to Shaft Pitch, Configuration 5, μ = 0.60, 850 RPM (P = 1.15)

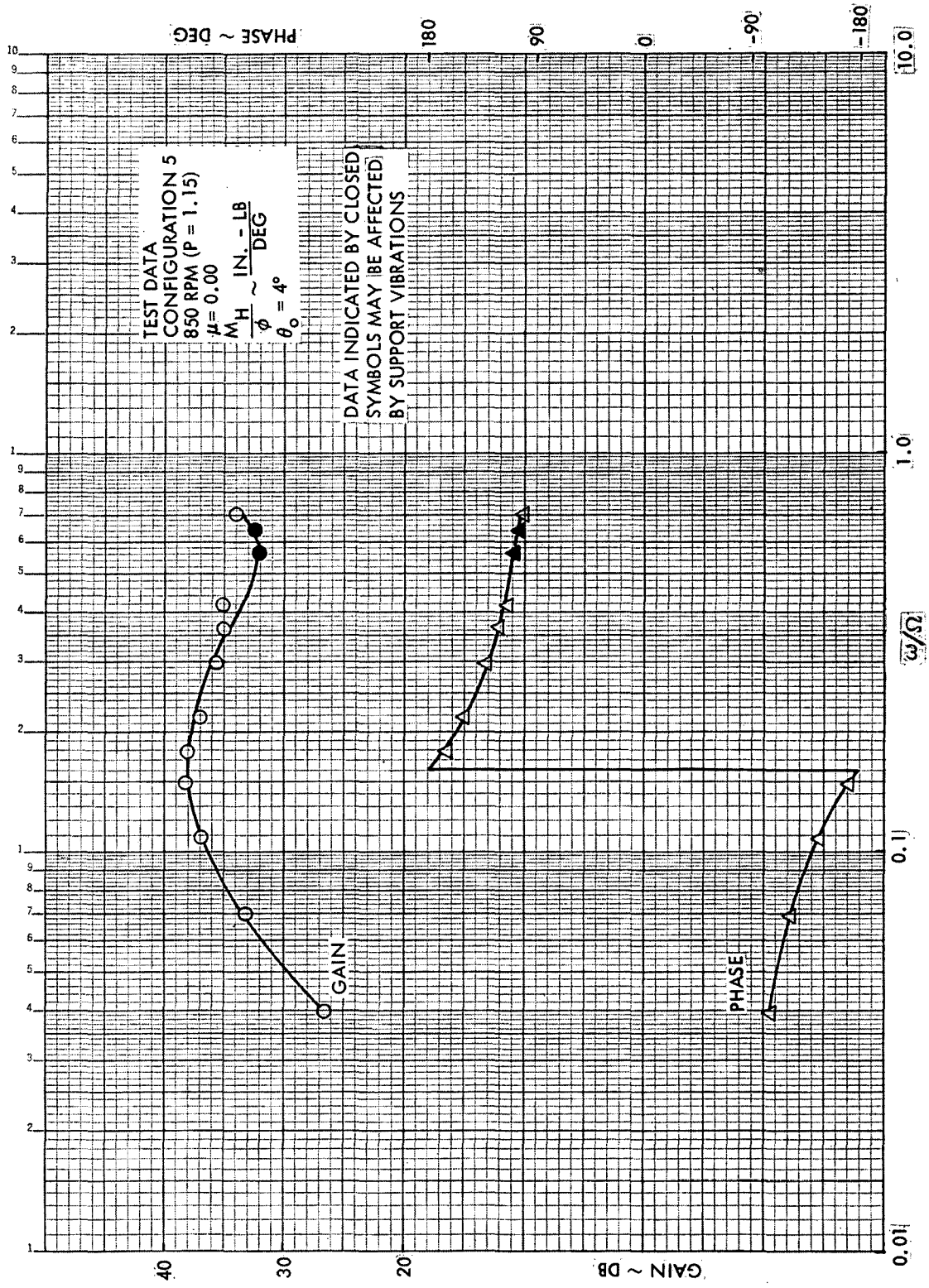

Figure C11. Rotor Hub Pitch Moment Frequency Response to Shaft Roll, Configuration 5, μ = 0.0, 850 RPM (P = 1.15)

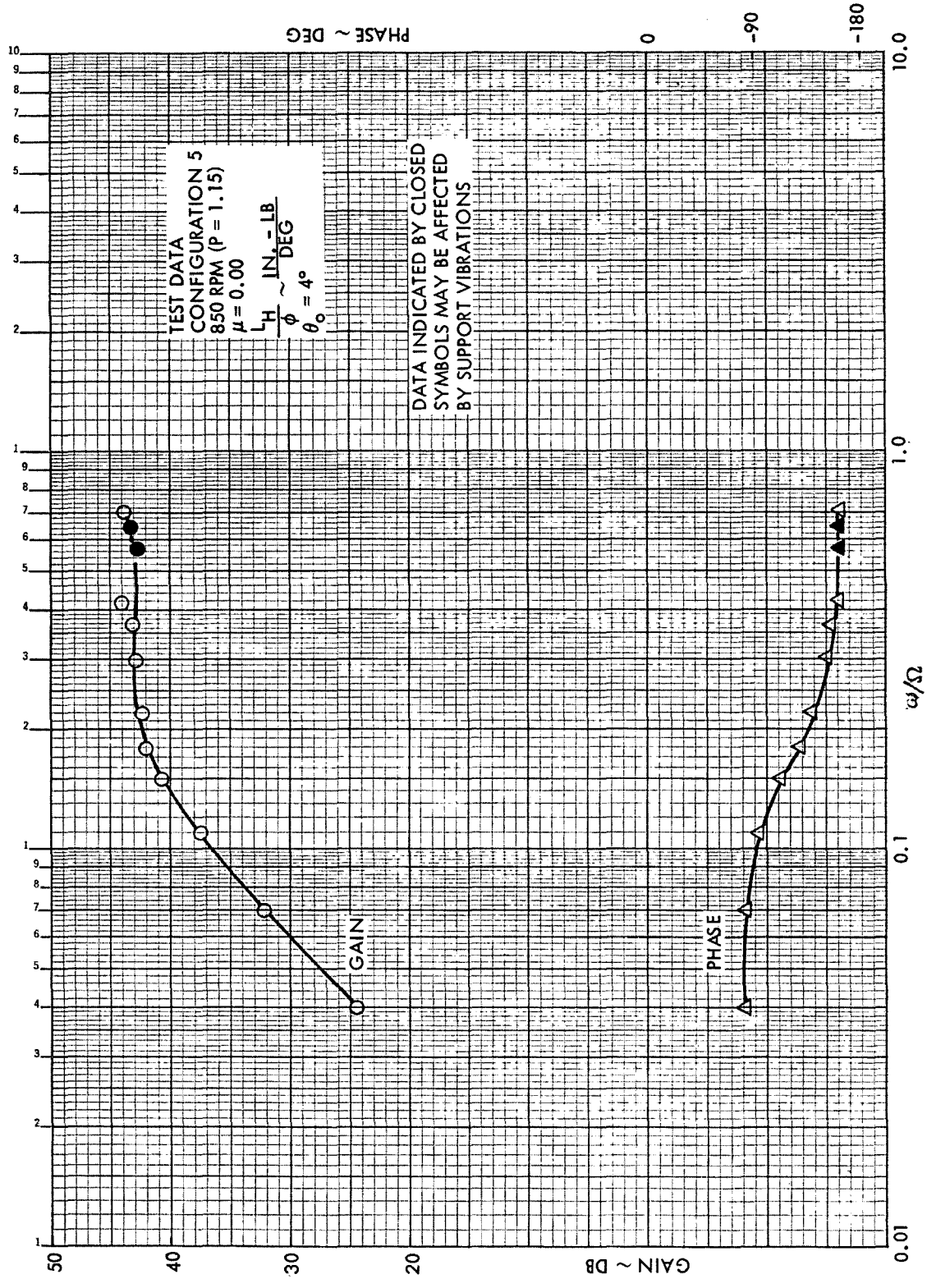

Figure C12. Rotor Hub Roll Moment Frequency Response to Shaft Roll, Configuration 5, μ = 0.0, 850 RPM (P = 1.15)

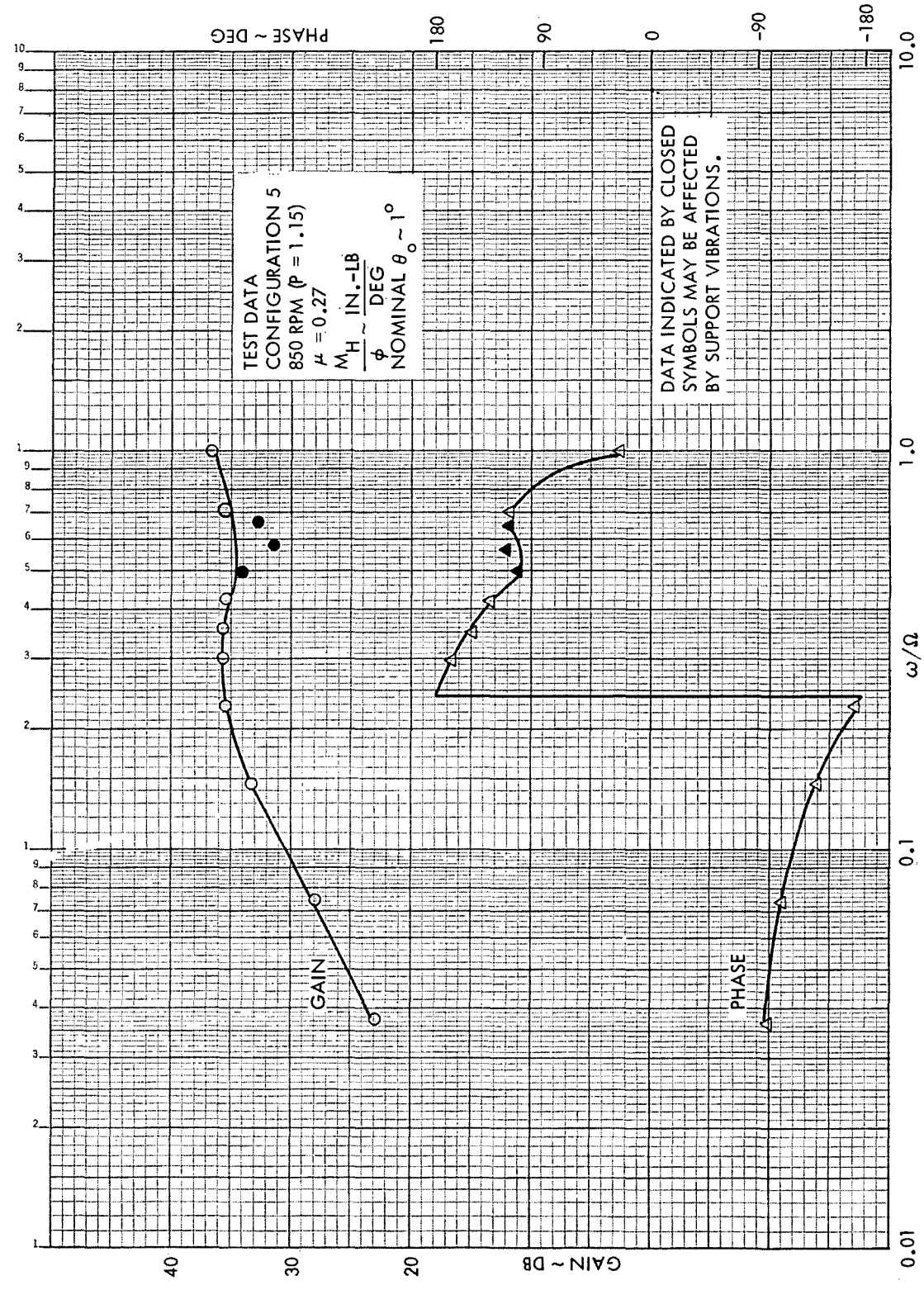

Figure C13. Rotor Hub Pitch Moment Frequency Response to Shaft Roll, Configuration 5, μ = 0.27, 850 RPM (P = 1.15)

LOCKHEED CALIFORNIA COMPANY

B

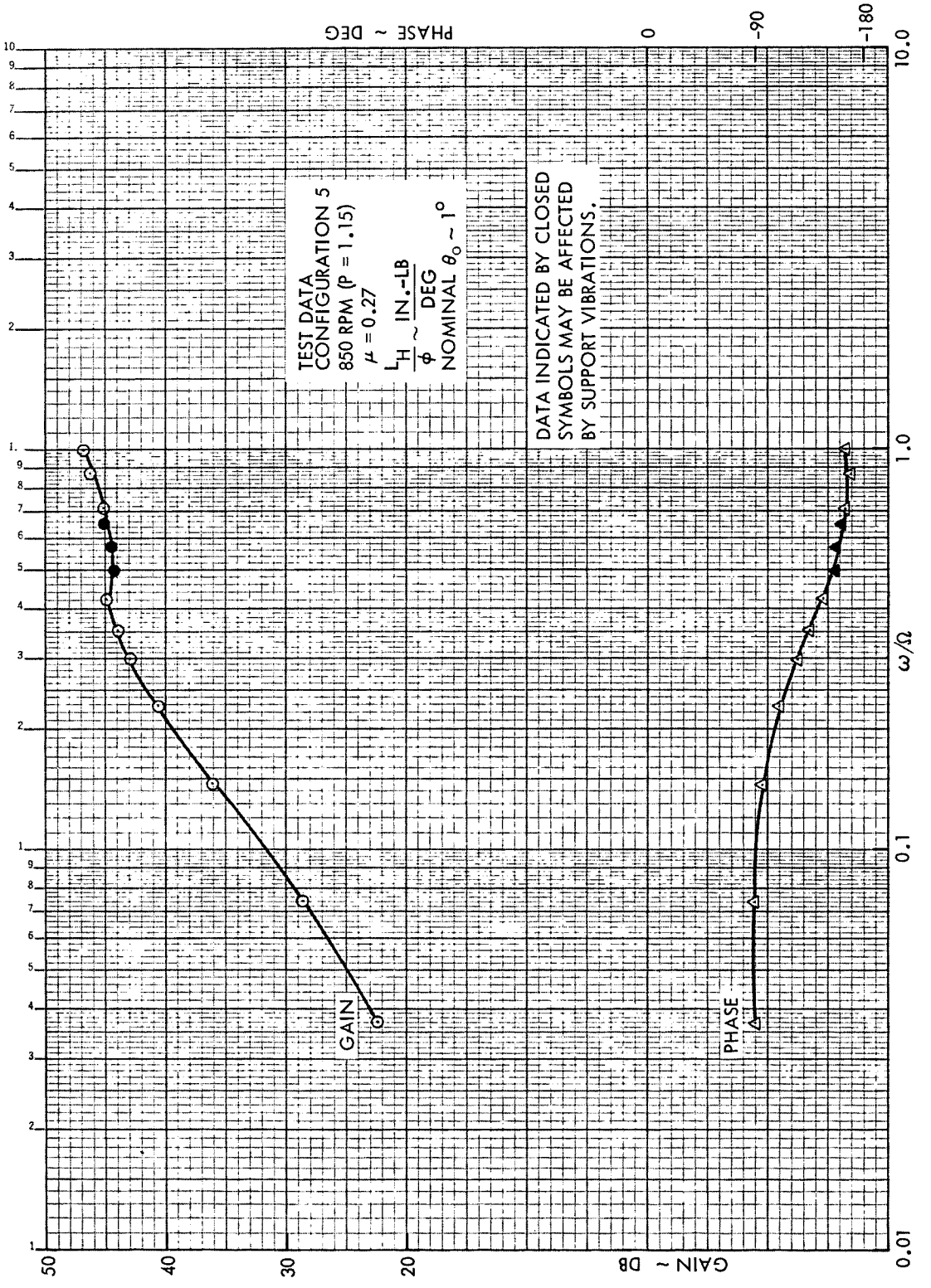

Figure C14. Rotor Hub Roll Moment Frequency Response to Shaft Roll, Configuration 5, μ = 0.27, 850 RPM (P = 1.15)

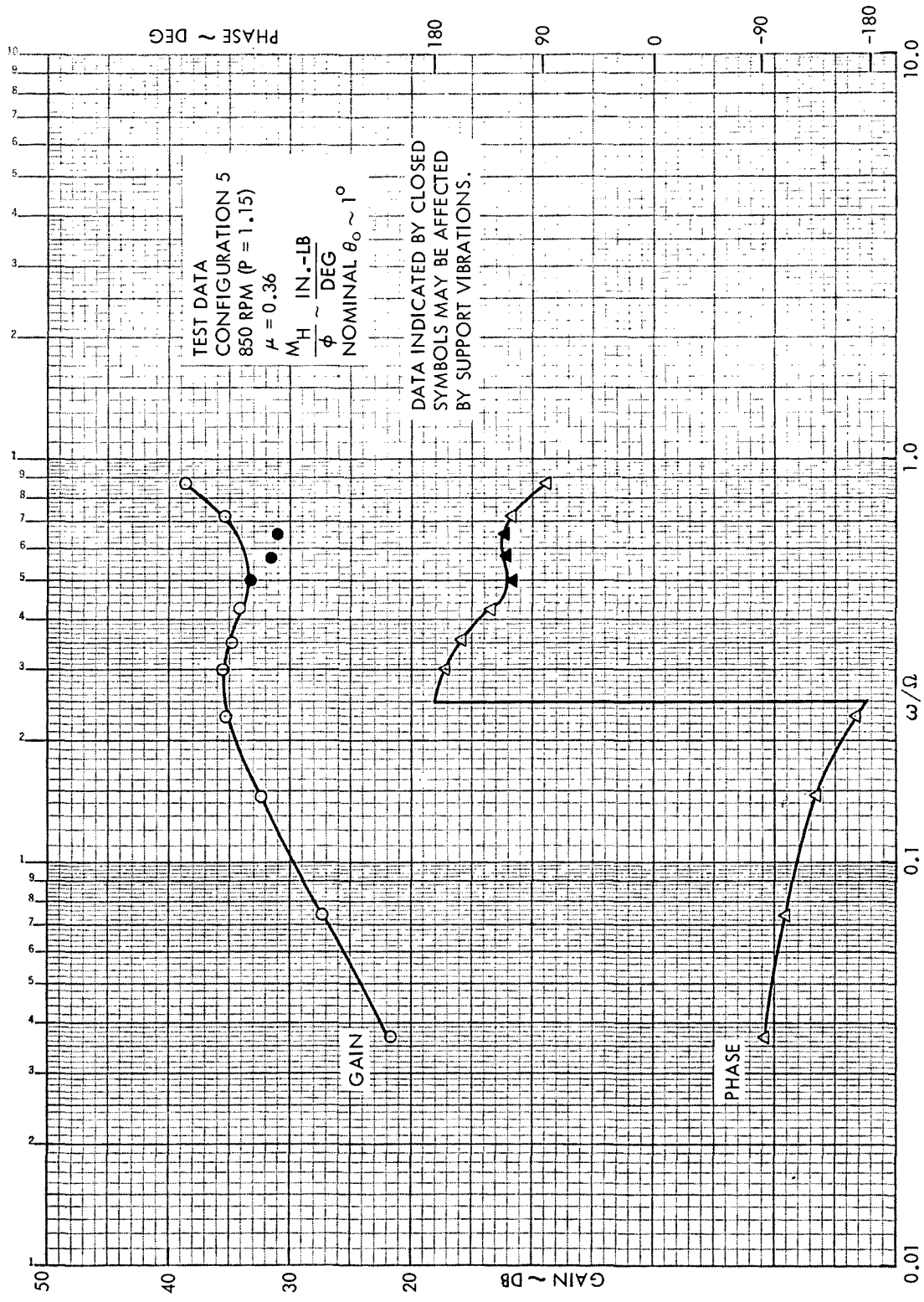

Figure C15. Rotor Hub Pitch Moment Frequency Response to Shaft Roll, Configuration 5, μ = 0.36, 850 RPM (P = 1.15)

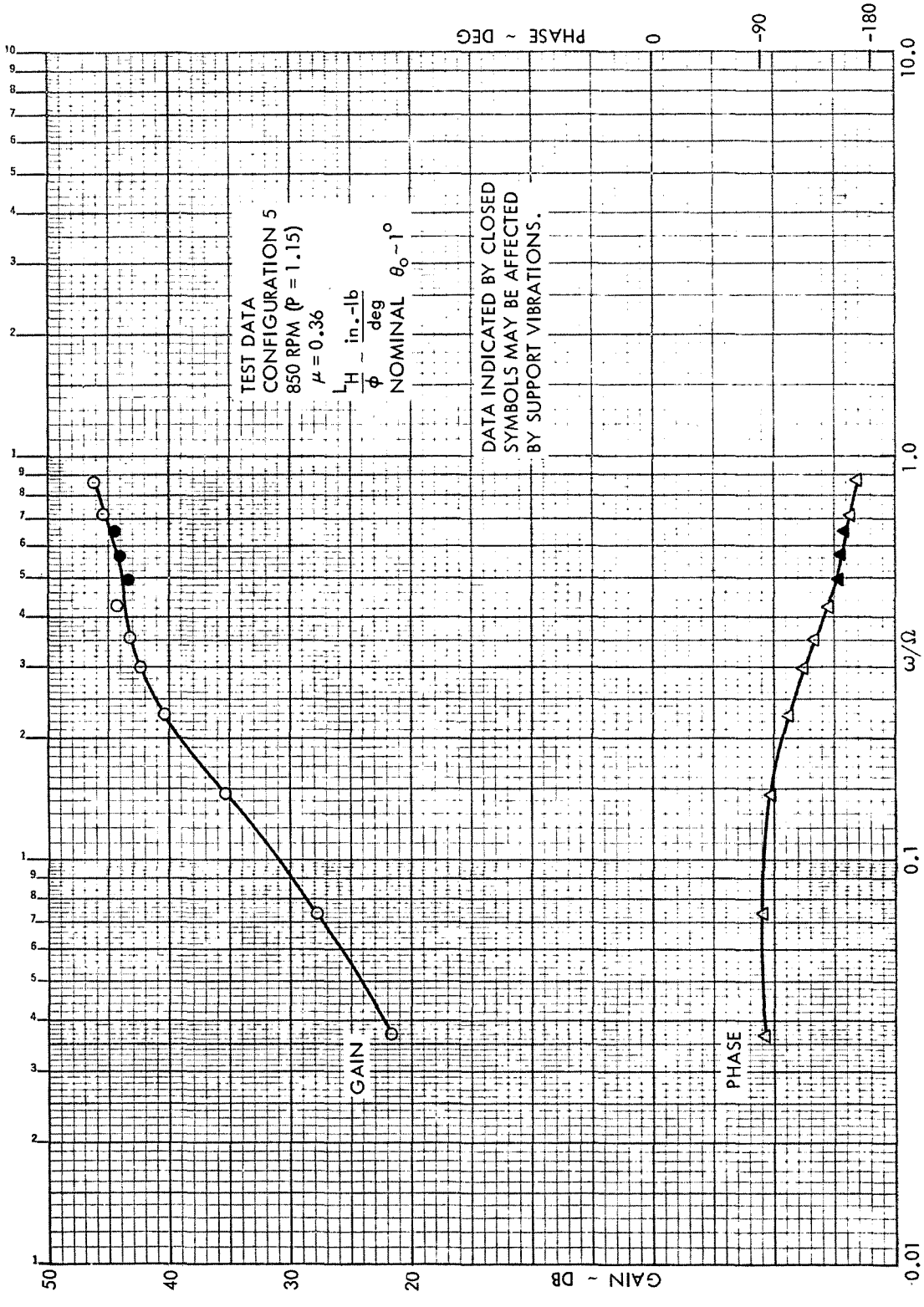

Figure C16. Rotor Hub Roll Moment Frequency Response to Shaft Roll, Configuration 5, μ = 0.36, 850 RPM (P = 1.15)

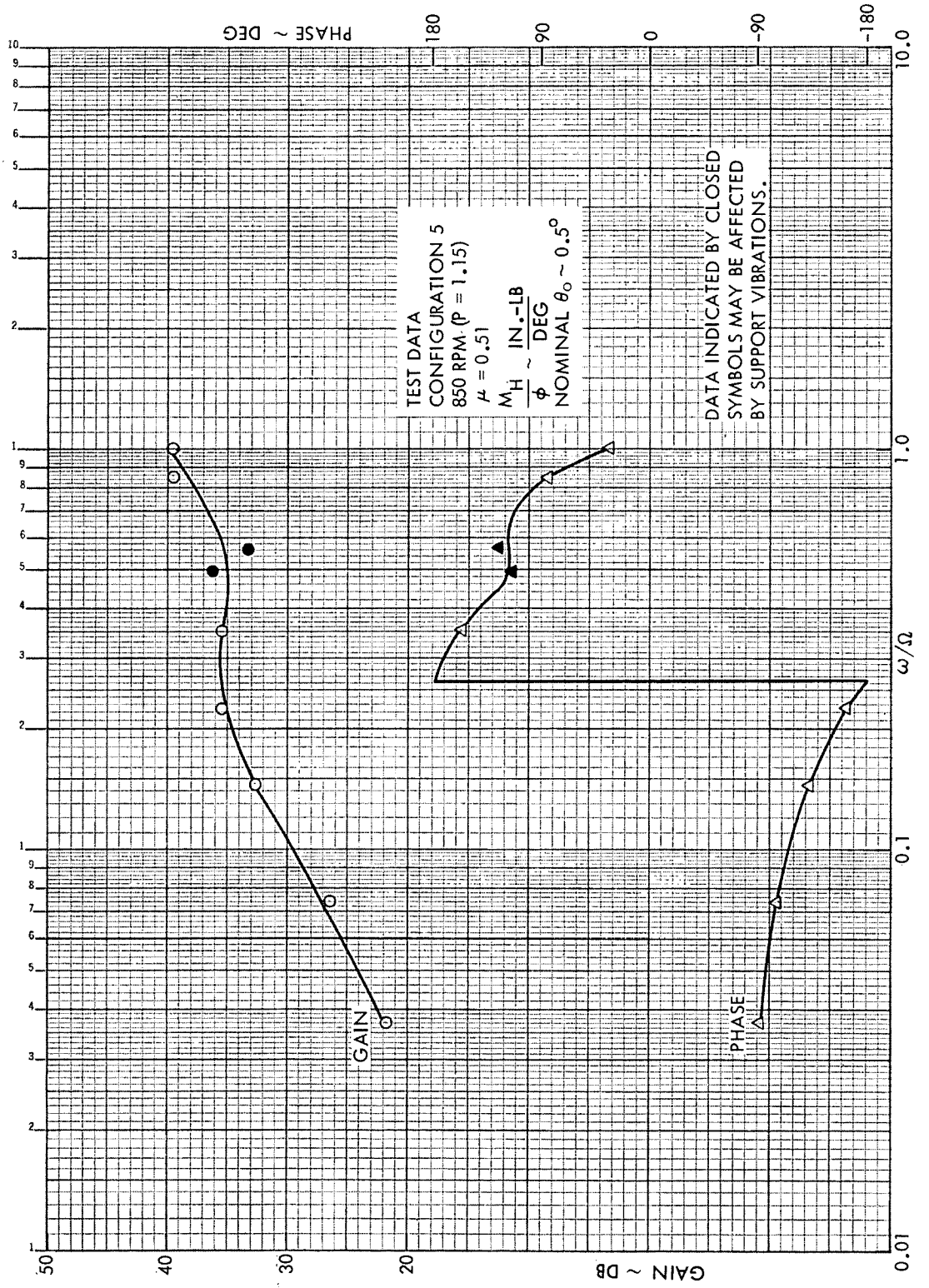

Figure C17. Rotor Hub Pitch Moment Frequency Response to Shaft Roll, Configuration 5, μ = 0.51, 850 RPM (P = 1.15)

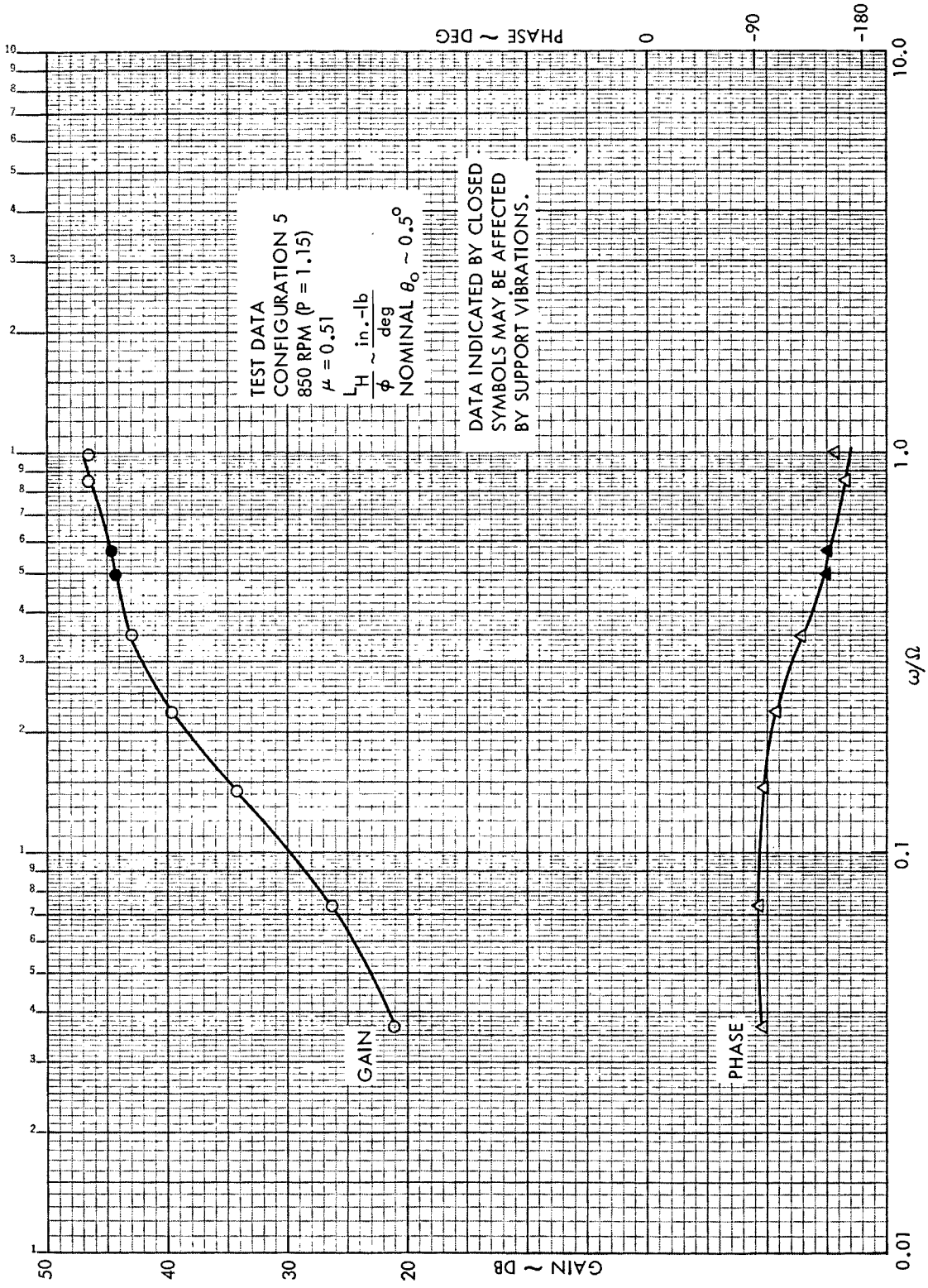

Figure C18. Rotor Hub Roll Moment Frequency Response to Shaft Roll, Configuration 5, μ = 0.51, 850 RPM (P = 1.15)

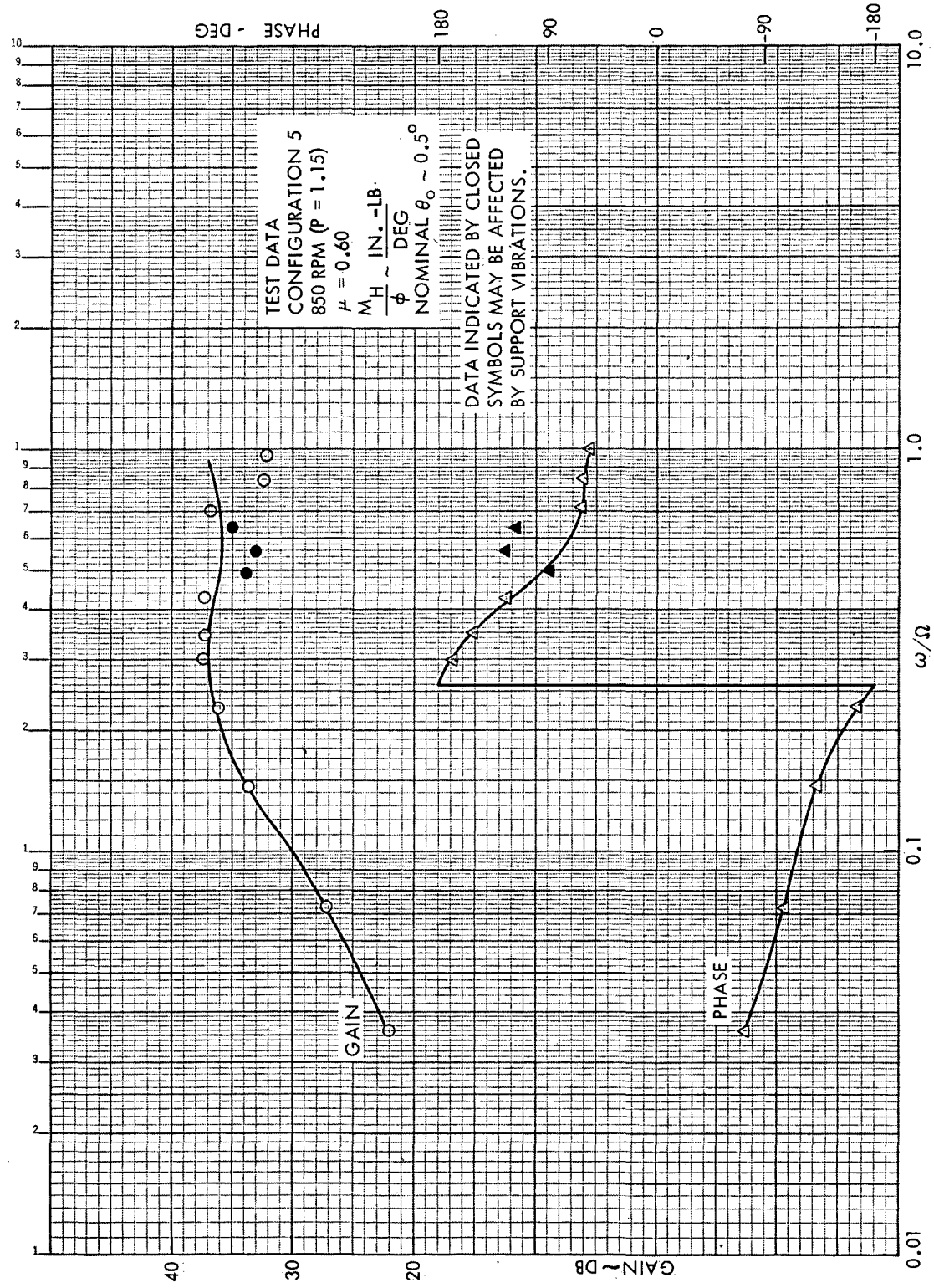

Figure C19. Rotor Hub Pitch Moment Frequency Response to Shaft Roll, Configuration 5, μ = 0.60, 850 RPM (P = 1.15)

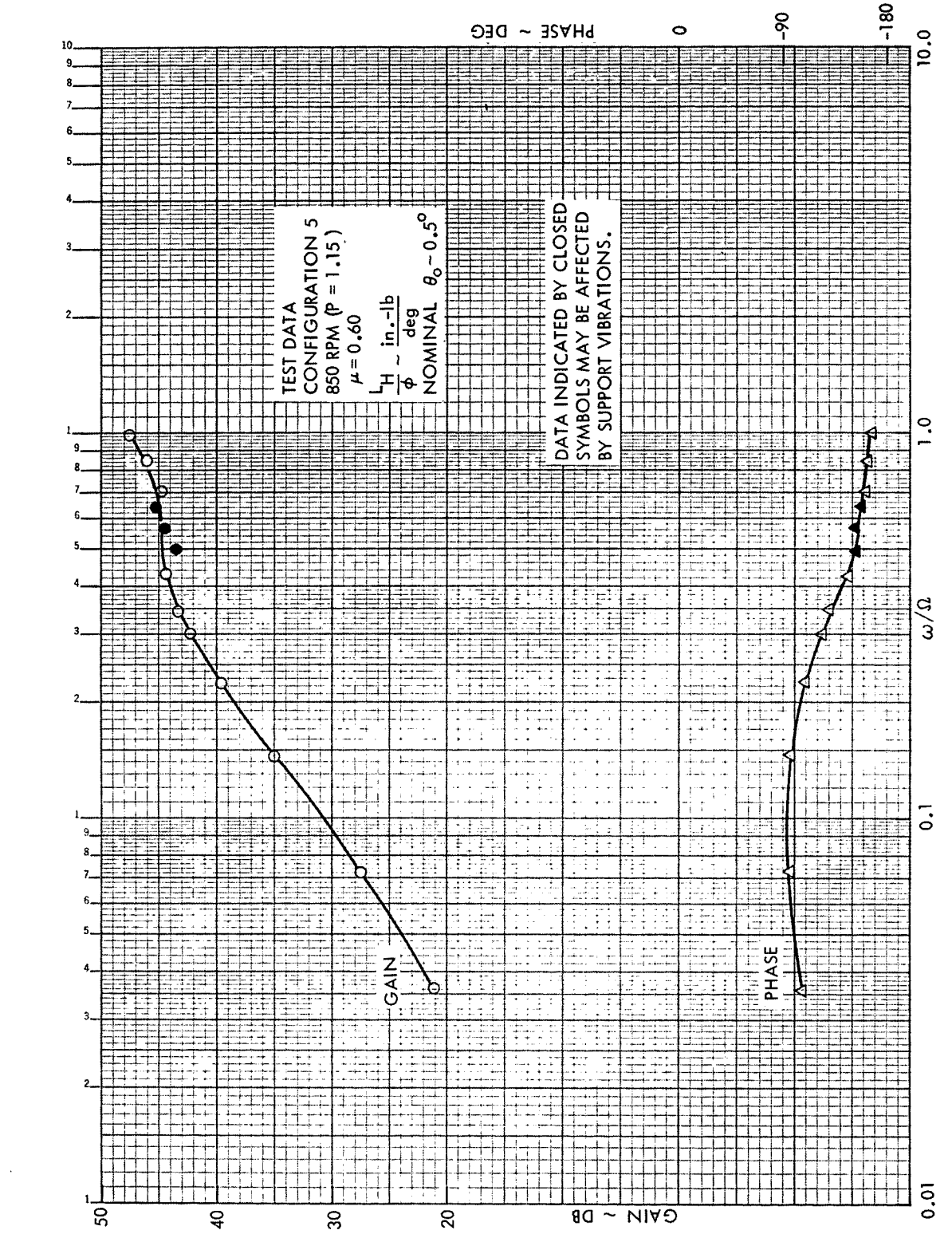

Figure C20. Rotor Hub Roll Moment Frequency Response to Shaft Roll, Configuration 5, μ = 0.60, 850 RPM (P = 1.15)

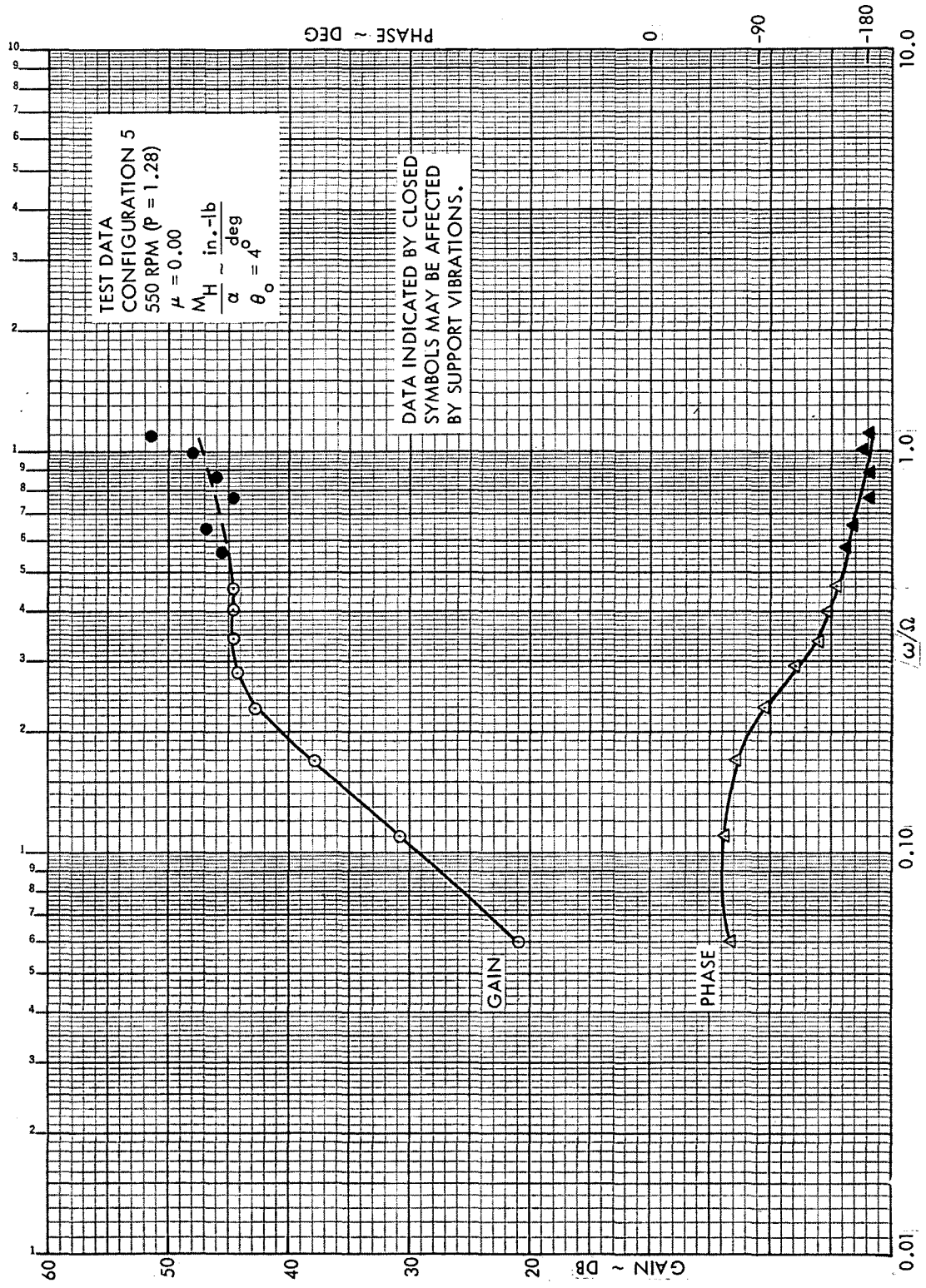

Figure C21. Rotor Hub Pitch Moment Frequency Response to Shaft Pitch, Configuration 5, μ = 0.0, 550 RPM (P = 1.28)

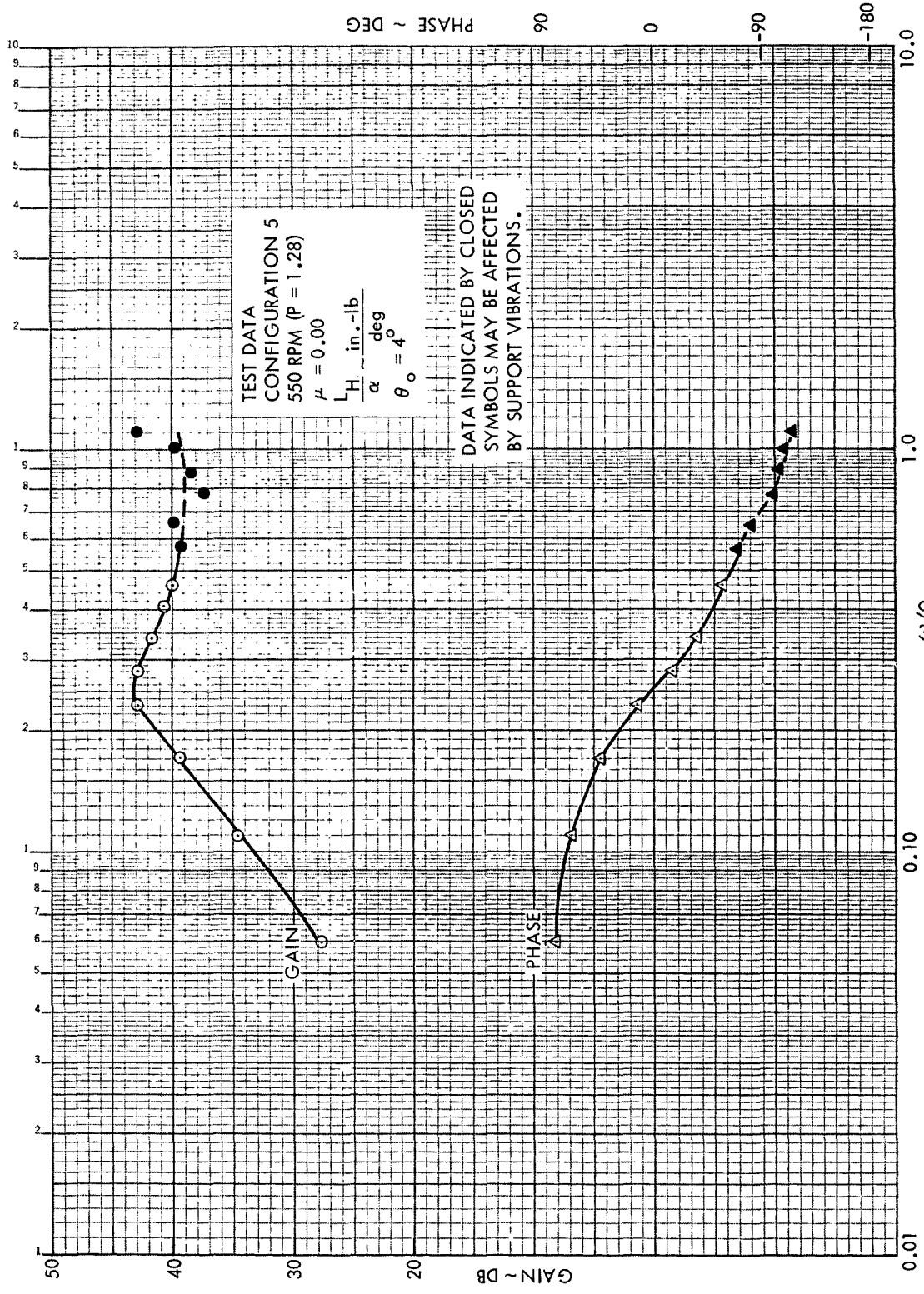

Figure C22. Rotor Hub Roll Moment Frequency Response to Shaft Pitch, Configuration 5, μ = 0.0, 550 RPM (P = 1.28)

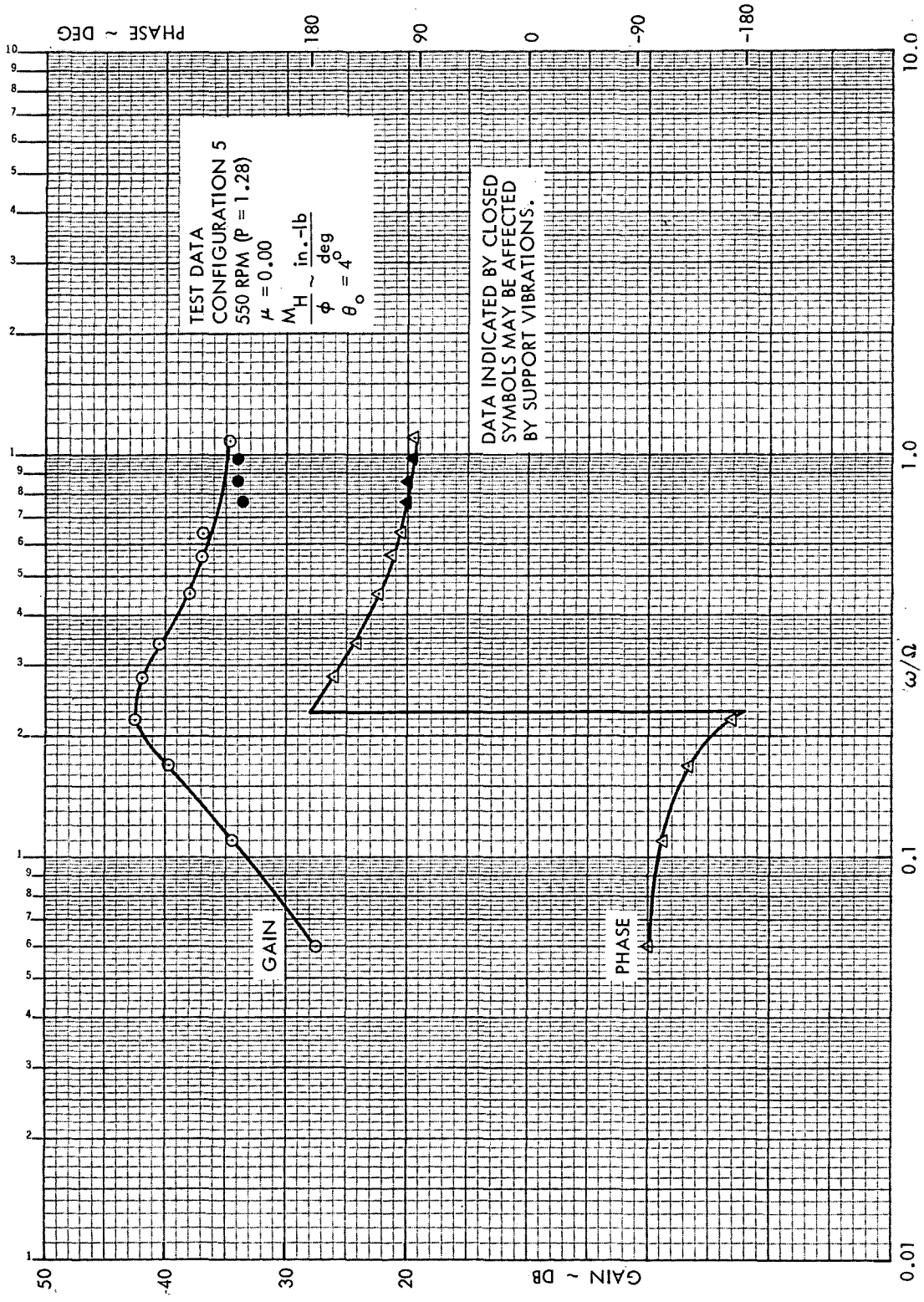

Figure C23. Rotor Hub Pitch Moment Frequency Response to Shaft Roll, Configuration 5, μ = 0.0, 550 RPM (P = 1.28)

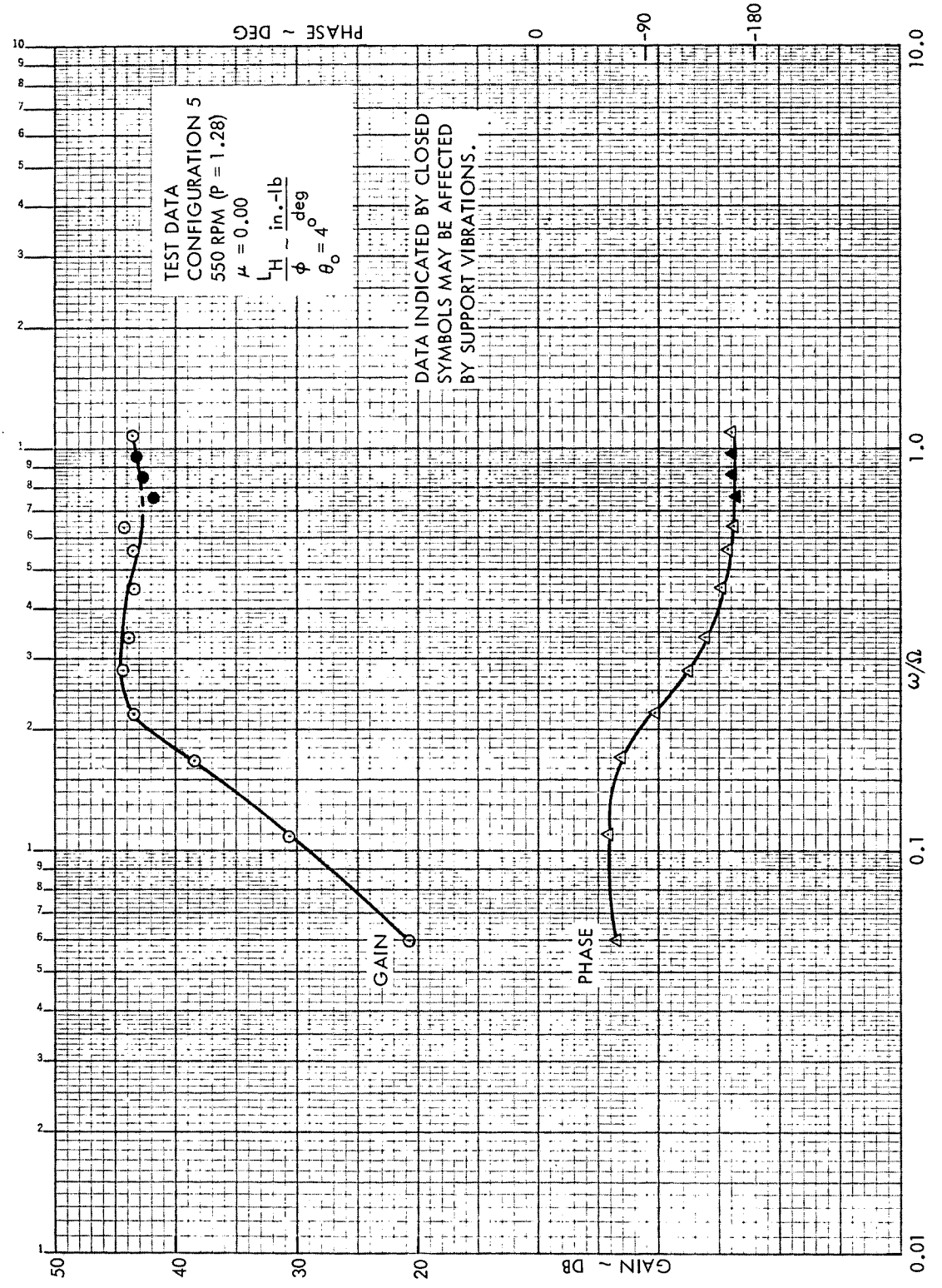

Figure C24. Rotor Hub Roll Moment Frequency Response to Shaft Roll, Configuration 5, μ = 0.0, 550 RPM (P = 1.28)

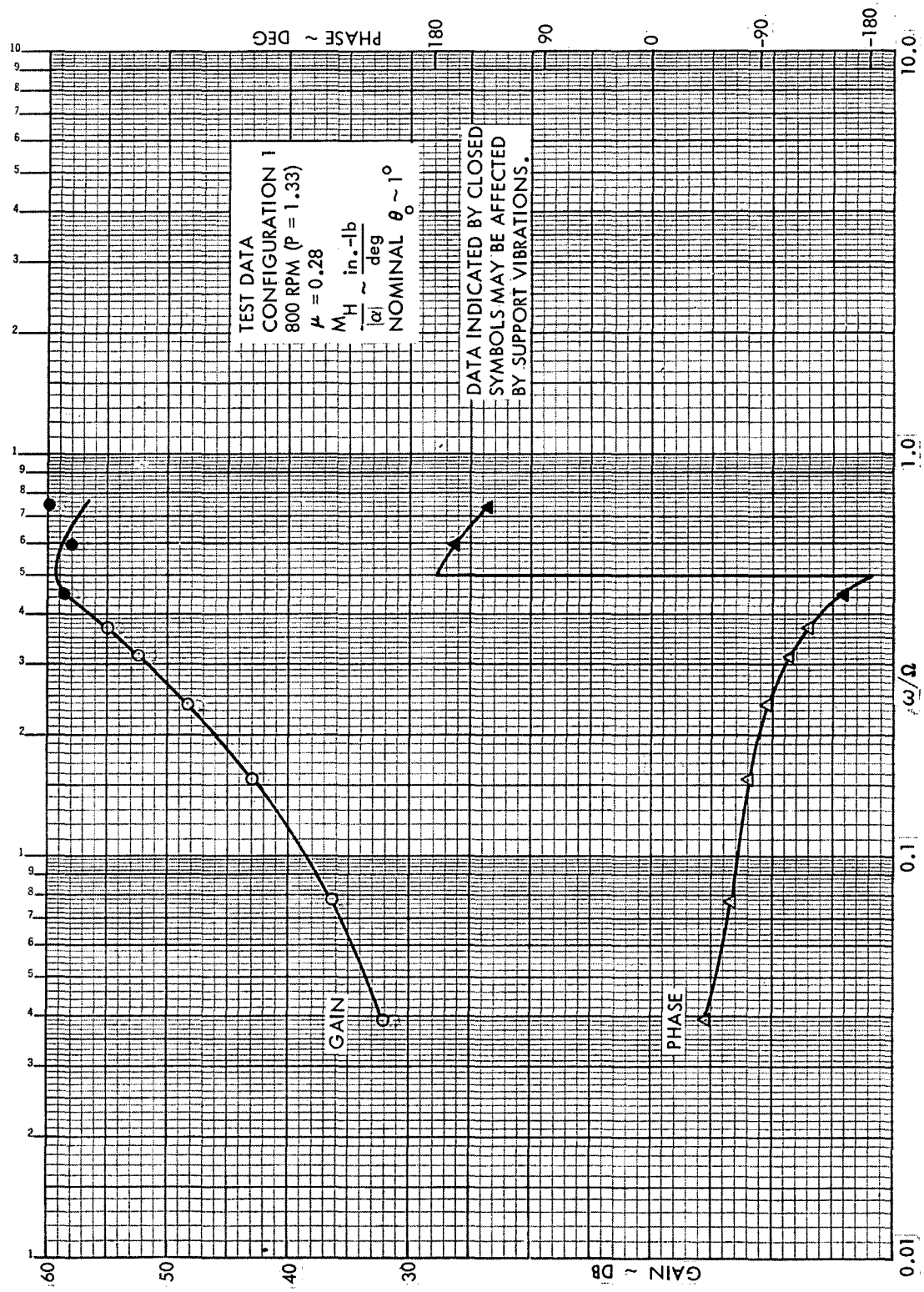

Figure C25. Rotor Hub Pitch Moment Frequency Response to Shaft Pitch, Configuration 1, μ = 0.28, 800 RPM (P = 1.33)

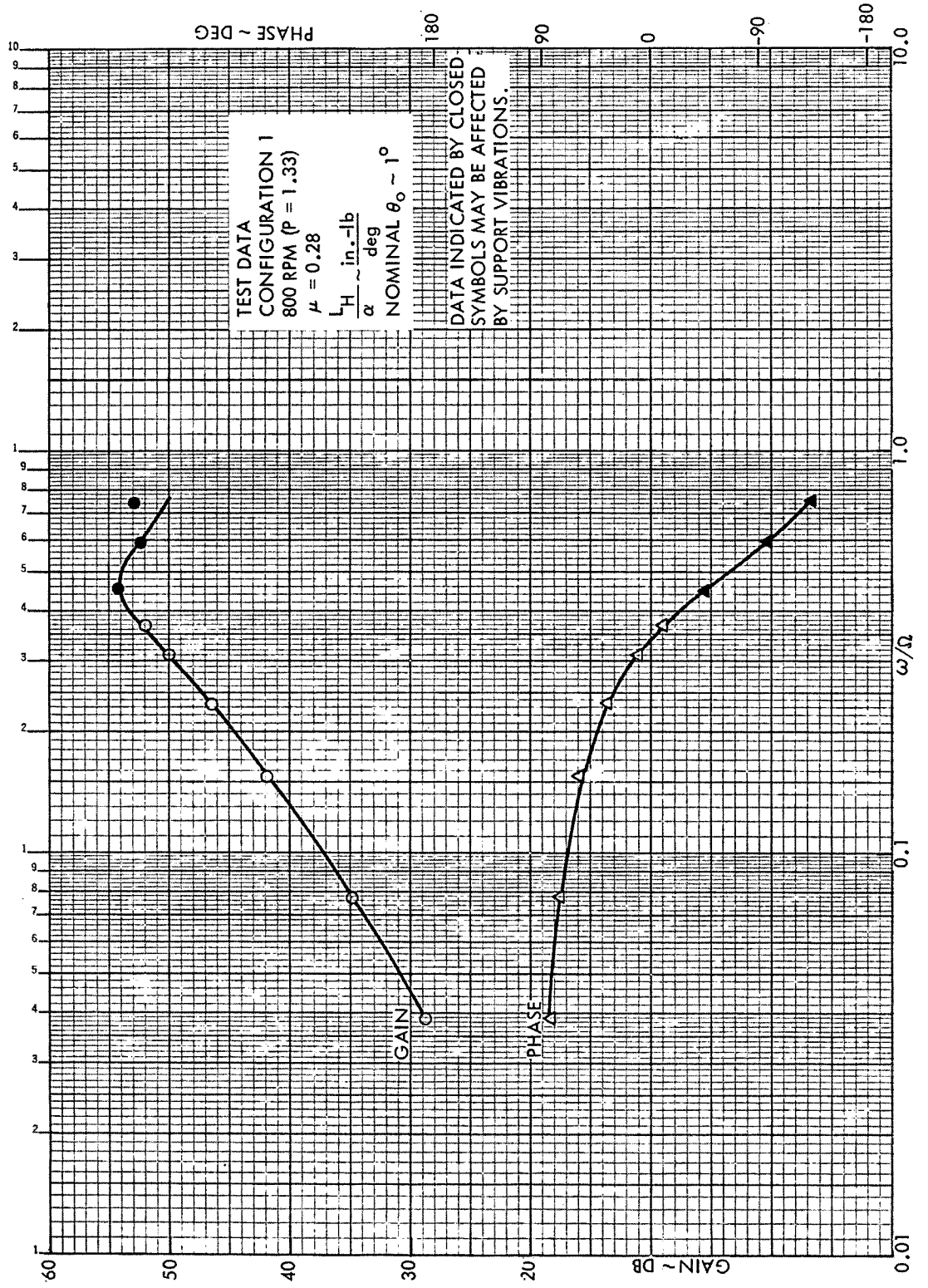

Figure C26. Rotor Hub Roll Moment Frequency Response to Shaft Pitch, Configuration 1, μ = 0.28, 800 RPM (P = 1.33)

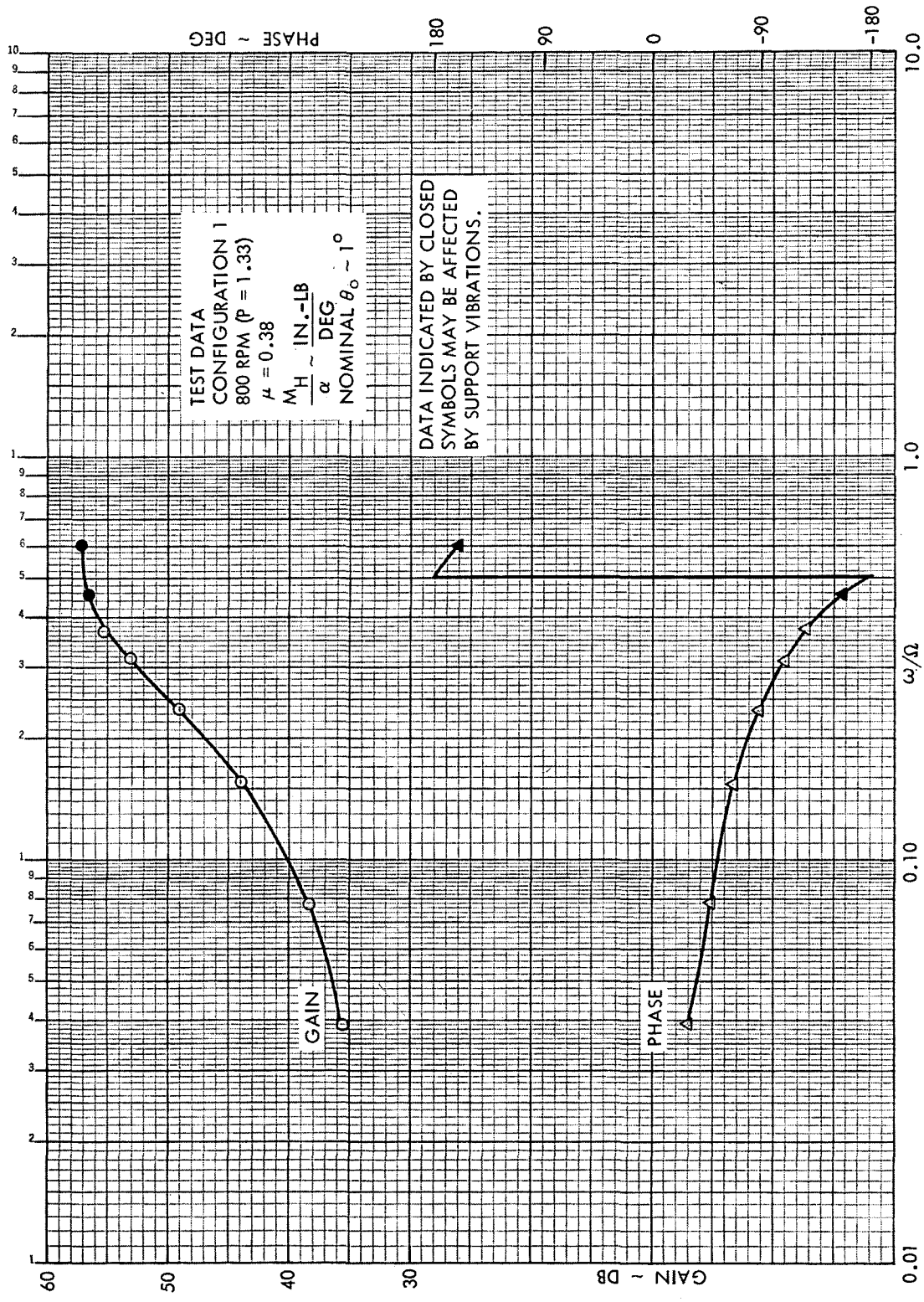

Figure C27. Rotor Hub Pitch Moment Frequency Response to Shaft Pitch, Configuration 1, μ = 0.38, 800 RPM (P = 1.33)

LOCKHEED
CALIFORNIA COMPANY

C

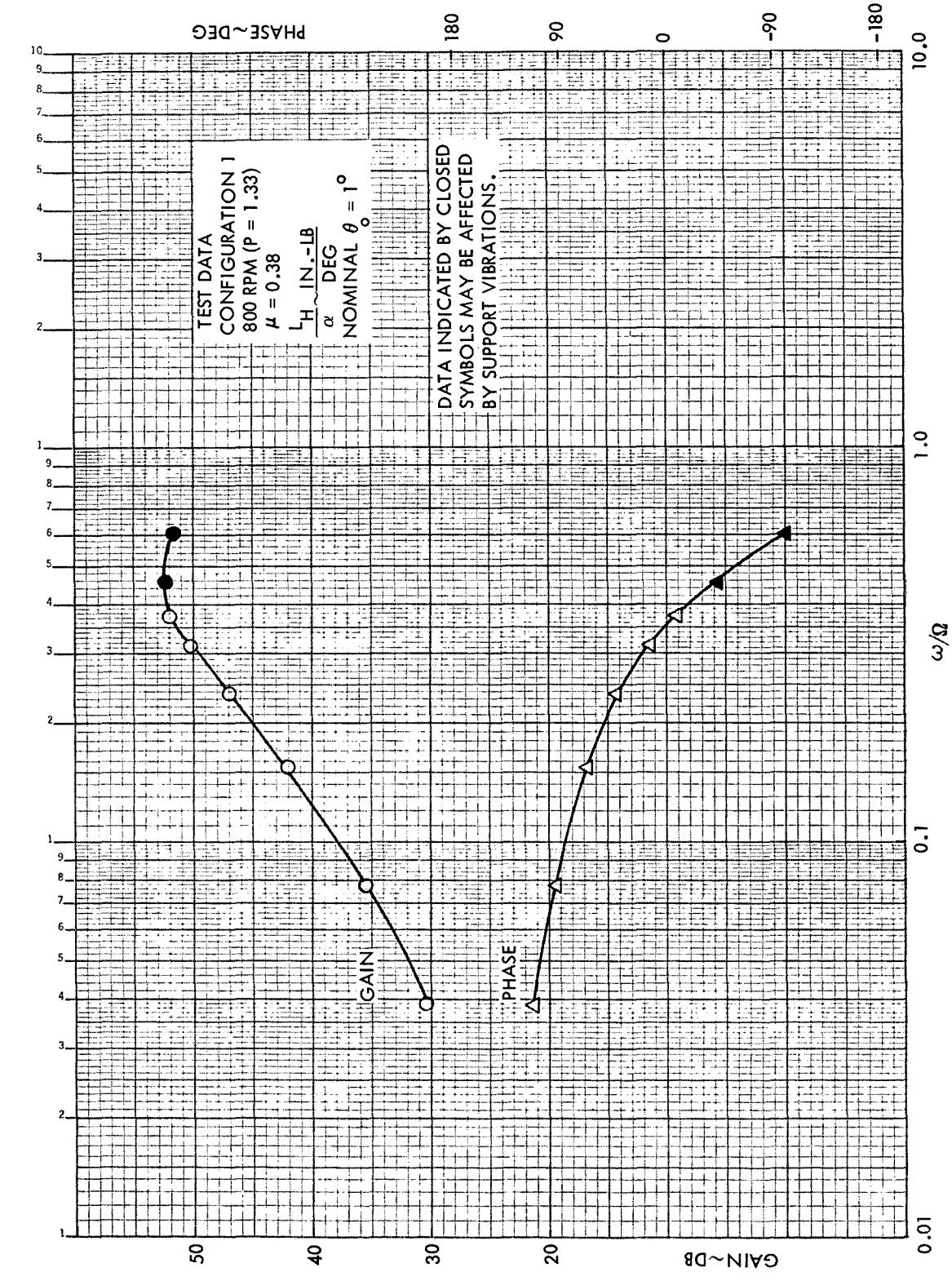

Figure C28. Rotor Hub Roll Moment Frequency Response to Shaft Pitch, Configuration 1, μ = 0.38, 800 RPM (P = 1.33)

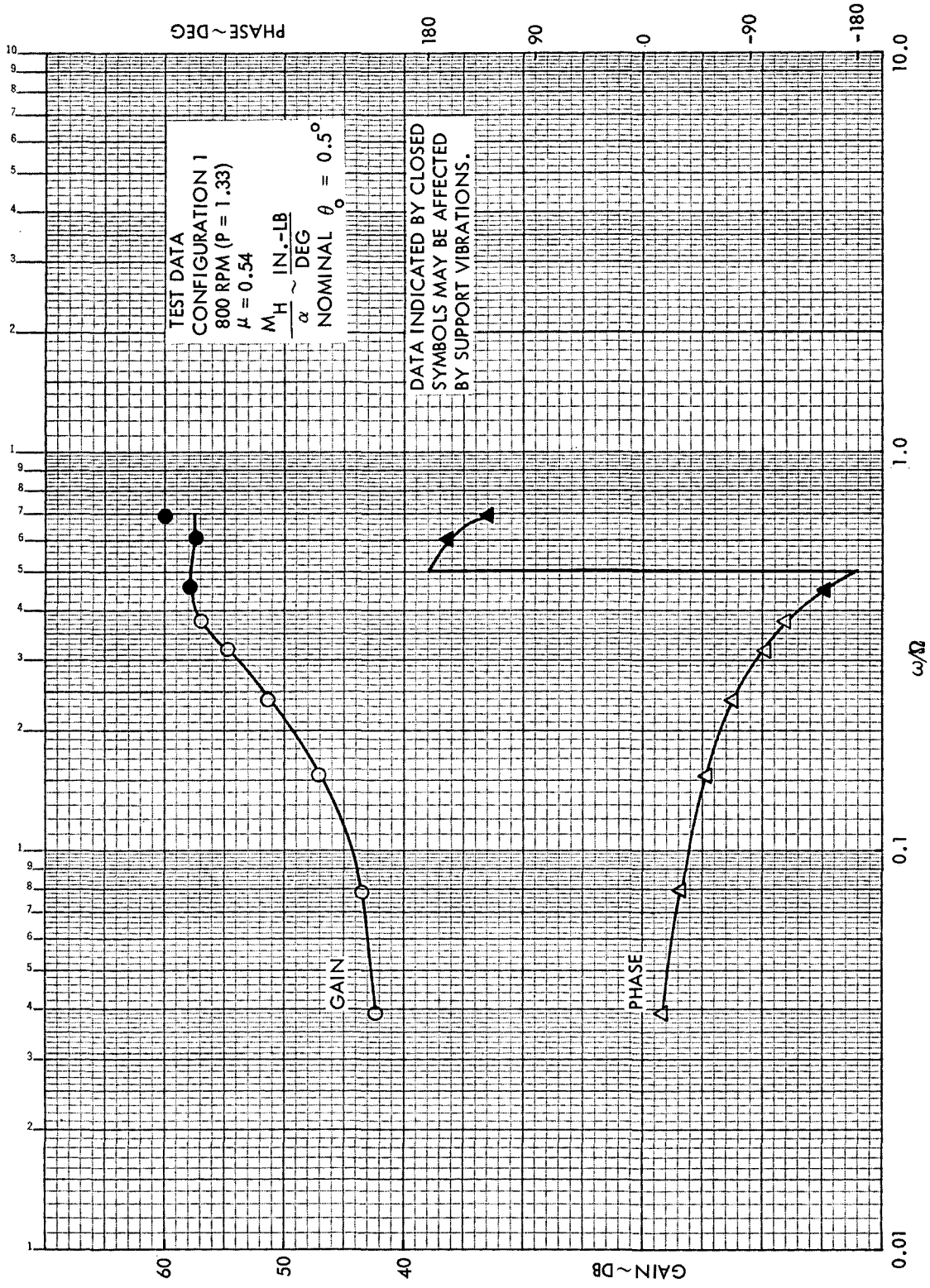

Figure C29. Rotor Hub Pitch Moment Frequency Response to Shaft Pitch, Configuration 1, μ = 0.54, 800 RPM (P = 1.33)

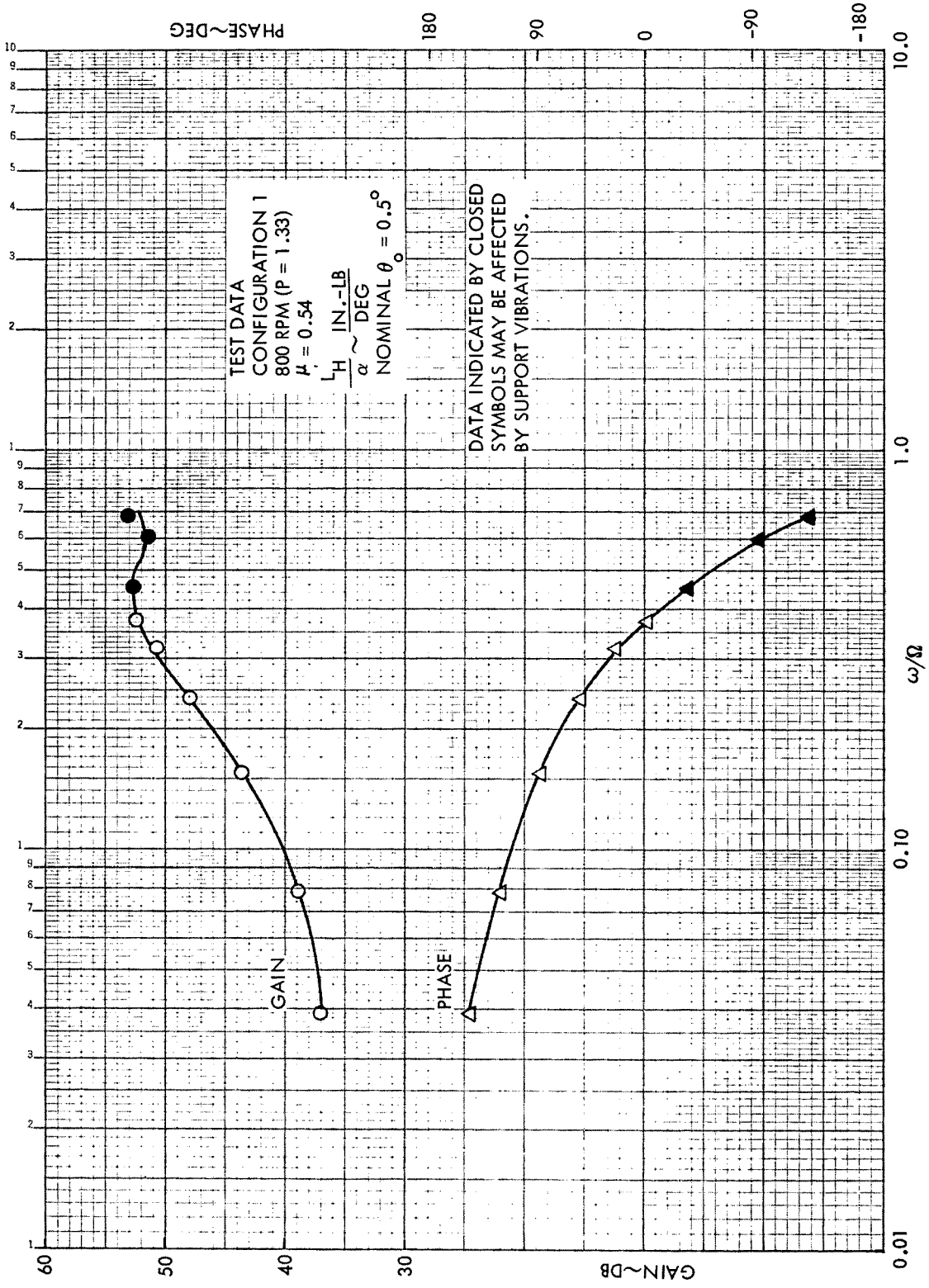

Figure C30. Rotor Hub Roll Moment Frequency Response to Shaft Pitch, Configuration 1, μ = 0.54, 800 RPM (P = 1.33)

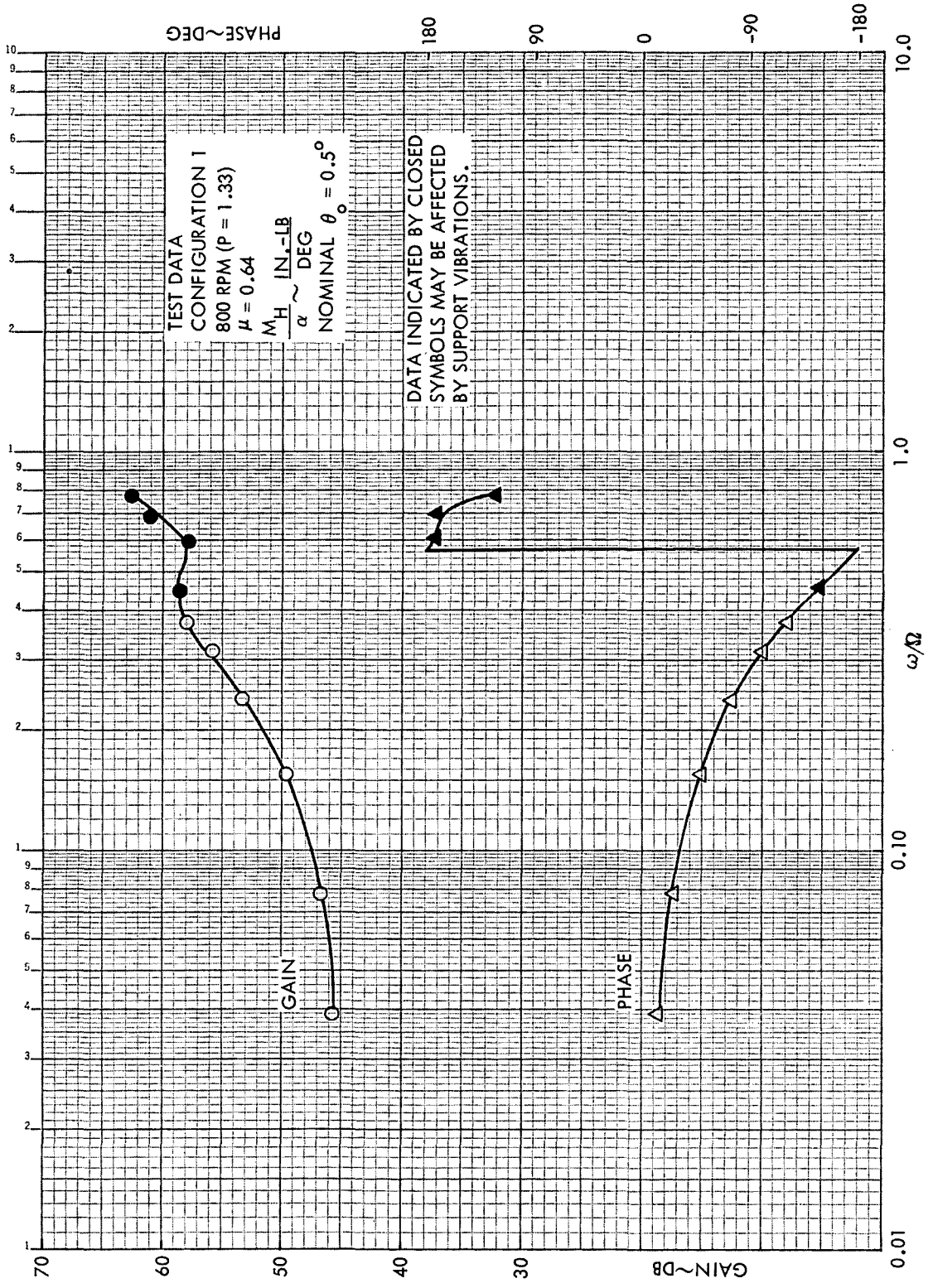

Figure C31. Rotor Hub Pitch Moment Frequency Response to Shaft Pitch, Configuration 1, μ = 0.64, 800 RPM (P = 1.33)

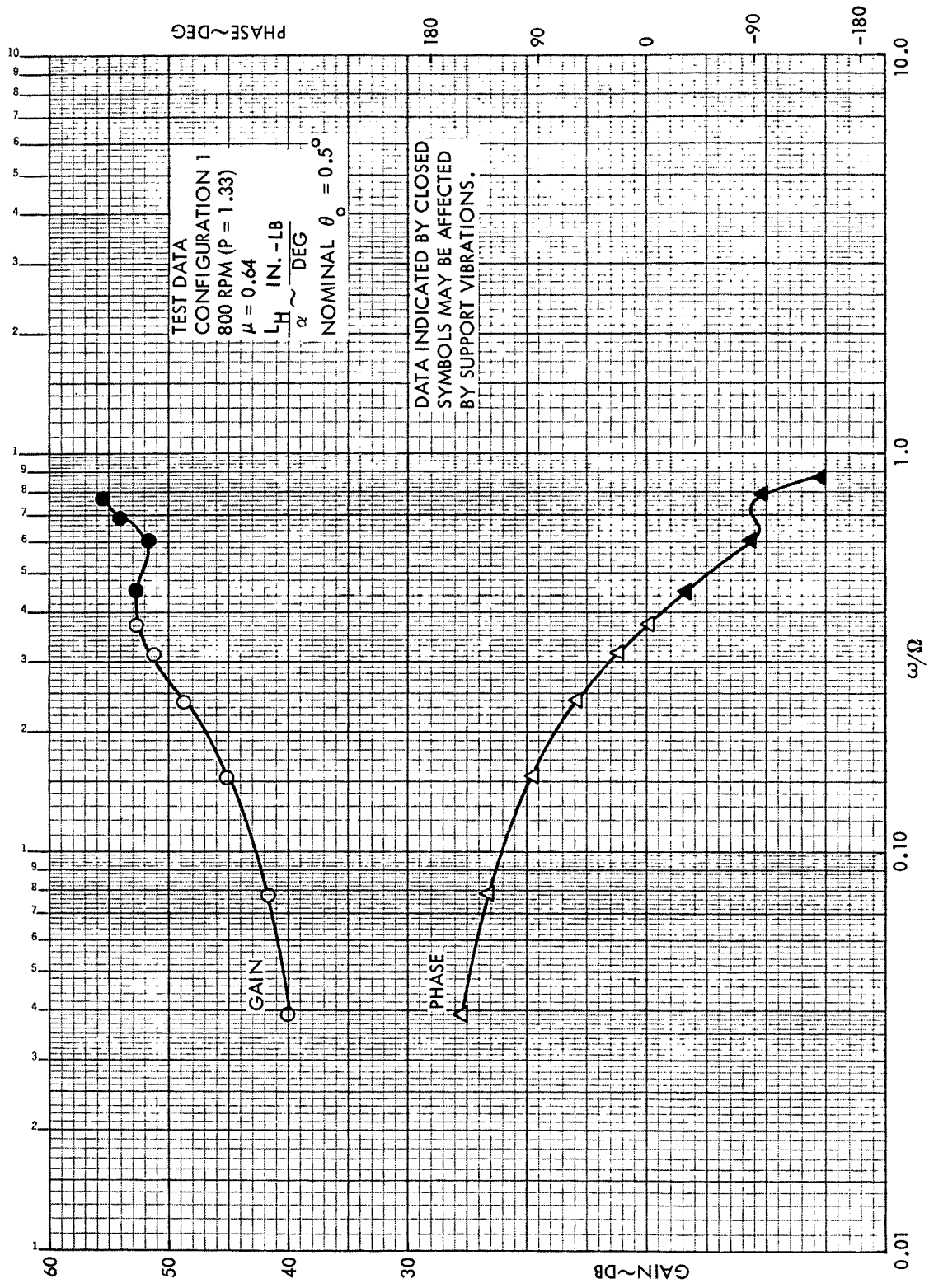

Figure C32. Rotor Hub Roll Moment Frequency Response to Shaft Pitch, Configuration 1, μ = 0.64, 800 RPM (P = 1.33)

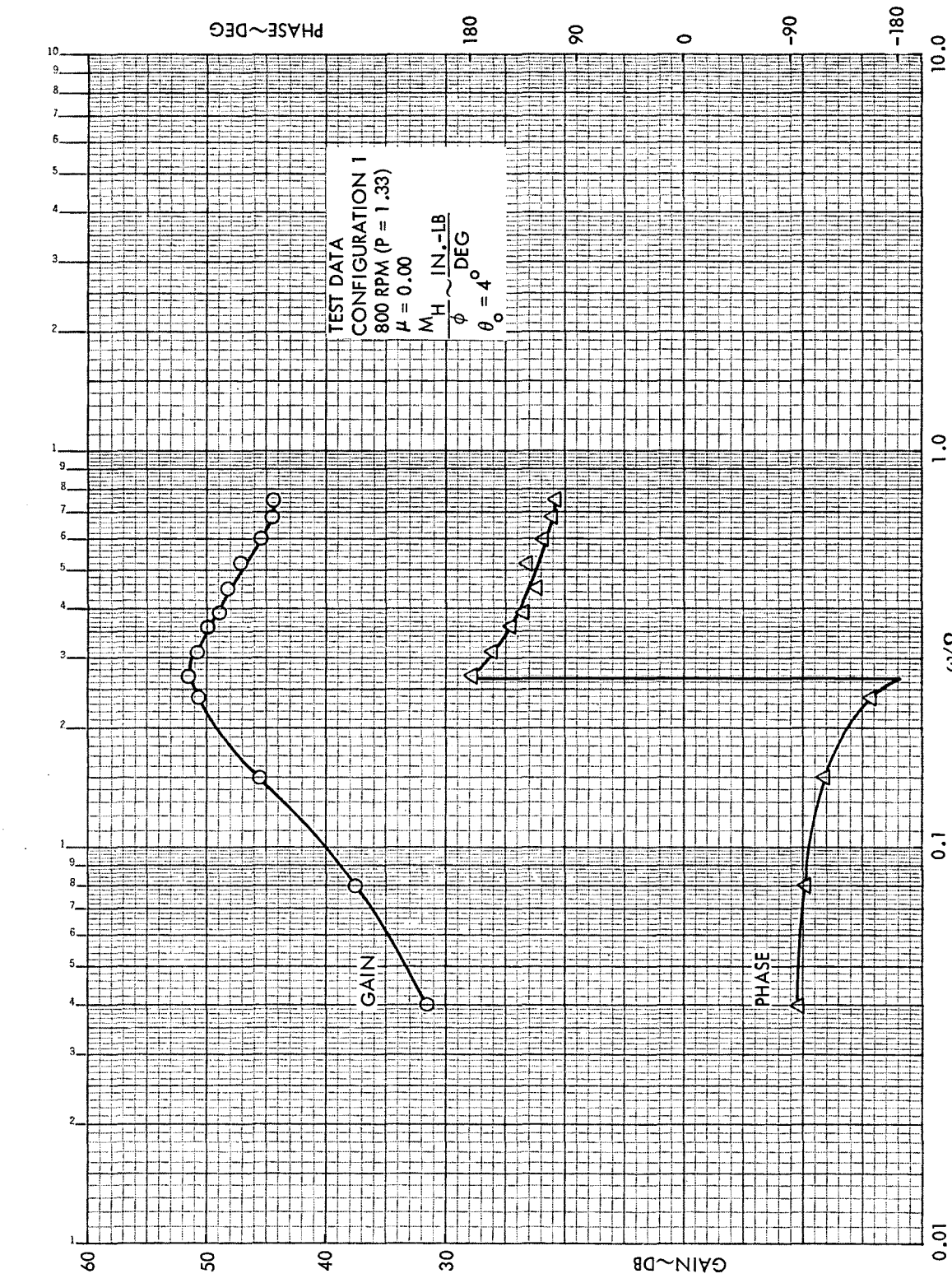

Figure C33. Rotor Hub Pitch Moment Frequency Response to Shaft Roll, Configuration 1, μ = 0.0, 800 RPM (P = 1.33)

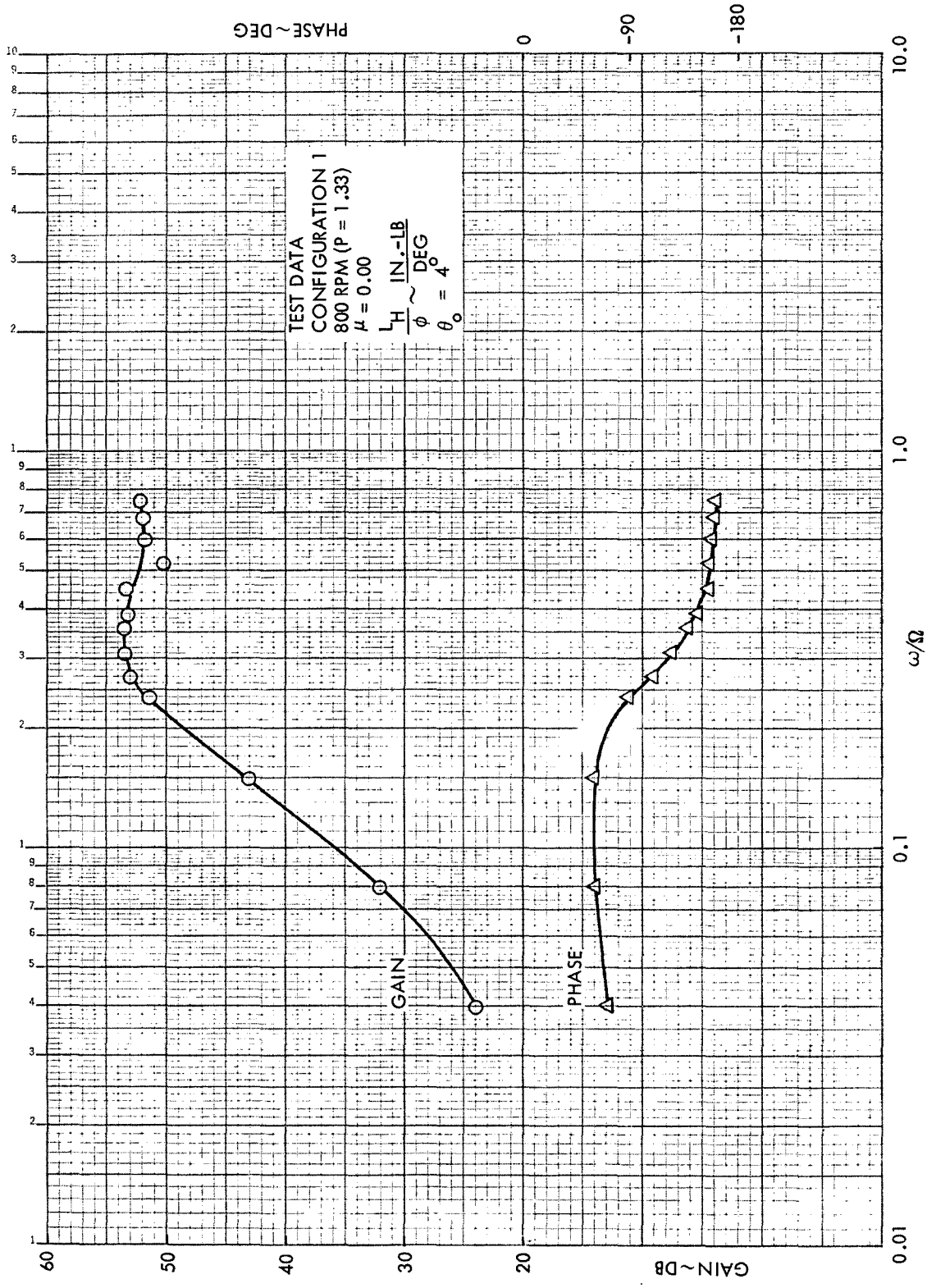

Figure C34. Rotor Hub Roll Moment Frequency Response to Shaft Roll, Configuration 1, μ = 0.0, 800 RPM (P = 1.33)

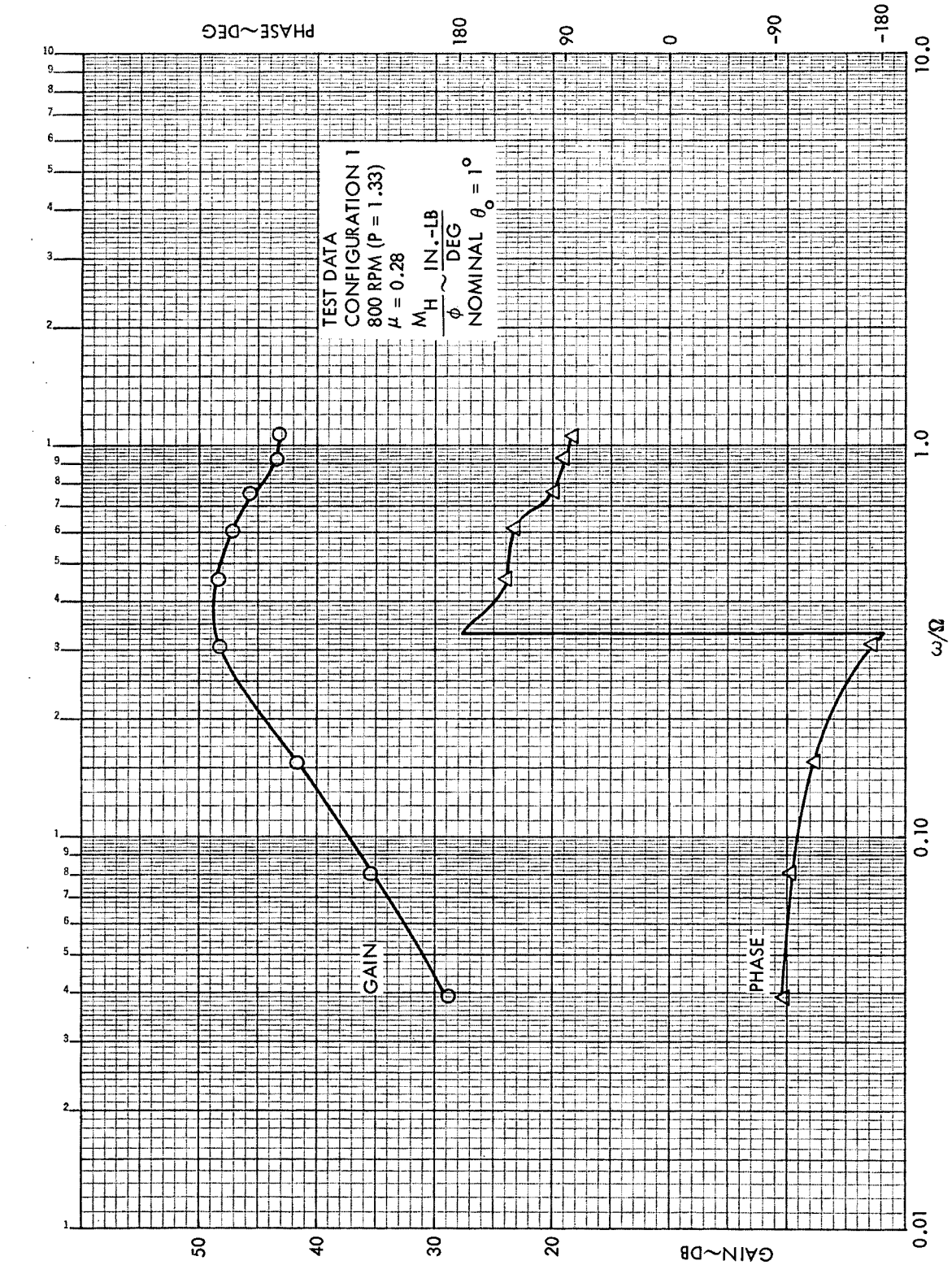

Figure C35. Rotor Hub Pitch Moment Frequency Response to Shaft Roll, Configuration 1, μ = 0.28, 800 RPM (P = 1.33)

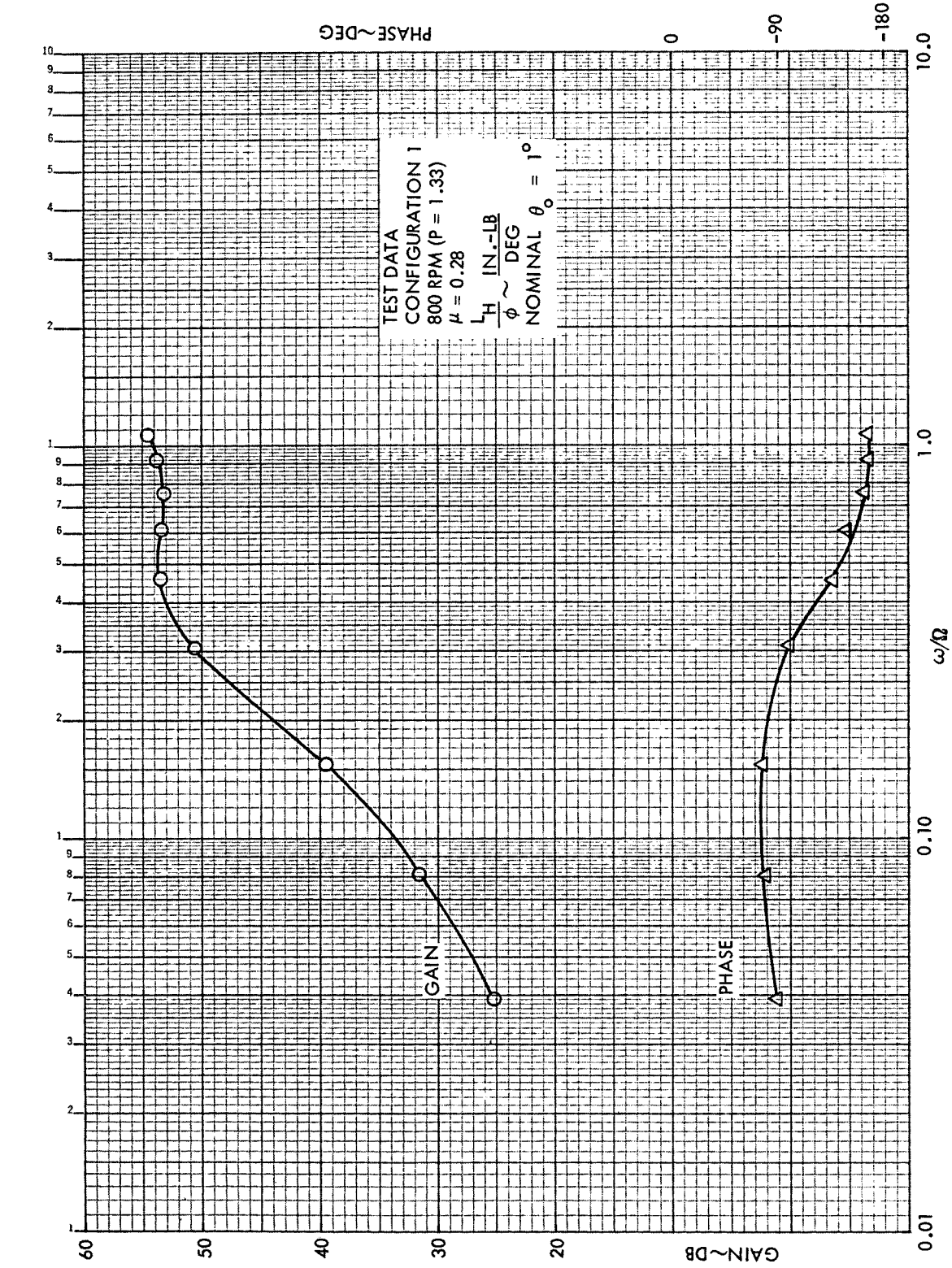

Figure C36. Rotor Hub Roll Moment Frequency Response to Shaft Roll, Configuration 1, μ = 0.28, 800 RPM (P = 1.33)

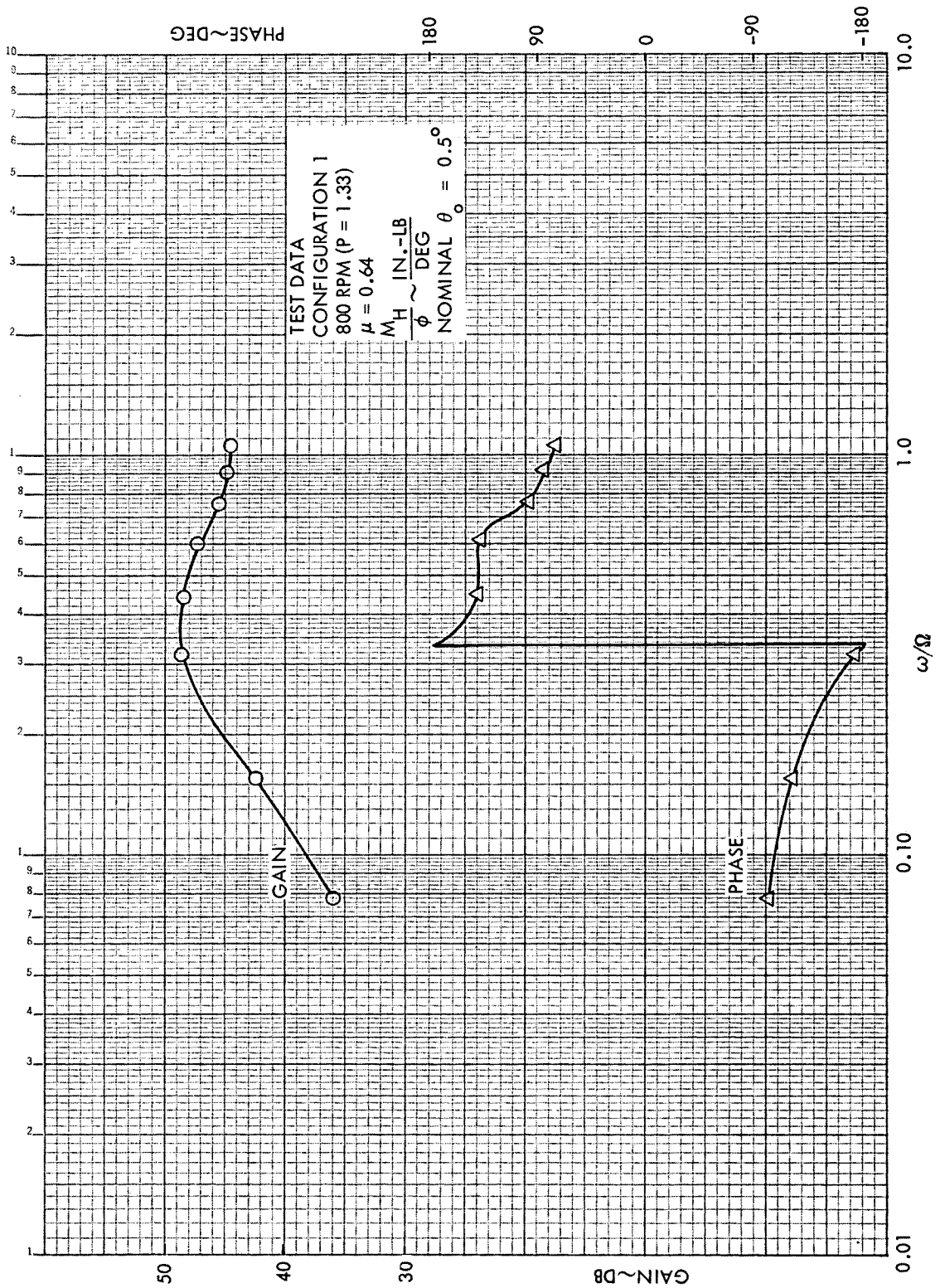

Figure C37. Rotor Hub Pitch Moment Frequency Response to Shaft Roll, Configuration 1, μ = 0.64, 800 RPM (P = 1.33)

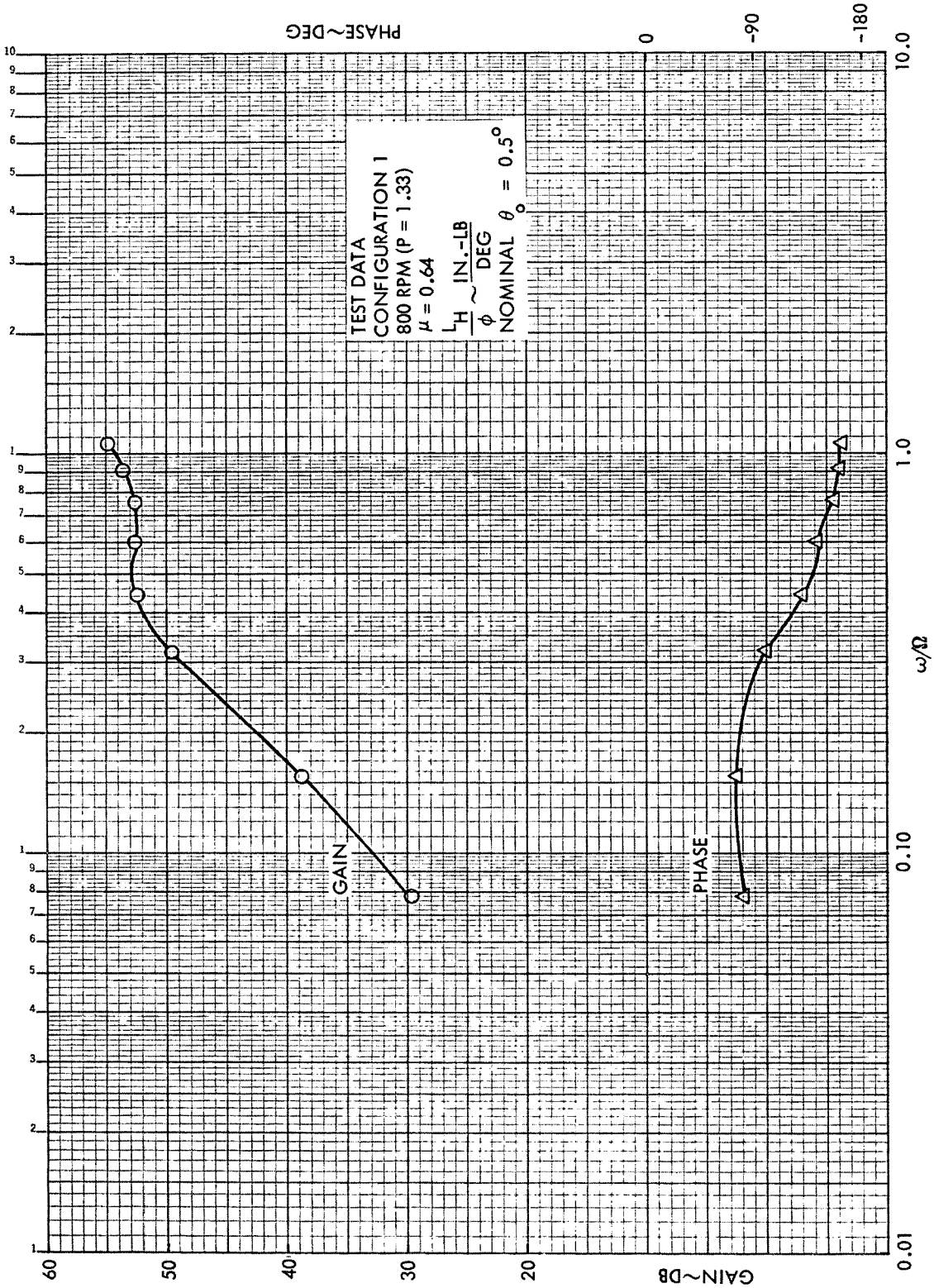

Figure C38. Rotor Hub Roll Moment Frequency Response to Shaft Roll, Configuration 1, μ = 0.64, 800 RPM (P = 1.33)

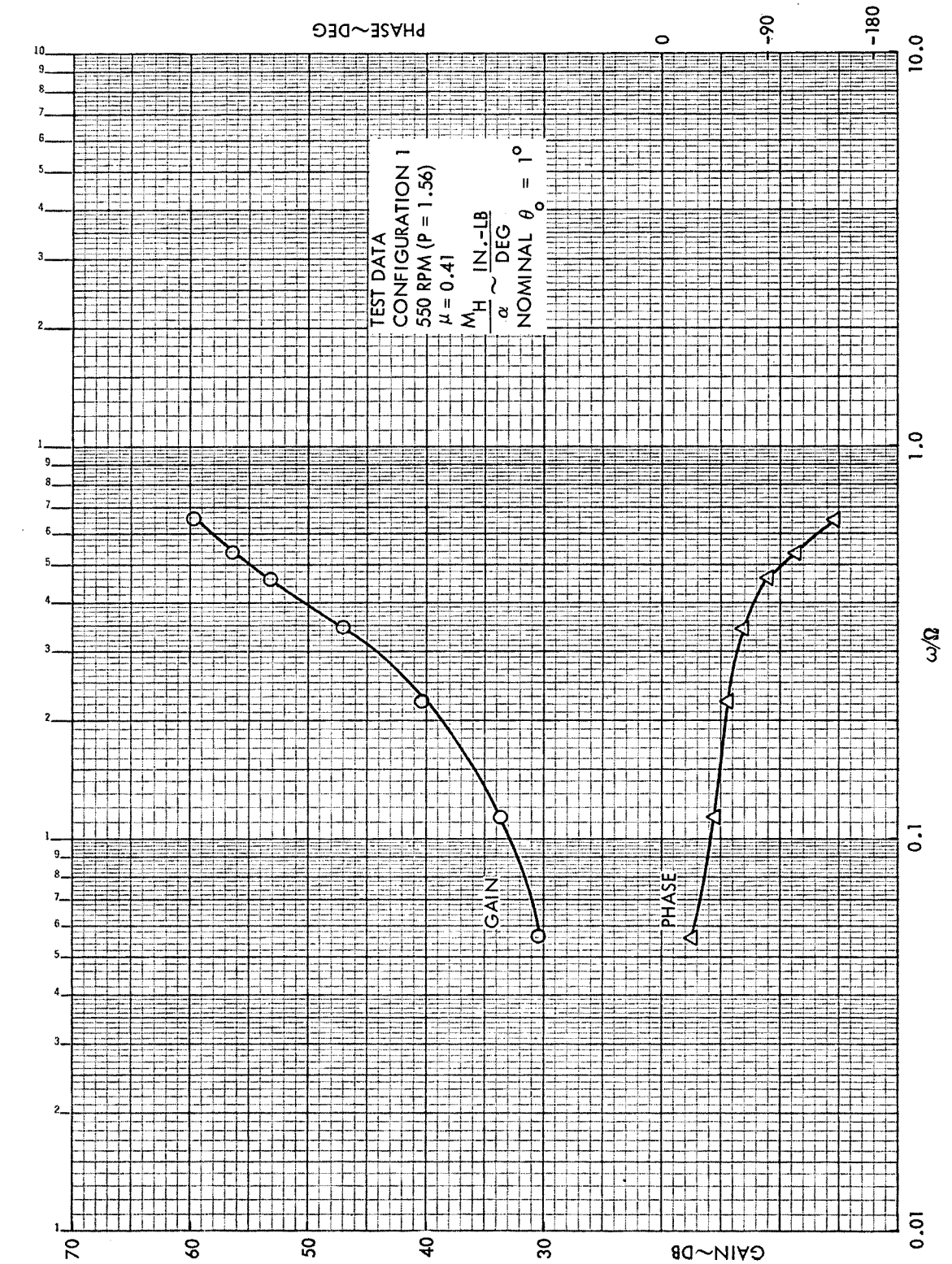

Figure C39. Rotor Hub Pitch Moment Frequency Response to Shaft Pitch, Configuration 1, μ = 0.41, 550 RPM (P = 1.56)

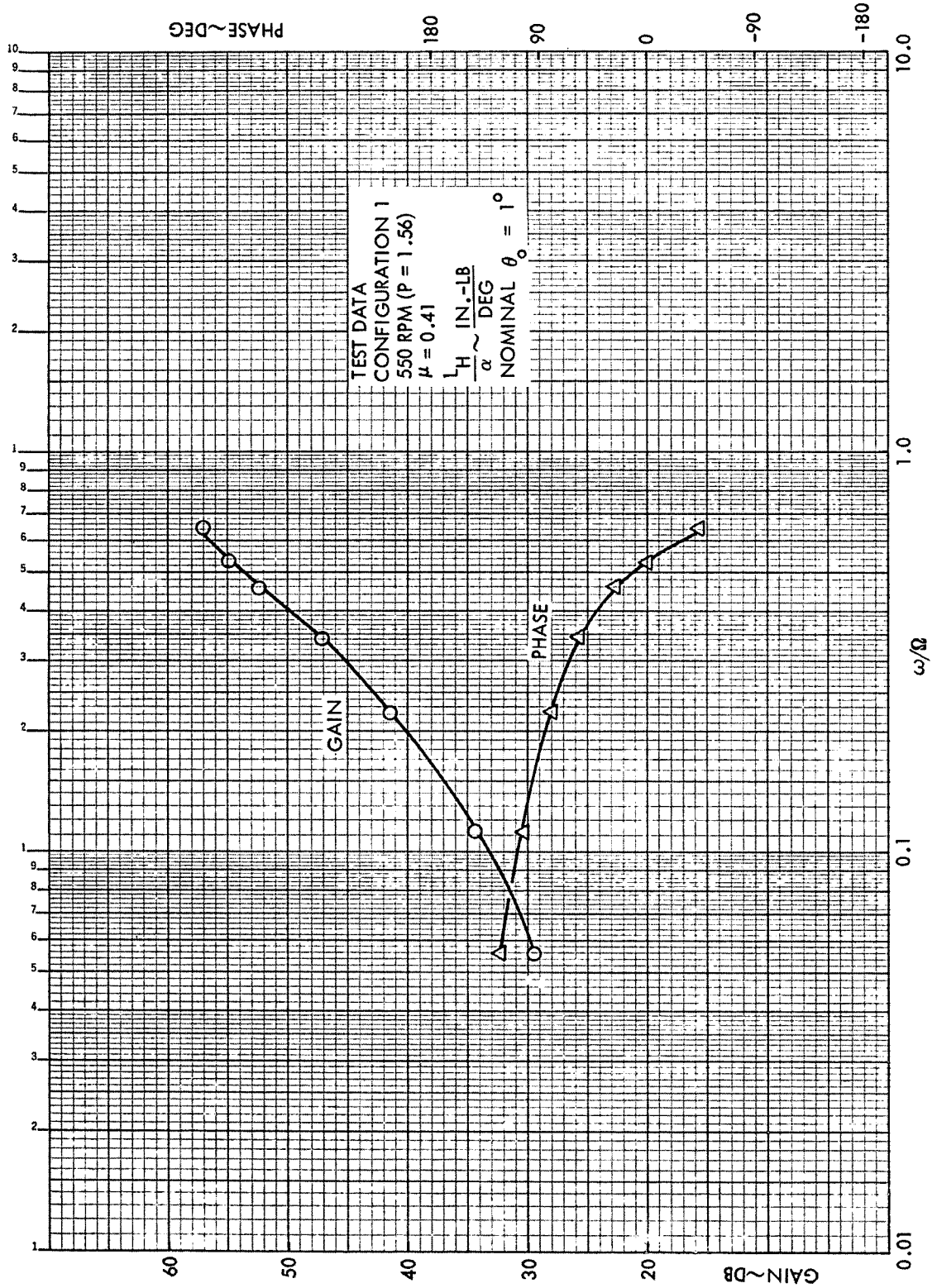

Figure C40. Rotor Hub Roll Moment Frequency Response to Shaft Pitch, Configuration 1, μ = 0.41, 550 RPM (P = 1.56)

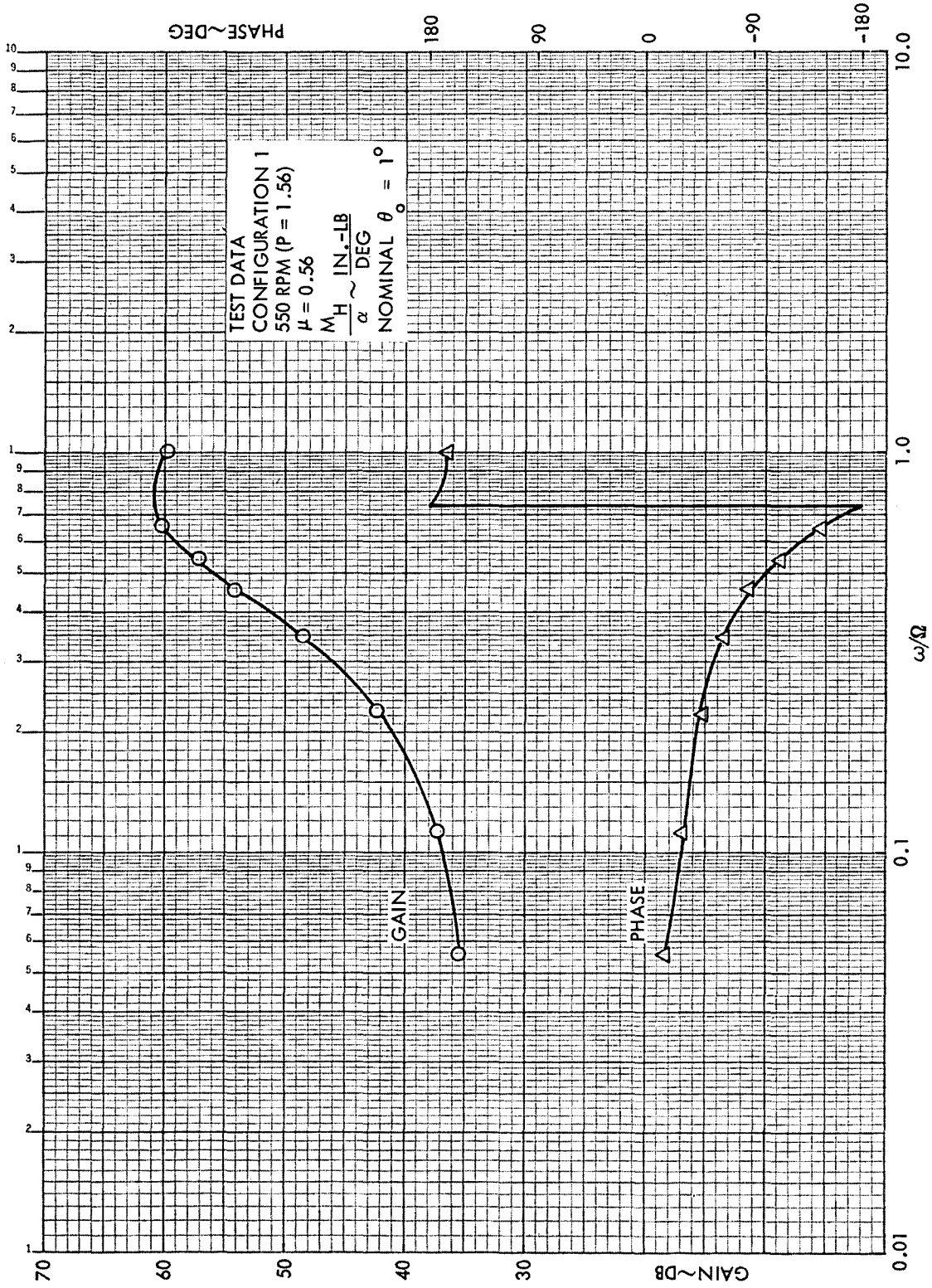

Figure C41. Rotor Hub Pitch Moment Frequency Response to Shaft Pitch, Configuration 1, μ = 0.56, 550 RPM (P = 1.56)

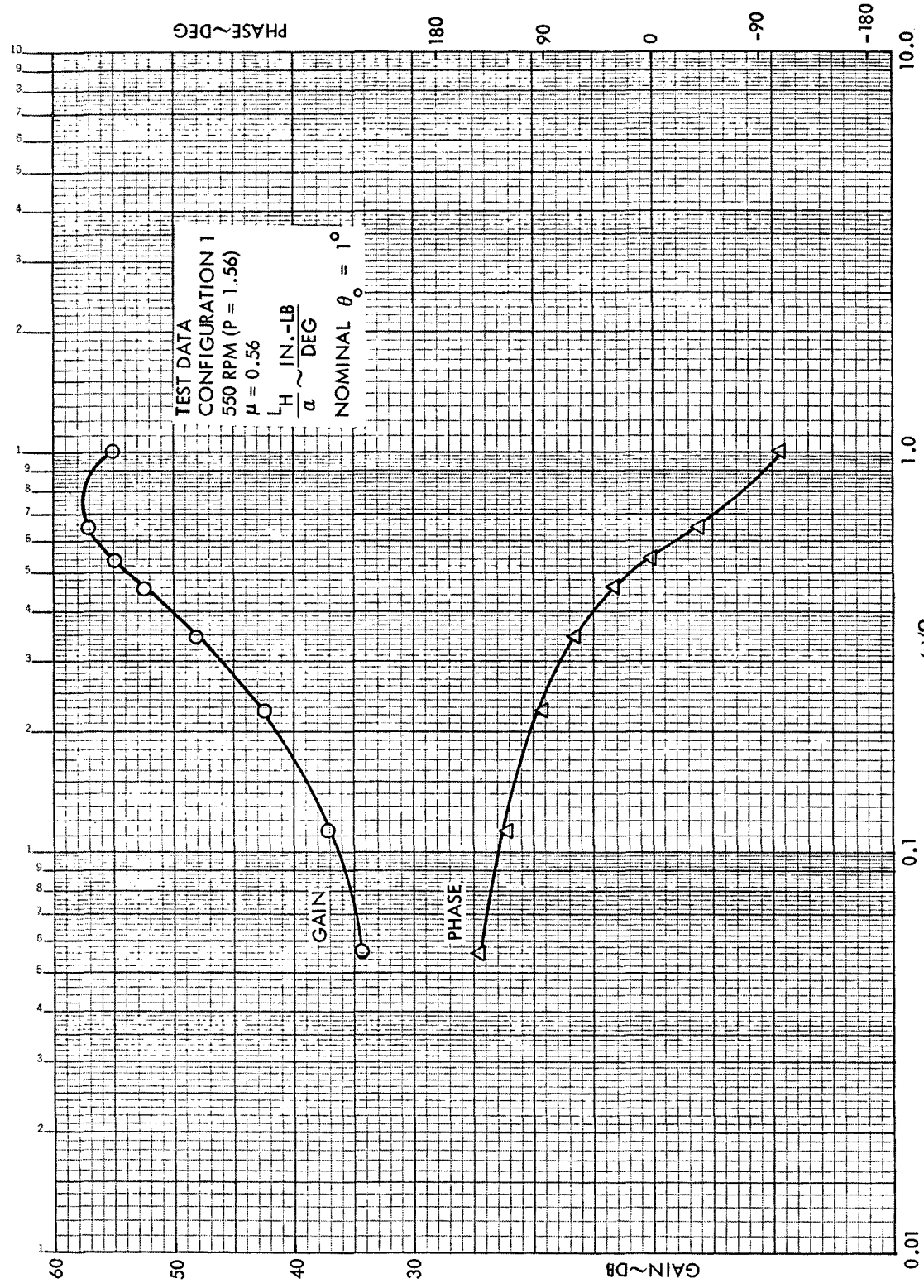

Figure C42. Rotor Hub Roll Moment Frequency Response to Shaft Pitch, Configuration 1, μ = 0.56, 550 RPM (P = 1.56)

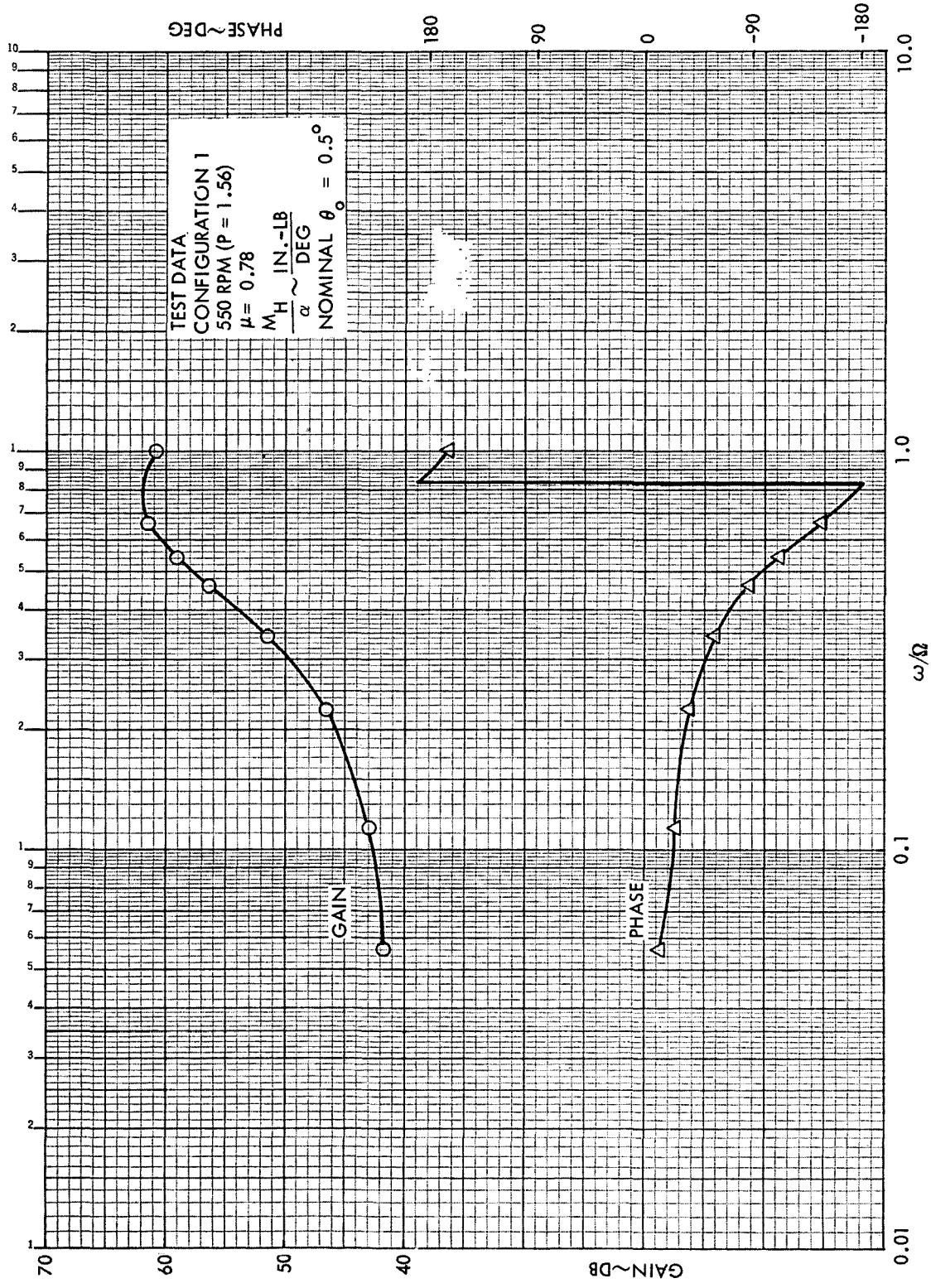

Figure C43. Rotor Hub Pitch Moment Frequency Response to Shaft Pitch, Configuration 1, μ = 0.78, 550 RPM (P = 1.56)

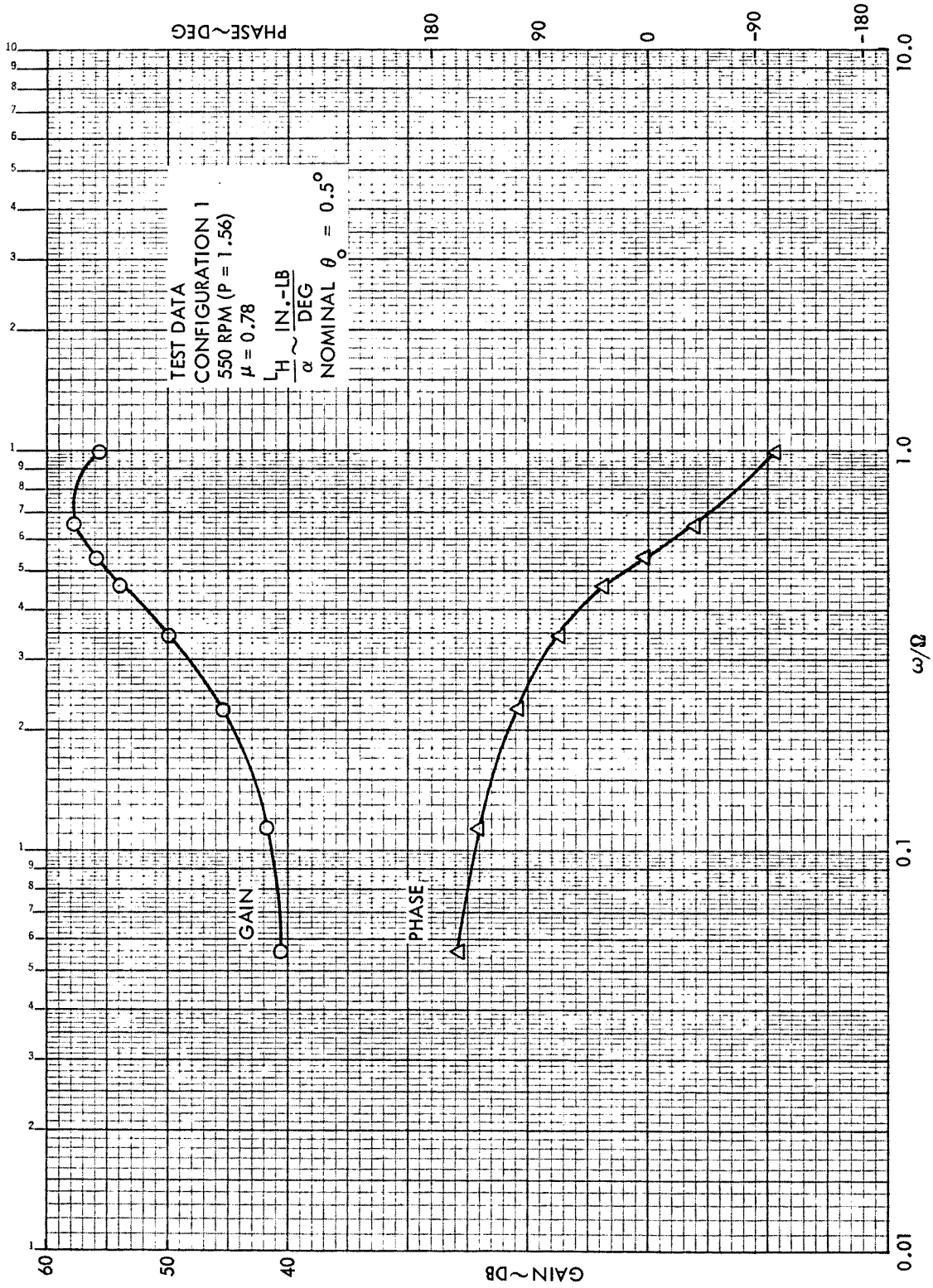

Figure C44. Rotor Hub Roll Moment Frequency Response to Shaft Pitch, Configuration 1, μ = 0.78, 550 RPM (P = 1.56)

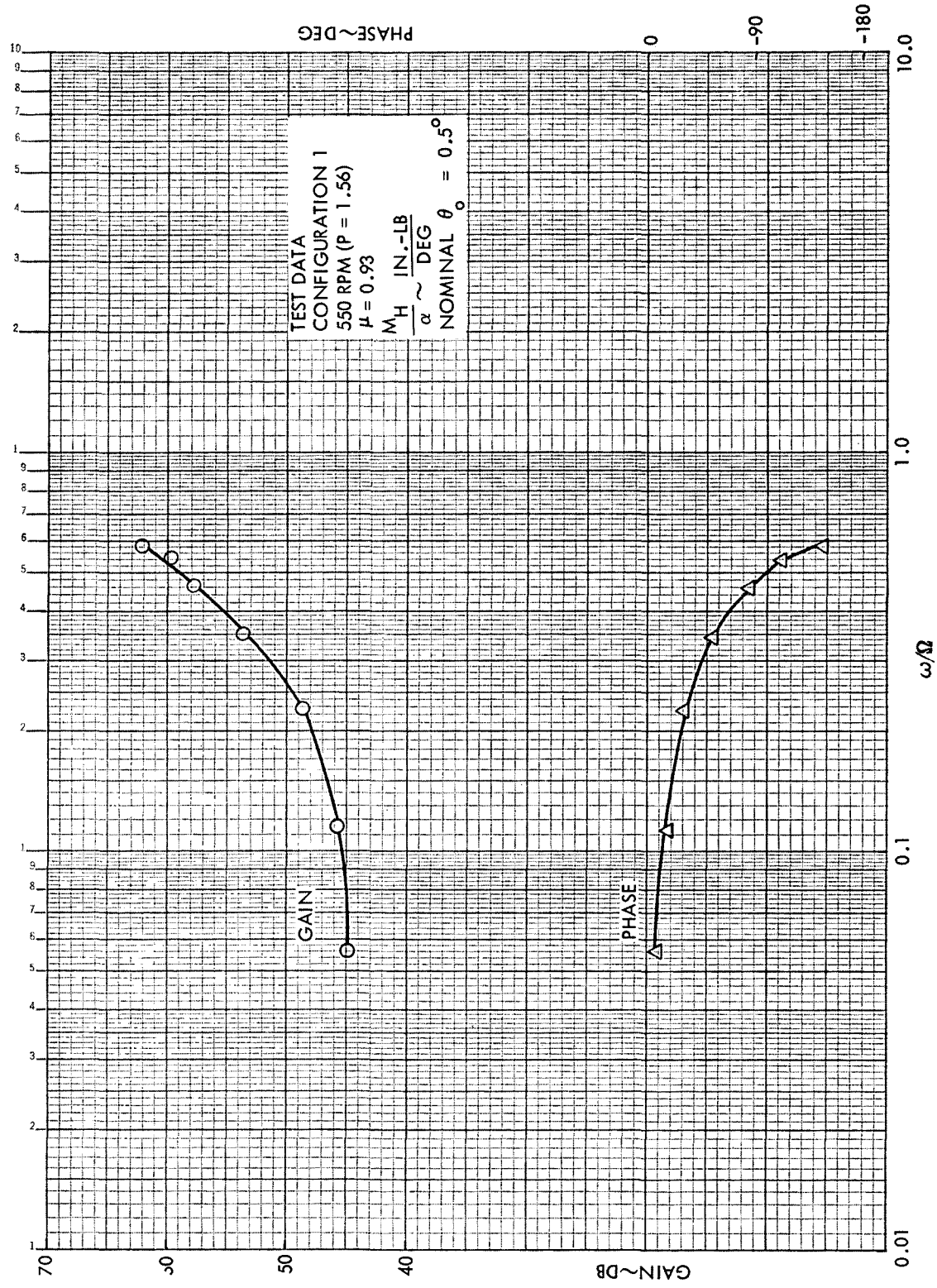

Figure C45. Rotor Hub Pitch Moment Frequency Response to Shaft Pitch, Configuration 1, μ = 0.93, 550 RPM (P = 1.56)

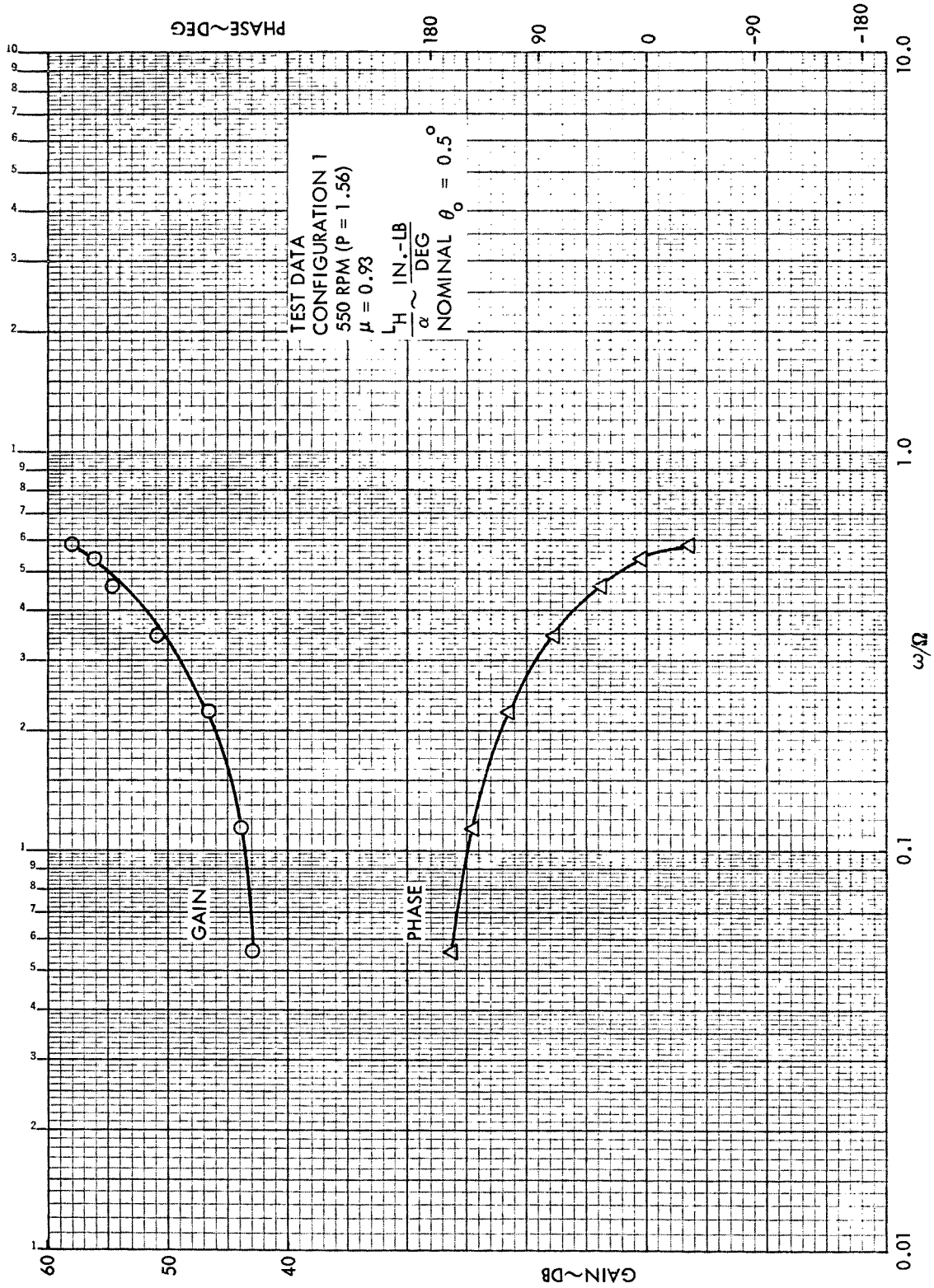

Figure C46. Rotor Hub Roll Moment Frequency Response to Shaft Pitch, Configuration 1, μ = 0.93, 550 RPM (P = 1.56)

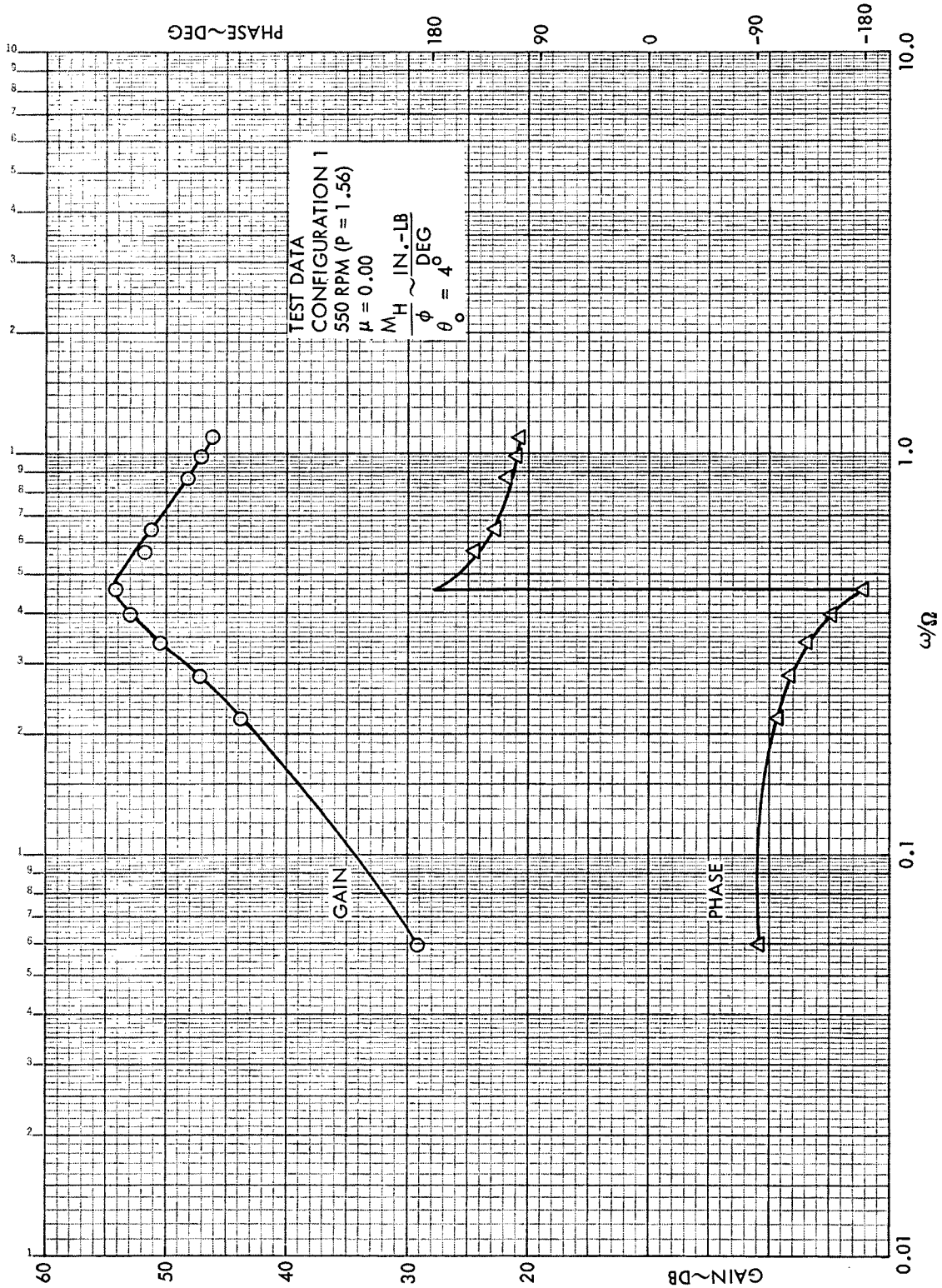

Figure C47. Rotor Hub Pitch Moment Frequency Response to Shaft Roll, Configuration 1, μ = 0.0, 550 RPM (P = 1.56)

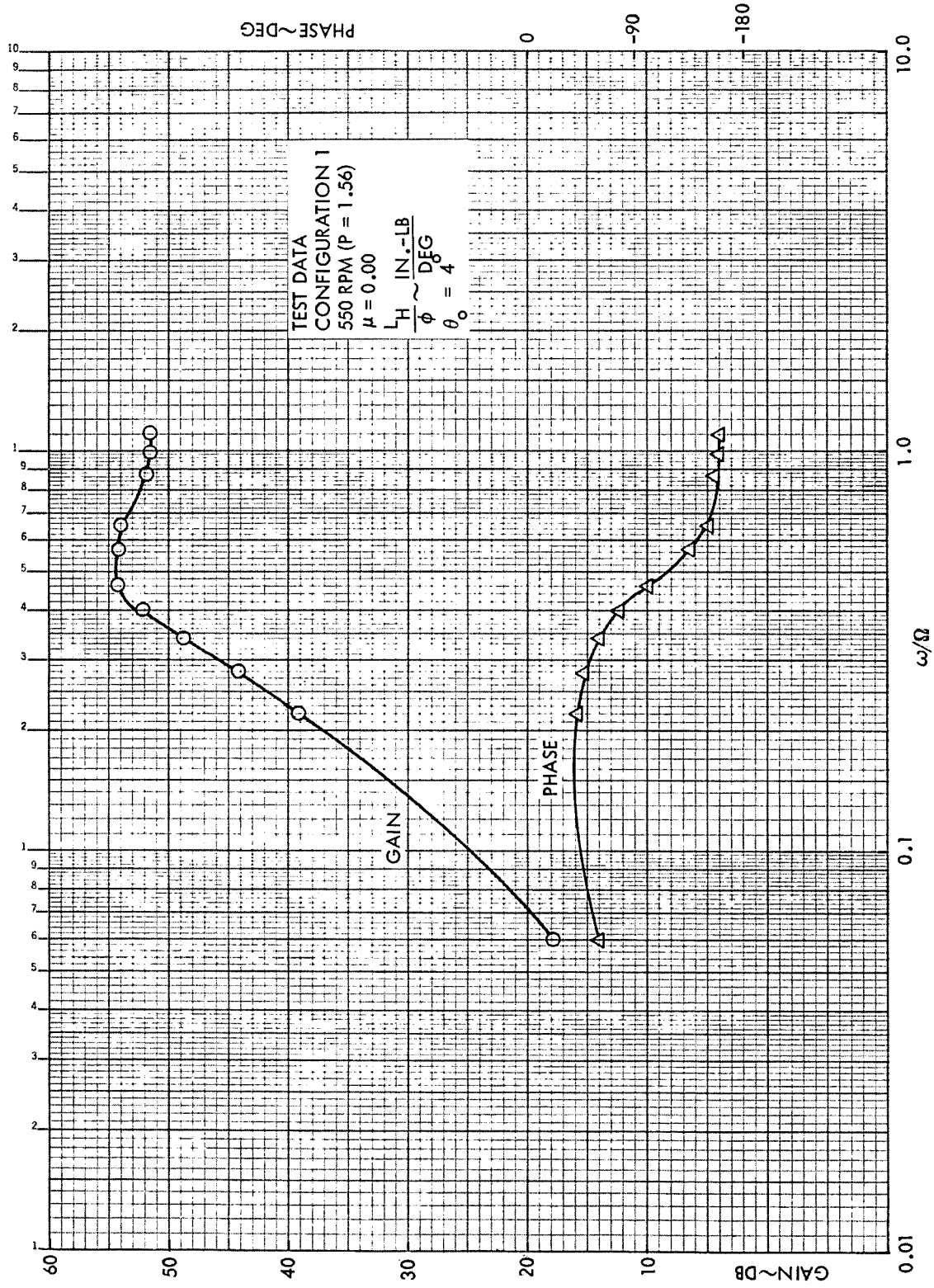

Figure C48. Rotor Hub Roll Moment Frequency Response to Shaft Roll, Configuration 1, μ = 0.0, 550 RPM (P = 1.56)

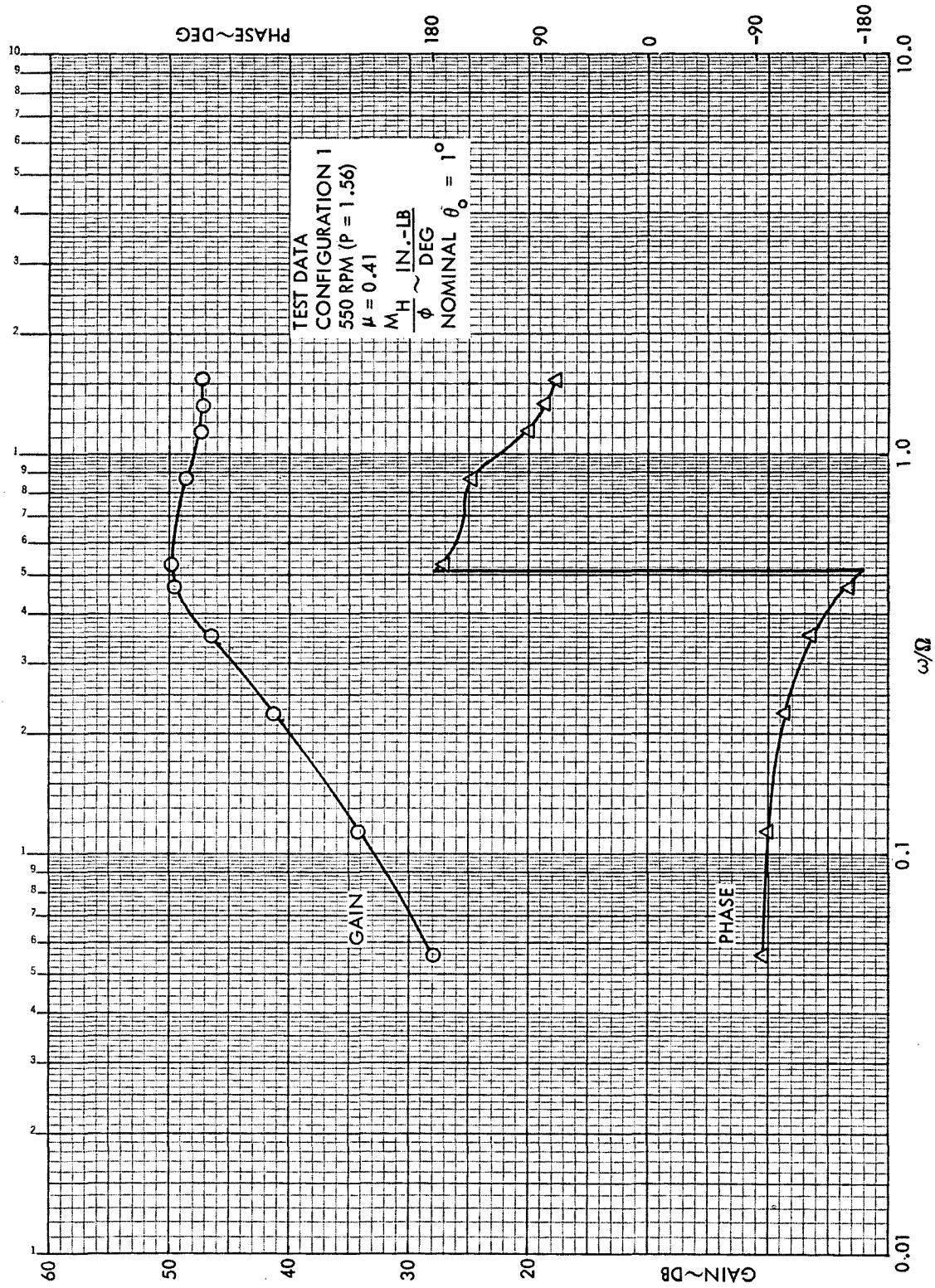

Figure C49. Rotor Hub Pitch Moment Frequency Response to Shaft Roll, Configuration 1, μ = 0.41, 550 RPM (P = 1.56)

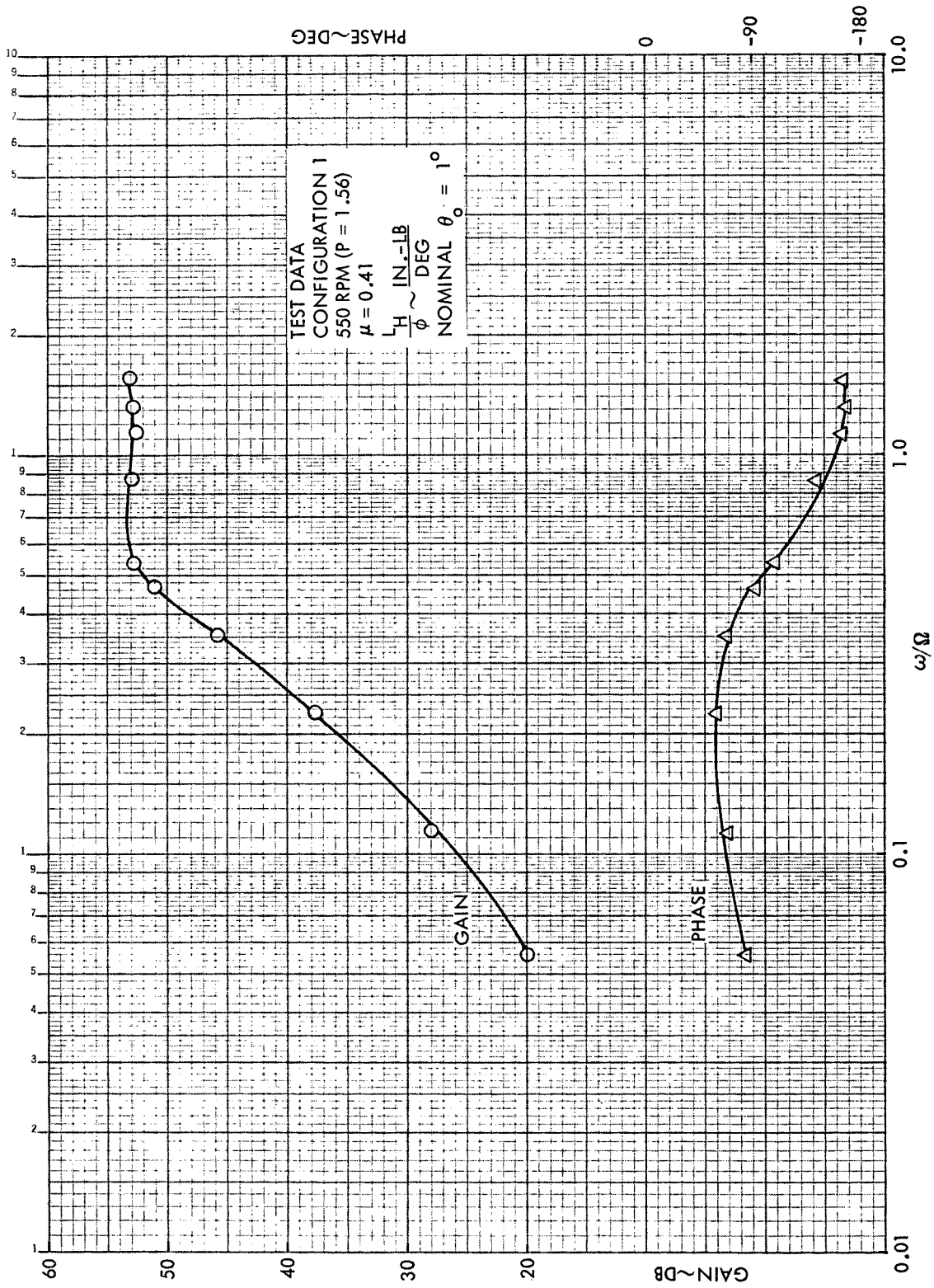

Figure C50. Rotor Hub Roll Moment Frequency Response to Shaft Roll, Configuration 1, μ = 0.41, 550 RPM (P = 1.56)

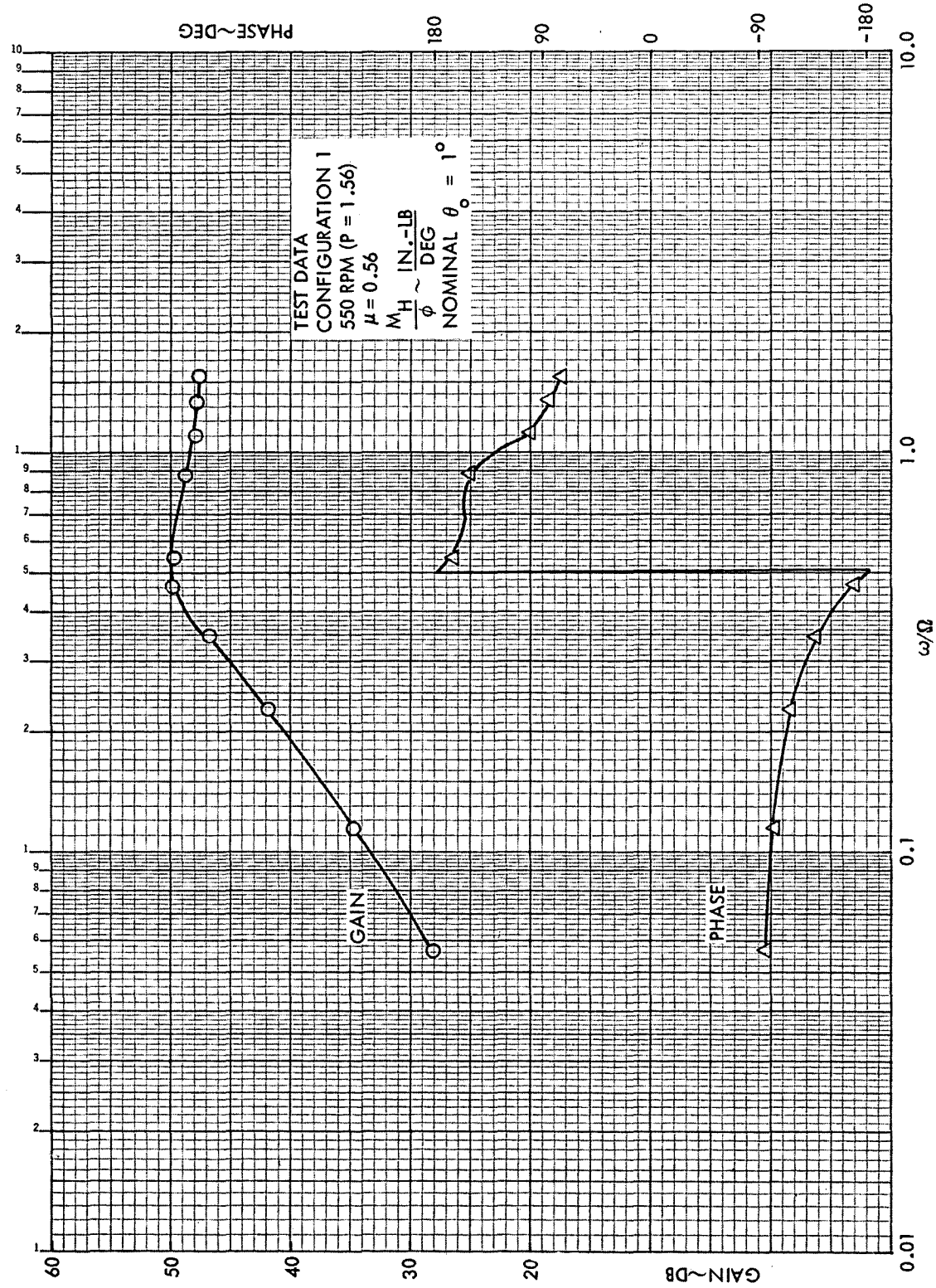

Figure C51. Rotor Hub Pitch Moment Frequency Response to Shaft Roll, Configuration 1, μ = 0.56, 550 RPM (P = 1.56)

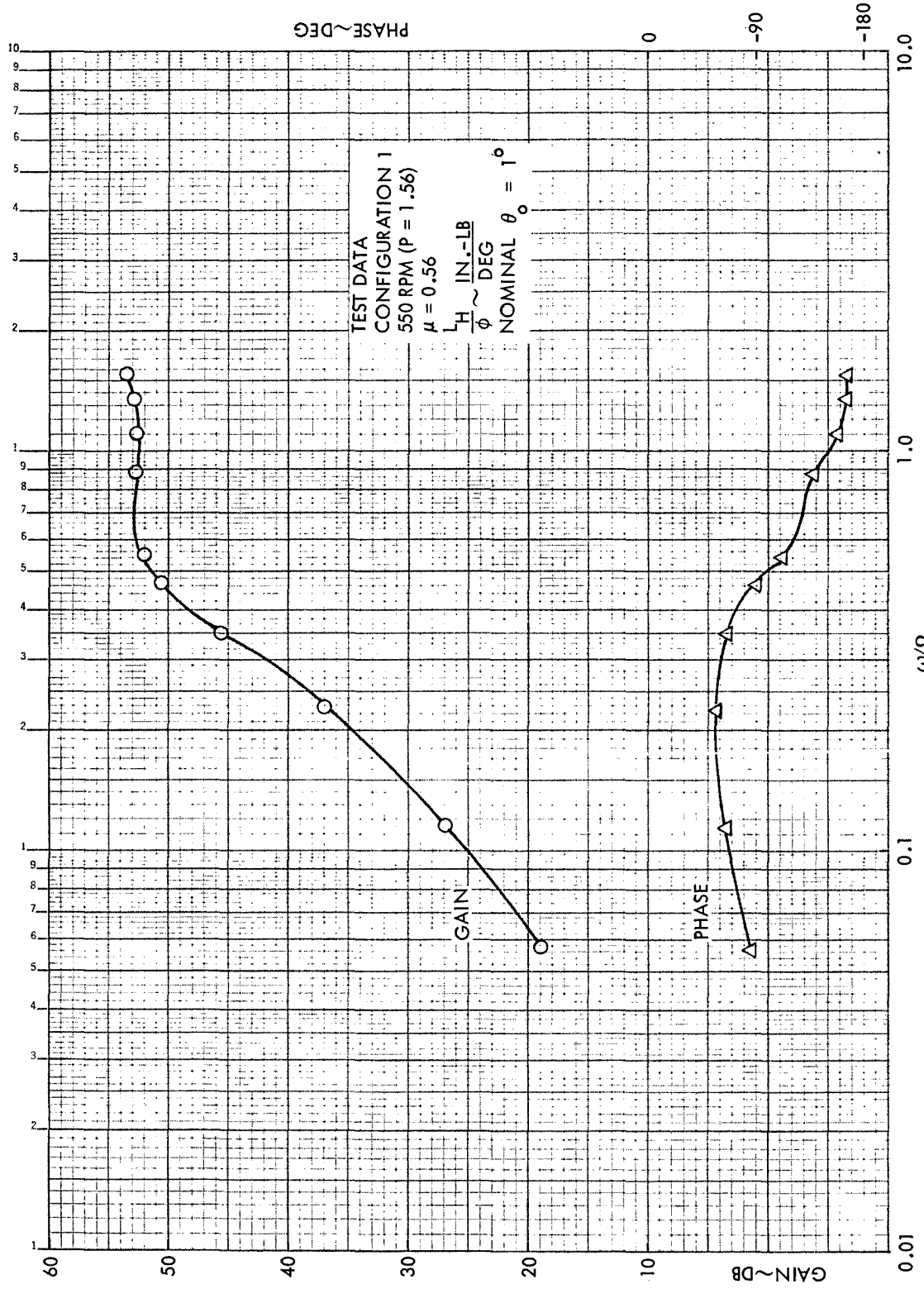

Figure C52. Rotor Hub Roll Moment Frequency Response to Shaft Roll, Configuration 1, μ = 0.56, 550 RPM (P = 1.56)

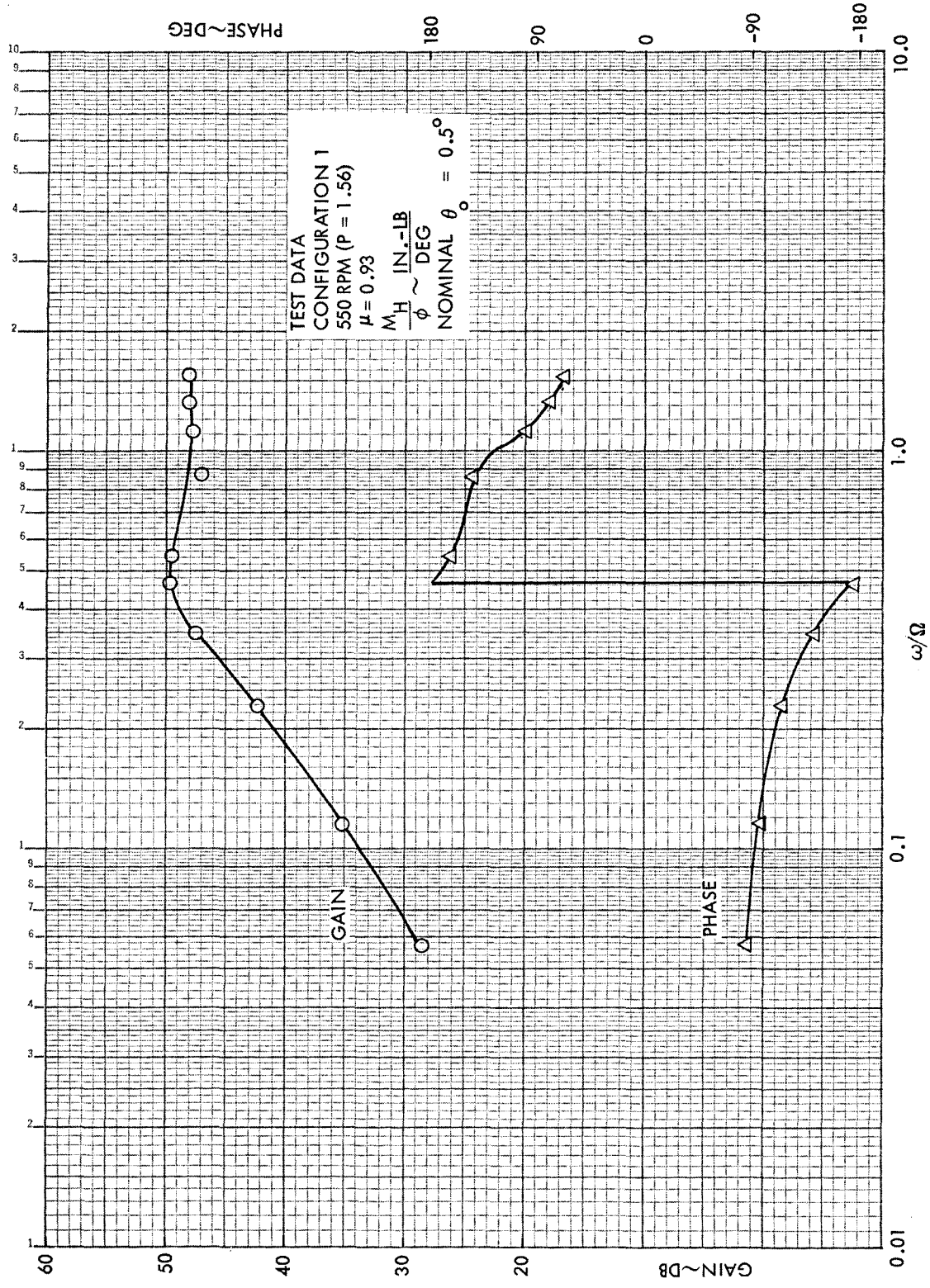

Figure C53. Rotor Hub Pitch Moment Frequency Response to Shaft Roll, Configuration 1, μ = 0.93, 550 RPM (P = 1.56)

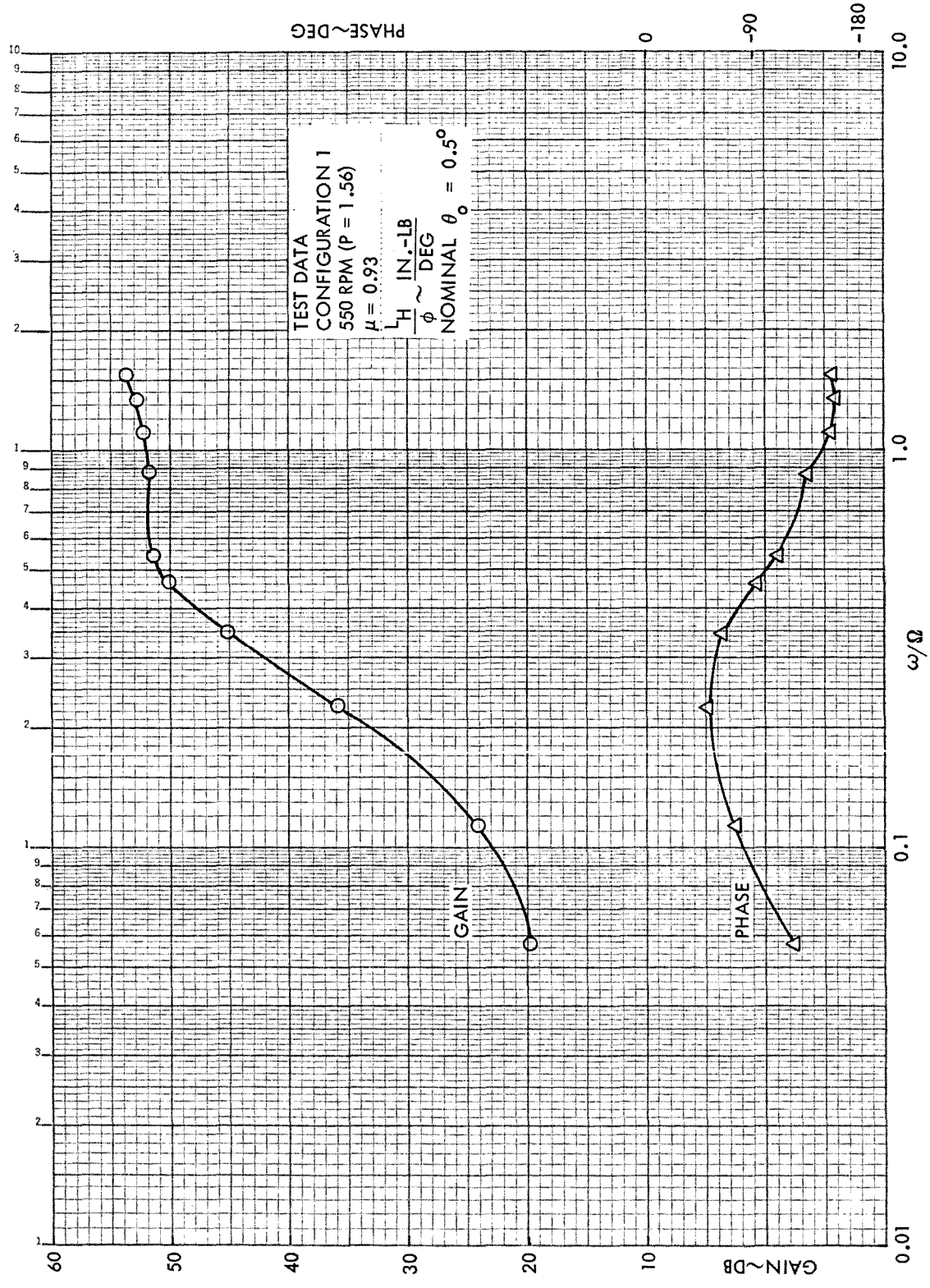

Figure C54. Rotor Hub Roll Moment Frequency Response to Shaft Roll, Configuration 1, μ = 0.93, 550 RPM (P = 1.56)